

Synthesis of Functionalized 2-Oxindoles and 3-Spirocyclic-2-Oxindoles from Morita-Baylis-Hillman Adduct of Isatin

THESIS SUBMITTED TO
THE UNIVERSITY OF KERALA
IN FULFILMENT OF THE REQUIREMENTS
FOR THE DEGREE OF
DOCTOR OF PHILOSOPHY
IN CHEMISTRY
UNDER THE FACULTY OF SCIENCE

BY

K. SELVAKUMAR

ORGANIC CHEMISTRY SECTION
NATIONAL INSTITUTE FOR INTERDISCIPLINARY SCIENCE AND TECHNOLOGY (CSIR)
THIRUVANANTHAPURAM-695 019
KERALA, INDIA

2012

...To my beloved family

DECLARATION

I hereby declare that Ph. D. thesis entitled “**Synthesis of Functionalized 2-Oxindoles and 3-Spirocyclic-2-Oxindoles from Morita-Baylis-Hillman Adduct of Isatin**” is an independent work carried out by me and it has not been submitted anywhere else for any other degree, diploma or title.

K. Selvakumar

Thiruvananthapuram

2012

राष्ट्रीय अंतर्विषयी विज्ञान तथा प्रौद्योगिकी संस्थान

(वैज्ञानिक एवं प्रौद्योगिकी अनुसंधान परिषद्)

(पहले क्षेत्रीय अनुसंधान प्रयोगशाला)

NATIONAL INSTITUTE FOR INTERDISCIPLINARY SCIENCE AND TECHNOLOGY

(Council of Scientific & Industrial Research)

(formerly Regional Research laboratory)

इन्डस्ट्रियल इस्टेट डाक घर, तिरुवनन्तपुरम 695 019, भारत

Industrial Estate P.O., Thiruvananthapuram 695 019, India



आई एस ओ 9001 प्रमाणित



CERTIFICATE

This is to certify that the work embodied in the thesis entitled “**Synthesis of Functionalized 2-Oxindoles and 3-Spirocyclic-2-Oxindoles from Morita-Baylis-Hillman Adduct of Isatin**” has been carried out by **Mr. K. Selvakumar** under our combined supervision at the Chemical Sciences and Technology Division of National Institute for Interdisciplinary Science and Technology (CSIR), Thiruvananthapuram and the same has not been submitted elsewhere for any other degree.

Dr. R. LUXMI VARMA

(Thesis supervisor)

Dr. P. SHANMUGAM

(Thesis supervisor)

Thiruvananthapuram

ACKNOWLEDGEMENTS

At the outset, I express my sincere and heartfelt gratitude to my research supervisor **Dr. P. Shanmugam** for suggesting me interesting research topic and for his care, constructive criticism and continuous support throughout my doctoral studies.

I would like to offer special thanks to **Dr. R. Luxmi Varma**, Co-guide for her suggestions, encouragement and timely help during the tenure of this work.

I am grateful to Dr. Suresh Das, Directors, NIIST and Prof. T. K. Chandrasekhar, Dr. B. C. Pai, former Directors, NIIST, for providing all the laboratory facilities to carry out this work.

My sincere thanks are also due to

- ✓ Dr. G. Vijay Nair for his inspiration and support.
- ✓ Dr. Mangalam S. Nair, Dr. A. Jayalekshmy and Dr. K.V. Radhakrishnan, Scientists, Organic Chemistry Section for their help and support extended to me.
- ✓ Dr. Baby Viswambharan, Dr. V. Vaithiyathan, Ms. M. V. Suchithra for the excellent companionship and support throughout these studies.
- ✓ Mr. Arun prasath lingam, Mr. Periya raja, Ms. Solai selvi, Mr. Gouthaman, Mr. Nithiyatham Vasagam, and Dr. Dhamoathan, CLRI, Chennai for their help and cooperation.
- ✓ Mrs. S. Viji for HRMS, Mrs. Saumini Mathew, Mr. Thirumalai Kumaran, Mr. B. Adarsh, and Mr. P. Preethanuj for recording NMR spectra
- ✓ Dr. Gokulsapathi, Dr. Pannerselvam, Dr. Balasubramanian, Dr. L. Praveen, Dr. Sreeja, Dr. S. P. Rajasingh, Dr. K. Syam Krishnan, Dr. Jubi John, Dr. P. B. Beneesh, for sharing their research experiences and creative suggestions.
- ✓ Ms. Sholly Clair George, Ms. Rani Rajan, Mr. Ramesh reddy, Mr. Jinesh M. Kuthanapillil, Ms. Anu priya, Mr. Adharsh, Mr. Rony Rajan Paul, Mr. C.R. Sinu, Ms. Jisha Babu, Ms. Nayana Joseph, Ms. Jijy, Ms. Anu Jose, Mr. Sarath, Mr. Ajish, Mr. Praveen, Ms. Maya, Ms. Dhanya, Mr. Aneesh, Ms. Parvathy for their camaraderie and valuable support.

- ✓ Dr. S. Savithri, Dr. T.P.D. Rajan, Dr. U.T.S. Pillai, Dr. Sundrarajan, Dr. Anbu, Dr. Srinivasan, Dr. Ravi, Dr. Karunakaran and Mr. Gurusamy for their care and general help.
- ✓ Mr. Arumugam, Mr. Dharanipathi, Mr. Suresh kannan, Mr. Bala murugan, Mr. Naran, Mr. Suresh, Mr. Sabari Nathan, Mr. Balaji, Mr. Karthik, Mr. Sivaguru, Mr. Vethanarayanan, Mr. Shanmugasundram, Mr. Sasiganesh raja, Mr. Jegan, Mr. Rama krishanan, Mr. Shanmugam, Mr. Bhasha, Mr. Presanth kumar and Mr. Ajith kumar for their deep friendship and sincere help during my stay in NIIST
- ✓ All the present and former members of the Organic Chemistry Section and my friends at NIIST.
- ✓ The University Grants Commission (UGC), for financial assistance.

My deepest gratitude goes to my parents for their unflagging love, support and encouragement to pursue my interests. It is inevitable to say a word of gratitude, besides love to my brother who was there for me at each and every moment. I also owe heartfelt thanks to my wife Dr. S. Gomathi and other family members for their support, patience and understanding.

K. Selvakumar

Content

Declaration	i
Certificate	ii
Acknowledgements	iii
List of Tables	xix
List of Figures	xix
Abbreviations	xxiii
Preface	xi

Chapter I

Recent Developments on Morita-Baylis-Hillman Reaction

1.1	General introduction	2
1.2	The Morita-Baylis-Hillman reaction	3
1.2.1	Classical mechanism of MBH reaction	3
1.2.2	Recent developments on the mechanism of MBH reaction	5
1.3	Recent evaluation of MBH chemistry	5
1.3.1	Homologous aldol adducts formation under MBH reaction condition	6
1.3.2	Alkyl halides and epoxides as electrophiles in MBH reaction	7
1.3.3	Silylcyclopropene-3-carboxylates as nucleophile in MBH reaction	8
1.3.4	Quinols as nucleophile in MBH reaction	8
1.3.5	Cationic metal complex catalyzed MBH reaction	8
1.3.6	Organo borate catalyzed stereo selective β -substituted MBH reaction	9
1.3.7	Aza-MBH reaction of ferrocene aldehyde	10
1.4	Synthetic application of Morita-Baylis-Hillman adducts and their derivatives	10
1.4.1	Regiospecific allylic amination and dynamic kinetic resolution (DKR)	11
1.4.2	Phosphine catalyzed diastereoselective domino reaction	11
1.4.3	Biscinchona alkaloid catalyzed asymmetric allylic-alkylation (AAA)	12

1.4.4	Synthesis of highly functionalized oxindoles by asymmetric allylic alkylation (AAA)	12
1.4.5	Regio- and stereoselective synthesis of α -dehydro- β -amino esters nitrile	13
1.4.6	Iron catalyzed regioselective nucleophilic α -substitution on MBH adducts	14
1.4.7	Organo catalyzed δ -regioselective nucleophilic substitution	14
1.4.8	Synthesis of six member heterocyclic derivatives	15
1.4.9	Synthesis of seven member heterocyclic derivatives	16
1.5	Application of MBH adducts in natural product synthesis	16
1.5.1	Synthesis of (+)-heliotridine	16
1.5.2	Synthesis of Yuremamine	17
1.6	The Chemistry of Isatin	17
1.7	Isatin appended natural products and structurally important motifs	18
1.7.1	Synthesis of welwitindolinone C isocyanide scaffold	18
1.7.2	Synthesis of spiro- γ -butyrolactone oxindole	19
1.7.3	Synthesis of anti-tubercular active spirothiazolidinone derivatives	19
1.8	Synthesis of MBH adduct of isatin and its synthetic applications	20
1.8.1	Isatin as an electrophile in MBH chemistry	20
1.8.2	Synthesis of enantioenriched MBH adduct of isatin	21
1.8.3	Asymmetric allylic alkylation (AAA) of MBH adduct of isatin	22
1.8.4	Reductive cyclization of MBH adduct of isatin	23
1.8.5	Synthesis of Lactam	23
1.8.6	Synthesis of 3-spirocyclopropane-2-oxindoles from MBH adduct of isatin	24
1.8.7	Synthesis of 3-spiro- α -methylene- γ -butyrolactone-2-oxindoles	24
1.8.8	Synthesis of 3-spiropyrrrolidine-2-oxindole derivatives via azomethine ylide cycloaddition reaction	26

1.8.9	Synthesis of dimerized 3-spirocyclopropane-2-oxindoles from MBH adduct of isatin	27
1.9	Definition of problem	28

Chapter II

A Mild and Efficient CAN Mediated Oxidation of Morita-Baylis-Hillman Adducts of 5-Methyl-*N*-Alkylisatin to 5-Formyl-*N*-Alkylisatin

2.1	Introduction	31
2.2	A brief introduction on Cerium (IV) Ammonium Nitrate (CAN) reagent	32
2.3	CAN mediated synthetic transformations	33
2.3.1	Synthesis of benzimidazole	33
2.3.2	Deprotection of sultam	34
2.3.3	Stoichiometric CAN induced electrophilic substitution of indole	34
2.3.4	Synthesis of Xanthenes	35
2.3.5	<i>N</i> -Methyl activation of MBH adduct of isatin	35
2.4	Miscellaneous transformations	36
2.4.1	Alkoxylation reaction	36
2.4.2	Synthesis of Aminotetralin derivatives	37
2.4.3	CAN induced aromatic side chain oxidation of benzyl derivatives	37
2.5	Objective of the present work	38
2.6	Results and Discussion	39
2.6.1	Preparation of MBH adducts of isatin	39
2.6.1.1	Synthesis of <i>N</i> -alkyl derivatives of isatin	39
2.6.2	CAN mediated side chain oxidation of MBH adducts of 1,5-dimethyl isatin	40
2.6.3	Optimization of aromatic side chain oxidation of MBH adduct of isatin: Effect of solvent and catalyst load	42

2.6.4	Comparison of CAN reagent with other oxidizing reagents	43
2.6.5	Substrates screening for side chain oxidation of oxindole derivative	44
2.6.6	Substrate scope of CAN oxidation with various activated alkene derived MBH adducts of isatin	47
2.6.7	Generality of side chain oxidation of CAN with various <i>N</i> -substituted MBH adduct of isatin	50
2.7	Mechanistic postulates: CAN mediated aromatic side chain oxidation of MBH adduct of isatin	55
2.8	Conclusion	57
2.9	Experimental	58
2.9.1	General considerations	58
2.9.2	General experimental procedure for alkylation of isatin	58
2.9.3	General procedure for the preparation of MBH adducts	58
2.9.4	Characterization of compounds	59
2.9.5	General procedure for CAN oxidation 5-methyl MBH adduct of isatin	59
2.9.6	Characterization of compounds	60
2.9.7	Procedure for protection of 3 ^o -Hydroxyl group of MBH adduct of isatin	63
2.9.8	Characterization of compounds	64
2.2.9	General procedure for CAN oxidation reaction of <i>N</i> -alkylated MBH adduct of isatin	65
2.9.	Procedure for protection of 3 ^o -Hydroxyl group of MBH adduct of isatin	65
2.9.10	Characterization of compounds	65

Chapter III

Synthesis of Highly Functionalized Allene and Dihydrofuran Appended Oxindoles *via* Claisen Rearrangement and Base Induced Cyclization

3.1	Introduction	71
3.1.1	Claisen rearrangement	72
3.2	Types of [3,3]-sigmatropic Claisen rearrangements	74
3.2.1	Carroll rearrangement	74
3.2.2	Johnson-Claisen rearrangement	74
3.2.3	Ireland- Claisen rearrangement	75
3.2.4	Synthesis of enantio-enriched amino acid derivatives <i>via</i> Eschenmoser-Claisen rearrangement	75
3.2.5	Total synthesis of (\pm)-debromoflustramine <i>B</i> and <i>E</i> and (\pm)-debromoflustramide <i>B</i> <i>via</i> Claisen rearrangement	76
3.2.6	Aza-Claisen rearrangement	77
3.2.7	Characteristic reactions of vinyl propargyl ether	78
3.3	Objective of the work	79
3.4	Synthesis of various MBH adduct of substituted isatin	80
3.4.1	Isomerization of MBH adduct of isatin with propargyl alcohol	80
3.4.2	Optimization of propargyl isomerization under microwave irradiation: Synthesis of allyl propargyl ether derivatives	81
3.5	Synthesis of vinyl propargyl ethers from allyl propargyl ethers	84
3.5.1	Generalization of [1,3]-hydride shift	87
3.6	Synthesis of allene appended multi-functional oxindole derivatives <i>via</i> Claisen rearrangement	90
3.6.1	Generality of Claisen rearrangement reactions	93

3.6.2	Mechanistic postulates of Claisen rearrangements	95
3.7	Synthetic application of allene appended oxindole derivatives	96
3.7.1	Differentiation of two geometrical isomers 70a and 70b	101
3.8	Mechanistic postulate of base induced cyclization	102
3.9	Conclusions	103
3.10	Experimental section	104
3.10.1	General considerations	104
3.10.2	Experimental procedure	104
3.10.3	General experimental procedure for Propargyl isomerization (Conventional heating)	104
3.10.4	Microwave irradiation	104
3.10.5	Characterization of new compounds	105
3.10.6	General experimental procedure for allylic isomerization	105
3.10.7	Characterization of new compounds	105
3.10.8	General experimental procedure for Claisen rearrangement	110
3.10.9	Characterization of new compounds	110
3.10.10	Synthesis of dihydrofuran derivatives	116
3.10.11	Characterization of new compounds	116

Chapter IV

Diastereoselective Synthesis of 3-Spirocyclopentene and 3-Spiropyrazole-2-Oxindole Derivatives *via* [3+2]-Annulation Reaction

4.1	Introduction	120
4.2	Synthesis of cyclic and spirocyclic derivatives <i>via</i> annulation strategy	121
4.2.1	Lewis acids promoted [5+2]-annulation	121
4.2.2	Epoxy annulation: reagent vs. kinetic resolution of substrate controlled	122

	reaction	
4.3	Recent reports on phosphorous and sulphur ylide annulation reactions using MBH adducts and their derivatives	123
4.3.1	Phosphine catalyzed cascade [3+2]-cyclization-allylic alkylation and [2+2+1]-annulation	123
4.3.2	Phosphine catalysed [3+N]-annulation reaction	124
4.3.3	Phosphine-catalyzed [4+1]-annulation	125
4.3.4	Phosphine-catalyzed intramolecular [3+2]-cycloaddition	126
4.3.5	Sulphide induced [3+2]-annulation strategy	126
4.3.6	Synthesis of vinyl cyclopropane <i>via</i> sulphur ylide chemistry	127
4.4	Present work	127
4.5	Retrosynthetic analysis	128
4.6	Results and Discussion	128
4.6.1	Preparation of allyl bromide from MBH adduct of isatin	128
4.6.2	Optimization study for the isomerization reaction of MBH adduct with aqueous HBr	129
4.6.3	Distinction of <i>E/Z</i> -isomers 36a/b by ¹ H NMR	130
4.6.4	Isomerization of MBH adduct: Generality of the reaction	131
4.6.5	Synthesis of 3-spirocyclopentene oxindole derivative from allyl bromide of oxindole <i>via</i> phosphine mediated [3+2]-annulation strategy	131
4.6.6	Optimization study: Effect of solvent and base	135
4.6.7	Formation of α -methylene reduced alkene compounds 41a/b	136
4.6.8	Synthesis of spirocyclopentene derivatives <i>via</i> [3+2]-annulation: Generality of the reaction	139
4.6.9	A diastereoselective synthesis of spirocyclopentene: Plausible reaction mechanism	141
4.6.10	Synthesis of 3-spiropyrazole-2-oxindole derivatives from allyl bromide	143

	of oxindole <i>via</i> sulphur ylide [3+2]-annulation reaction	
4.6.11	Diastereoselective synthesis of 3-spiropyrazole-2-oxindole derivatives <i>via</i> [3+2]-annulation: Generality of the reaction	146
4.6.12	Reaction mechanism of the formation of diastereoselective 3- spiropyrazoles-2-oxindole	151
4.7	Conclusions	153
4.8	Experimental part	154
4.8.1	General considerations	154
4.9	General experimental procedure	154
4.9.1	General experimental procedure for the preparation of Morita- Baylis- Hillman adducts of isatin	154
4.9.2	General experimental procedure for the preparation of bromo isomerized Morita-Baylis-Hillman adducts of isatin	154
4.9.3	Spectral data for isomerized MBH adducts	155
4.9.4	General experimental procedure for the preparation of spirocyclopentene derivatives <i>via</i> [3+2]-annulation strategy	155
4.9.5	Characterization of new compounds	156
4.9.6	General experimental procedure for the preparation of spiro pyrazole derivatives	160
4.9.7	Characterization of new compounds	161

Chapter V

Pyridine Core Activation *via* 1, 5-Electrocyclization of Vinyl Pyridinium Ylide Generated from Bromo Isomerized Morita- Baylis-Hillman Adduct of Isatin: Synthesis of 3- Spirodihydroindolizine-2-Oxindoles

5.1	Introduction	169
5.1.1	Electrocyclization Reactions	170

5.2	A literature review on the synthesis of nitrogen heterocyclics and pyridine core activation	172
5.2.1	Synthesis of partially saturated pyrrolopyridines and spiro- β -lactams <i>via</i> pyridine core activation	172
5.2.2	Copper catalyzed [3+2]-annulation <i>via</i> pyridine activation	173
5.2.3	Electrophilic activation of lactam with pyridine	174
5.2.4	Regioselective <i>N</i> -heterocycle activation <i>via</i> 1,5-electrocyclization	174
5.2.5	Pyridine core activation <i>via</i> MBH adduct/ <i>N</i> -alkylation	175
5.2.6	Pyridine core activation <i>via</i> <i>N</i> -alkylation/nucleophilic substitution	176
5.2.7	Synthesis of imidazole derivative <i>via</i> 1,5-electrocyclization	177
5.3	Present work	178
5.4	Retrosynthetic analysis	179
5.5	Results and Discussion	179
5.5.1	Preparation of allyl bromide of oxindole from MBH adduct of isatin	179
5.5.2	Synthesis of 3-spirodihydroindolizine-2-oxindole derivative <i>via</i> 1,5 electrocyclization	180
5.5.3	Optimization study: Effect of solvent and catalyst load	183
5.5.4	Generality of pyridine core activation <i>via</i> 1,5-electrocyclization reaction	184
5.5.5	Substituted pyridine and poly cyclic pyridine core involved 1,5-electrocyclization	189
5.5.6	Limitations of 1, 5-electrocyclization reaction in pyridine derivative with allyl bromide of oxindole	193
5.6	Reaction mechanism of pyridine core activation <i>via</i> 1,5-electrocyclization	194
5.7	Conclusions	196
5.8	Experimental section	197
5.8.1	General remarks	197

5.8.2	General experimental procedure for the preparation of Morita-Baylis-Hillman adducts of isatin	197
5.8.3	General experimental procedure for the preparation of bromo isomerized Morita-Baylis-Hillman adducts of isatin	197
5.8.4	General experimental procedure for 1, 5-electrocyclization	198
5.8.5	Characterization of new Compounds	198
	Bibliography and References	207
	Summary	238
	List of Publications	241

List of Tables

2.1	Optimization of CAN oxidation of 5-methyl MBH adduct of isatin 31	43
2.2	Comparative studies between CAN and other oxidative reagents for side chain oxidation of compound 31	44
2.3	Generality of CAN oxidation with various activated alkene derived MBH adducts	47
2.4	Generality of the reaction with various N-alkylated MBH adducts	50
3.1	Optimization of propargyl isomerization under microwave reaction condition	82
3.2	Synthesis of vinyl propargyl ethers from allyl propargyl ethers	87
3.3	Generality of the Claisen rearrangement reactions	94
4.1	Optimization of allyl bromide of oxindole derivative synthesis	130
4.2	Optimization of phosphine catalyzed [3+2]-annulation reaction	136
4.3	Generality of phosphine catalyzed [3+2] annulation	139
4.4	Diastereoselective synthesis of 3-spiropyrazole-2-oxindole derivatives	147
5.1	Woodward-Hoffmann rule for electrocyclization reaction	170
5.2	Optimization of 1,5-electrocyclization reaction with allyl bromide of oxindole	184
5.3	Generality of 1,5-electrocyclization with a various allyl bromide of oxindole derivatives	185
5.4	Activation of pyridine derivatives core via 1,5-electrocyclization	190

List of figures

1.1	A typical MBH adduct and reactive sites	1
2.1	Structure of Cerium (IV) Ammonium Nitrate (CAN) reagent	32
2.2	¹ H NMR Spectrum of 5-formyl MBH adduct of isatin compound 32	41
2.3	¹³ C NMR Spectrum of 5-formylMBH adduct of isatin 32	42
2.4	Substrate screening of oxindole derivatives for aromatic side chain oxidation	44
2.5	Feasible resonance structure of MBH derivatives	46
2.6	¹ H NMR Spectrum of compound 50	49
2.7	¹³ C NMR Spectrum of compound 50	49
2.8	¹ H NMR Spectrum of compound 66	52
2.9	¹³ C NMR Spectrum of compound 66	52
2.10	¹ H NMR Spectrum of compounds 68 and 69	54
2.11	¹³ C NMR Spectrum of compounds 68 and 69	54
2.12	FAB Mass spectrum of compounds 68 and 69	55
3.1	General representation of allyl vinyl analogue of Claisen rearrangement reaction	72
3.2	Pictorial representation of Claisen rearrangement transition states and orbital interactions	73
3.3	Various MBH adducts of substituted isatin	80
3.4	¹ H NMR Spectrum of propargyl isomerized compound 43	83
3.5	¹³ C NMR Spectrum of propargyl isomerized compound 43	83
3.6	¹ H NMR Spectrum of compound 44	84
3.7	¹³ C NMR Spectrum of compound 44	86

3.8	FAB-Mass spectrum of compound 44	86
3.9	¹ H NMR Spectrum of compound 55	89
3.10	¹³ C NMR Spectrum of compound 55	89
3.11	FAB-Mass spectrum of compound 55	90
3.12	¹ H NMR Spectrum of compound 61	92
3.13	¹³ C NMR Spectrum of compound 61	92
3.14	FAB-Mass spectrum of compound 61	93
3.15	¹ H NMR spectrum of compound 70a	98
3.16	¹³ C NMR spectrum of compound 70a	98
3.17	FAB-Mass spectrum of compound 70a	99
3.18	¹ H NMR Spectrum of compound 70b	100
3.19	¹³ C NMR Spectrum of compound 70b	100
3.20	NOE correlation of compounds 70a and 70b	101
3.21	NOE spectrum of compound 70b	101
4.1	Structurally unique spirocyclic frameworks	120
4.2	Spirooxindole natural product isolated from <i>Aspergillus fumigates</i>	121
4.3	Retrosynthetic strategy for spirocyclic oxindole derivatives	128
4.4	Differentiation of E- and Z-isomers 36 a/b by ¹ H NMR spectrum	130
4.5	¹ H NMR Spectrum of spirocyclopentene derivative 40	132
4.6	¹ H- ¹ H-COSY Spectrum of spirocyclopentene derivative 40	133
4.7	¹³ C NMR Spectrum of spirocyclopentene derivative 40	134
4.8	DEPT-135 Spectrum of spirocyclopentene derivative 40	134

4.9	Mass spectrum of spirocyclic compound 40	135
4.10	¹ H NMR Spectrum of compound 41a E-isomer.	137
4.11	¹ H NMR Spectrum of compound 41b Z- isomer	138
4.12	¹³ C NMR Spectrum of compound 41b Z- isomer	138
4.13	ORTEP diagram of spirocyclopentene compound 46	141
4.14	¹ H NMR Spectrum of spiropyrazole compound 53	144
4.15	¹³ C NMR Spectrum of spiropyrazole compound 53	145
4.16	Mass spectrum of compound 53	146
4.17	¹ H NMR Spectrum of spiropyrazole compound 61	149
4.18	¹³ C NMR Spectrum of pyrazole compound 61	150
4.19	Mass spectrum compound 61	150
4.20	ORTEP diagram of compound 61	151
5.1	Thermal and photochemical electrocyclization of 1,3-disubstituted butadiene with molecular orbital energy diagram (4n system).	171
5.2	Thermal and photochemical cyclization of 5,6-dimethylcyclohexa-1,3-diene with molecular orbital energy diagram (4n+2 system)	172
5.3	Natural products with 3-Spirooxindole core structure	178
5.4	Retrosynthetic analysis of pyridine activation	179
5.5	¹ H NMR Spectrum of compound 42	181
5.6	¹ H- ¹ H-COSY Spectrum of compound 42 (Expanded region δ 4-8)	181
5.7	¹³ C NMR Spectrum of compound 42	182
5.8	Mass spectrum of compound 42	183

ABBREVIATIONS

AcOH	: acetic acid	Hz	: hertz
Ar	: argon	IR	: infra red
AIBN	: azo bis isobutyro nitrile	J	: coupling constant
AMY	: azomethine ylide	LUMO	: lowest unoccupied molecular orbital
CSA	: camphor sulphonic acid	m	: multiplet
d	: doublet	MBH	: Morita-Baylis-Hillman
dd	: doublet of doublet	Me	: methyl
DABCO	: 1,4-diazabicyclo[2.2.2]-octane	mg	: milligram
DBU	: 1,8-diazabicyclo[5.4.0]undec-7-ene	mL	: milliliter
DEPT	: distortionless enhancement by polarization transfer	MS	: molecular sieves
DMAP	: dimethylamino pyridine	MVK	: methyl vinyl ketone
DMDO	: dimethyl dioxirane	NMR	: nuclear magnetic resonance
DMSO	: dimethyl sulphoxide	<i>p</i>	: para
DMF	: dimethyl formamide	Ph	: phenyl
EDG	: electron donating group	PEG	: poly ethelene glycol
Et	: ethyl	PTSA	: <i>para</i> -toluene sulphonic acid
FAB	: fast atom bombardment	ppm	: parts per million
HOMO	: highest occupied molecular orbital	q	: quartet
		rt	: room temperature
		s	: singlet
		t	: triplet

TMSOTf : Trimethylsilyl triflate
TMSI : Trimethylsilyl iodide
THP : Tetrahydro pyranyl
THF : tetrahydrofuran
TLC : thin layer chromatography
TMS : tetramethylsilyl
Tert : tertiary
UV : ultra violet
COSY : correlation spectroscopy
Ph : phenyl

PREFACE

Among the various carbon-carbon bond forming reactions, Morita-Baylis-Hillman (MBH) reactions play an important role in synthetic chemistry, since they serve as versatile synthons in the construction of complex molecular frameworks including biologically important drugs, natural products. The Particular charm of the reaction is its capability to produce a huge reservoir of diverse classes of densely functionalized molecules in an atom economic fashion. Also we can able to fine-tune the chiral center in the case of a prochiral electrophile thus offering challenges and opportunities for developing its asymmetric version. Hence, the MBH adducts are having proximity of functional groups, these offered the highly useful synthons in a number of synthetic processes.

Due to the excellent substrate scope of MBH reactions, there were a number of MBH counterparts were reported as electrophiles and nucleophiles in this reaction. Biologically and pharmacologically important isatin has very recently been incorporated as a reactive electrophile in classical MBH chemistry [Garden, S. J. *et al.* 2002; Chung, Y. M. *et al.* 2002] which furnished oxindole appended MBH adduct. Until 2006 this valuable synthetic building blocks remain unexplored. In 2006, we have first utilized this functionalized molecule as starting material to synthesize the bioactive γ -butyrolactone with sodium borohydride *via* reductive cyclization as a key step. The same strategy has explored to synthesize tricyclic lactam from MBH adduct of isatin *via* benzylamine induced ring opening condensation cyclization instead hydride ring opening reaction by Kim and co-workers.

The MBH adducts have further proved to be valuable counterparts in dipolar cycloaddition reactions. Recently we have reported synthesis of a variety oxindole appended spiro and dispirocyclic derivatives utilising MBH adduct of isatin as dipolarophile against various azomethine ylides in [3+2] cycloaddition reaction. Very recently, two separate groups [Peddibhotla, S. 2009; and Peng, J. *et al.* 2010] have reported asymmetric version of oxindole derivatives synthesis *via* reductive cyclization and chemoselective functionalization followed by base induced spiro cyclization. However, the literature investigation showed that functionalization of MBH adducts of isatin and its synthetic utility is still in its infancy. Inspired by the setting, we undertook a

Chapter I

Recent Developments on Morita-Baylis-Hillman Reaction

Chapter I

Recent Developments on Morita-Baylis-Hillman Reaction

1.1 General introduction:

To develop a simple, convenient, highly chemo- and diastereoselective methodologies for the synthesis of organic compounds have been, and continue to be, a challenging endeavour in front of synthetic chemists, even though the construction of complex molecular frameworks is a simple carbon-carbon bond forming reaction and/or small functional group transformations. To address these goals, a number of groups have been working on their interested research areas to craft a short, efficient method to construct a variety of selective C-C and C-X bond forming reactions. There are several carbon-carbon bond forming reactions discovered and their applications are explored towards value added compound synthesis. Among them, the Morita-Baylis-Hillman reactions (MBH) also play a valuable contribution to construct a variety of C-C and C-X bond forming reaction towards bio-active molecule and natural products synthesis. The main features of this reaction are as follows: (1) It is a three-component involving carbon-carbon bond forming reaction providing diverse products on the basis of substrates selection with atom economic mode. (2) This creates a chiral center in the case of a prochiral electrophile and thus offering challenging opportunities for developing its asymmetric version. (3) Since the MBH adducts are densely functionalized molecules due to its proximity of functional groups, these adducts are highly useful synthons in a number of synthetic transformations. These advantages are projecting the MBH reactions as unique and central research theme for a number of research groups in recent past years (Figure 1.1).

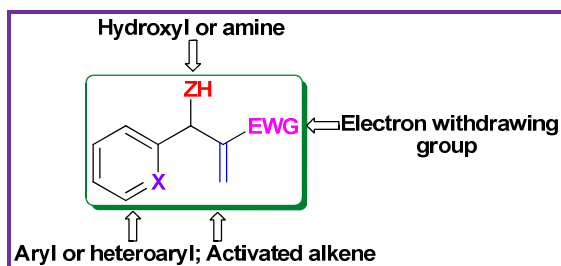
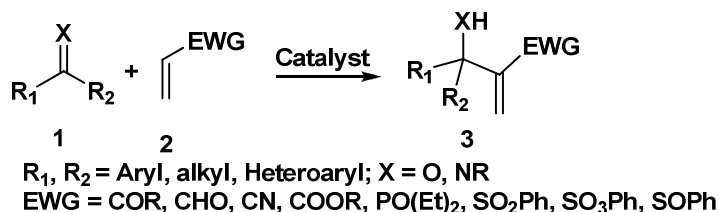


Figure 1.1: A typical MBH adduct and reactive sites.

1.2 The Morita-Baylis-Hillman reaction:

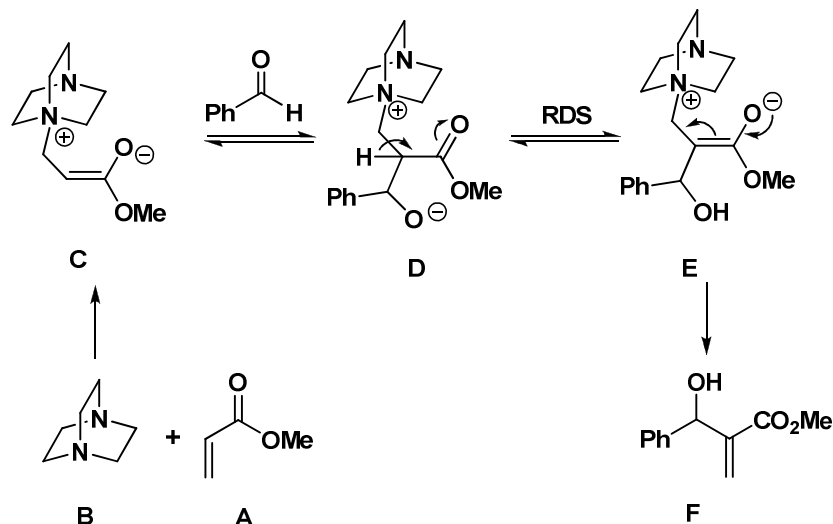
Ever since the discovery of the reaction of an electrophile **1** with α -position of an activated alkene **2** that catalyzed by trialkylphosphine or a tertiary amine, usually diazobicyclo[2.2.2]-octane (DABCO), by Baylis and Hillman in 1972, organic practitioners are looking at the various synthetic aspects of the reaction (Scheme 1.1) [Baylis, A. B. *et al.* 1972; Drewes, S. E. *et al.* 1988; Mortia, K. *et al.* 1968]. Named after that, the MBH reaction has become a powerful tool for the atom-economical construction of C-C bond, giving α -methylene- β -hydroxyl carbonyl or α -methylene- β -amino carbonyl derivatives **3**, which comprises a contiguous assembly of three different functional groups. Properly activated imines can also participate in this reaction and the reaction is called *aza*-MBH reaction [Declerck, V. *et al.* 2009].



Scheme 1.1: Morita-Baylis-Hillman reaction /Aza-MBH reaction

1.2.1 Classical mechanism of MBH reaction:

According to the proposal of Hill and Isaacs, the reaction was initiated by amine with methyl acrylate (activated olefin) and benzaldehyde (electrophile) to form MBH adduct under catalytic influence of DABCO as a model case. It is believed to proceed through the Michael initiated addition–elimination sequence (Scheme 1.2) [Basavaiah, D. *et al.* 2003, 2010; Singh, V. *et al.* 2008]. In the first step, this catalytic cycle involves the Michael-type nucleophilic addition of activated alkene **A** (methyl acrylate) with tertiary amine **B** to produce a Zwitterionic enolate **C**. The enolate **C** can make an Aldol type nucleophilic attack on to the aldehyde and generates another Zwitterion intermediate **D**, subsequent proton migration and electron resettlement simultaneously trigger the catalyst and MBH adduct **F**.

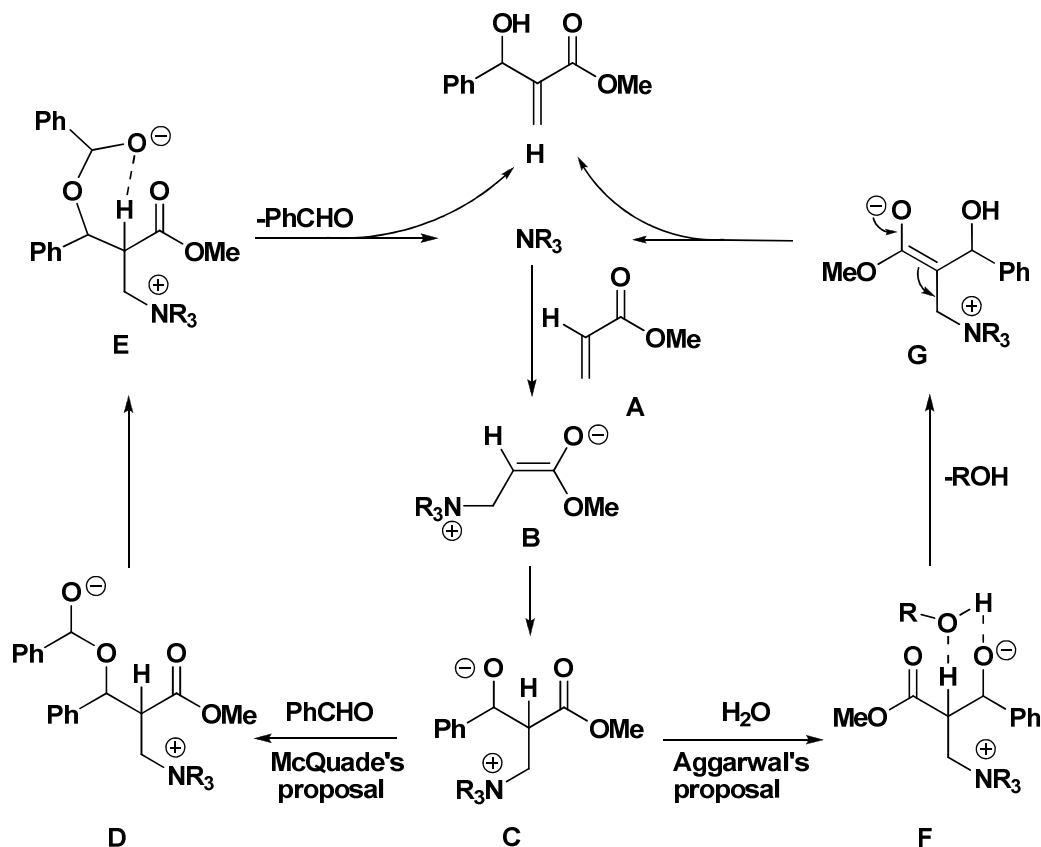


Scheme 1.2: Mechanism of MBH reaction.

1.2.2 Recent developments on the mechanism of MBH reaction:

Very first, Hill and co-workers proposed the existing and widely accepted mechanism of the MBH adduct. According to the mechanism, the proton 1,3-shift was the rate-determining step (RDS) [Hill, J. S. *et al.* 1986; 1990]. With this idea, they attempted to shed light more on the reaction mechanism through kinetic studies and proposed that the RDS was assumed to be the carbon-carbon bond formation in the aldol type reaction between the Zwitterionic amine-acrylate adducts **C** and an aldehyde molecule (Scheme 1.3). This proposal was further supported by subsequent independent investigations including the interception of all key intermediates using electron spray ionization mass, tandem mass spectrometry [Santos, L. S. *et al.* 2004] and X-ray analysis of one the intermediates of the catalytic cycle [Drewes, E. *et al.* 1993]. However, recently two separate groups McQuade lead by [Price, K. E. *et al.* 2005^a; 2005^b] and Aggarwal [Aggarwal, V. K. *et al.* 2005] independently reinvestigated the kinetics of the MBH reaction by means of kinetic isotope effect (KIE) employing an acrylate precursor and proposed the RDS is the proton transfer step **E** and **F** (Scheme 1.3). The above conclusion has been arrived due to the first-order dependence on solvent could be interpreted as a medium effect or as a molecular (aldehyde) interaction (Scheme 1.3). The first-order dependence of solvent demonstrated that the rate increase was a medium effect by which the ionic transition states received stabilized by polar solvents. Very recently, Cantillo *et. al.*, reported that the experimental determination chemical kinetic

and theoretical calculation of thermodynamics of MBH reaction using the M06-2X computational method, which further supported the McQuade and Aggarwal proposal [Cantillo, D. *et al.* 2010].



Scheme 1.3: *New interpretation of mechanism of MBH reaction.*

Finally, the recent studies all together concluded that the 1,3-shift proton could be the rate-determining step (RDS) which was assisted and stabilized either by polar protic solvent **F** or by another molecule of aldehyde **D** in an aprotic medium *via* the ionic transition states.

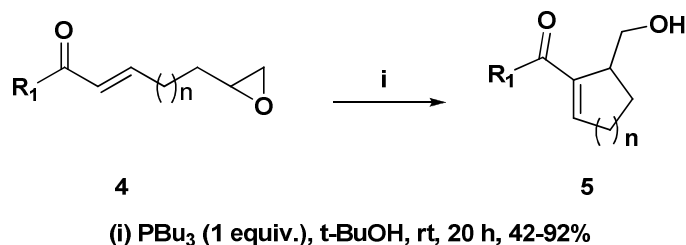
1.3 Recent evaluation of MBH chemistry:

The fascinating chemistry of MBH reaction has inspired both the synthetic and theoretical aspect of the chemists. Consequently, several leading organic chemists all over the world have been working on various directions of the MBH reaction [Masson, G. *et al.* 2007; Basavaiah, D. *et al.* 2007]. Among them, the recent growth on the MBH reaction particularly screening of new classes electrophiles, nucleophiles and catalysts in

adduct formation and various synthetic transformation of MBH adducts have been dealt in the following sections.

1.3.1 Homologous aldol adducts formation under MBH reaction condition:

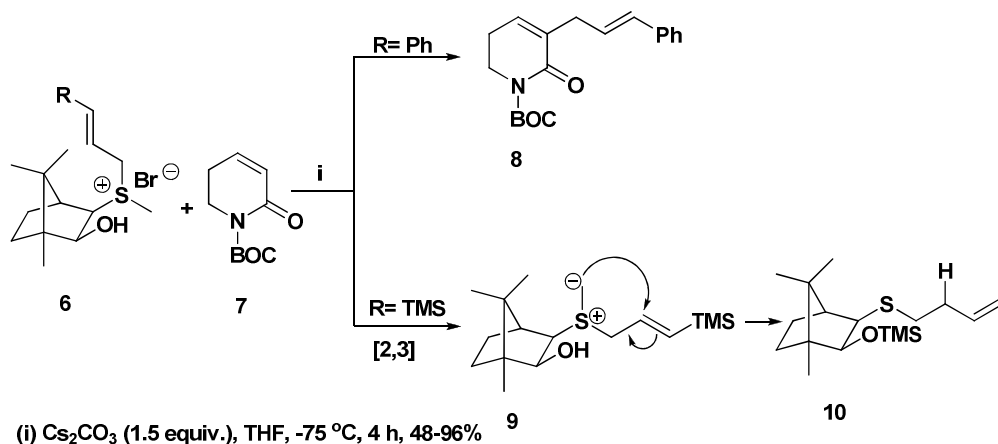
Epoxide ring opening is an essential posture of organic synthesis and also plays a crucial role to construct a diverse carbon–carbon and carbon–oxygen bonds forming reactions [Bonney, K. J. *et al.* 2011; Morten, C. J. *et al.* 2009; Byers, J. A. *et al.* 2009]. Krafft and co-workers have described an unprecedented ring opening of epoxide **4** to afford homologous aldol adduct **5** under MBH reaction condition [Krafft, M. E. *et al.* 2006^d]. The formation of observed homologous aldol adduct **5** from epoxy enone **4** reveals that the phosphine induced Zwitterionic enolate preferably undergoes intramolecular endo mode ring opening with epoxide under MBH reaction condition (Scheme 1.4).



Scheme 1.4: *Synthesis of homologous aldol adduct via MBH reaction.*

1.3.2 Alkyl halides and epoxides as electrophiles in MBH reaction:

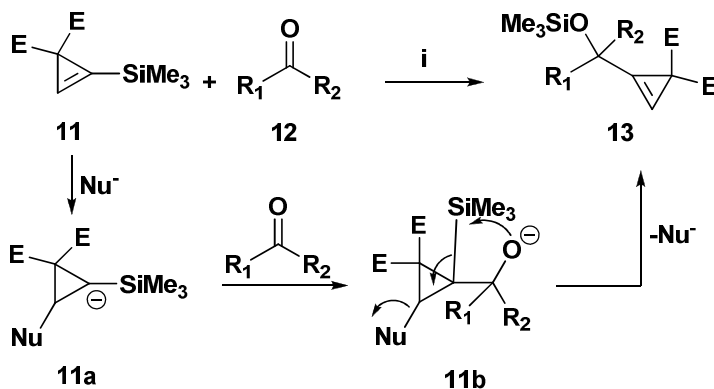
The poor reactive electrophiles substrates such as alkyl halide and epoxide [Basavaiah, D. *et al.* 2001; 2002] involve in MBH reaction **8** with weak nucleophile lactam **7** [Krafft, M. E. *et al.* 2005;^a 2005;^b 2006^c] under hydroxyl sulphide catalyzed basic condition [del Villar, I. S. *et al.* 2010]. The observed selective formation of MBH adduct competing with cyclopropanation **10** under basic reaction condition was emphasised. The formation of MBH product was controlled by the judicial selection of substrates (R = Ph) which overcome the competing cyclopropanation (Scheme 1.5).



Scheme 1.5: MBH reaction vs sigmatropic shift.

1.3.3 Silylcyclopropene-3-carboxylates as nucleophile in MBH reaction:

Sila-MBH adduct have been reported from readily available 1-silylcyclopropene-3-carboxylate **11** with aldehyde or ketone **12** in the presence of phosphine catalyst under room temperature [Chuprakov, S. *et al.* 2007]. This new protocol allowed to synthesize 1-(silyloxymethyl) cyclopropane derivative **13**, which does not easily obtainable through existing methods. The combined effect of highly reactive double bond of cyclopropane and the ability of stabilization of α -silylcyclopropyl α -carbanion **11a** generated from the nucleophilic addition (catalyst) of 1-silylcyclopropene was the driving force for the adduct formation **13** (Scheme 1.6).



E = CO_2Me , CO_2Et ; R_1 = aryl, hetero aryl, aliphatic
 R_2 = H, aryl, aliphatic

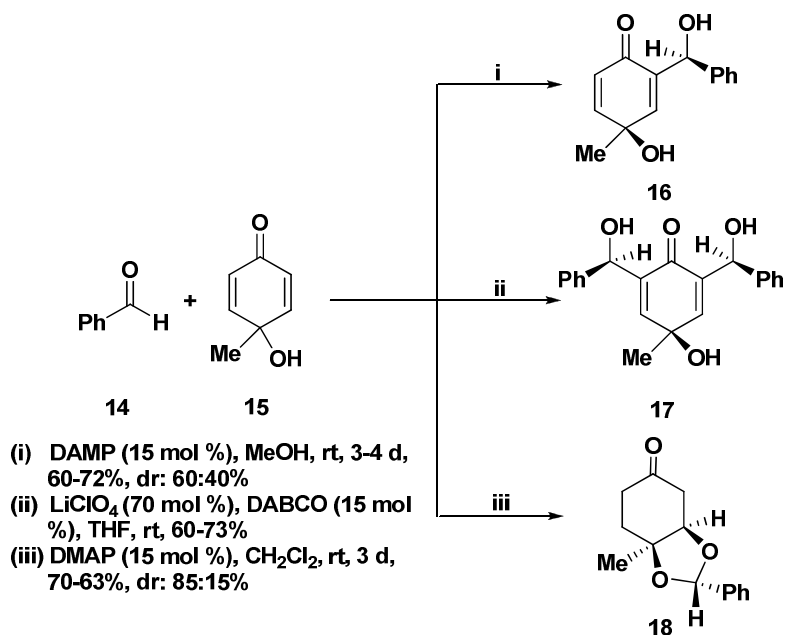
(i) TTMPP (5 mol %), dioxane, rt

Scheme 1.6: Preparation of sila-MBH adduct.

The formation of sila-MBH adduct was rationalized mechanistically where the intermediate **11a** underwent an addition with electrophile **12** to produce alkoxide **11b** followed by 1,3-Brook rearrangement/elimination cascade reaction.

1.3.4 Quinols as nucleophile in MBH reaction:

Like 1-silylcyclopropene-3-carboxylates, Carreño and co-workers have reported the synthesis of mono **16**, bis-MBH adduct **17** and cyclic ketal **18** compounds from *p*-methyl quinols as Michael acceptor with aromatic aldehydes under the MBH reaction condition [Redondo, M. C. *et al.* 2010]. The formation of all three products was preceded *via* a domino intramolecular oxa-Michael/aldol condensation/elimination, instead of the commonly accepted MBH reaction mechanism. The formation of diverse set of compound from *p*-methyl quinols depends on the catalyst system, solvent and additives used in the reaction (Scheme 1.7).

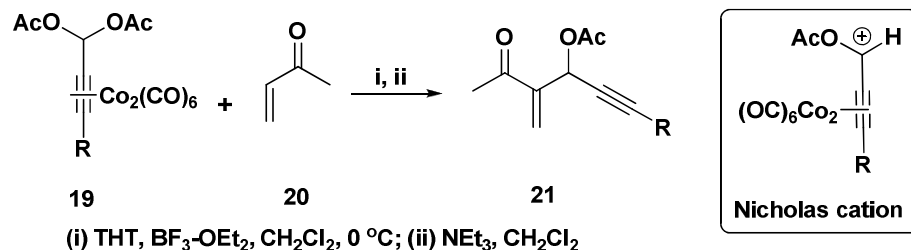


Scheme 1.7: Synthesis of MBH adducts from *p*-methyl quinol as nucleophile.

1.3.5 Cationic metal complex catalyzed MBH reaction:

A number of electrophilic components of MBH reaction have already been explored and yet some new variants of MBH components are seeking scheduled. Recently, Krafft *et al.* reported one pot synthesis of acyl protected MBH adduct achieved from dicobalt hexacarbonyl complexed acetylenic acetal **19** as electrophile with methyl vinyl ketone (MVK) **20** and Lewis acid as catalytic system [Krafft, M. E. *et al.* 2011].

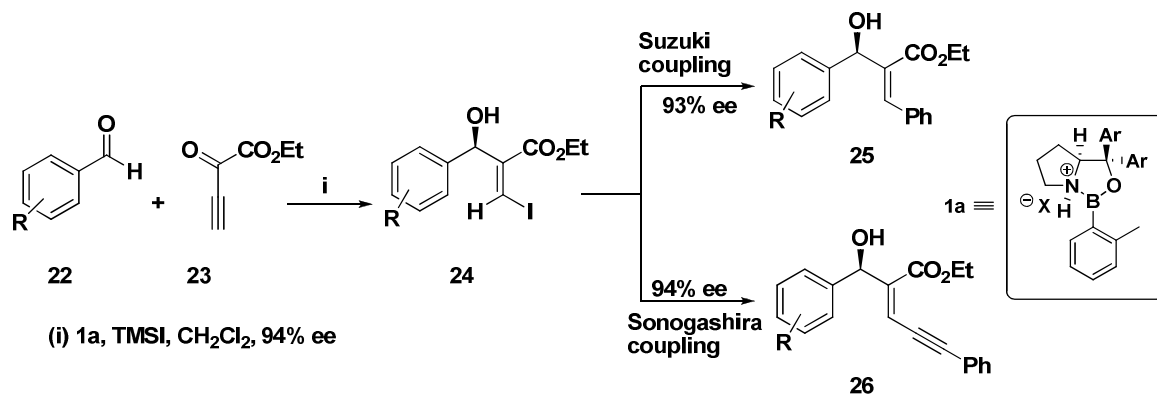
The metal stabilized cationic intermediate was known as Nicholas cation generated from *in-situ* reaction between dicobalthexacarbonyl alkynes complex with Lewis acid. This Nicholas cation can undergo intermolecular MBH reaction with activated alkene **20** and provided one pot acyl protected MBH adduct **21** (Scheme 1.8).



Scheme 1.8: Synthesis of MBH adduct from Nicholas cation as electrophiles.

1.3.6 Organo borate catalyzed stereo selective β -substituted MBH reaction:

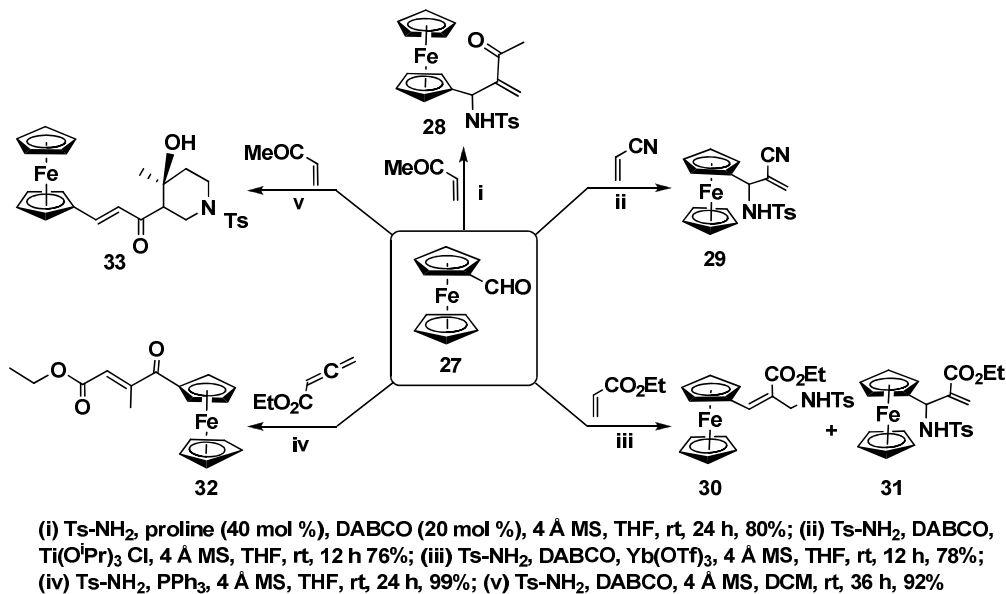
Stereoselective synthesis of β -substituted MBH derivatives is a challenging task [Perez, R. *et al.* 2006; Kim, J. M. *et al.* 2008] and Ruy and co-workers achieved it *via* organoborate salt catalyzed reaction (Scheme 1.9). A highly enantio-enriched (*Z*)- β -iodo derivative **24** was synthesized from a three-component coupling reaction between an aldehyde **22**, ethyl propiolate **23**, and trimethyl silyl iodide (TMSI) in the presence of organo-borate as catalyst [Senapati, B. K. *et al.* 2009]. The observed geometrical isomer (*Z*-isomer) and absolute configuration was assisted by a pentacyclic coordinated transition state of the catalyst **1a** during the aldol reaction between trimethylsilyl β -iodo allenolate and aldehyde.



Scheme 1.9: Synthesis of β -substituted MBH derivatives using organoborate catalyst.

1.3.7 Aza-MBH reaction of ferrocene aldehyde:

Previously, we have proven that ferrocene carboxaldehyde **27** can act as a counterpart electrophile to synthesize simple MBH adduct and can be stereoselectively functionalized *via* isomerization reaction [Shanmugam, P. *et al.* 2007^a; 2009]. Recently, our group have explored miscellaneous ferrocenyl derivatives from ferrocene carboxaldehyde, tosylamine and various activated alkenes under aza-MBH reaction condition [Madhavan, S. *et al.* 2011]. The activated alkene dependent products such as piperidine derivative **33**, β -amino acid residues **30** and **31** and γ -ketoester derivative **32** were observed from ferrocene carboxaldehyde by the aza-MBH reactions with various activated alkenes. Interestingly, the methyl vinyl ketone (MVK) has led to an unexpected diastereoselective ferrocenyl piperidine derivative **33** *via* domino aza- Michael/double Aldol pathway. The usual aza-MBH product **28** with MVK has also been achieved by judicious selection of catalyst and reaction condition (Scheme 1.10).



Scheme 1.10: Synthesis of miscellaneous ferrocene derivatives via aza-MBH reaction of ferrocene aldehyde.

1.4 Synthetic application of Morita-Baylis-Hillman adducts and their derivatives:

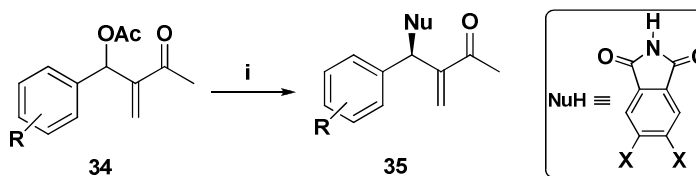
MBH adducts have been proved as versatile starting materials toward a number synthetic transformation, heterocycles synthesis and value added total synthesis. In the recent years, the MBH adducts and their derivatives are mainly focusing on the regio-

and stereoselective synthetic transformation and enantiomerically enriched heterocycle synthesis *via* organo catalytic methods. Hence, the following part of the introduction deals with the recent developments on the regio- and stereoselective synthetic transformation and natural product synthesis using MBH adducts and their derivatives.

1.4.1 Regiospecific allylic amination and dynamic kinetic resolution (DKR):

Dynamic kinetic resolution is a method to access stereospecific products from the racemic starting materials in a particular reaction condition without any loss of the yield [Jurkauskas, V. *et al.* 2002; Lapierre, A. J. B. *et al.* 2007; Cho, C.-W. *et al.* 2004] Stereoselective and regiospecific allylic amination was enabled from chiral racemic MBH adduct **34** *via* chiral phosphine catalysis [Cho, C.-W. *et al.* 2004].

The observed selectivity of product **35** explained by the generation of an electrophile-nucleophile ion pair, presumably suppresses direct nucleophile addition which led to the less substituted enone moiety of MBH acetate. The allylic amination with up to 56% ee was achieved *via* deracemization of racemic MBH acetate **34**, using 4,5-dichlorophthalimide as pro-nucleophile and commercially available phosphine catalyst (*R*)-Cl-MeO-BIPHEP (Scheme 1.11).

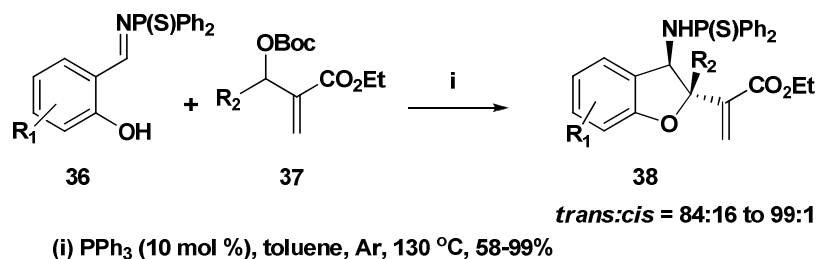


(i) (*R*)-Cl-MeO-BIPHEP, NuH (2 equiv.), THF, 56-80%, 56% ee

Scheme 1.11: Stereo- and regioselective allylic amination of MBH adduct.

1.4.2 Phosphine catalyzed diastereoselective domino reaction:

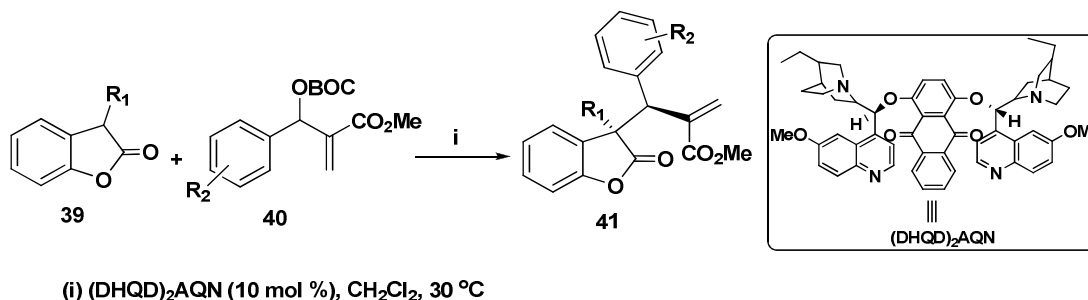
Modified allyl MBH derivatives have been used as versatile C3 synthon for a number of [3+2], [3+3], [3+6] and [3+4]-annulation reactions [Du, Y. *et al.* 2003; 2005; Ye, L.-W. *et al.* 2007; 2008; Zheng, S. *et al.* 2008; 2009^a; 2009^b]. The modified allylic carbonate **37** serve as a new kind of 1,1-dipole with salicyl *N*-thiophosphyne imines **36** under phosphine catalyst and afforded highly substituted diastereoselective *trans*-2,3-dihydrobenzofuran **38** skeleton [Xie, P. *et al.* 2010] (Scheme 1.12).



Scheme 1.12: Phosphine catalyzed diastereoselective synthesis of *trans*-2,3-dihydrobenzofuran

1.4.3 Biscinchona alkaloid catalyzed asymmetric allylic-alkylation (AAA):

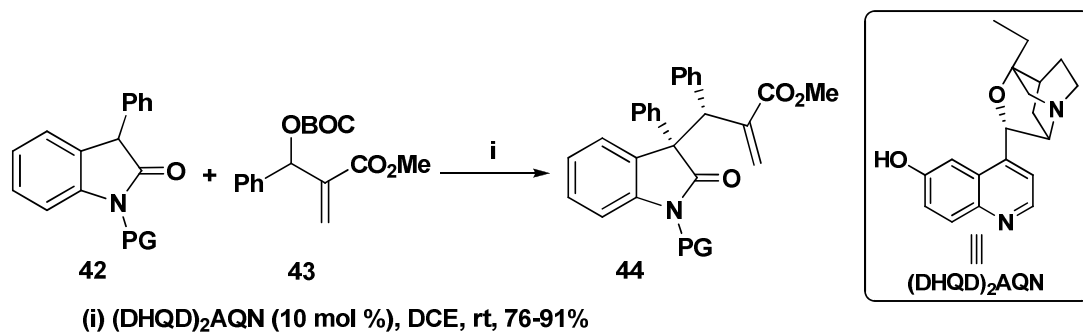
Recently, Cheng and co-workers described a Biscinchona alkaloid induced asymmetric allylic-alkylation (AAA) reaction between the benzofuran-2(3H)-one **39** as pro-nucleophile and modified MBH carbonate **40** as electrophiles [Liu, C. *et al.* 2011]. The observed transformation has been explained where the MBH adduct underwent nucleophilic substitution with *in-situ* generated reactive enolate by means of deprotonation of methine at C3 position of 3-substituted benzofuran-2(3H)-one under chiral amine base (Scheme 1.13).



Scheme 1.13: Enantioselective synthesis of homoallylic benzofuran derivatives.

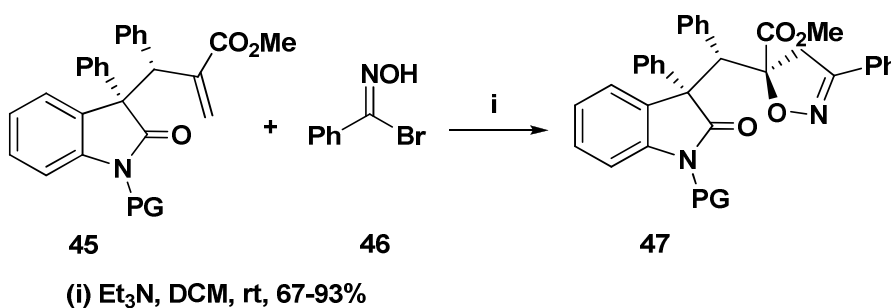
1.4.4 Synthesis of highly functionalized oxindoles by asymmetric allylic alkylation (AAA):

Cinchona alkaloid induced asymmetric C3 allylic alkylated compound **44** has been synthesized by the reaction between modified MBH carbonate **43** with achiral oxindole moiety **42** [Jiang, K. *et al.* 2009] (Scheme 1.14).



Scheme 1.14: Synthesis of enantioselective homoallylic oxindole derivatives.

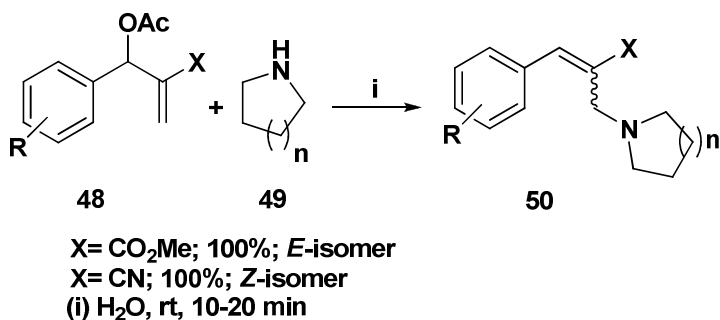
In order to increase molecular complexity, the compound **44** has further subjected to [3+2]-cycloaddition with *in-situ* generated nitric-oxide and afforded enantioenriched oxindole derivative **47** (Scheme 1.15).



Scheme 1.15: Synthesis of highly substituted enantioenriched oxindole derivatives.

1.4.5 Regio- and stereoselective synthesis of α -dehydro- β -amino esters nitrile:

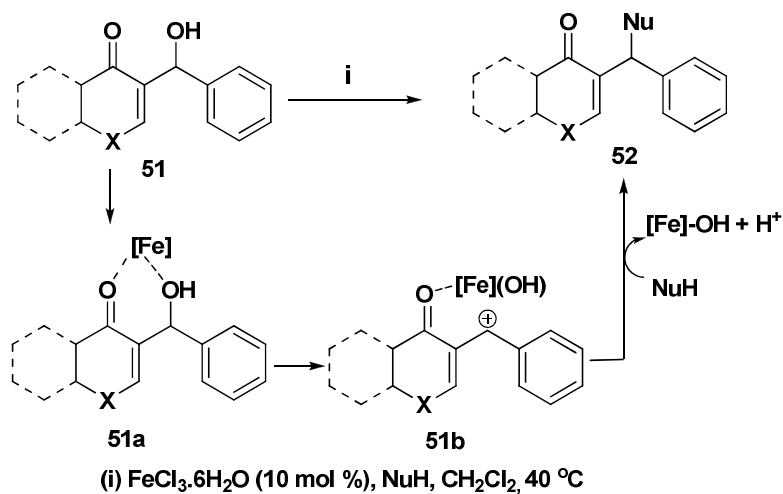
Ghosh, *et al.* reported a mild and efficient regioselective synthesis α -dehydro- β -amino ester and nitrile derivative **50** from modified MBH adduct **48** in water medium [Ghosh, S. *et al.* 2009]. The regiospecific γ -addition furnished with stereoselective (*E*)-isomer from MBH adducts bearing carboxylic ester moiety and (*Z*)-isomers from MBH adduct bearing nitrile functionality with excellent yield. This simple reaction has been tolerated with a variety of amines and with excellent regio- and stereoselectivity (Scheme 1.16).



Scheme 1.16: Synthesis of regio- and stereoselective β -amino ester.

1.4.6 Iron catalyzed regioselective nucleophilic α -substitution on MBH adducts:

A stoichiometric Iron-catalyzed α -regioselective nucleophilic substitution reaction was reported for the MBH adduct **51** with structurally diverse set of pro-nucleophiles including alcohols, 1,3-dicarbonyl compounds, sulfamates and thiols under moisture-free reaction condition in excellent yields [Zhang, X. *et al.* 2009](Scheme 1.17). The observed selectivity has been explained as Iron forms a coordination complex **51a** which subsequently generate carbocation **51b** by the elimination of hydroxyl group. The generated carbocation **51b** underwent nucleophilic attack and protodemetalation of [Fe]-OH delivers the α -substituted MBH compound **52** and the catalyst.

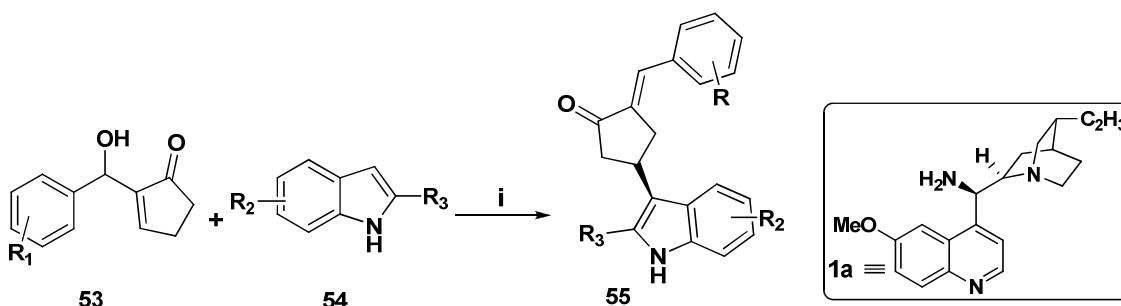


Scheme 1.17: Regioselective nucleophile substitution of MBH adducts.

1.4.7 Organo catalyzed δ -regioselective nucleophilic substitution:

Recently, a direct enantioselective δ -nucleophilic substitution of MBH adduct was reported by Qiao, and co-workers by the reaction between cyclic MBH adduct **53**

and indole **54** under the combined catalytic influence of organo-catalyst and Brønsted acid [Qiao, Z. *et al.* 2010]. This synthetic protocol has furnished exclusive enantioenriched δ -regioselective product **55** up to 93% ee. The observed regioselectivity can be explained by the iminium ion generated from the cyclic enone and organo catalyst **1a** which also assisted dehydration of allylic alcohol and addition of a carbon nucleophile to the unsaturated unit of **53**. Brønsted acid played a dual role to assist the formation of iminium ion and removal of OH group in the MBH adducts (Scheme 1.18).

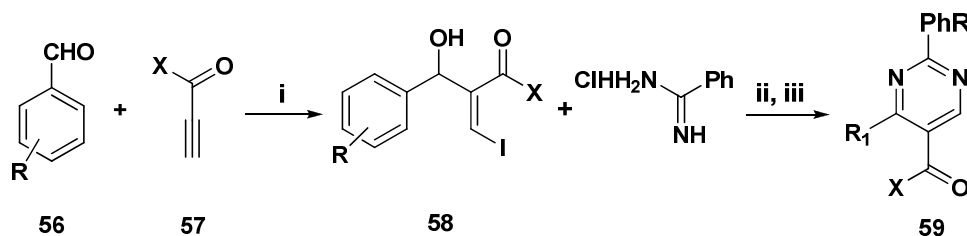


(i) **1a** (20 mol %), TFA (40 mol %), THF (1:1), 5 days, 30 °C

Scheme 1.18: Synthesis of δ -regio-selective nucleophilic substituted MBH adducts.

1.4.8 Synthesis of six member heterocyclic derivatives:

Pyrimidine and their derivatives have been found as constitutional core for many drug molecules. This tri-substituted pyrimidine derivative **59** was synthesized by the reaction of *in-situ* generated ketone from β -iodo substituted MBH derivatives **58** by Dess-Martin periodinane oxidation with various amidines [Sharma, V. *et al.* 2010]. The β -iodo derivatives **58** was synthesized by means of magnesium iodide mediated reaction between aryl aldehyde **56** and propiolate derivative **57** (Scheme 1.19).

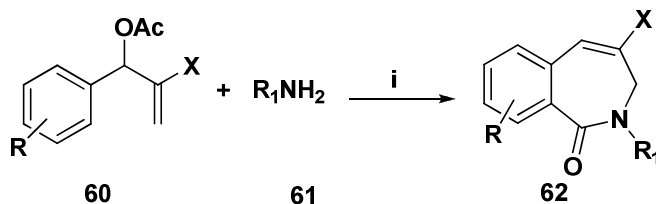


(i) MgI_2 , CH_2Cl_2 ; (ii) Dess-Martin periodinane
(iii) TEA, EtOH

Scheme 1.19: Synthesis of 2,5,6- tri-substituted pyrimidine derivatives from MBH adduct.

1.4.9 Synthesis of seven member heterocyclic derivatives:

A number of biologically important natural and un-natural benzazepine derivative **62** has been synthesized from the modified MBH adduct **60** with a various amines **61** using palladium catalyst one-pot sequential amination followed by intramolecular carbonylation as a key step [Cao, H. *et al.* 2011] (Scheme 1.20).



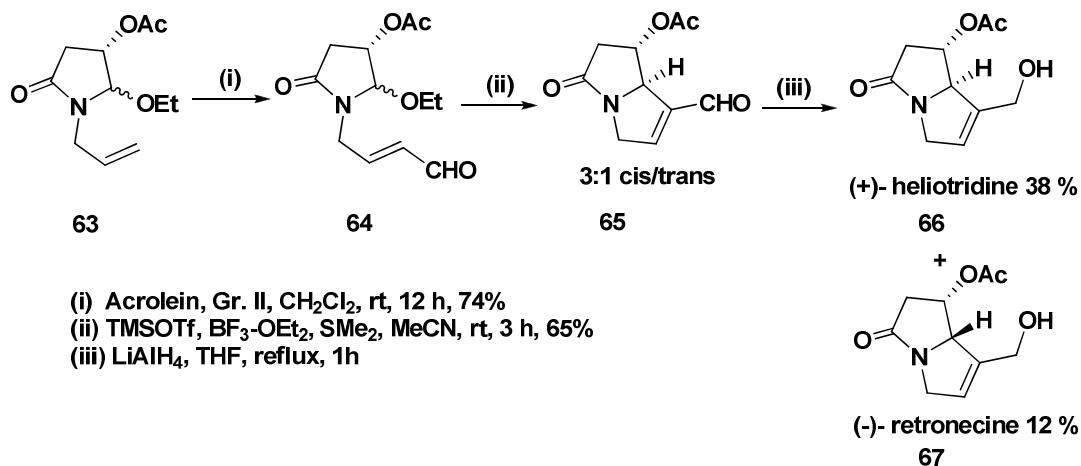
X = CN, CO₂Me; R₁ = aryl, aliphatic
(i) Pd(OAc)₂ / dppb, K₂CO₃, 100 psi CO, 30 h, toluene, 100 °C

Scheme 1.20: Synthesis of benzazepine derivatives from MBH adduct.

1.5 Application of MBH adducts in natural product synthesis:

1.5.1 Synthesis of (+)-heliotridine:

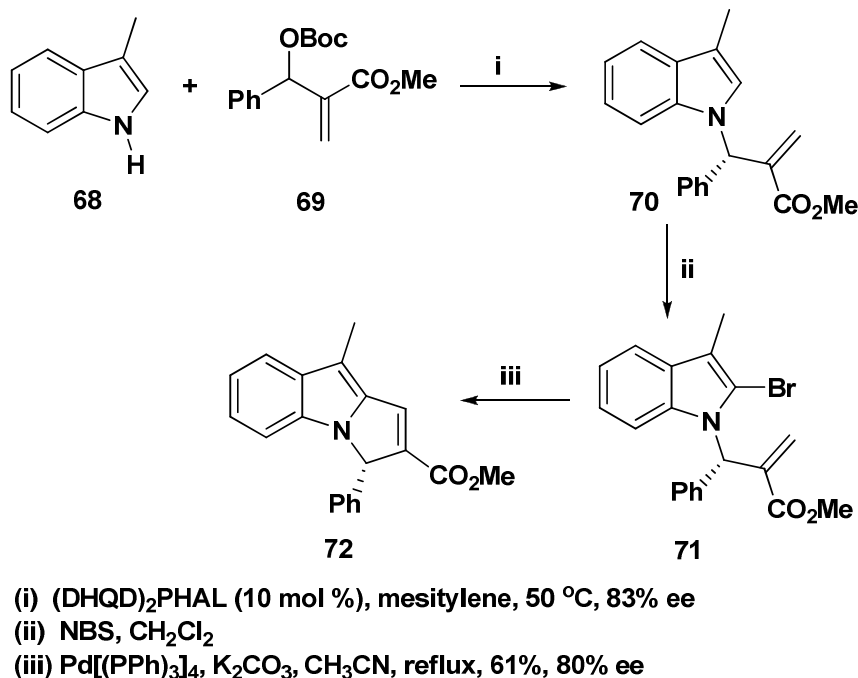
Aggarwal and co-workers have reported a novel method to synthesize densely functionalized heterocycles, where a broad range of Michael acceptors were allowed to couple with readily available iminium ion *via* inter- and intramolecular MBH-type reaction [Myers, E. L. *et al.* 2007]. The iminium ion was generated from masked N, O-acetal **64** by TMSOTf and BF₃.Et₂O in the presence of Me₂S. More importantly, the process is highly enantioselective for cyclic enones. By employing this methodology, they have reported a short synthesis of (+)-heliotridine **66**, as shown in Scheme 1.21.



Scheme 1.21: Synthesis of (+)-heliotridine from MBH adduct.

1.5.2 Synthesis of Yuremamine:

The cinchona alkaloid induced asymmetric allylic alkylation (AAA) reaction has been used as a key step to synthesize yuremamine by the reaction between indole **68** and modified MBH adduct **69** [Cui, H.-L. *et al.* 2009^b]. The chemoselective asymmetric *N*-allylic alkylated compound **70** was further utilized to synthesize natural product **72** via intra-molecular Heck reaction from the bromo derivative **71** (Scheme 1.22).



Scheme 1.22: Synthesis of yuremamine from MBH adduct.

1.6 The Chemistry of Isatin:

Isatin (1H-indole-2,3-dione) was first reported from the oxidation of indigo using nitric and chromic acids by Erdman and Laurent in the year 1841 (Figure 1.2). The synthetic versatility of isatin has led to the extensive use in organic synthesis.

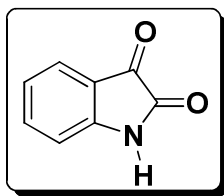


Figure 1.2: Isatin.

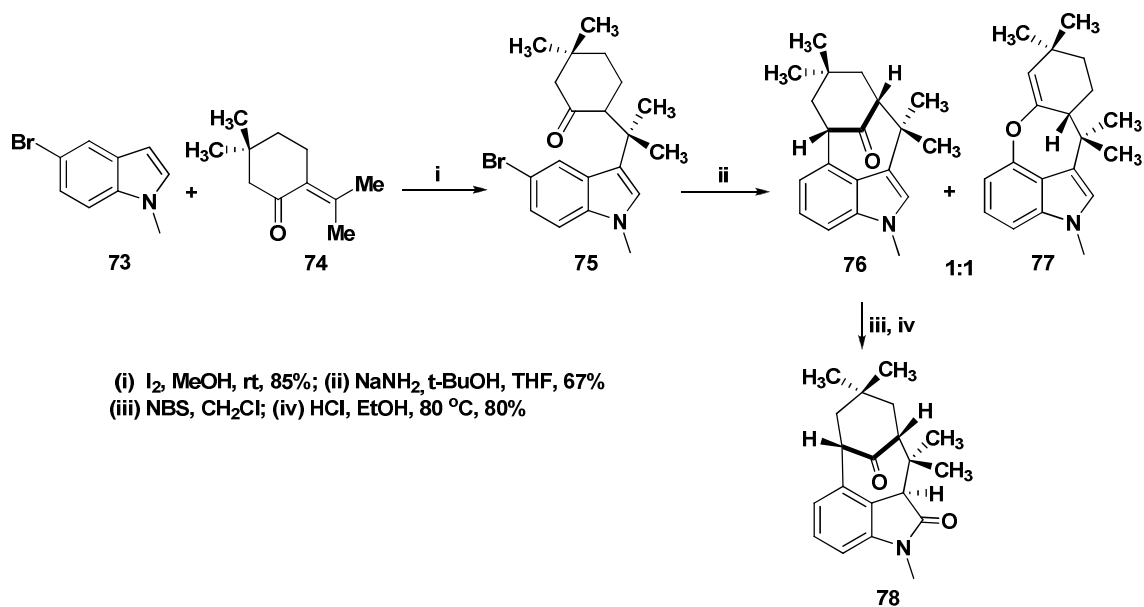
Four reviews have been published on the chemistry of isatin. The very first review by Sumpter in 1945 [Sumpter, W.C. 1945], second by Popp in 1975 [Popp, F. D.

et al. 1982], and the third on the utility of isatin as a precursor for various heterocyclic compounds synthesis were reported [Shvekhgeimer, M. G. A. *et al.* 1996]. In 2001 da Silva *et al.* have published one more review [da Silva J. F. M. *et al.* 2001] by updating the chemistry of isatin. The synthetic versatility of isatin and its derivatives has stemmed from the interest in its biological and pharmacological properties. In nature, isatin is found in plants of the genus *Isatis*, in *Calanthe discolor* LINDL [Yoshikawa, M. *et al.* 1998]. Isatin has also been found as a component of the secretion from the parotid gland of *Bufo* frogs, and in humans as it is a metabolic derivative of adrenaline [Ischia, M. *et al.* 1988; Palumbo, A. *et al.* 1989; Halket, J. M. *et al.* 1991]. With this introduction, the following section outlines a few syntheses of biologically important derivatives with isatin core.

1.7 Isatin appended natural products and structurally important motifs:

1.7.1 Synthesis of welwitindolinone C isocyanide scaffold:

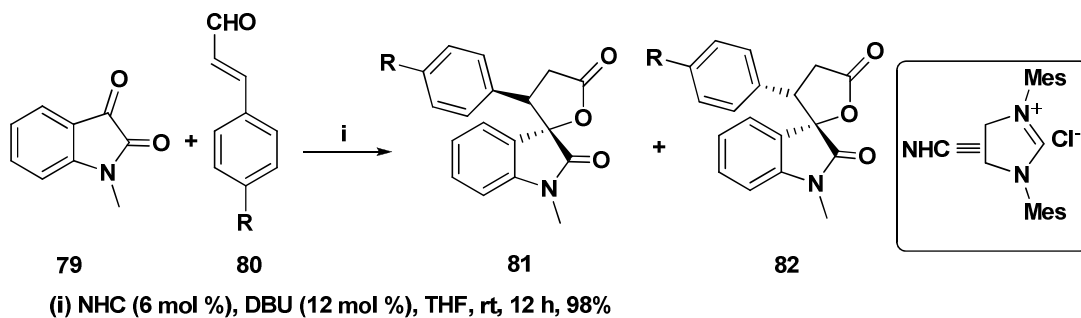
The *N*-methyl welwitindolinone C isocyanide is an important natural product first isolated from blue-green algae *Hapalosiphon welwitschii*. It has showed reverse multiple drug resistance (MDR) to a variety of anticancer drugs [Smith, C. D. *et al.* 1995; 1996]. Two key steps are involved in the synthesis of bicyclic-oxindole derivative **78** from indole precursor. i. Initially, the bicyclic derivatives derivative **76** and **77** were enabled through indolyne intermediate from Michael addition product **75** which was attained by iodine induced Michael reaction between indole **73** and enone **74**. ii. The diastereoselective bicyclic indole **78** was achieved enabled from the intermediate **76** by the treatment with NBS followed by acid hydrolysis reaction in 80% yield [Tian, X. *et al.* 2009] (Scheme 1.23).



Scheme 1.23: Synthesis of *N*-methyl welwitindolinone *C* isocyanide scaffold.

1.7.2 Synthesis of spiro- γ -butyrolactone oxindole:

The oxindole appended spiro- γ -butyrolactone derivative is an important structural unit in a number of bio-active natural products such as *mycotoxin triptoquivaline*. The mixture of diastereomeric spiro- γ -butyrolactone motifs **81** and **82** have been synthesized from the reaction between enal **80** and cyclic 1,2-diketone compound **79** via nucleophilic heterocyclic carbene (NHC) annulation [Nair, V. *et al.* 2005]. Usually, the ketone showed poor reactivity with NHC, which conquered by the use of diketones (Scheme 1.24).

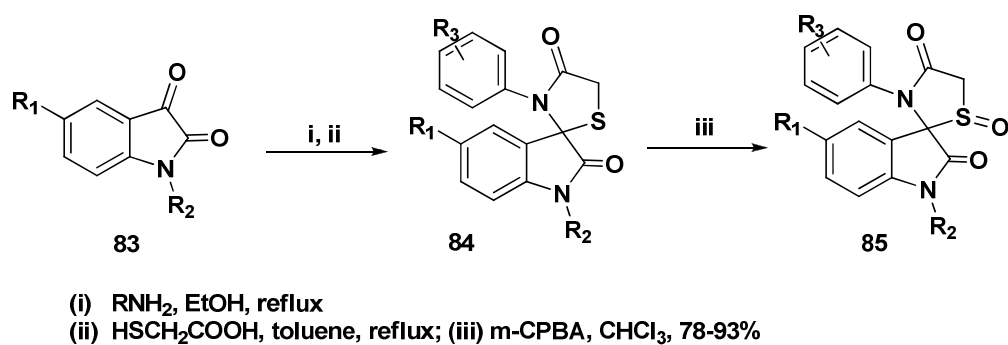


Scheme 1.24: Synthesis of spiro- γ -butyrolactone-2-oxindole derivatives.

1.7.3 Synthesis of anti-tubercular active spirothiazolidinone derivatives:

Thiazolidinone derivatives are an important class of medicinal compounds and this core structure found in a number of biological active molecules [Havrylyuk, D. *et al.*

2010]. In 2010, Vintonyak and co-workers have reported the synthesis of spirothiazolidinone indolone-2-one derivatives from the condensation between amine and isatin **83** followed by cyclization with mercaptoacetic acid at reflux condition. The *m*-chloroperbenzoic acid (*m*-CPBA) oxidation of spirosulphides **84** has led to the target compound **85** (Scheme 1.25). Biological evaluation of spirothiazolidinone derivative **85** showed potent and selective inhibitor activity against *Mycobacterium tuberculosis* protein tyrosine phosphatases B (MtpB) [Vintonyak, V. V. *et al.* 2010].



Scheme 1.25: Synthesis of 3-spirothiazolidinone-2-one derivatives.

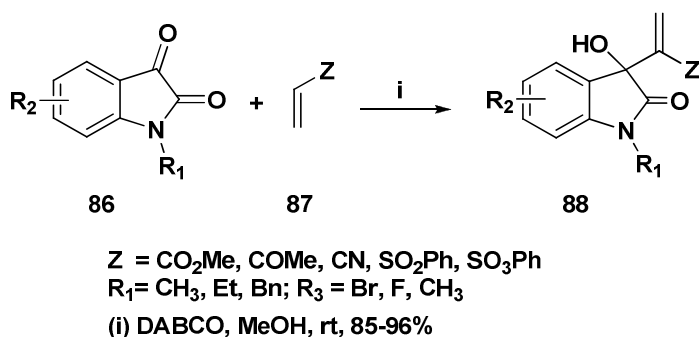
1.8 Synthesis of MBH adduct of isatin and its synthetic applications:

A vast number of natural products and biologically important drug units have been identified with oxindole core as a basic skeleton. Interestingly, the classical MBH chemistry very recently incorporated isatin as a reactive electrophile and furnished oxindole appended MBH adducts. The emblem of MBH reaction is its atom economic nature, with the arrangement of proximate functionalities in MBH adduct of oxindole have gained much interest in synthetic transformation. In fact, very limited work has been published by utilising the MBH adduct of isatin and their derivatives as starting material, and a major part has been reported by our group. A brief detail about the synthesis of MBH adducts of isatin and their synthetic transformations are discussed in the following section.

1.8.1 Isatin as an electrophile in MBH chemistry:

In 2002 Garden and Kim and their co-workers independently first utilized this activated ketone **86**, as an electrophilic partner in the MBH reaction [Garden, S. J. *et al.* 2002; Chung, Y. M. *et al.* 2002] (Scheme 1.26). Generally, the ketones are reacting with activated alkene at drastic condition in MBH reaction (high pressure and often gave low

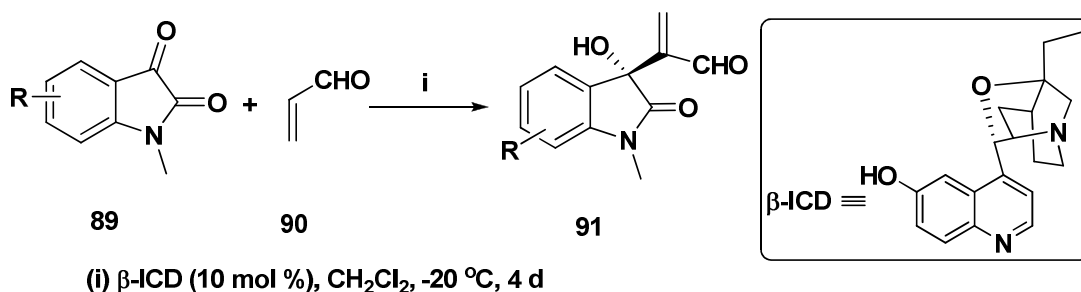
yields). However, the formation of 3-hydroxy-2-oxindole derivatives **88** from isatin at room temperature was realized with the aid of electron withdrawing amide carbonyl group which activates the ketone. Thus, it can readily undergo nucleophilic substitution with enolate ion formed from Michael addition between activated alkene and DABCO resulting into highly functionalized MBH adduct of isatin.



Scheme 1.26: Synthesis of MBH adducts of isatin.

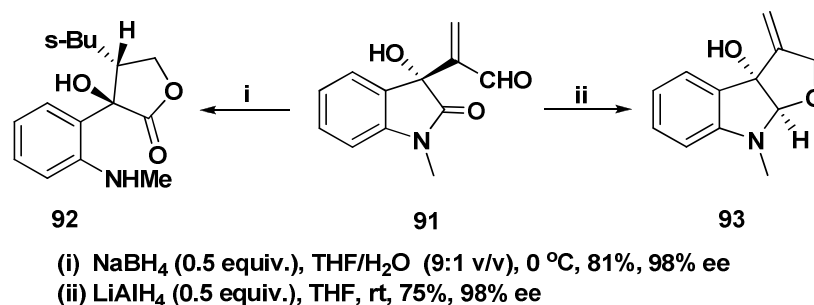
1.8.2 Synthesis of enantioenriched MBH adduct of isatin:

Structural activity relationship (SAR) studies have revealed that biological activities of 3-hydroxy-2-oxindole compound must deeply be affected by the configuration of the C3 position hydroxyl group and *N*-substitution of the oxindole moiety [Peddibhotla, S. 2009]. Accordingly, the asymmetric version of MBH adduct of isatin would be able to provide the highly warranted stereo defined 3-hydroxyl-2-oxindole derivatives. With this idea, Liu and co-workers have reported a variety of enantioenriched MBH adducts of isatin **91** with reactive acrolein **90** under organo catalytic reaction condition [Liu, Y.-L. *et al.* 2010] (Scheme 1.27).



Scheme 1.27: Synthesis of enantioselective MBH adduct of isatin.

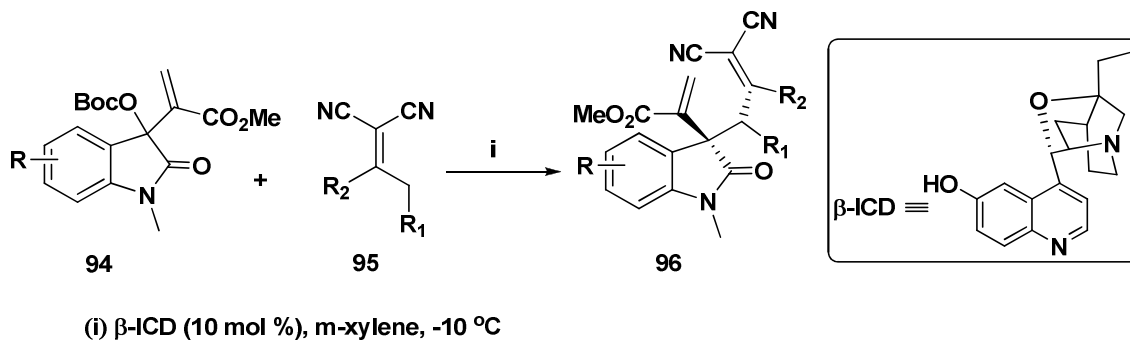
Thus, the enantioenriched 3-hydroxyl-2-oxindole derivative **91** has led the bioactive molecule **93** and natural product core **92** *via* reductive cyclization (Scheme 1.28).



Scheme 1.28: Synthesis of enantioselective natural product core from MBH adduct of isatin.

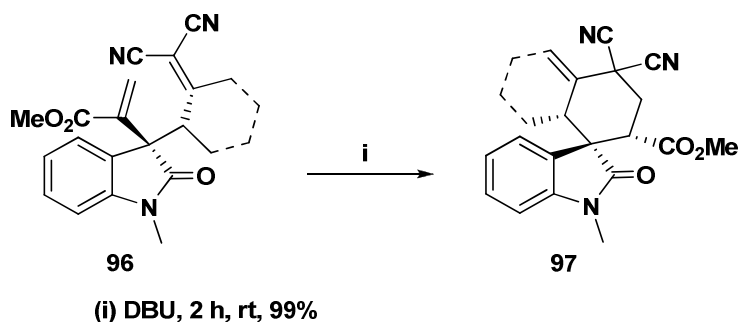
1.8.3 Asymmetric allylic alkylation (AAA) of MBH adduct of isatin:

Organo-catalyzed AAA reactions have been well explored for the synthesis of enantiomerically pure heterocycle derivatives from simple MBH adducts [Cui, H.-L. *et al.* 2009^a]. For the first time, Chen and co-workers have reported enantioenriched allylic alkylated MBH adduct of isatin **96** enabled from racemic isatin adduct **94**, by means of organo-catalyzed C3 nucleophilic substitution process [Peng, J. *et al.* 2010]. The asymmetric synthesis of oxindole at C3 position was addressed and rectified *via* nucleophilic alkylation using β -ICD catalyst (Scheme 1.29).



Scheme 1.29: Asymmetric allylic alkylation of MBH adduct of isatin.

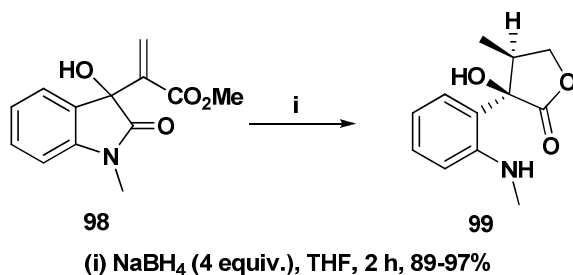
This functionalized allylic alkylated compound **96** was further used as a starting material to synthesize enantioselective spirocyclic derivatives **97** *via* intra-molecular Michael addition under basic condition (Scheme 1.30).



Scheme 1.30: Synthesis of spirooxindole derivative from MBH adduct of isatin.

1.8.4 Reductive cyclization of MBH adduct of isatin:

Our group embarked upon the synthetic application of natural product core synthesis. The γ -butyrolactone **99** using synthesized from MBH adduct of isatin **98** and sodium borohydride *via* reductive cyclization as the key step [Shanmugam, P. *et al.* 2007^b] (Scheme 1.31). Mechanistically, the formation of γ -butyrolactone from MBH adduct of isatin was explained by the sequential of reduction olefin followed by hydrolysis of ester MBH adduct which provided the corresponding methyl and primary alcohol. The primary alcohol underwent lactonization with amide carbonyl followed by the cleavage of weak C-N bond and furnished the desired product **99**.

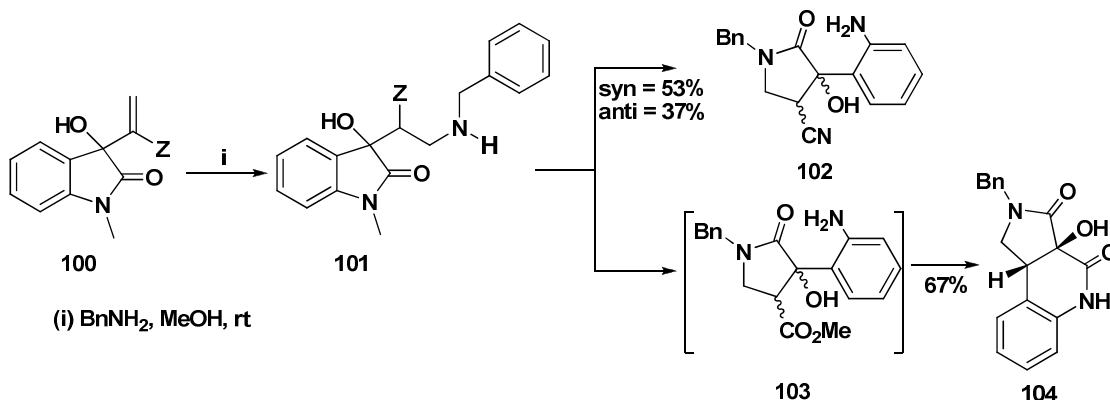


Scheme 1.31: Synthesis of γ -butyrolactone from MBH adduct of isatin.

1.8.5 Synthesis of Lactam:

Kim and co-workers have also been utilized nucleophilic ring opening reaction as a key step to synthesize pyrrolidine-2-one derivatives *via* Michael addition-condensation-ring opening reaction sequence [Kim, S. C. *et al.* 2006]. Interestingly, the nitrile bearing MBH adduct furnished mixture of *syn* and *anti* isomer of lactam **102** from racemic adducts. In the case of ester bearing derivatives mainly tricyclic derivative **104** with trace of expected product **103** was observed (Scheme 1.32). The formation of tricyclic derivative **104** was explained as the reaction proceed *via* sequential Michael addition,

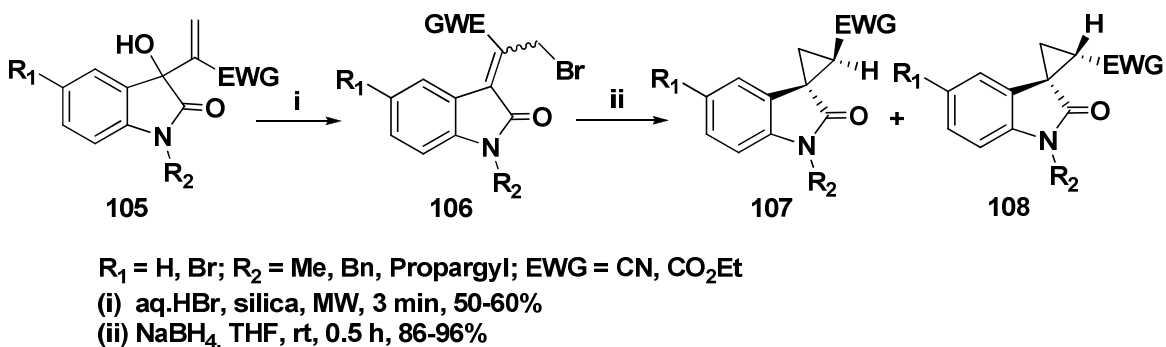
intramolecular cyclization and concomitant ring opening of lactam which eventually led to the formation of new lactam ring.



Scheme 1.32: Synthesis of lactam from MBH adduct of isatin.

1.8.6 Synthesis of 3-spirocyclopropane-2-oxindoles from MBH adduct of isatin:

The synthesis of 3-spirocyclopropane-2-oxindole from allyl bromide of oxindole **106** via reductive cyclization has been demonstrated by our group [Shanmugam, P. *et al.* 2006^b]. A tandem hydride addition followed by bromide elimination resulted into a mixture of diastereomer of spirocyclopropane derivatives **107** and **108** in combined excellent yield (Scheme 1.33). Interestingly, both the *Z*- and *E*-allyl bromide of oxindole upon individual reductive cyclization reactions afforded the same mixture of diastereomeric 3-spirocyclopropane-2-oxindole.



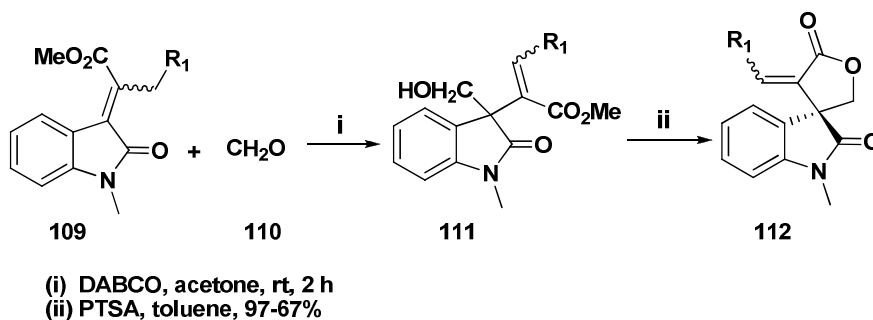
Scheme 1.33: Synthesis of 3-spirocyclopropane-2-oxindoles via reductive cyclization.

1.8.7 Synthesis of 3-spiro- α -methylene- γ -butyrolactone-2-oxindoles:

The medium size lactams and macrolides with α -methylene- γ -butyrolactone backbone are well known for its antitumor, phytotoxic and antibacterial activities.

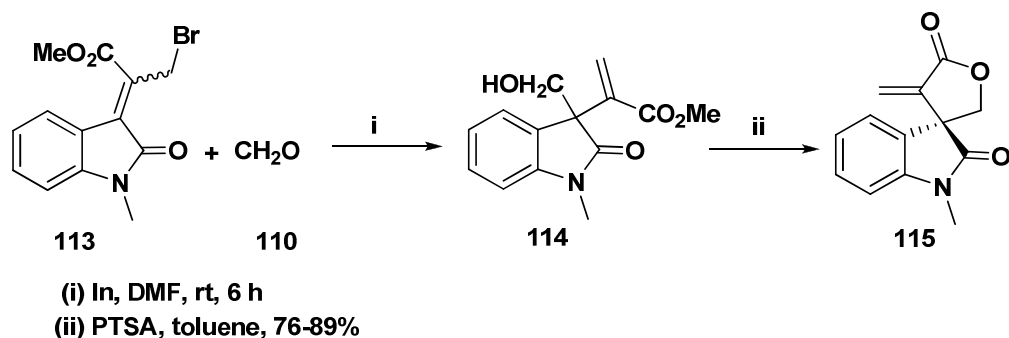
Consequently, there has been considerable interest to develop an efficient method for the synthesis of spiro lactones. Thus, our group have developed two simple methodologies for the construction of spiro lactone from MBH adduct of isatin as discussed below.

i. The stereoselective synthesis of 3-spiro- α -methylene- γ -butyrolactone oxindole derivative **112** was achieved from MBH adducts of isatin *via* three-step reaction sequences [Shanmugam, P. *et al.* 2008^a] *viz.* (1) Isomerization of the MBH adducts of isatin **109** with trimethyl orthoformate using montmorillonite K10 clay catalyst. (2) a second MBH reaction with formaldehyde **110** in the presence of DABCO. (3) Finally, the target molecule **112** was achieved by a solid acid catalyzed lactonization (Scheme 1.34).



Scheme 1.34: *Synthesis of α -methylene- γ -butyrolactone-2-oxindole from isomerized MBH adduct of isatin.*

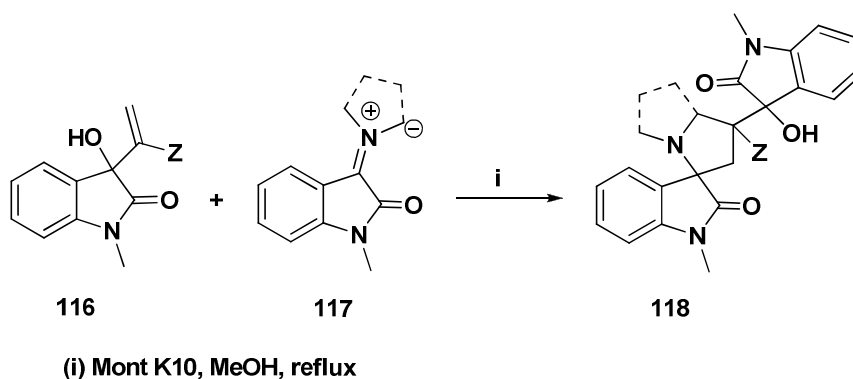
ii. Similarly, the allyl bromides of oxindole have also been used as starting materials to synthesize spiro lactone *via* Barbier allylation as a key step [Shanmugam, P. *et al.* 2008^b]. The Barbier allylation between the formaldehyde **110** and allyl bromide of oxindole **113** has furnished homoallylic alcohol **114** in the presence of indium catalyst. The resultant homoallylic alcohol underwent lactonization with solid acid catalyst and afforded diastereoselective 3-spiro- α -methylene- γ -butyrolactone oxindole **115** (Scheme 1.35) in excellent yield.



Scheme 1.35: Synthesis of α -methylene- γ -butyrolactone-2-oxindoles from bromo isomerized MBH adduct of isatin.

1.8.8 Synthesis of 3-spiropyrrolidine-2-oxindole derivatives via azomethine ylide cycloaddition reaction:

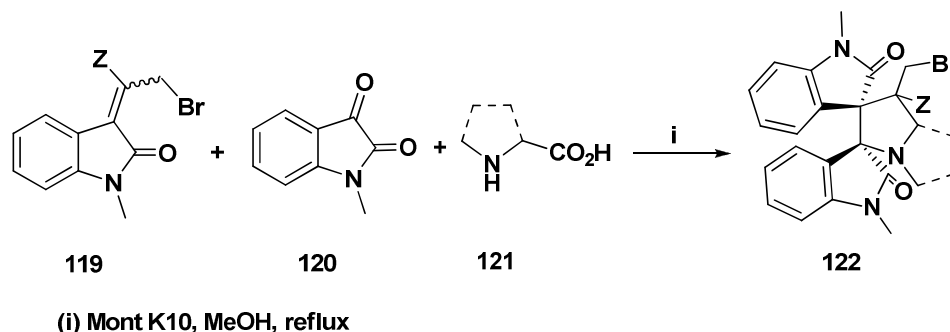
Based on the concept of azomethine ylide (AMY) [3+2]-cycloaddition chemistry [Pandey, G. *et al.* 2006; Coldham, I. *et al.* 2005], a variety of 3-spirooxindole derivatives **118** from MBH adduct of isatin **116** as dipolarophile with *in-situ* generated cyclic or acyclic AMY-ylides have been reported by our group. This cyclic/acyclic ylides **117** can be generated *in-situ* from the reaction between L-proline or sarcosine with isatin derivatives in the presence of K10 clay under reflux condition [Shanmugam, P. *et al.* 2007^c]. Interestingly, the less stable hetero-aryl MBH adduct also furnished the cycloaddition product with excellent yield (Scheme 1.36).



Scheme 1.36: Synthesis of 3-spiropyrrolidine-2-oxindoles via AMY [3+2]-cycloaddition.

This [3+2]-cycloaddition strategy has also been extended to isomerized MBH adduct of isatin **119** which afforded highly functionalized dispiropyrrolidine and

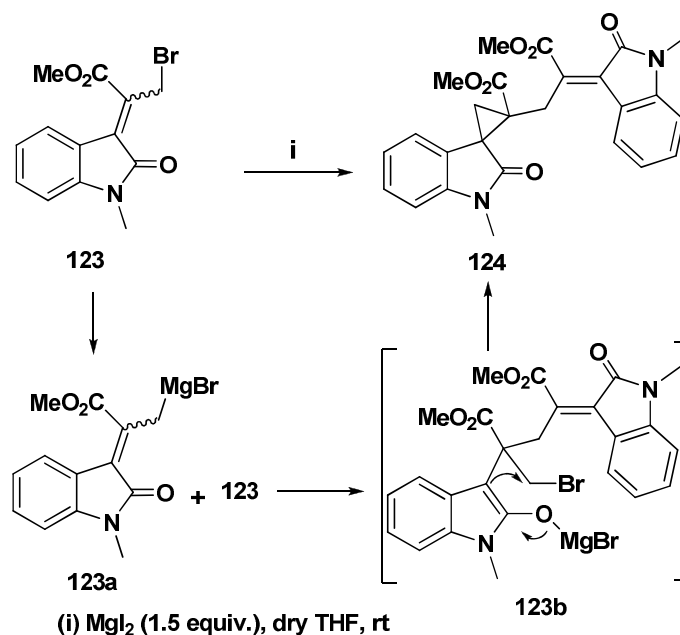
dispiropyrrolizidine oxindoles derivatives **122** in excellent yield [Shanmugam, P. *et al.* 2008^c] (Scheme 1.37).



Scheme 1.37: Synthesis of 3-spirodipyrrolidines-2-oxindoles.

1.8.9 Synthesis of dimerized 3-spirocyclopropane-2-oxindoles from MBH adduct of isatin:

Very recently we have reported an unforeseen magnesium iodide mediated synthesis of diastereomeric mixture of self dimerized spirocyclopropane derivatives **124** from bromo isomerized MBH adducts of isatin **123** in combined good yield [Lingam, K. A. P. *et al.* 2011]. The reaction was accounted by *in-situ* generated magnesium allyl complex **123A** which has led to a 1,2-Michael type addition with another molecule of allyl bromide of oxindole derivative **123** and afforded the spirocyclic product **124** via intermediate **123B** by the bromide elimination (Scheme 1.38).



Scheme 1.38: Synthesis of dimerized 3-spirocyclopropane-2-oxindoles.

1.9 Definition of problem:

From the above literature it is clear that functionalized isatin and its derivatives are used wide spread as core structural motifs in a number of natural products and closely related to pharmacologically important drug molecules. Recently, the chemo- and stereoselective functionalization and synthetic transformation of MBH adducts have received much attention and also well explored. Even though MBH adduct became a substrate for complexity-generating reactions and there is an exponential increase in the synthetic utility of this reaction, the chemo- and stereoselective synthetic transformation was very limited in the case of MBH adduct of isatin and its derivatives. Especially, the C3 functionalization of oxindoles has been paid less attention. With this back ground, we initiated our work with MBH adduct of isatin as starting material towards the selective functionalization and developing new methods for the synthesis of spirocyclic systems in a stereo- and regioselective fashion. The results of our investigation in this direction form the subject matter of the thesis.

With a general introduction in Chapter 1, the thesis is broadly divided into two phases. The first phase of the thesis deals with selective functionalization of MBH adducts of isatin and is the subject matter of Chapters two and three. The second phase of the thesis focuses on the diastereoselective synthesis of spirocycle derivatives at C3 position of MBH adduct of isatin from allyl bromide of oxindole.

In brief, the second Chapter of the thesis deals with a mild and efficient CAN mediated regioselective aromatic side chain oxidation of MBH adduct of isatin. Substrate scope, comparative study with other oxidising reagents and a plausible mechanism are also discussed in this Chapter. The highly functionalized allene appended oxindole derivative synthesis from MBH adduct of isatin *via* consecutive propargyl isomerisation, 1, 3-hydride shift and [3,3]-sigmatropic reactions is the subject matter of third Chapter. Finally, the functionalized allene derivatives were synthetically transformed into oxindole appended furan derivatives and a plausible mechanism is also discussed in this chapter.

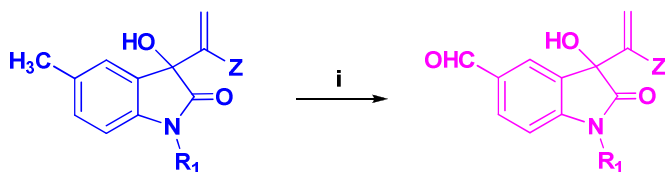
The diastereoselective syntheses of 3-spirocyclopentene and 3-spiropyrazole-2-oxindole derivatives from isomeric mixture of allyl bromide of oxindoles derived on MBH adduct of isatin *via* [3+2]-annulation reaction is the central theme of the fourth Chapter. The final and the fifth Chapter describes pyridine core activation as a key step to synthesise 3-spirodihydroindolizine-2-oxindole derivatives from isomeric mixture of allyl bromide of oxindole *via* 1,5 electrocyclization strategy. In order to make molecular complexity at C3 position of oxindole, quinoline, isoquinoline and 4-bromoquinoline were used as starting material in place of pyridine.

Chapter II

A Mild and Efficient CAN Mediated Oxidation of Morita-Baylis-Hillman Adducts of 5-Methyl-*N*-Alkylisatin to 5-Formyl-*N*-Alkylisatin

Abstract:

A simple, mild and efficient CAN mediated oxidation of Morita–Baylis–Hillman adducts of 5-methyl-*N*-alkylisatins to 5-formyl-*N*-alkylisatins under ambient reaction conditions is reported. Simple and isomerized 5-methyl-*N*-alkylisatin derivatives have also been tested and failed to provide the corresponding formylated products. A plausible reaction mechanism has been proposed.



$R_1 = \text{H, CH}_3, \text{CH}_2\text{Ph, CH}_2\text{CCH, CO}_2\text{Me, CH}_2\text{CHCH}_2, \text{CH}(\text{CH}_3)_3$
 $Z = \text{CO}_2\text{Me, CO}_2\text{Et, CO}_2^t\text{Bu, CN, SO}_2\text{Ph, SO}_3\text{Ph}$

(i) CAN (4.1 equiv.), MeOH:CH₃CN (1:0.5), rt, 48 h - >95%

Shanmugam, P. *et al. Tetrahedron Lett.*, 2008, 49, 2119–2123.

Chapter II

A Mild and Efficient CAN Mediated Oxidation of Morita-Baylis-Hillman Adducts of 5-Methyl-N-Alkylisatin to 5-Formyl-N-Alkylisatin

2.1 Introduction:

Oxidation of aromatic side chain is an important and essential task to make a diverse set of bond forming reactions in organic synthesis. Thus, the resulting functionalities such as -OH, -COOH, CH₂OH and -CHO are valuable chromophores in a variety of synthetic transformation and themselves are present in a number of active pharmaceutical intermediates (API), and natural product core structures [F. Brühne 1999; Haque, A.-M. 2011; Pryde, D. C. *et al.* 2010]. Due to rather poor performance of various direct oxidative methods, the aromatic aldehydes are still manufactured in traditional ways of organic synthesis. Traditionally, benzaldehyde is produced by the chlorination of side-chain of toluene and followed saponification of the resulting dichloromethyl group to furnish aldehyde. Unfortunately, these products still contain the chlorinated impurities and did not meet food and drug grade specifications. In addition to this issue, the aromatic aldehydes can easily undergo over oxidation and gives its corresponding acid derivatives [Gupta, M. *et al.* 2005]. To rectify this limitation, few groups were concerned about the direct oxidation of aromatic alkanes with air and catalyzed by metalloporphyrin, because of the inertness of aromatic alkane and air. Since 1938, numerous oxidative reagents and processes have been implemented to synthesize aromatic aldehydes from methylarenes, *viz.* Na₂S₂O₈/AgNO₃, [Bacon, R. G. R. *et al.* 1960] O₂/NBS, [Laundon, B. *et al.* 1971] 2,3-dichloro-5,6-dicyanobenzoquinone (DDQ)/O₂/NBS/hy, [Naidu, M. V. *et al.* 1979] CrO₃/Me₃SiCl, [Aizpurua, J. M. 1989] KMnO₄/NEt₃, [Li, W.-S. *et al.* 1989] cerium (IV) trifluoromethanesulfonate [Ce(OTf)₄], [Imamoto, T. *et al.* 1990] Ag(Py)₄S₂O₈, [Firouzabadi, H. *et al.* 1991] KMnO₄/Al₂O₃, [Zhao, D. *et al.* 1994] (MeO)₂CHNMe₂/ NaIO₄, [Vetelino, M. G. 1994] laccase/ABTS-(NH₄)₂/O₂, [Potthast, A.

et al. 1995] O-iodoxybenzoic acid (IBX) as mediator, [Nicolaou, K. C. 2002] and pyridinium chlorochromate (PCC) [Hosseinzadeh, R. *et al.* 2005]. Nevertheless, these procedures generally require multisteps for the preparation of catalyst or the reaction process, special apparatus in some cases, strong oxidants and also long reaction time which are not applicable to the entire aromatic alkane derivatives.

These remarkable limitations of aromatic side chain oxidation reaction has led to an unurge of interest in controlled aromatic side chain oxidation. To address the issue, we initiated to work on aromatic side chain oxidation of MBH adduct of 5-methyl isatin using cerium (IV) ammonium nitrate (CAN) as a mild oxidizing reagent. Among the various oxidative reagents known for synthetic transformation, the single-electron transfer (SET) reactions undoubtedly occupied a predominant position [Nair, V. *et al.* 2010]. Hence, a detailed study on the aromatic side chain oxidation of MBH adduct of 5-methyl isatin with single electron oxidative reagent (CAN) is the subject matter of this chapter.

2.2 A brief introduction on Cerium (IV) Ammonium Nitrate (CAN) reagent:

The IUPAC name of the CAN reagent is Diammonium Cerium (IV) Nitrate and the structure of the complex is shown in Figure 2.1.

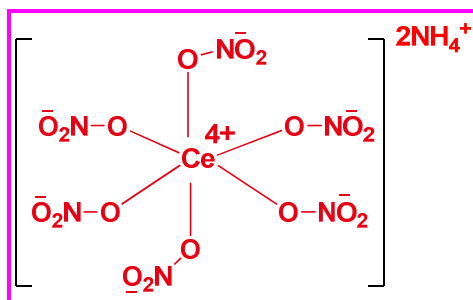


Figure 2.1: Structure of Cerium (IV) Ammonium Nitrate (CAN) reagent.

CAN has been emerged as a versatile reagent for a number of oxidative synthetic transformations. The reasons for its general acceptance as a one-electron oxidant may be attributed due to the following advantages.

- Large reduction potential value of +1.61 V
- Cheap and ready availability

- Low toxicity
- Easy handling
- Experimental simplicity
- Soluble in a variety of organic solvents

The enormous growth in the usage of CAN reagent has been evidenced by the publication of a large number of research papers and several major reviews on CAN-mediated synthetic transformation [Hwu, J. R. *et al.* 2001; Nair, V. *et al.* 1997; 2003; 2004; 2007^a; 2009]. Due to its wide application in organic synthesis demonstrated as a versatile reagent, one can broadly classify the types of reactions and applications catalyzed by this reagent under the following categories.

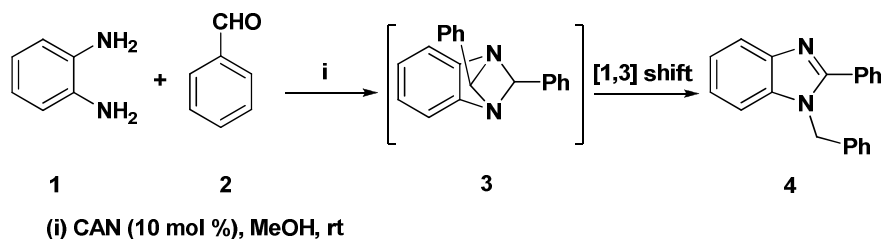
- Reaction involving carbon-carbon bond-formation
- Intramolecular reactions
- Carbon-heteroatom bond formation
- Stoichiometric CAN involving oxidative transformation
- Protection-deprotection reactions

From the list mentioned above, a few selected CAN mediated synthetic transformations are discussed in the following section.

2.3 CAN mediated synthetic transformations:

2.3.1 Synthesis of benzimidazole:

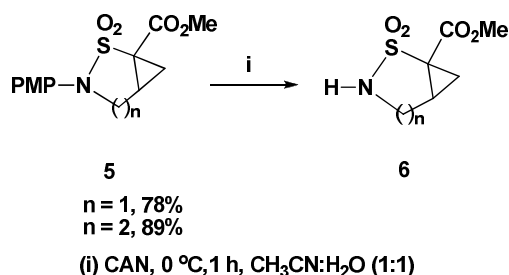
A variety of benzimidazole derivatives **4** have been prepared by the treatment of diamine **1** and aldehyde **2** *via* the sequential reaction of condensation followed by CAN oxidation (Scheme 2.1). The formation of the dihydro-2-arylbenzimidazole as a key intermediate can condense with another molecule of aldehyde afforded 1,4-diazobicyclo hexane intermediate **3**. The 1,4-diazobicyclo derivatives **3** undergo thermally allowed 1,3- hydrogen shift and afforded compound **4** [Sadeka, K. U. *et al.* 2010].



Scheme 2.1: Synthesis of benzimidazole derivatives via catalytic CAN mediated oxidation.

2.3.2 Deprotection of sultam:

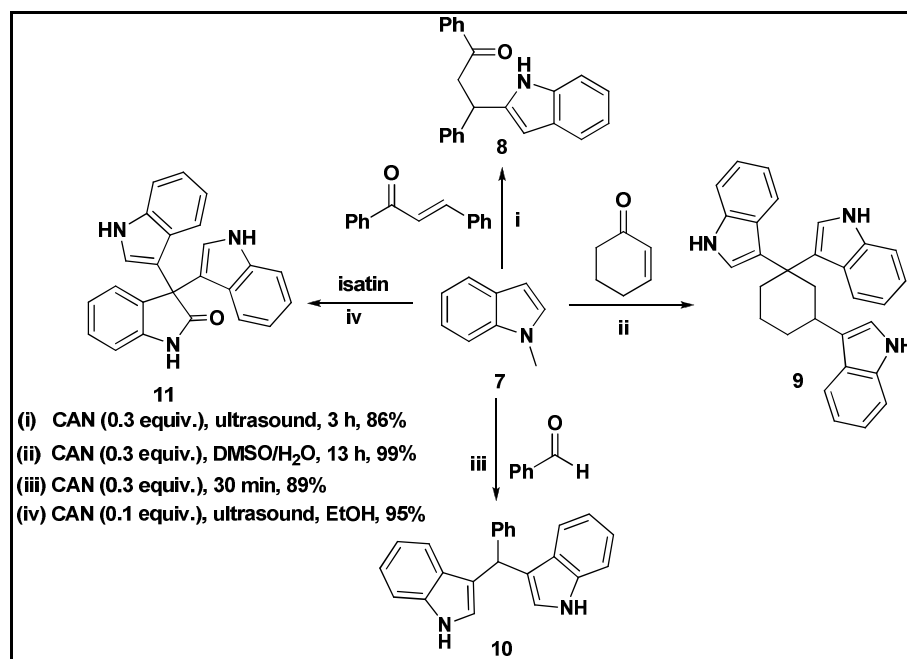
In a routine organic synthesis, the frequently encountered functional group transformations such as protection and deprotection sequence have been achieved efficiently using CAN as an oxidant [Cotelle, P. *et al.* 1992; Ates, A. *et al.* 1999; Marko, I. E. *et al.* 1999]. In 2009, Meijere *et al.* reported a pharmaceutically important deprotected sultam **6** from the PMP protected derivative **5** via oxidative deprotection as a key step by the use of CAN as an oxidative reagent (Scheme 2.2) [Rassadin, V. A. *et al.* 2009].



Scheme 2.2: CAN induced oxidative PMP deprotection of sultam.

2.3.3 Stoichiometric CAN induced electrophilic substitution of indole:

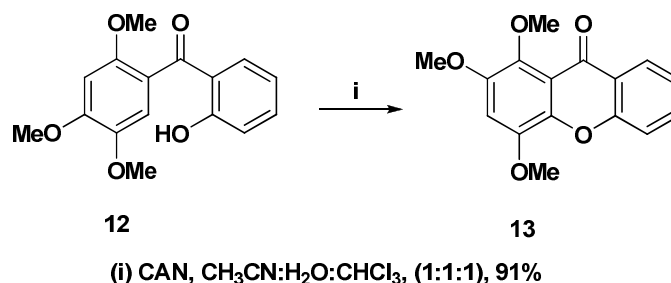
Catalytic amount of CAN assisted electrophilic substitution reactions with indole under different reaction conditions were summarized in Scheme 2.3. Michael addition of indole **7** with α,β -unsaturated ketones under ultrasonic irradiation afforded corresponding adduct **8** in excellent yield [Ji, S. *et al.* 2003]. Interestingly, the reaction between the indole **7** and cyclic α,β -unsaturated ketone or aldehyde using catalytic amount of CAN reagent afforded 1,2-addition derivatives **9** and **10** [Ko, S. *et al.* 2006]. However, with stoichiometric amount of CAN has led to the symmetrical 3,3-(indolyl)indolin-2-one derivatives **11** from the reaction between isatin and indole under ultrasonic irradiation [Wang, S.-Y. *et al.* 2006].



Scheme 2.3: Catalytic CAN assisted electrophilic substitution of indoles.

2.3.4 Synthesis of Xanthenes:

Xanthone is an important class of natural product compound, such derivatives synthesized by intramolecular cyclization of phenolic derivative **12** via CAN mediated oxidative cyclization have been reported by Koning and co-workers. The nucleophilic substitution of radical cation intermediate to the aromatic ring was a key step to synthesize the Xanthone derivative **13** (Scheme 2.4) [Johnson, M. M. *et al.* 2010].

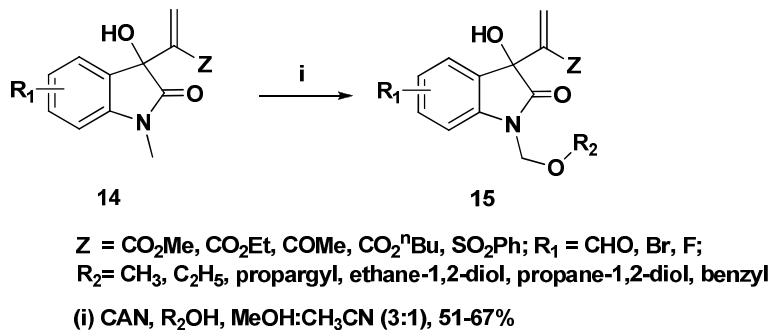


Scheme 2.4: Synthesis of Xanthone via CAN mediated aromatic nucleophilic substitution.

2.3.5 N-Methyl activation of MBH adduct of isatin:

Recent investigation from our group has explored an unforeseen CAN mediated N-methyl activation of MBH adduct of isatin derivative [Shanmugam, P, *et al.* 2006^a]. The N-alkylated MBH adduct of isatin **14** was treated with CAN and alcohol in acetonitrile afforded the ethers of corresponding alcohol **15** and the results were found

applicable only with MBH adduct of isatin rather than other isatin derivatives (Scheme 2.5).



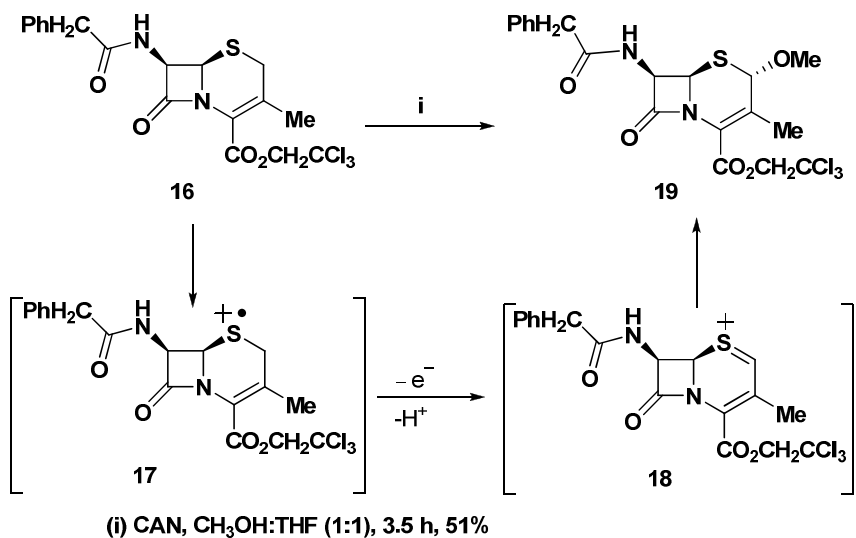
Scheme 2.5: CAN Mediated N-methyl activation of MBH adduct of isatin.

2.4 Miscellaneous transformations using CAN oxidant:

In addition to the reactions described above, CAN have also been found to be effective to brought about some novel and interesting transformations. Such reactions also provide insight into the mechanistic details of several CAN mediated transformations. A few illustrative examples are depicted as below.

2.4.1 Alkoxylation reaction:

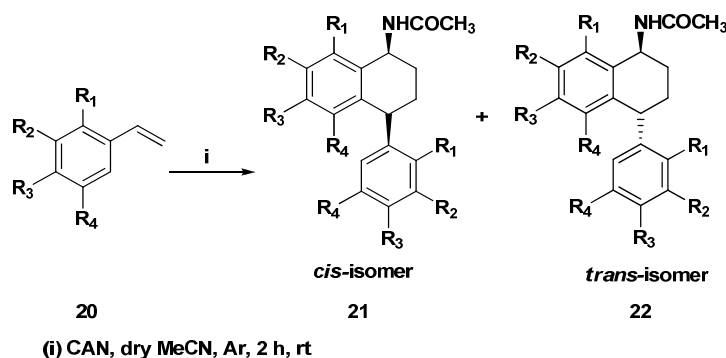
Cephalosporins **16** react with CAN in methanol under mild condition to afford the corresponding 2-methoxy derivative **19** as a major product which has been reported by Fletton and co-workers [Fletton, R. A. *et al.* 1985]. Mechanistically, a single-electron transfer from sulphur to Ce(IV) reagent initiates the radical cation **17**. The 2-methoxy derivative **19** enabled from radical cation **17** by subsequent loses of a proton and an electron to form intermediate **18** which has been quenched with alcohol (Scheme 2.6).



Scheme 2.6: Synthesis of 2-methoxy Cephalosporin via CAN mediated oxidation.

2.4.2 Synthesis of amino tetralin derivatives:

Amino tetralin derivatives are therapeutically useful bio-active molecules, they specifically act as immunomodulator and antitumor agents. Styrene **20** with CAN in acetonitrile solvent as well as reactant was found to be a starting material to synthesize *cis* and *trans* tetralins **21/22** (Scheme 2.7) [Nair, V. *et al.* 2002]. For instance, the reaction of 4-methylstyrene with CAN in acetonitrile yielded *cis* and *trans*-isomer **21/22** of α -acetamido tetralines *via* oxidative cyclization.

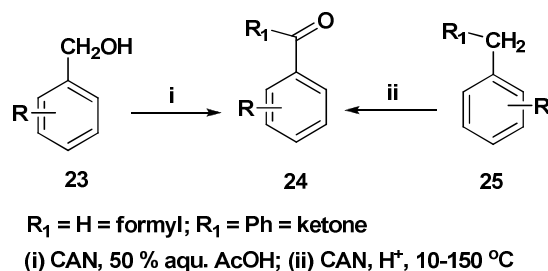


Scheme 2.7: Synthesis of α -amino tetralin derivatives via CAN mediated oxidation.

2.4.3 CAN induced aromatic side chain oxidation of benzyl derivatives:

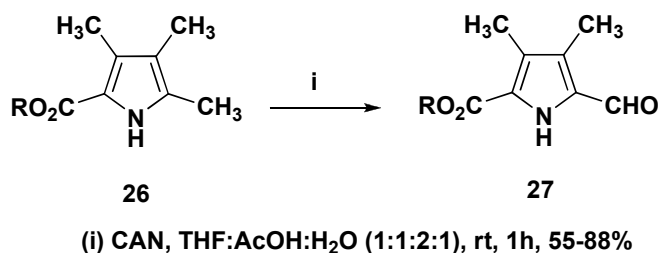
Among the various known aromatic side chain oxidative reagents in organic synthesis, CAN has led such type of synthetic transformation in a controlled fashion. Trahanovsky, reported the CAN induced controlled oxidation of benzyl alcohol **23** to their corresponding aldehyde **24** under the acidic condition [Trahanovsky, *et al.* 1966].

Syper has also been reported a variety of aldehyde and ketone derivatives **25** from toluene and its analogs *via* aromatic side chain oxidation by CAN reagent under acidic condition (Scheme 2.8) [Syper, L. 1966].



Scheme 2.8: CAN Mediated aromatic side chain oxidation

In 1995 Thyran, and co-workers have been reported the hetero-aryl derivative as a starting material used for the regioselective oxidation of α -methyl pyrrole derivative **26** produce the corresponding formyl derivative **27** by means of CAN oxidant (Scheme 2.9) [Thyran, T. *et al.* 1995]. Mechanistically, the formyl compound **27** had arrived from *in-situ* generated alcohol *via* the second oxidation from the α -methyl derivative **26** under CAN mediated acidic condition.



Scheme 2.9: CAN induced regioselective pyrrole α -methyl oxidation.

2.5 Objective of the present work:

Due to the various oxidation states of transition metal salts under strong acidic medium and at elevated temperature, controlled oxidations at that stage of benzyl derivative to their corresponding aldehyde are remaining a challenging task in synthetic chemistry. The aromatic aldehydes are valuable and dynamic resource for further valuable synthetic transformations. Such aldehyde functionality attached with biologically important derivative like isatins are more reliable source for further value added synthetic transformation. In this aspect, we attempted to carry out the controlled and regioselective aromatic methyl group oxidation of the 5-methyl MBH adduct of isatin to corresponding aldehydes using CAN as a mild oxidant. Thus, an efficient CAN

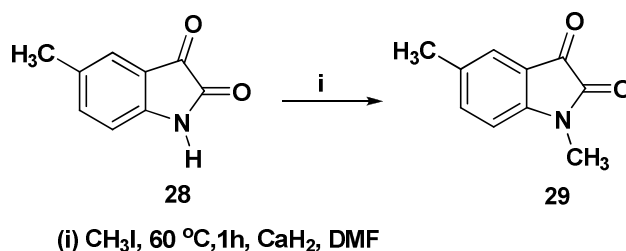
mediated controlled oxidation of 5-methyl MBH adducts of isatin to 5-formyl MBH adducts of isatin (aldehydes), substrate scope and plausible reaction mechanism are elaborated in this Chapter.

2.6 Results and Discussion:

2.6.1 Preparation of MBH adducts of isatin:

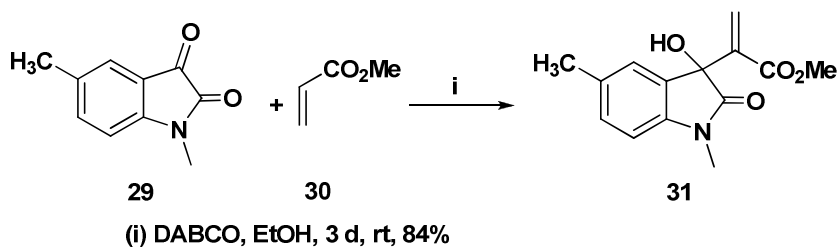
2.6.1.1 Synthesis of *N*-alkyl derivatives of isatin:

The first stage of our target compound synthesis begun with the preparation of MBH adduct of isatin from various *N*-alkylated isatin. Hence, we initiated the preparation of *N*-alkylation of isatin as shown in Scheme 2.10. Thus, the alkylation of 5-methyl isatin **28** was conducted using methyl iodide and CaH₂ as a base in DMF at 60 °C for 1h reaction time provided the corresponding *N*-methyl isatin compound **29**. The same strategy further extended to synthesize a variety of *N*-alkylated derivatives from isatin with alkyl halides such as propargyl bromide, benzyl iodide, allyl bromide etc. and all the reactions afforded corresponding alkylated compounds.



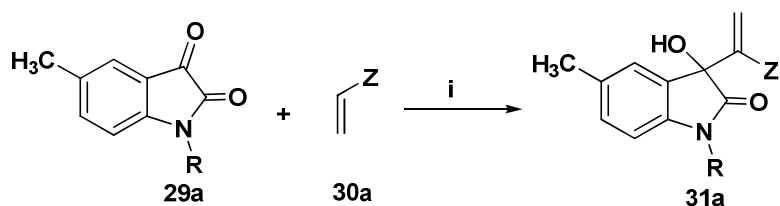
Scheme 2.10: Synthesis of *N*-Alkylation of isatin derivatives.

Model substrate for initial studies, the *N*-methyl MBH adduct of isatin **31** has been prepared by the treatment of *N*-methyl isatin **29** in ethanol with methyl acrylate **30** using DABCO (10 mol %) as catalyst at room temperature afforded compound **31** in good yield (84%) and the reaction is shown in Scheme 2.11.



Scheme 2.11: Synthesis of 5-methyl-*N*-methyl MBH adduct of isatin **31**

The structure of synthesized compound **31** was characterized by ^1H NMR spectroscopic technique and also compared with the literature data. In a similar fashion described above, a variety of MBH adducts of isatin **31a** were prepared based on the standard literature procedure as showed in Scheme 2.12 [Garden, S. J. *et al.* 2002; Chung, Y. M. *et al.* 2002].



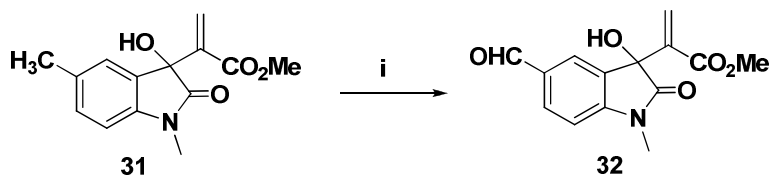
R= CH₃, CH₂Ph, CH₂CCH, CO₂Et, CH₂CHCH₂, CH(CH₃)₂
 Z= CO₂Me, CO₂Et, CO₂ⁿBu, CN, SO₂Ph, SO₃Ph

(i) DABCO, EtOH, 2-5 d, rt

Scheme 2.12: Synthesis of 5-methyl-N-alkyl MBH adduct of isatin derivatives.

2.6.2 CAN mediated side chain oxidation of MBH adducts of 1,5-dimethyl isatin:

The aromatic side chain oxidation studies were initiated using MBH adduct of 1,5-dimethyl isatin **31** as a model substrate. In a preliminary reaction, the adduct **31** when treated with 2.1 equivalents of CAN in methanol (2 mL) afforded the side chain oxidized product **32** in 48% yield after 4 hour (Scheme 2.13). Even though the reaction mixture was allowed to stir up to 8h, the starting materials remained unaltered without any further improvement of yield.



(i) CAN, 8 h, MeOH (2 mL), 48%

Scheme 2.13: CAN oxidation of 5-methyl N-methyl MBH adduct of isatin **31**

Before initiating the optimization, we were interested in characterizing the structure of the resulted compound **32**. Hence, the structure of functionalized compound **32** was confirmed by the analysis of detailed spectroscopic data (FTIR, ^1H , ^{13}C NMR and FAB-MS). Thus, the FTIR of compound **32** showed two carbonyl absorptions at 1710

and 1725 cm^{-1} which corresponds to the presence of aldehyde and ester groups, respectively and the hydroxyl group absorption was observed at 3382 cm^{-1} .

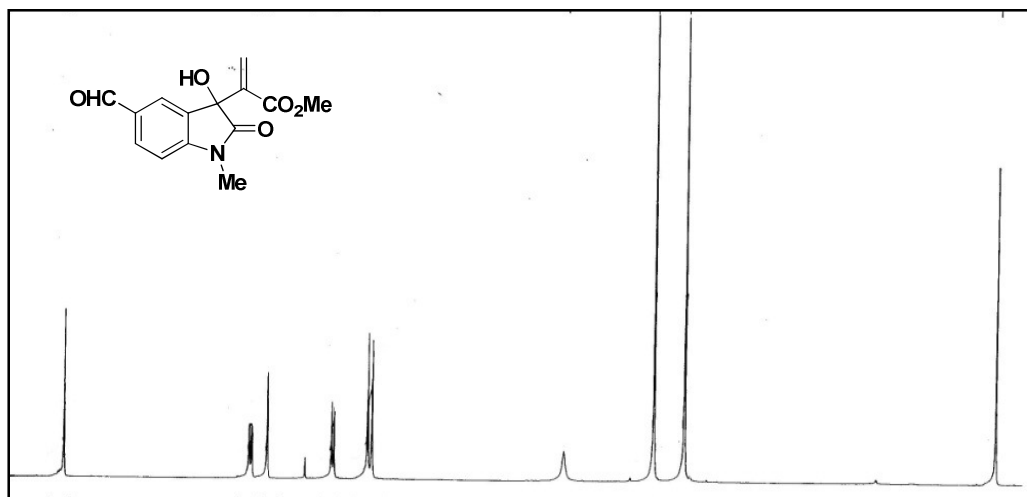


Figure 2.2: ^1H NMR spectrum of 5-formyl MBH adduct of isatin compound **32**

In the proton NMR spectrum, both the *N*-methyl and ester methyl protons appeared as two separate singlets at δ 3.26 and 3.58 ppm, respectively and also the 5-methyl protons in the starting compound **31** had disappeared (Figure 2.2). The MBH adduct olefinic protons discernible as two separate singlets at δ 6.55 and 6.60 ppm. Among the three aromatic protons, two protons appeared as a doublet centered at δ 6.97 and 7.83 ppm with a coupling constant $J = 8.4$ Hz and the remaining one proton appeared as singlet at δ 7.66 ppm. The aldehyde proton appeared as a sharp singlet at δ 9.80 ppm. In addition, the newly appeared proton was further confirmed as an aldehyde instead of carboxylic acid through D_2O exchange studies. The D_2O exchange study exhibited that there was no chemical shift change in the δ value of aldehyde proton.

The ^{13}C NMR spectrum of compound **32** showed signals at δ 27.21, 52.03 and 75.27 ppm corresponding to *N*-methyl, ester methyl and quaternary carbons, respectively (Figure 2.3). The six aromatic and two olefinic carbons were resonated in the region between δ 124.65-149.98 ppm. The three carbonyl carbons *viz.* ester, amide and aldehyde appeared at δ 164.58, 176.85 and 190.38 ppm, respectively.

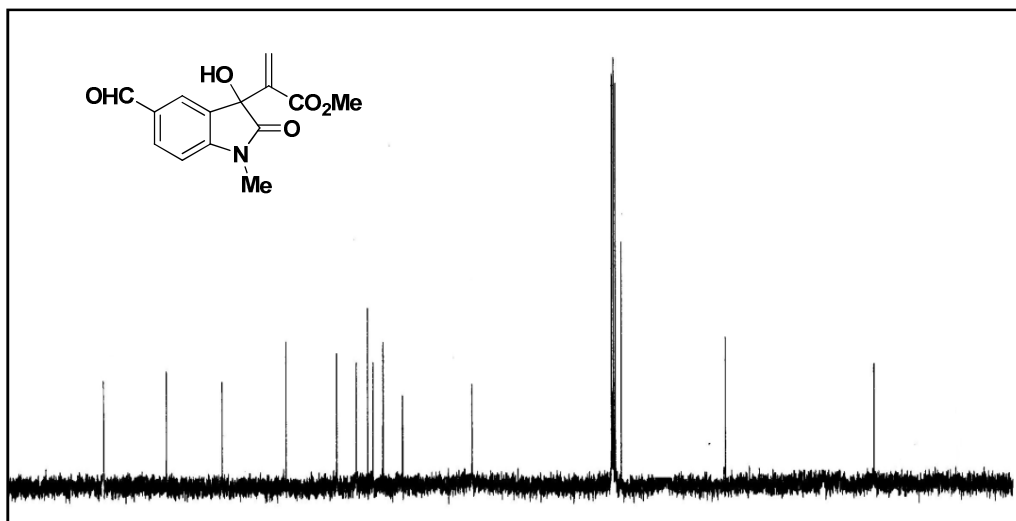


Figure 2.3: ^{13}C NMR Spectrum of 5-formyl MBH adduct of isatin **32**

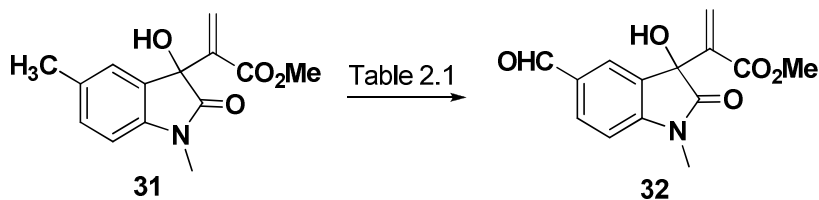
Finally, the structure of synthesized compound **32** was supported by the FAB mass spectrum as it showed a molecular ion $[\text{M}^+]$ peak at $m/z = 275.48$ as against calculated value $m/z = 275.07$. The structure was further confirmed by the elemental analysis.

2.6.3 Optimization of aromatic side chain oxidation of MBH adduct of isatin: Effect of solvent and catalyst load:

To optimize the reaction conditions, we have chosen MBH adduct of 1,5-dimethyl isatin **31** as a model substrate. Repeating the reaction with various solvents and 2.1 equiv. of CAN provided nearly 48-50% yield at various time intervals (Table 2.1, entries 1-5). While in aqueous medium, the reaction provided a trace of expected product **32** after 30 min. The reaction was further allowed stir up to 3h, and there was no improvement in yield (Table 2.1, entry 3). The reason may be due to the lack of the solubility of starting material **31** in water. Hence, we have used binary solvent system $\text{CH}_2\text{Cl}_2/\text{H}_2\text{O}$ (1:1) to improve the solubility of the starting material, unfortunately that did not improve the yield (Table 2.1, entry 4). The use of another binary solvent system MeOH: CH_3CN (1:0.5) afforded the desired product in 50% yield within 5 min. reaction time (Table 2.1, entry 5). Hence, we have turned our attention to increase the number of equivalents of CAN in this reaction. Surprisingly, the gradual increase in the mole equivalents of CAN in the reaction significantly increase the yield of the product **32** (Table 2.1, entry 6-8). Further fine-tuning the catalytic load in this reaction showed that the 4 equivalents of

CAN was necessary to complete (>95%) oxidation (Table 2.1, entry 7). In addition, excess load of CAN did not provide any valuable result in this reaction.

Table 2.1 Optimization of CAN oxidation of 5-methyl MBH adduct of isatin **31**



Entry	Solvent (2 mL)	CAN (equiv.)	Time (min)	Yield (%)
1	MeOH	2	60	48
2	CH ₃ CN	2	60	47
3	H ₂ O	2	180	Trace
4	CH ₂ Cl ₂ /H ₂ O (1:1)	2	60	23
5	MeOH:CH ₃ CN (1:0.5)	2	5	50
6	MeOH:CH ₃ CN (1:0.5)	3	5	74
7	MeOH:CH₃CN (1:0.5)	4	5	>95
8	MeOH:CH ₃ CN (1:0.5)	5	5	>95

2.6.4 Comparison of CAN reagent with other oxidizing reagents:

The efficiency of CAN mediated aromatic side chain oxidation of MBH adducts of isatin was compared with other well known oxidizing reagents. The oxidizing reagents such as Mn(OAc)₃·2H₂O, SeO₂, KMnO₄ and DDQ were screened against 5-methyl MBH adduct **31** as model substrate under the optimized condition. The results are given in the Table 2.2. Among the various oxidative reagents screened, only CAN was found to be effective than other oxidizing reagents. The failure of other reagents with 5-methyl MBH adduct of isatin **31** may be due to the absence of harsh reaction conditions such as acidic or basic condition and elevated temperatures.

Table 2.2 Comparative studies between CAN and other oxidative reagents for side chain oxidation N-alkyl MBH adduct of isatin.



Entry	Reagent	Yield (%) after 5 min.	Yield (%) after 12 h
1	CAN (4.1 equiv.)	>95	>95
2	Mn(OAc) ₃ ·2H ₂ O (1.2 equiv.)	-	trace
3	SeO ₂ (1.2 equiv.)	-	-
4	KMnO ₄ (1.2 equiv.)	-	-
5	DDQ (1.2 equiv.)	-	decomposed

Notably, manganese (III) acetate gave a trace of expected product **32** after 12 h (Table 2.2, entry 2). All other reagents showed inertness toward MBH adduct **31** and quantitative amount of starting material was recovered. However, the decomposition of starting material was observed with DDQ due to over oxidation (Table 2.2, entries 3-5). Thus, we can conclude that CAN is an efficient reagent for aromatic side chain oxidation of 5-methyl MBH adduct of isatin under acid free and mild reaction condition.

2.6.5 Substrates screening for side chain oxidation of oxindole derivative:

In order to explore the substrate scope of this mild aromatic side chain oxidation, we have selected and tested various oxindole derivatives **33-38** as shown in Figure 2.4.

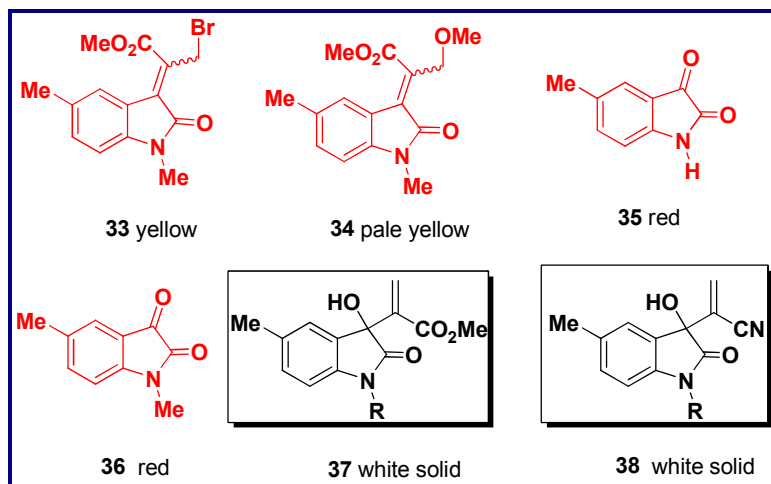
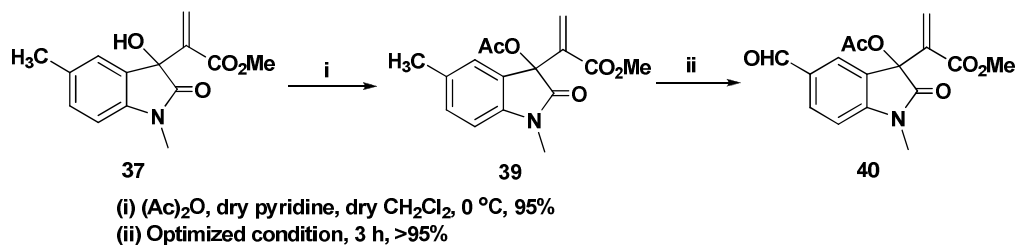


Figure 2.4: Substrate screening of oxindole derivatives for aromatic side chain oxidation.

Under the optimized reaction conditions, only the 5-methyl MBH adducts such as **37** and **38** afforded oxidized products in excellent yield (>95%). Unfortunately, other 5-methyl oxindole derivatives **33-36** did not provide any oxidized product. This preliminary

investigation suggests that the sp^3 hybridization at C3 position of isatin core is a necessary factor rather than sp^2 hybridization for a mild CAN oxidation.

Hence, we have further fine tuned the screening studies concentrating on retaining the C3 position with sp^3 hybridization. Thus, the 3^o-hydroxyl protected MBH adduct of isatin **39** prepared from adduct **37** under standard hydroxyl protecting condition. Interestingly, the compound **39** furnished the oxidized product **40** in excellent yield after 3 h under the optimized conditions (Scheme 2.14).



Scheme 2.14: CAN Oxidation of 3^o-hydroxyl protected MBH adduct of isatin.

The experimental studies with protected MBH adducts revealed the importance of hydroxyl group on C3 position of oxindole derivatives for CAN oxidation. In the absence of hydroxyl group at C3 position, the structure **33-36** has failed to furnish the oxidized products. The failure of these substrates **33-36** may be due to the planarity (sp^2 hybridization) at C3 position. Due to the planar structure, the lone pair of electrons in oxindole nitrogen is in resonance with adjacent carbonyl group as shown in **B** and is not available for the CAN mediated oxidation (Figure 2.5). This argument further supported in the presence of double bond at C3 position the colour was persist in the substrates **33-36** due extent of conjugation, which disappeared in MBH adduct of isatin (Figure 2.4, entries **33-36**). That is way structures **33-36** failed to furnish the expected oxidized products. However, in the case of MBH adduct of isatin, the hydroxyl group at C3 position is involved in intramolecular hydrogen bonding with amide carbonyl group, which disrupted the planarity at C2 position. Hence the lone pair of electrons on the nitrogen atom is readily available for CAN oxidation and generated the radical cation on nitrogen as shown in **A** (Figure 2.5). The generation of radical cation is a driving force for 5-methyl oxidation of MBH adducts of isatin and the mechanism is described in detail at the end of this chapter.

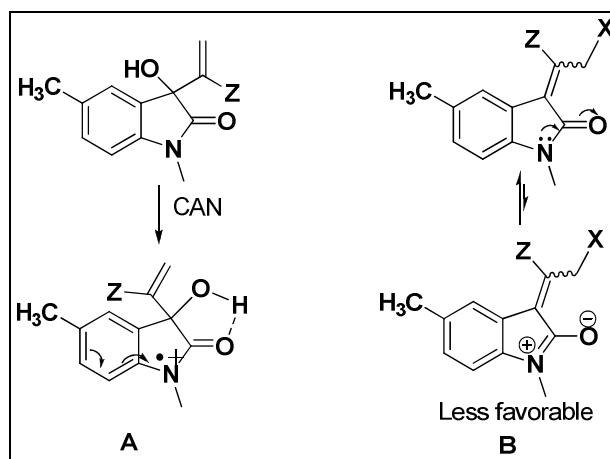
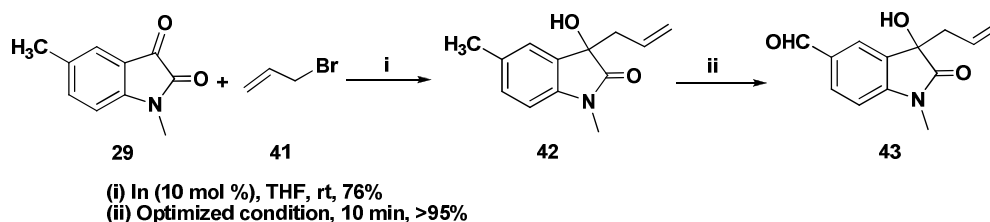


Figure 2.5: Feasible resonance structure of MBH derivatives

The importance of hydroxyl group at C3 position in CAN oxidation was further supported by the following experiments. The oxindole derived homoallylic alcohol **42** was synthesized from *N*-methyl isatin and allyl bromide **41** in presence of indium catalyst (Scheme 2.15). The synthesized compound **42** was characterized and compared with the reported data by Nair and co-workers [Nair, V. *et al.* 2001]. Under optimized reaction conditions, the homoallylic alcohol **42** was subjected to CAN mediated oxidation and the reaction yielded corresponding formyl derivative **43** in >95% after 10 min. It is to be noted that in the case of 3^o-hydroxyl group protected MBH adduct, the side chain oxidation is a slow process compared with unprotected MBH adduct and homoallyl alcohol under the optimized conditions. These observations implied that the rate of CAN oxidation was assisted by hydroxyl group at C3 position *via* intra molecular hydrogen bonding. In other words, the intramolecular hydrogen bonding is responsible in enhancing the acidity of 5-methyl MBH adduct of isatin. The detailed spectral data of the compound **40** and **43** are given the experimental section.



Scheme 2.15: CAN mediated side chain oxidation of oxindole appended homoallylic alcohol.

The substrate screening studies showed that the MBH adduct of 5-methyl isatin derivatives with sp³ hybridization at C3 position and a hydroxyl group at the same are necessary in substrates for CAN mediated facile side chain oxidation.

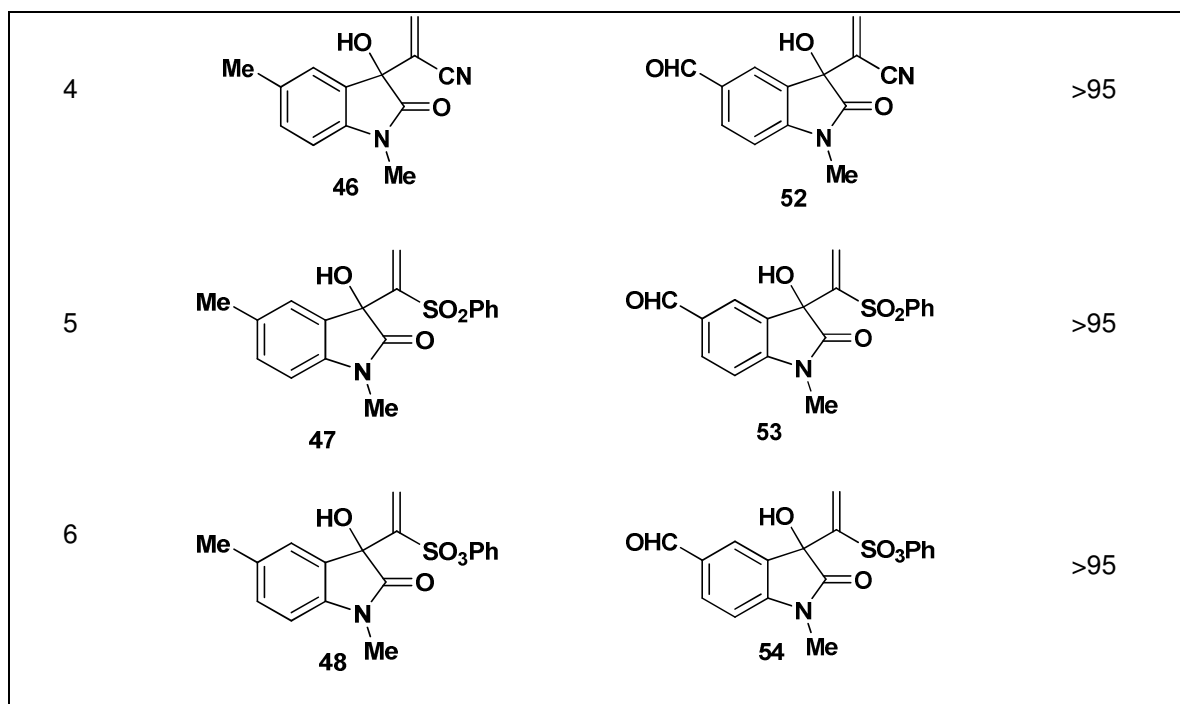
With excellent preliminary results, we were interested in studying the systematic screening of the aromatic alkene oxidation of various 5-methyl MBH adduct isatin derivatives. Thus, we have chosen and prepared a number of *N*-substituted MBH adducts with various activated alkene derivatives.

2.6.6 Substrate scope of CAN oxidation with various activated alkene derived MBH adducts of isatin:

In order to exemplify the generality of CAN mediated aromatic side chain oxidation, we have subjected a number of MBH derivatives **43-48** under the optimized conditions. All reactions underwent smoothly and furnished the corresponding highly functionalized 5-formyl MHB adducts of isatin in excellent yield and the results are given in Table 2.3.

Table-2.3 Generality of CAN oxidation with various activated alkene derived MBH adducts.

Entry	Substrates 43 - 48	Products 49 - 54	Yield (%)
1			>95
2			>95
3			>95



It should be noted that the radical sensitive groups such as ester, nitrile and ketone appended MBH adduct derivative furnished the corresponding oxidized compound in excellent yields without any compensation of rate of the reaction.

For detailed structural characterization, the compound **50** was chosen and established by spectroscopic data analysis. The ^1H NMR spectrum of compound **50** showed a sharp singlet at δ 3.24 ppm which corresponds to *N*-methyl proton and the three aromatic protons and two olefinic protons appeared in the deshielding region at δ 6.55 to 7.88 ppm (Figure 2.6). The ester methylene ($-\text{CO}_2\text{CH}_2$) and the hydroxyl proton resonated as a triplet centered at δ 3.96 ppm and a broad singlet at δ 4.53 ppm, respectively. Remaining aliphatic protons were accounted and appeared in the region at δ 0.87-1.88 ppm. The characteristic aldehyde proton appeared as a singlet at δ 9.84 ppm.

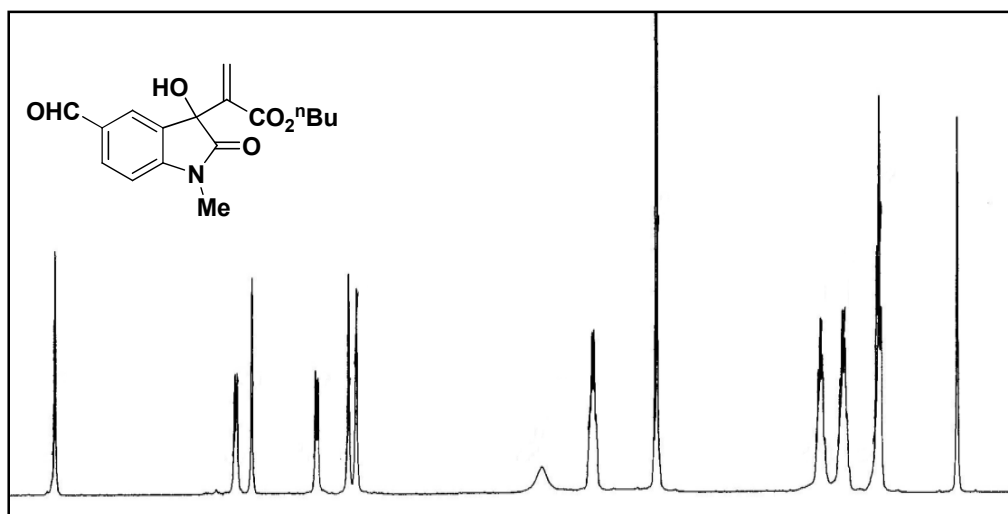


Figure 2.6: ^1H NMR Spectrum of compound **50**

The ^{13}C NMR spectrum of compound **50** showed *N*-methyl carbon appearing at 26.61 ppm (Figure 2.7). The aliphatic *n*-butyl carbons resonated at δ 13.53, 18.87 and 30.23 ppm and the adduct ester methylene carbon ($-\text{CO}_2\text{CH}_2-$) resonated at δ 65.01 ppm. The characteristic isatin quaternary carbon appeared at δ 75.27 ppm and the six aromatic carbons and two olefinic carbons were appeared in the region at δ 108.55-149.97 ppm. The three carbonyl groups *viz.* ester, amide and formyl groups were visible at δ 164.32, 176.76 and 190.73 ppm, respectively.

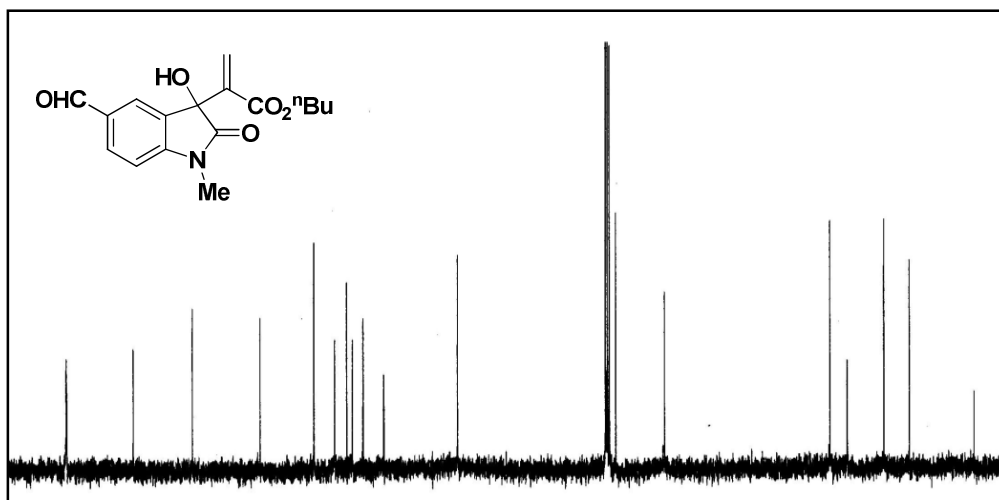


Figure 2.7: ^{13}C NMR Spectrum of compound **50**

Finally, the assigned structure of compound was supported by FAB mass spectrum as it showed a molecular ion $[\text{M}+1]$ peak at $m/z = 318.45$ as against the

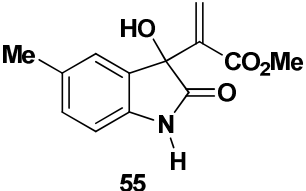
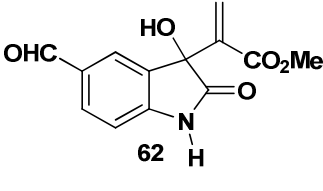
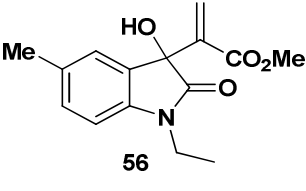
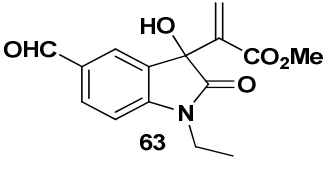
calculated value $m/z = 317.36$. The elemental analysis further supported the synthesized compound **50**.

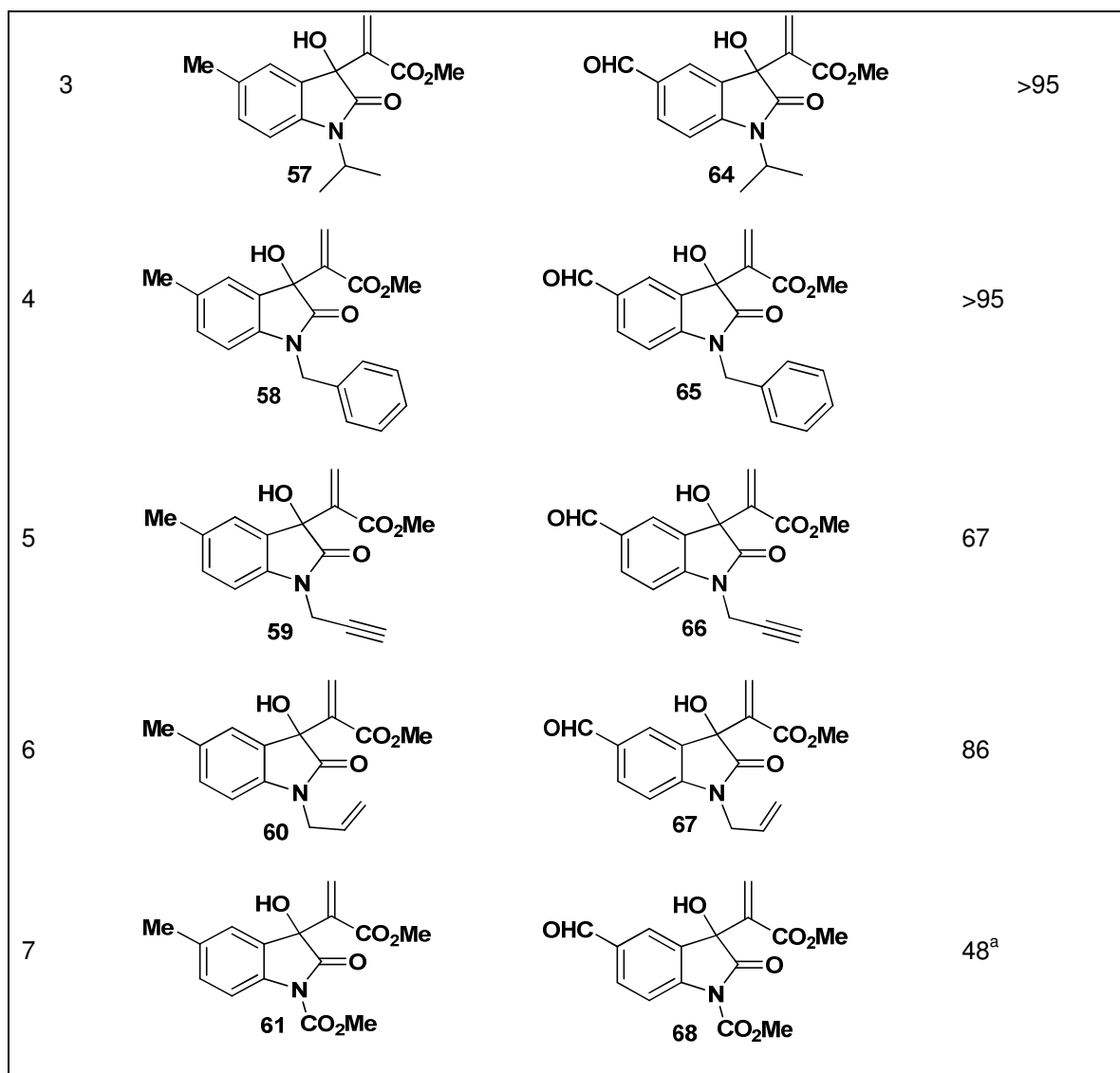
Complete spectroscopic data of all the tabulated compounds were collected in the experimental section. All the above experiments supported that the substitution at the activated alkene part of the MBH adduct of isatin did not have any role in the yield of the side chain oxidation.

2.6.7 Generality of CAN mediated side chain oxidation with various *N*-substituted MBH adduct of isatin:

Systematic screening of various *N*-substituted MBH adduct of isatin furnished the expected product and the results are given in Table 2.4. Unlike the activated alkene derivatives of MBH adduct of isatin, the CAN oxidation of *N*-alkyl derived MBH adducts was slightly affected by the substituent on nitrogen. Specifically, the un-substituted isatin derived MBH adduct **55** and *N*-propargyl, *N*-allyl and *N*-ester derivatives **59-61** provided lesser yields even with prolonged reaction time (Table 2.4, entries 1, 5-7). In the case of *N*-ester derivative along with oxidized product **68**, nitrated product **69** was also observed as an inseparable mixture (1:1 ratio) by silica gel column chromatography with an overall combined yield was 98% (Table 2.4, entry 7). The formation of nitro substituted product is rationalized through a plausible mechanism and is discussed at the end of the chapter.

Table-2.4: Generality of the reaction with various *N*-alkylated MBH adducts.

Entry	Substrates 55 - 61	Products 62 - 68	Yield (%)
1	 <p style="text-align: center;">55</p>	 <p style="text-align: center;">62</p>	87 ^a
2	 <p style="text-align: center;">56</p>	 <p style="text-align: center;">63</p>	>95



^aMixture of two products, over all yield 98%.

The structure of synthesized compound **66** was determined based on the detail of spectroscopic analysis (FTIR, ¹H, ¹³C NMR, and FAB-MS). The FTIR spectrum of compound **66** showed the carbonyl absorptions at 1676, 1710 and 1724 cm⁻¹ due to the presence of aldehyde amide, and ester, respectively. The absorption of hydroxyl group was observed at 3387 cm⁻¹.

In ¹H NMR spectrum, the propargyl terminal proton was visible as a triplet centered at δ 2.33 ppm and the methylene proton appeared as a doublet centered at δ 4.55 ppm with a coupling constant $J = 2.3$ Hz (Figure 2.8). The ester methyl and hydroxyl proton appeared as a singlet and a broad singlet at δ 3.62 ppm and 3.68 ppm, respectively.

The aromatic and olefinic protons resonated in the deshielding region at δ 6.54-7.90 ppm. The characteristic aldehyde proton appeared as a singlet at δ 9.88 ppm.

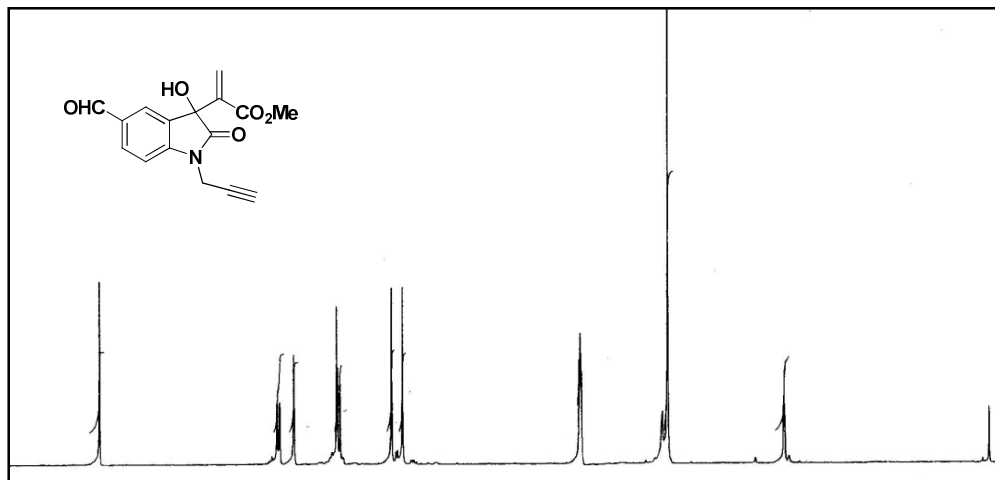


Figure 2.8: ¹H NMR Spectrum of compound 66

The proposed structure was further supported by ¹³C NMR spectrum, which showed a signal at δ 56.42 ppm assigned to ester methyl carbon (Figure 2.9). The characteristic acetylene carbons of propargyl functionality were visible at δ 67.43 ppm and 71.02 ppm, respectively. The *N*-methylene carbon (*N*-CH₂-) and quaternary carbons resonated at δ 29.78 ppm and 75.79 ppm, respectively. The remaining six aromatic carbons, two terminal olefinic carbons were accounted and appeared in the region at δ 109.27-149.53 ppm. The carbonyl functionality of amide, ester and formyl groups appeared at δ 164.37, 178.25 and 198.21 ppm, respectively.

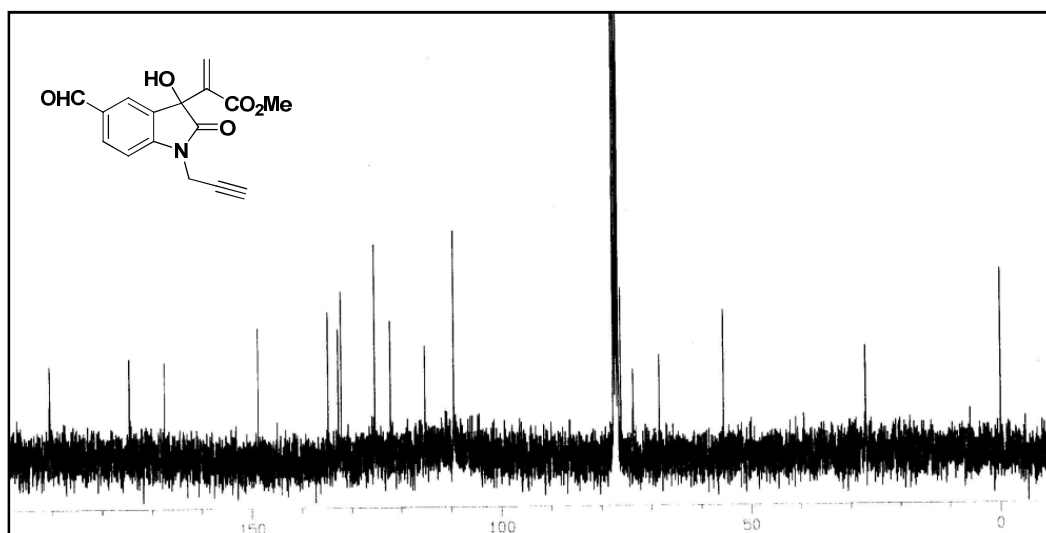
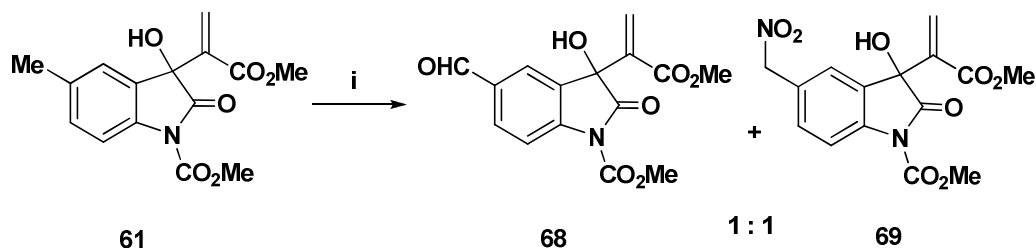


Figure 2.9: ¹³C NMR Spectrum of compound 66

The structure of the compound was supported by FAB mass spectrum showing the [M+1] peak at $m/z = 300.67$ as against calculated value $m/z = 299.06$. The elemental analysis confirmed the assigned structure.

All the *N*-substituted MBH derivatives furnished the 5-formyl MBH adduct under the optimized reaction condition with CAN except *N*-ester MBH adduct (Scheme 2.16). The *N*-ester MBH derivatives **61** furnished the desired product **68** along with 5-methyl nitrated MBH derivatives **69** as a inseparable mixture (1:1 ratio) by silica gel column chromatography in excellent combined yield (>95%). This nitrated derivative characterized by spectroscopic technique and the compound formation has been rationalized through a mechanistic postulate as discussed in the following section.



(i) CAN, MeOH:CH₃CN, rt, 30 min, 95%

Scheme 2.16: Aromatic side chain oxidation of *N*-ester MBH adduct of isatin **61**

The FTIR spectrum of mixture of compounds showed the presence of functional groups such as nitro, aldehyde, ester and amide absorption peaks at 1356, 1678, 1710 and 1726 cm⁻¹, respectively. The hydroxyl group absorption appeared at 3377 cm⁻¹.

In the ¹H NMR spectrum, the *N*-methyl proton of the compounds **68** and **69** merged with each other and appeared as a singlet at δ 3.63 ppm (Figure 2.10). The ester methyl group of compounds **68** and **69** appeared as two separate singlets at δ 4.00 ppm and 4.02 ppm. The characteristic NO₂CH₂- group methyl proton resonated as singlet at δ 5.29 ppm. The compound **68** and **69** aromatic and olefinic protons were accounted and appeared in deshielding region at δ 6.52 -8.12 ppm. The characteristic formyl proton was visible at δ 9.26 ppm.

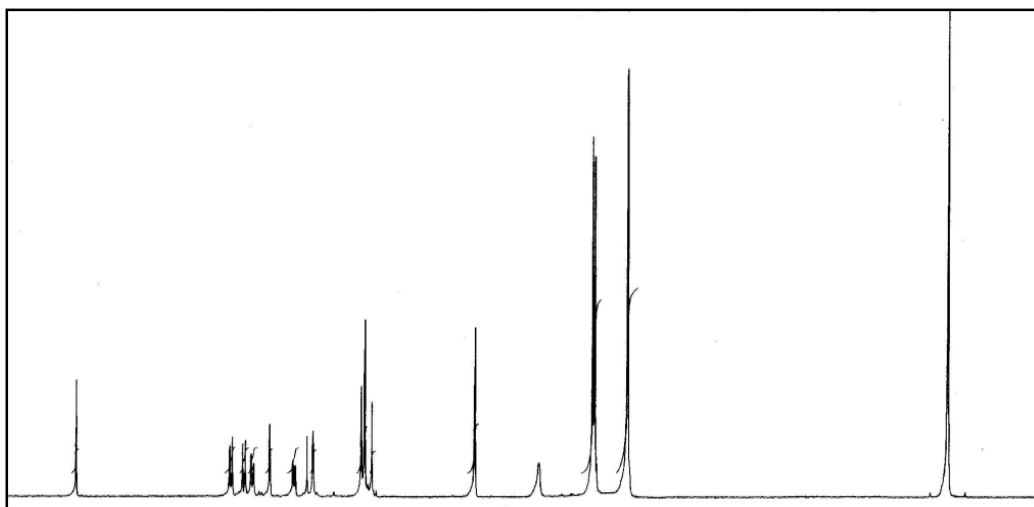


Figure 2.10: ^1H NMR Spectrum of compounds **68** and **69**

The ^{13}C NMR spectrum of the compounds **68** and **69** supported the characterized structure and the nitromethylene (O_2NCH_2 -) carbon appeared at δ 48.35 ppm and the aldehyde carbonyl carbon at δ 196.26 ppm (Figure 2.11). All the remaining carbons were resonated on their respective characteristic region of assigned structures.

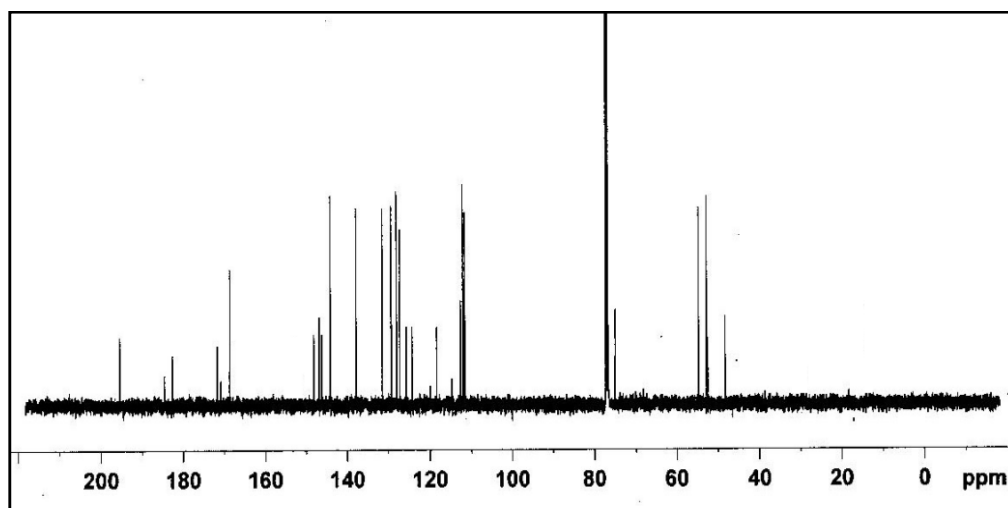


Figure 2.11: ^{13}C NMR Spectrum of compounds **68** and **69**

Finally, the structure of the compounds **68** and **69** were further supported by FAB mass spectrum as it showed the molecular ion $[\text{M}^+]$ and $[\text{M}+1]$ peak at $m/z = 319.17$ and $m/z = 351.29$ corresponding to structure **68** and **69** as against the calculated values $m/z = 319.06$ and $m/z = 350.07$, respectively (Figure 2.12).

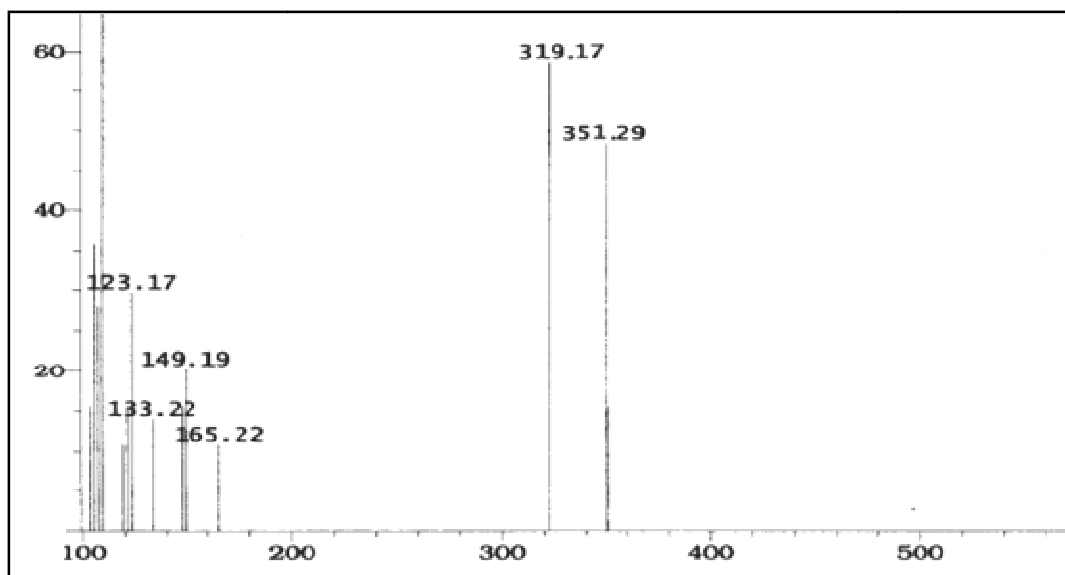
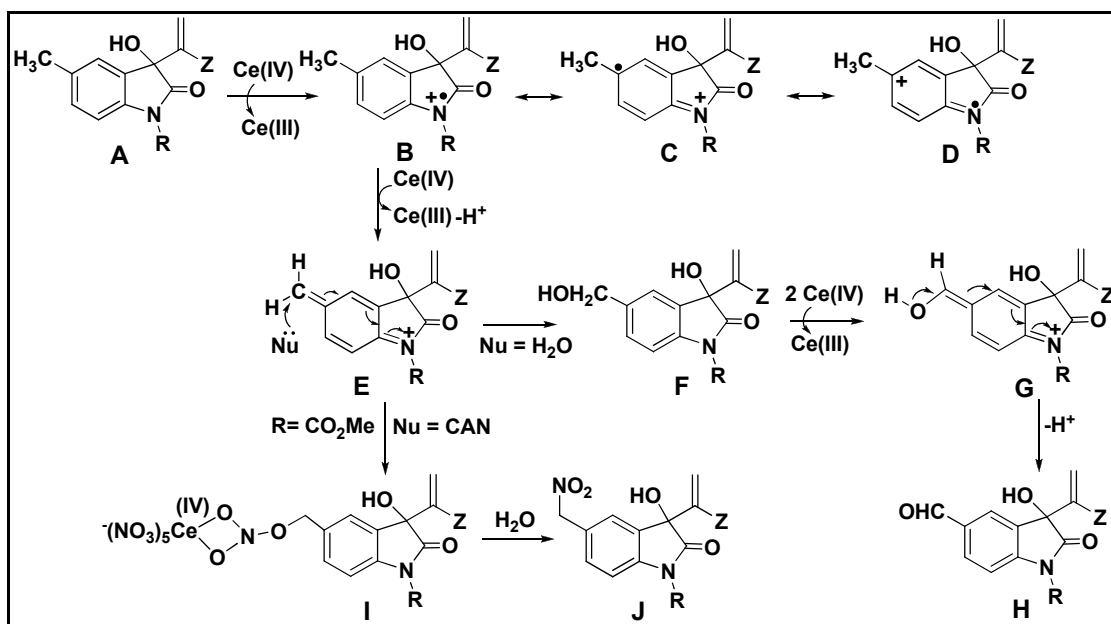


Figure 2.12: FAB Mass spectrum of compounds 68 and 69

2.7 Mechanistic postulates: CAN mediated aromatic side chain oxidation of MBH adduct of isatin:

Initially, the lone pair of electron on the nitrogen atom of MBH adduct of isatin **A** underwent oxidation with 1 equiv. of CAN reagent and generated resonance stabilized radical cation intermediate **B**. This resonance stabilized structure **B** subsequently loses a proton and an electron with second equiv. of CAN to form intermediate **E**. Now the generated intermediate **E** can readily undergoes the nucleophilic attack either with water or CAN reagent based on the electronic environment on the nitrogen of MBH adduct.

The formation of product **J** can be accounted, when **R** = CO₂Me as it diminished the electronic flow toward 5-methyl group through the stabilization of radical at the nitrogen centre. As a result, the third equivalent of CAN helped to cleavage of nitro group of CAN in the MBH adduct. While in the case of **R** = alkane, water undergoes nucleophilic attack with intermediate **E** and furnished the alcohol intermediate [Syper 1966]. The intermediate undergoes further oxidation with two equiv. of CAN furnished the final product **H**. This mechanistic scenario is accounted and it highlights the essential requirement of 4 equiv. of CAN for the side chain oxidation of 5-methyl MBH adduct of isatin (Scheme 2.17).



Scheme 2.17: Mechanistic rationalization of CAN mediated side chain oxidation and nitration of MBH adduct of isatin.

2.8 Conclusions:

- We have developed a mild and efficient synthetic route for the regioselective oxidation of 5-methyl MBH adduct of isatin to 5-formyl MBH adduct of isatin with CAN in an acid free reaction condition.
- The methodology has been demonstrated with a number of substrates. These highly functionalized MBH derivatives can be used as synthon for the synthesis of oxindole core natural products.
- The aromatic side chain oxidation and 5-methyl nitrated product formation are explained *via* plausible reaction mechanism. The number of equivalents of CAN used in the reaction and formation of unexpected product was explained by a mechanistic outlook.
- All the synthesized new compounds were characterized by spectroscopic methods.

2.9 Experimental section:

2.9.1 General considerations:

All the reactions were carried out in oven-dried glassware. Progress of reactions was monitored by Thin Layer Chromatography (TLC) while purification of crude compounds was done by column chromatography using silica gel (100-200 mesh). Melting points were recorded on a Buchi melting point apparatus and are uncorrected. NMR spectra were recorded at 500 and 300 MHz (based on availability of instruments) 125 and 75 MHz (for ^{13}C) respectively on Bruker Avance DPX-500 MHz. and Bruker Avance DPX-300 MHz. Chemical shifts are reported in δ (ppm) relative to TMS (^1H) or CDCl_3 (^{13}C) as internal standards. Mass spectra were recorded using JEOL JMS 600H mass spectrometer. IR spectra were recorded on Bomem MB series FT-IR spectrometer; absorbencies are reported in cm^{-1} . Yields refer to quantities obtained after chromatography.

2.9.2 General experimental procedure for alkylation of isatin:

A mixture of isatin (1 mmol), alkyl bromide/iodide (1.5 equiv.) and calcium hydride (3 equiv.) in DMF was stirred at $60\text{ }^\circ\text{C}$ for 1 hour. After completion of the reaction (monitored by TLC), the crude mixture was diluted with water, neutralized with 2N HCl and extracted using ethyl acetate. The organic layer was separated and dried over anhydrous Na_2SO_4 and concentrated *in vacuo*. The crude product obtained was purified by silica gel chromatography using EtOAc:Hexane (20:80) as eluent to afford the desired *N*-alkyl isatin derivatives in excellent yield (89-95%).

2.9.3 General procedure for the preparation of MBH adducts:

A mixture of *N*-alkyl isatin (1 mmol), activated alkene (1.2 equiv.), DABCO (20 mol %) in EtOH (5 mL) was stirred at room temperature for 3-4 days. After completion of the reaction (monitored by TLC), the reaction mixture was diluted with ethyl acetate. The organic layer was washed successively with 2N HCl, water and brine. The organic layer was separated and dried over (Na_2SO_4) and concentrated *in vacuo*. The crude product obtained was purified by silica gel column chromatography using EtOAc:Hexane (20: 80) as eluent to afford the desired MBH adducts of *N*-alkyl isatin.

2.9.4 Characterization of compounds:

Colourless solid, Mp: 148-150 °C;

R_f : 0.48 (25% EtOAc-Hexane);

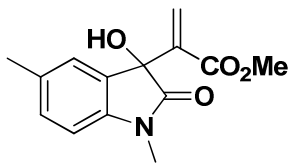
IR (CH₂Cl₂) ν_{\max} : 1615, 1711, 1723, 2856, 3096, 3317 3341cm⁻¹;

¹H NMR (CDCl₃/TMS, 300.1 MHz): δ 2.34 (s, 3H), 2.45 (bs, 1H), 3.26 (s, 3H), 3.72 (s, 3H), 6.41 (s, 1H), 6.56 (s, 1H), 6.88 (d, *J* = 7.80 Hz, 1H), 7.19 (s, 1H), 7.32 (d, *J* = 7.80 Hz, 1H);

¹³C NMR (CDCl₃/TMS, 75.4 MHz): δ 22.73, 24.75, 52.26, 70.55, 110.39, 123.62, 124.13, 128.03, 129.08, 130.72, 139.24, 143.27, 165.33, 176.47;

FAB mass: Calcd. for C₁₄H₁₅NO₄ *m/z* = 261.10; Found: 261.12 (M⁺);

Elemental Analysis: Calcd. for C₁₄H₁₅NO₄: C, 64.36; H, 5.79; N, 5.36; Found: C, 64.35; H, 5.75; N, 5.38.



Compound 31

2.9.5 General procedure for CAN oxidation 5-methyl MBH adduct of isatin:

A mixture of various activated alkene derived MBH adduct (1 mmol), with cerium ammonium nitrate (4.1 equiv.) in MeOH: CH₃CN (1:0.5; 3 mL) was allowed to stir at room temperature for 5–30 min. The progress of the reaction was monitored by TLC. After the completion of the reaction, the solvent was removed under reduced pressure. The crude reaction mixture was extracted with dichloromethane and washed with water and brine. The organic layer was separated and dried over (Na₂SO₄) and concentrated in *vacuo* to afford pure functionalized aldehyde product after passing through a silica gel column chromatography.

2.9.6 Characterization of compounds:

Colourless viscous liquid;

R_f: 0.48 (20% EtOAc-Hexane);

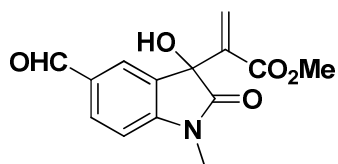
IR (Neat) ν_{\max} : 1607, 1679, 1710, 1725, 2767, 2854, 3095, 3382 cm^{-1} ;

¹H NMR (CDCl_3/TMS , 300.1 MHz): 3.26 (s, 3H), 3.58 (s, 3H), 4.53 (bs, 1H), 6.55 (s, 1H), 6.60 (s, 1H), 6.97 (d, $J = 8.4$ Hz, 1H), 7.66 (s, 1H), 7.83 (d, $J = 8.4$ Hz, 1H), 9.80 (s, 1H);

¹³C NMR (CDCl_3/TMS , 75.4 MHz): 27.21, 52.03, 75.27, 124.65, 130.73, 131.85, 133.70, 133.91, 134.88, 138.72, 149.98, 164.58, 176.85, 190.38;

FAB mass: Calcd. for $\text{C}_{14}\text{H}_{13}\text{NO}_5$ $m/z = 275.07$; Found: 275.48 (M^+);

Elemental Analysis: Calcd. for $\text{C}_{14}\text{H}_{13}\text{NO}_5$: C, 61.09; H, 4.76; N, 5.09; Found: C, 61.06; H, 4.73; N, 5.06.



Compound 32

Colourless viscous liquid;

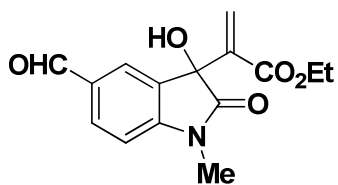
R_f: 0.46 (20% EtOAc-Hexane);

IR (Neat) ν_{\max} : 1611, 1676, 1711, 1728, 2761, 2856, 3096, 3389 cm^{-1} ;

¹H NMR (CDCl_3/TMS , 300.1 MHz): 1.22 (t, $J = 6.2$ Hz, 3H), 3.24 (s, 3H), 4.01 (q, $J = 6.2, 5.5$ Hz, 2H), 4.43 (bs, 1H), 6.51 (s, 1H), 6.56 (s, 1H), 6.86 (d, $J = 7.9$ Hz, 1H), 7.42 (s, 1H), 7.55 (d, $J = 7.9$ Hz, 1H), 9.81 (s, 1H);

¹³C NMR (CDCl_3/TMS , 75.4 MHz): 14.32, 23.65, 52.67, 75.54, 108.23, 124.65, 130.65, 131.34, 133.21, 134.76, 138.72, 149.92, 164.43, 176.56, 190.38;

FAB mass: Calcd. for $\text{C}_{15}\text{H}_{15}\text{NO}_5$ $m/z = 289.09$; Found: 290.48 ($\text{M}+1$);



Compound 49

Elemental Analysis: Calcd. for C₁₅H₁₅NO₅: C, 62.28; H, 5.23; N, 4.84. Found: C, 62.22; H, 5.21; N, 4.80.

Colourless viscous liquid;

R_f: 0.48 (20% EtOAc-Hexane);

IR (Neat) ν_{\max} : 1607, 1673, 1712, 1728, 2771, 2876, 3100, 3391;

¹H NMR (CDCl₃/TMS, 300.1 MHz): 0.87 (t, *J* = 4.2 Hz, 3H), 1.25 (m, 2H), 1.88 (q, *J* = 4.2, 3.5 Hz, 2H), 3.24 (s, 3H), 3.96 (t, *J* = 4.2 Hz, 2H), 4.53 (bs, 1H), 6.55 (s, 1H), 6.64 (s, 1H), 6.98 (d, *J* = 8.5 Hz, 1H), 7.69 (s, 1H), 7.86 (d, *J* = 8.5 Hz, 1H), 9.84 (s, 1H);

¹³C NMR (CDCl₃/TMS, 75.4 MHz): 13.53, 18.87, 26.61, 30.23, 65.01, 75.27, 108.55, 123.99, 128.37, 130.54, 131.83, 134.40, 138.72, 149.97, 164.32, 176.76, 190.73;

FAB mass: Calcd. for C₁₇H₁₉NO₅ *m/z* = 317.36; Found: 318.45 (M+1);

Elemental Analysis: Calcd. for C₁₇H₁₉NO₅: C, 64.34; H, 6.03; N, 4.41; Found: C, 64.32; H, 6.01; N, 4.40.

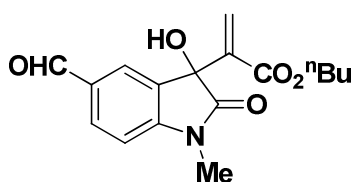
Colourless viscous liquid;

R_f: 0.42 (20% EtOAc-Hexane);

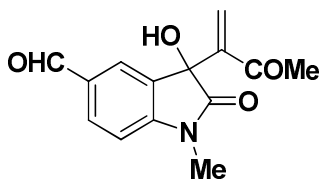
IR (Neat) ν_{\max} : 1612, 1686, 1716, 1724, 2767, 2876, 3086, 3399;

¹H NMR (CDCl₃/TMS, 300.1 MHz): 2.64 (s, 3H), 3.22 (s, 3H), 3.87 (bs, 1H), 6.58 (s, 1H), 6.63 (s, 1H), 6.85 (d, *J* = 8.0 Hz, 1H), 7.41 (s, 1H), 7.65 (d, *J* = 8.5 Hz, 1H), 9.84 (s, 1H);

¹³C NMR (CDCl₃/TMS, 75.4 MHz): 23.24, 31.04, 75.27, 108.75, 123.38, 124.65, 130.73, 131.85, 133.91,



Compound 50



Compound 51

134.88, 148.98, 176.85, 190.34, 192.52;

FAB mass: Calcd. for $C_{14}H_{13}NO_4$ $m/z = 259.34$; Found: 259.12 (M^+);

Elemental Analysis: Calcd. for $C_{14}H_{13}NO_4$: C, 64.86; H, 5.05; N, 5.40. Found : C, 63.66; H, 5.11; N, 5.32.

Colourless viscous liquid;

R_f: 0.44 (20% EtOAc-Hexane);

IR (Neat) ν_{max} : 1611, 1687, 1706, 1726, 2254, 2765, 2967, 3391 cm^{-1} ;

¹H NMR ($CDCl_3/TMS$, 300.1 MHz): 3.29 (s, 3H), 4.55 (bs, 1H), 6.26 (s, 1H), 6.46 (s, 1H), 7.08 (d, $J = 8.1$ Hz, 1H), 7.42 (s, 1H), 7.66 (d, $J = 8.1$ Hz, 1H), 9.93 (s, 1H);

¹³C NMR ($CDCl_3/TMS$, 75.4 MHz): 27.06, 76.01, 105.42, 115.16, 122.14, 125.30, 127.99, 132.11, 132.72, 134.77, 148.69, 174.52, 190.40;

FAB mass: Calcd. for $C_{13}H_{10}N_2O_3$ $m/z = 242.23$; Found: 243.48 ($M+1$);

Elemental Analysis: Calcd. for $C_{13}H_{10}N_2O_3$: C, 64.46; H, 4.16; N, 11.56. Found: C, 63.32; H, 4.09; N, 11.50.

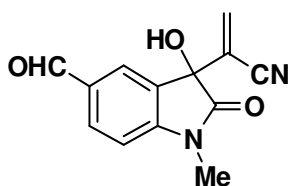
Colourless viscous liquid;

R_f: 0.45 (20% EtOAc-Hexane);

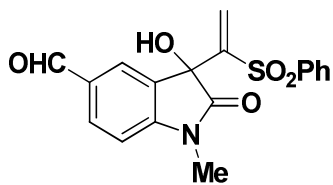
IR (Neat) ν_{max} : 1056, 1613, 1690, 1711, 1727, 2776, 2967, 3391 cm^{-1} ;

¹H NMR ($CDCl_3/TMS$, 300.1 MHz): 3.21 (s, 3H), 4.59 (bs, 1H), 6.45 (s, 1H), 6.53 (s, 1H), 6.99 (m, 3H), 7.35 (m, 3H), 7.42 (d, $J = 7.5$ Hz, 1H), 7.43 (d, $J = 7.5$ Hz, 1H), 9.75 (s, 1H);

¹³C NMR ($CDCl_3/TMS$, 75.4 MHz): 23.46, 75.65, 108.23, 122.61, 125.45, 126.87, 126.91, 128.32, 129.02



Compound 52



Compound 53

(2C), 129.89 (2C), 131.76, 133.43, 133.54, 142.84, 172.45, 191.85;

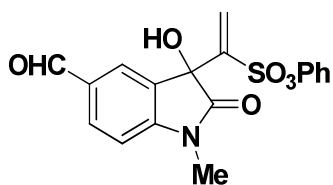
FAB mass: Calcd. for $C_{18}H_{15}NO_5S$ $m/z = 357.06$;
Found: 358.12 (M+1);

Elemental Analysis: Calcd. for $C_{18}H_{15}NO_5S$: C, 60.49;
H, 4.23; N, 3.92. Found: C, 60.01; H, 4.13; N, 3.72.

Colourless viscous liquid;

R_f: 0.43 (20% EtOAc-Hexane);

IR (Neat) ν_{max} : 1370, 1611, 1685, 1712, 1726, 2785, 2967, 3391 cm^{-1} ;



Compound 54

¹H NMR ($CDCl_3/TMS$, 300.1 MHz): 3.22 (s, 3H), 4.42 (bs, 1H), 6.54 (s, 1H), 6.59 (s, 1H), 6.81 (m, 3H), 7.28 (m, 3H), 7.39 (d, $J = 7.5$ Hz, 1H), 7.41 (d, $J = 7.5$ Hz, 1H), 9.87 (s, 1H);

¹³C NMR ($CDCl_3/TMS$, 75.4 MHz): 23.45, 75.35, 108.46, 121.61, 124.32, 124.52 (2C), 125.67, 126.31 (2C), 128.30, 129.89, 131.21, 133.24, 133.56, 143.25, 172.46, 191.36;

FAB mass: Calcd. for $C_{18}H_{15}NO_6S$ $m/z = 373.06$;
Found: 374.25 (M+1);

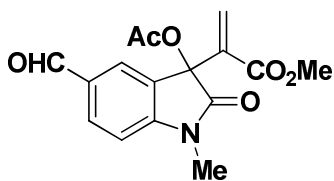
Elemental Analysis: Calcd. for $C_{18}H_{15}NO_6S$: C, 57.90;
H, 4.05; N, 3.75; Found: C, 56.92; H, 3.95; N, 3.76.

2.9.7 Procedure for protection of 3^o-Hydroxyl group of MBH adduct of isatin:

A mixture of MBH adduct of isatin (1 mmol), acetic anhydride (1.5 equiv.) in dry CH_2Cl_2 with dry pyridine (0.3 mmol) was allowed to stir at 0 °C for 4 hour. After the completion of the reaction, the solvent was removed under reduced pressure. The crude reaction mixture was work up with 2N HCl and extracted with dichloromethane and washed with water and brine. The organic layer was separated and dried over

(Na₂SO₄) and concentrated in *vacuo*, to afford pure 3-hydroxyl protected MBH adduct after passing through a silica gel column chromatography.

2.9.8 Characterization of compounds:



Compound 40

Colourless viscous liquid;

R_f: 0.46 (20% EtOAc-Hexane);

IR (Neat) ν_{\max} : 1606, 1681, 1713, 1722, 2765, 2855, 3092, 3387 cm⁻¹;

¹H NMR (CDCl₃/TMS, 300.1 MHz): 2.13 (s, 3H), 3.25 (s, 3H), 3.56 (s, 3H), 6.55 (s, 1H), 6.61 (s, 1H), 6.95 (d, *J* = 8.1 Hz, 1H), 7.66 (s, 1H), 7.83 (d, *J* = 8.1 Hz, 1H), 9.81 (s, 1H);

¹³C NMR (CDCl₃/TMS, 75.4 MHz): 19.23, 27.21, 52.03, 74.24, 123.65, 131.73, 131.86, 133.71, 133.92, 134.87, 138.73, 149.97, 164.38, 166.85, 176.83, 190.35;

FAB mass: Calcd. for C₁₆H₁₅NO₆ *m/z* = 317.09. Found: 317.48 (M⁺);

Elemental Analysis: Calcd. for C₁₆H₁₅NO₆: C, 60.57; H, 4.77; N, 4.41. Found: C, 61.56; H, 4.73; N, 4.39.

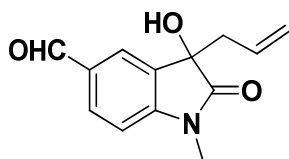
Colourless viscous liquid;

R_f: 0.44 (25% EtOAc-Hexane);

IR (CH₂Cl₂): ν_{\max} : 1343, 1476, 1481, 1634, 1725, 1781, 2938 cm⁻¹;

¹H NMR (CDCl₃/TMS, 500.1 MHz): 3.27 (s, 3H), 3.62 (m, 1H), 3.79 (m, 1H), 5.09 (d, *J* = 10.5 Hz, 1H), 5.15 (d, *J* = 10.5 Hz, 1H), 5.82 (m, 1H), 6.85 (d, *J* = 7.5 Hz, 1H), 7.03 (d, *J* = 7.5 Hz, 1H), 7.10 (s, 1H), 9.81 (s, 1H);

¹³C NMR(CDCl₃/TMS, 125.7 MHz): δ 26.43, 41.89, 80.28, 108.30, 116.75, 122.82, 126.87, 128.25, 130.39,



Compound 43

134.01, 145.31, 164.70, 174.19;

FAB mass: Calcd. for $C_{13}H_{13}NO_3$ $m/z = 231.09$; Found: 232.32 (M+1);

Elemental Analysis: Calcd. for $C_{13}H_{13}NO_3$: C, 67.52; H, 5.67; N, 6.06; Found: C, 67.56; H, 5.53; N, 6.02.

2.9.9 General procedure for CAN oxidation reaction of N-alkylated MBH adduct of isatin:

A mixture of various N-alkyl derived MBH adduct (1 mmol), 4.1 equiv. of cerium ammonium nitrate in MeOH: CH_3CN (1:0.5; 3 mL) was allowed to stir at room temperature for 5–30 min. The progress of the reaction was monitored by TLC. After the completion of the reaction, the solvent was removed under reduced pressure. The crude reaction mixture was extracted with dichloromethane and washed with water and brine. The organic layer was separated and dried over (Na_2SO_4) and concentrated in *vacuo* to afford pure functionalized aldehyde after passing through a silica gel column chromatography.

2.9.10 Procedure for protection of 3^o-Hydroxyl group of MBH adduct of isatin:

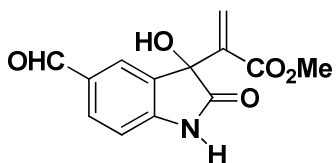
A mixture of MBH adduct of isatin (1 mmol), acetic anhydride (1.5 equiv.) in dry CH_2Cl_2 with dry pyridine (0.3 mmol) was allowed to stir at 0 °C for 4 hour. After the completion of the reaction, the solvent was removed under reduced pressure. The crude reaction mixture was work up with 2N HCl and extracted with dichloromethane and washed with water and brine. The organic layer was separated and dried over (Na_2SO_4) and concentrated in *vacuo*, to afford pure 3-hydroxyl protected MBH adduct after passing through a silica gel column chromatography.

2.9.11 Characterization of compounds:

Colourless viscous liquid;

R_f: 0.46 (20% EtOAc-Hexane);

IR (Neat) ν_{max} : 1606, 1680, 1706, 1726, 2768, 2854, 3095, 3382, 3492 cm^{-1} ;



Compound 62

¹H NMR (CDCl₃/TMS, 300.1 MHz): 3.59 (s, 3H), 4.07 (bs, 1H), 6.54 (s, 1H), 6.61(s, 1H), 7.04 (d, *J* = 7.5 Hz, 1H), 7.63 (s, 1H), 7.68 (d, *J* = 7.5 Hz, 1H), 8.21(s, 1H), 9.87 (s, 1H);

¹³C NMR (CDCl₃/TMS, 75.4 MHz): 52.32, 75.02, 108.23, 121.23, 123.64, 126.32, 131.31, 137.75, 139.25, 142.05, 162.26, 174.56, 192.82;

FAB mass: Calcd. for C₁₃H₁₁NO₅ *m/z* = 261.06; Found: 262.56 (M+1);

Elemental Analysis: Calcd. for C₁₃H₁₁NO₅: C, 59.77; H, 4.24; N, 5.36. Found: C, 58.13; H, 4.13; N, 5.16.

Colourless viscous liquid;

R_f: 0.44 (20% EtOAc-Hexane);

IR (CH₂Cl₂): 1607, 1675, 1710, 1728, 2768, 2890, 3386 cm⁻¹;

¹H NMR (CDCl₃/TMS, 300.1 MHz): 1.32 (t, *J* = 6.4 Hz, 3H), 3.60 (s, 3H), 3.82 (q, *J* = 6.4 Hz, 2H), 4.36 (bs, 1H), 6.57 (s, 1H), 6.63 (s, 1H), 7.00 (d, *J* = 8.0 Hz, 1H), 7.69 (s, 1H), 7.85 (d, *J* = 8.0 Hz, 1H), 9.83 (s, 1H);

¹³C NMR (CDCl₃/TMS, 75.4 MHz): 11.51, 35.75, 52.07, 75.28, 108.82, 123.60, 124.84, 128.44, 130.74, 131.66, 138.58, 149.26, 164.67, 176.38, 190.63;

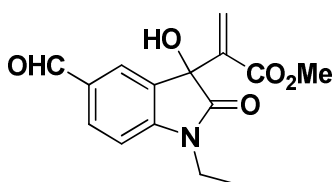
FAB mass: Calcd. for C₁₅H₁₅NO₅ *m/z* = 289.28; Found: 290.59 (M+1);

Elemental Analysis: Calcd. for C₁₅H₁₅NO₅: C, 62.28; H, 5.23; N, 4.84; Found: C, 61.16; H, 5.22; N, 4.23.

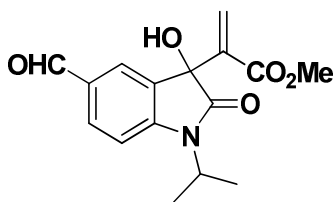
Colourless viscous liquid;

R_f: 0.43 (20% EtOAc-Hexane);

IR (Neat) *v*_{max}: 1606, 1678, 1710, 1728, 2772, 2890,



Compound 63



Compound 64

2900, 3386 cm^{-1} ;

$^1\text{H NMR}$ (CDCl_3/TMS , 300.1 MHz): 1.53 (d, $J = 7.8$ Hz, 6H), 3.60 (s, 3H), 4.28 (bs, 1H), 4.58 (sep, $J = 7.8$, 7.4 Hz, 1H), 6.56 (s, 1H), 6.60 (s, 1H), 7.11 (d, $J = 8.16$ Hz, 1H), 7.63 (s, 1H), 7.86 (d, $J = 8.16$ Hz, 1H), 9.81 (s, 1H);

$^{13}\text{C NMR}$ (CDCl_3/TMS , 75.4 MHz): 21.05 (2C), 42.31, 53.64, 75.63, 109.23, 121.76, 123.64, 126.89, 131.34, 137.46, 139.74, 142.23, 162.22, 174.54, 192.18;

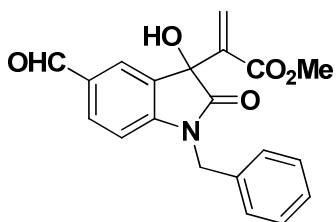
FAB mass: Calcd. for $\text{C}_{16}\text{H}_{17}\text{NO}_5$ $m/z = 303.11$; Found: 303.25 (M^+);

Elemental Analysis: Calcd. for $\text{C}_{16}\text{H}_{17}\text{NO}_5$: C, 63.36; H, 5.65; N, 4.62; Found: C, 62.24; H, 5.45; N, 4.36.

Colourless viscous liquid;

R_f: 0.48 (20% EtOAc-Hexane);

IR (Neat) ν_{max} : 1607, 1668, 1716, 2771, 2878, 3100, 3386 cm^{-1} ;



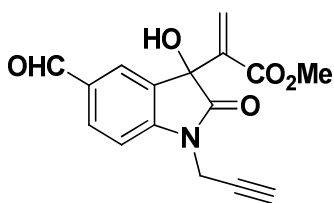
Compound 65

$^1\text{H NMR}$ (CDCl_3/TMS , 300.1 MHz): 3.60 (s, 3H), 4.28 (bs, 1H), 4.58 (m, 2H), 6.56 (s, 1H), 6.60 (s, 1H), 7.11 (m, 3H), 7.46 (m, 2H), 7.62 (m, 3H), 9.81 (s, 1H);

$^{13}\text{C NMR}$ (CDCl_3/TMS , 75.4 MHz): 42.23, 52.43, 74.98, 109.31, 121.24, 122.05, 123.66 (2C), 123.79, 124.29 (2C), 124.75, 125.79, 131.01, 132.56, 133.23, 133.67, 162.36, 174.33, 191.82;

FAB mass: Calcd. for $\text{C}_{20}\text{H}_{17}\text{NO}_5$ $m/z = 351.11$; Found: 352.32 ($\text{M}+1$);

Elemental Analysis: Calcd. for $\text{C}_{20}\text{H}_{17}\text{NO}_5$: C, 68.37; H, 4.88; N, 3.99. Found: C, 67.97; H, 4.45; N, 3.76.



Compound 66

Colourless viscous liquid;

R_f: 0.48 (20% EtOAc-Hexane);

IR (Neat) ν_{\max} : 1607, 1676, 1710, 1724, 2268, 2771, 2890, 3306, 3387 cm^{-1} ;

¹H NMR (CDCl_3/TMS , 300.1 MHz): 2.33 (t, $J = 2.3$ Hz, 1H), 3.62 (s, 3H), 3.68 (bs, 1H), 4.55 (d, $J = 2.3$ Hz, 2H), 6.54 (s, 1H), 6.66 (s, 1H), 7.24 (d, $J = 8.1$ Hz, 1H), 7.74 (s, 1H), 7.90 (d, $J = 8.1$ Hz, 1H), 9.88 (s, 1H);

¹³C NMR (CDCl_3/TMS , 75.4 MHz): 29.78, 56.42, 67.43, 71.02, 75.79, 109.27, 117.35, 123.67, 127.56, 133.76, 134.57, 138.23, 149.53, 164.37, 178.25, 198.21.

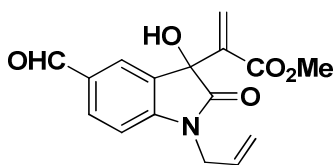
FAB mass: Calcd. for $\text{C}_{16}\text{H}_{13}\text{NO}_5$ $m/z = 299.06$; Found: 300.67 ($M+1$);

Elemental Analysis: Calcd. for $\text{C}_{16}\text{H}_{13}\text{NO}_5$: C, 64.21; H, 4.38; N, 4.68; Found: C, 63.91; H, 4.14; N, 4.46.

Colourless viscous liquid;

R_f: 0.48 (20% EtOAc-Hexane);

IR (Neat) ν_{\max} : 1608, 1667, 1715, 2772, 2878, 3103, 3389 cm^{-1} ;



Compound 67

¹H NMR (CDCl_3/TMS , 300.1 MHz): 3.57 (s, 3H), 4.23 (bs, 1H), 4.38 (m, 1H), 4.49 (m, 1H), 5.09 (d, $J = 10.5$ Hz, 1H), 5.16 (d, $J = 10.5$ Hz, 1H), 5.82 (m, 1H), 6.59 (s, 1H), 6.61 (s, 1H), 6.85 (d, $J = 7.5$ Hz, 1H), 7.02 (s, 1H), 7.10 (d, $J = 7$ Hz, 1H), 9.82 (s, 1H);

¹³C NMR (CDCl_3/TMS , 75.4 MHz): 42.91, 51.89, 74.98, 108.30, 116.75, 122.82, 124.14, 126.87, 128.25, 130.39, 134.01, 138.03, 145.31, 164.70, 174.19, 191.20;

FAB mass: Calcd. for $\text{C}_{16}\text{H}_{15}\text{NO}_5$ $m/z = 301.09$; Found: 301.45 (M^+);

Elemental Analysis: Calcd. for $\text{C}_{16}\text{H}_{15}\text{NO}_5$: C, 63.78;

H, 5.02; N, 4.65; Found: C, 62.88; H, 4.91; N, 4.61.

Colourless viscous liquid;

R_f: 0.45 (25% EtOAc-Hexane);

IR (Neat): 1356, 1546, 1609, 1678, 1726, 2776, 2856, 3377 cm⁻¹;

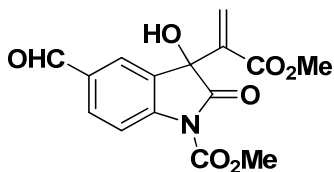
¹H NMR (CDCl₃/TMS, 300.1 MHz): 3.63 (s, 6H), 4.00 (s, 3H), 4.02 (s, 3H), 4.26 (bs, 2H), 5.29 (s, 2H), 6.58 (m, 4H), 7.19 (s, 1H), 7.41 (m, 1H), 7.68 (s, 1H), 7.86 (m, 1H), 7.89 (m, 1H), 8.12 (m, 1H), 9.26 (s, 1H);

¹³C NMR (CDCl₃/TMS, 75.4 MHz): 48.35, 52.53 (2C), 52.75 (2C), 75.91, 76.01, 111.60, 112.05, 112.62, 114.71, 118.35, 124.29, 125.71, 127.27, 128.07, 129.34, 131.47, 137.85, 144.18, 146.24, 146.92, 148.17, 168.65 (2C), 171.23, 173.25, 182.31, 184.65, 196.26;

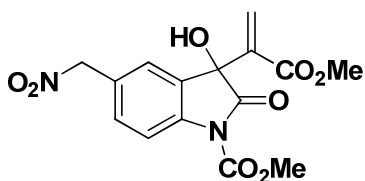
FAB mass: Calcd. for C₁₅H₁₃NO₇ *m/z* = 319.06; Found: 319.17 (M⁺);

FAB mass: Calcd for C₁₅H₁₄N₂O₈ *m/z* = 350.07; Found: 351.29 (M+1);

Elemental Analysis: Calcd. for C₂₉H₂₇N₃O₁₅: C, 52.97; H, 4.14; N, 6.39; Found: C, 52.81; H, 4.11; N, 6.12.



Compound 68

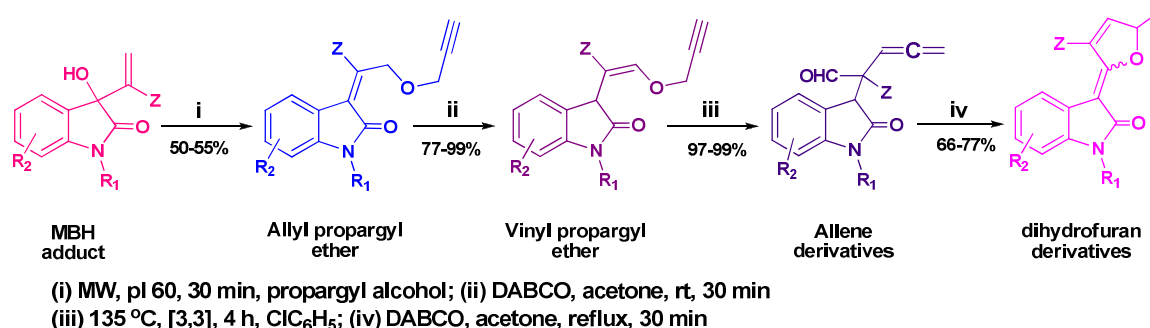


Compound 69

Chapter III

Abstract:

Synthesis of highly functionalized allene appended oxindoles derivatives from vinyl propargyl ether derivatives of Morita-Baylis-Hillman adducts of isatin *via* Claisen rearrangement has been achieved. Synthetic utility of allene derivatives obtained have been demonstrated with the synthesis of methyl 2,5-dihydro-5-methyl-2-(1-methyl-2-oxindolin-3-ylidene)furan-3-carboxylates in one-pot cyclization reaction under basic condition. A plausible mechanism of the reaction is described.



Shanmugam, P. *et al. Synlett.* 2012, 23, 278-284

Synthesis of Highly Functionalized Allene and Dihydrofuran Appended Oxindoles *via* Claisen Rearrangement and Base Induced Cyclization

3.1 Introduction:

The discovery of the Claisen rearrangement nearly a century ago offered a potentially useful synthetic tool to the organic chemist. Over the decades this usefulness has been realized and the reaction has drawn the attention of numerous research groups, which has been reflected in a number of papers published on this topic. [Dong, D. -J. *et al.* 2011; Hordern, B. K. 2010; Chen, Z. -H. *et al.* 2011; Knowles, R. R. *et al.* 2011]. Reactions that occur in tandem or generate functionality that is easily transformed in sequential processes provide an opportunity to rapid increase of complexity in organic structures. Use of the Claisen rearrangement reaction [Ziegler, F. E. 1977; 1988; Lutz, R. P. 1984; Ito, H. 1999] in these sequence with other processes such as the Heck reaction [Dounay, A. B. *et al.* 2003], Morita–Baylis–Hillman (MBH) [Basavaiah, D. *et al.* 2003], cycloaddition [Herndon, W. C. 1972], metathesis, and free radical reactions have greatly enhanced its value [Basset, J-M. *et al.* 2010; Ryu, I. *et al.* 1996]. An added advantage, the highly functionalized oxindoles frame work incorporated MBH adduct involved reaction are important and the resulted compounds were closely related to the numerous pharmacological structures [Smith, C. D. *et al.* 1995; Zhang, X. *et al.* 1996]. Hence, combined utilization of propargyl isomerized MBH isatin derivatives and Claisen rearrangement protocol would provide highly functionalized products which can be a new class of synthons for further synthetic modification. The synthesis of isolable allene derivatives from the propargyl derivatives is well documented and also utilized as active intermediate in a number of synthetic transformations. [Fandrick, D. R. *et al.* 2009; Zhou, H. *et al.* 2011]. To realize these themes, we synthesized molecules with consecutive two stereogenic centered, highly functionalized, allene appended oxindoles framework from MBH adduct of isatin *via* a classical [3,3]-Claisen rearrangement and

they are presented in this chapter. In addition, we dealt with the highly functionalized allene appended oxindoles framework for the synthesis dihydrofuran appended oxindole derivatives *via* base induced intramolecular cyclization process.

3.1.1 Claisen rearrangement:

The Claisen rearrangement reaction exhibits all the essential properties required by a synthetic procedure to be considered as efficient: it can be chemo-, regio-, diastereo-, and enantioselective, can be performed under mild conditions and affords potentially useful multi-functionalized molecules. The term “Claisen rearrangement” was originally applied to rearrangements of allyl aryl ethers to afford *ortho*- and occasionally *para*-substituted phenols [Woodward, R. B. *et al.* 1969]. Initially, a synchronic evolution for the Claisen rearrangement reactions through aromatic transition state was accepted, formed by a combination of π and σ overlap of 2p atomic orbitals of the carbon atoms of both the allyl fragments. Afterwards it was expanded to analogue rearrangement such as allyl vinyl derivatives into unsaturated carbonyl compounds, which is classified as [3,3]-sigmatropic rearrangement (Figure 3.1).

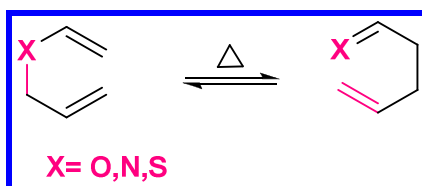


Figure 3.1: *General representation of allyl vinyl analogue of Claisen rearrangement reaction.*

It was concluded that the transformation of allyl vinyl ethers into unsaturated carbonyl compounds has been formed out of the two feasible transition states, the reaction proceeded through either chair like intermediates **A** or boat like intermediates **B** (Figure 3.2) [Doering, W. v. E. *et al.* 1962]. The formation of transition state in this reaction can also be controlled by the substitution on reactant and catalytic system involved in the reaction. According to the Woodward-Hoffmann rules for [3,3]-sigmatropic reactions, both transition states **A** and **B** are the only ones corresponding to *supra-supra* processes and therefore symmetry allowed process under thermal condition.

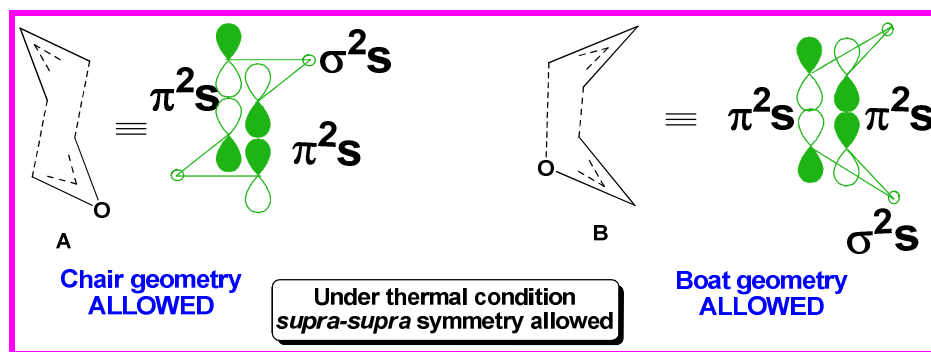


Figure 3.2: Pictorial representation of Claisen rearrangement transition states and orbital interactions.

The interest generated by the Claisen rearrangement prompted the development of a considerable number of diverse and *analogue* versions of [3,3]-sigmatropic rearrangement. Among them, a few of the most noteworthy [3,3]-sigmatropic rearrangement reactions are highlighted as follows.

- Carroll rearrangement
- Johnson-Claisen Rearrangement
- Ireland-Claisen Rearrangement
- Eschenmoser Rearrangement
- Reformatsky-Claisen Rearrangement
- Aza-Claisen rearrangement
- Retro-Claisen Rearrangement.

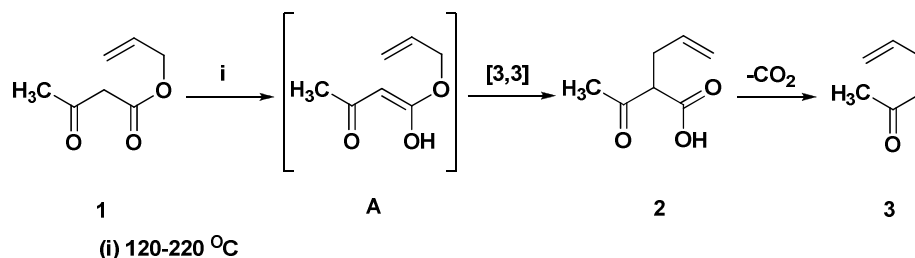
All the above Claisen rearrangements were categorized, based on the substrate selection or catalytic system used in the rearrangement. However, in the case of Retro-Claisen rearrangement reaction, the controlling factor is the stability of the products [Rhoads, S. J. *et al.* 1969].

3.2 Types of [3,3]-sigmatropic Claisen rearrangements:

This section deals with a brief introductory discussion on types of Claisen rearrangements and a literature survey on Claisen rearrangement reactions using vinyl propargyl ethers as starting materials.

3.2.1 Carroll rearrangement:

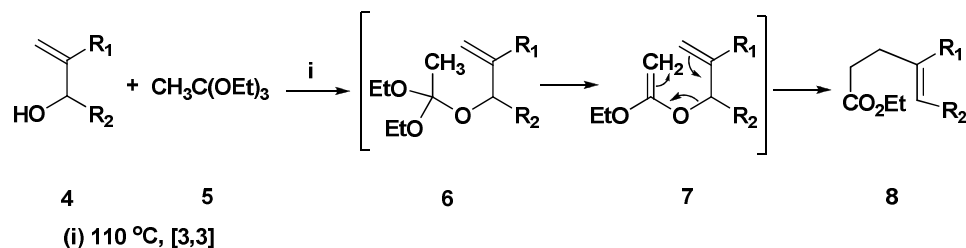
The Carroll reaction, initially described in 1940, is a thermal rearrangement of allyl β -ketoester **1** followed by decarboxylation to yield γ,δ -unsaturated ketone **3** (Scheme 3.1) [Carroll, M. F. 1940]. This reaction has not been widely developed due to the drastic reaction condition required to perform the transformation (temperatures of 120-220 °C after *in-situ* preparation of the β -ketoester).



Scheme 3.1: Carroll rearrangement reaction.

3.2.2 Johnson-Claisen rearrangement:

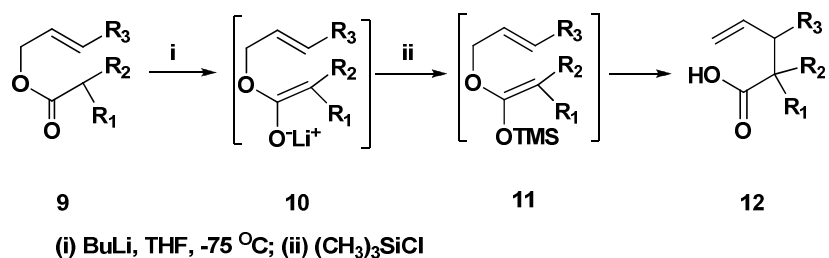
During the year 1970, the first Johnson rearrangement was reported and the reaction afforded *trans*-trisubstituted alkenes **8**, originally described as the process consisting of heating of an allylic alcohol **4** with an excess of ethyl orthoacetate **5** in the presence of trace amounts of a weak acid (typically propionic acid) [Johnson, W. S. *et al.* 1970]. The initially formed mixed ortho ester **6** loses ethanol to generate the ketene acetal **7**, which undergoes rearrangement leading to γ,δ -unsaturated ester **8** (Scheme 3.2).



Scheme 3.2: Johnson-Claisen rearrangement reaction.

3.2.3 Ireland- Claisen rearrangement:

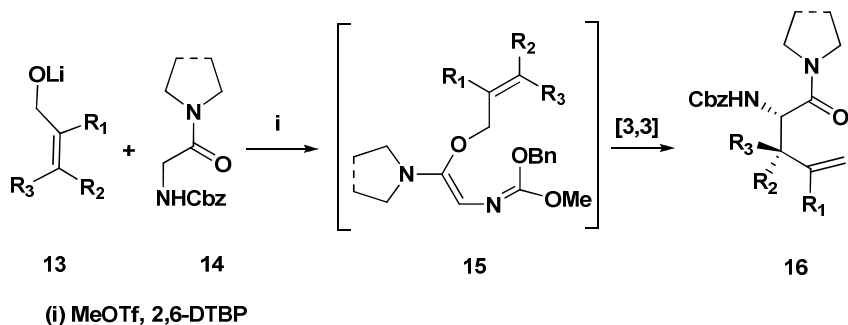
In 1972, Ireland *et al.* reported the rearrangement of allyl trimethylsilyl ketene acetal **11**, prepared by the reaction of allylic ester enolate **10** with trimethylsilyl chloride to yield γ,δ -unsaturated carboxylic acid **12** (Scheme 3.3) [Ireland, R. E. *et al.* 1972; 1976]. As compared with other reported rearrangements, this reaction proceeds under either mild basic or neutral reaction conditions.



Scheme 3.3: Ireland-Claisen rearrangement reaction.

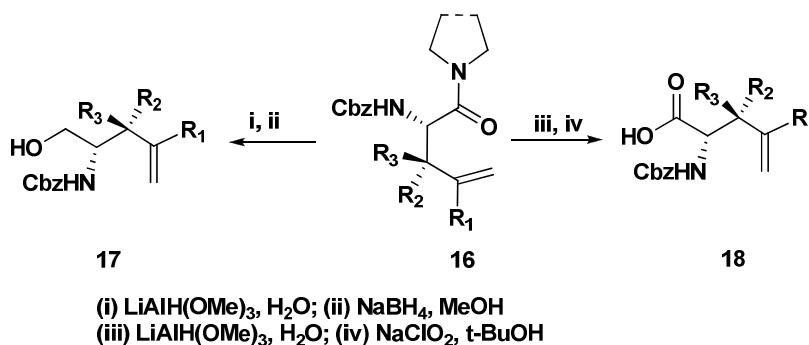
3.2.4 Synthesis of enantio-enriched amino acid derivatives via Eschenmoser-Claisen rearrangement:

In 2006, Qu *et al.* reported anti- β -substituted γ,δ -unsaturated amino acid derivative **16** via the Eschenmoser-Claisen rearrangement with excellent diastereoselectivity [Qu, H. *et al.* 2006]. The synthesis of anti- β -substituted amino acid derivative **16** with terminal olefin was difficult via usual Claisen rearrangement strategy (Scheme 3.4).



Scheme 3.4: Eschenmoser-Claisen rearrangement reaction.

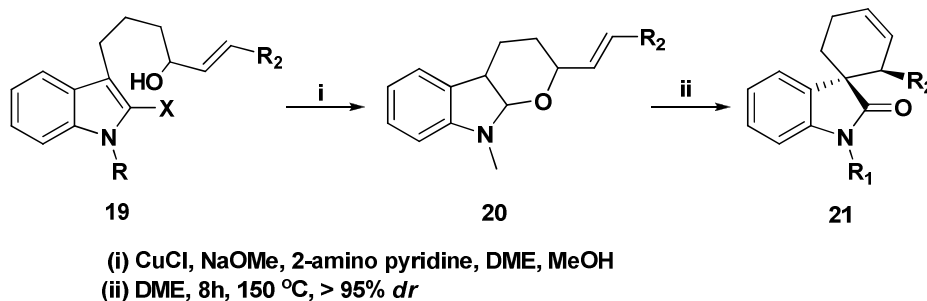
The hydrolysis of the rearranged amide **16** was a tricky step due to the presence of a terminal double bond and the *N*-Cbz protecting group, which was achieved by reductive hydrolysis offered the amino alcohol **17** and amino acid derivative **18** (Scheme 3.5) [Groves, J. T. *et al.* 1979; Gassmart, P. C. *et al.* 1976; Moghaddam, F. M. *et al.* 2001].



Scheme 3.5: Synthesis of anti- β -substituted γ,δ -unsaturated amino acids derivatives.

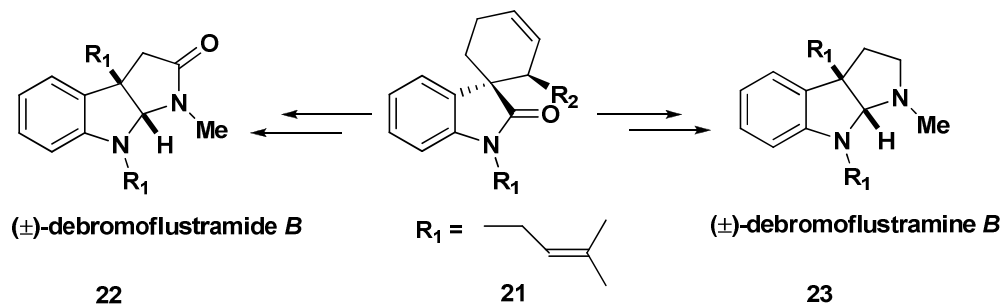
3.2.5 Total synthesis of (\pm)-debromoflustramine *B* and *E* and (\pm)-debromoflustramide *B* via Claisen rearrangement:

In 2006, Miyamoto *et al.* have shown one-pot diastereoselective formation of 3-spiro-2-oxindole derivative **21** via intramolecular Ullmann coupling (IUC) and Claisen rearrangement reaction from haloindole derivative **19** (Scheme 3.6) [Miyamoto, H. *et al.* 2006]. The IUC is a low-cost method for the preparation of the rearrangement precursors, alkenyl pyranoindoles **20**. The Claisen rearrangement of the pyranoindoles proceeded smoothly to spirocyclic oxindoles derivative **21** in good yield in a diastereoselective manner.



Scheme 3.6: Diastereoselective synthesis of spirocyclic compound.

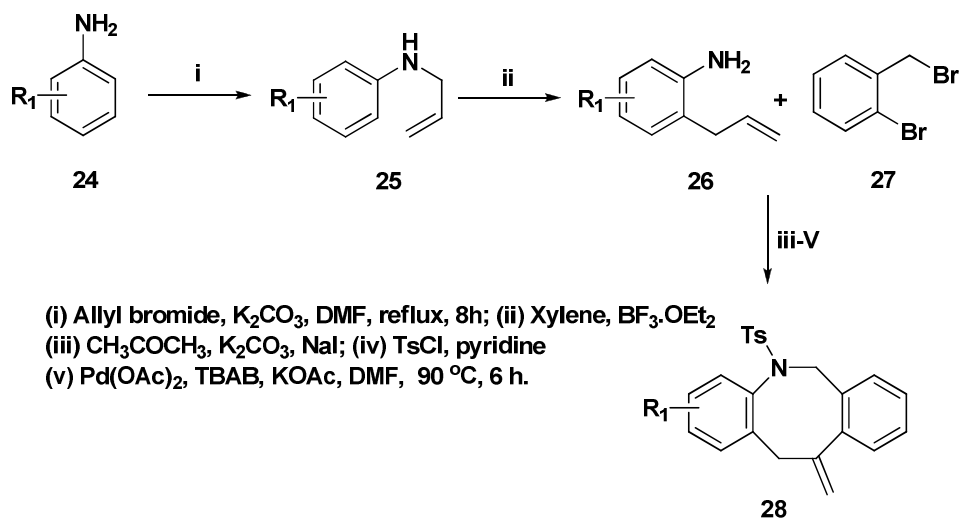
The synthesized spirocyclic oxindole **21** has been used as a common precursor for the synthesis (\pm)-debromoflustramine **B** **23** and lactam derivative **22** (Scheme 3.7) [Miyamoto, H. *et al.* 2007].



Scheme 3.7: Synthesis of (\pm)-debromoflustramine derivatives.

3.2.6 Aza-Claisen rearrangement:

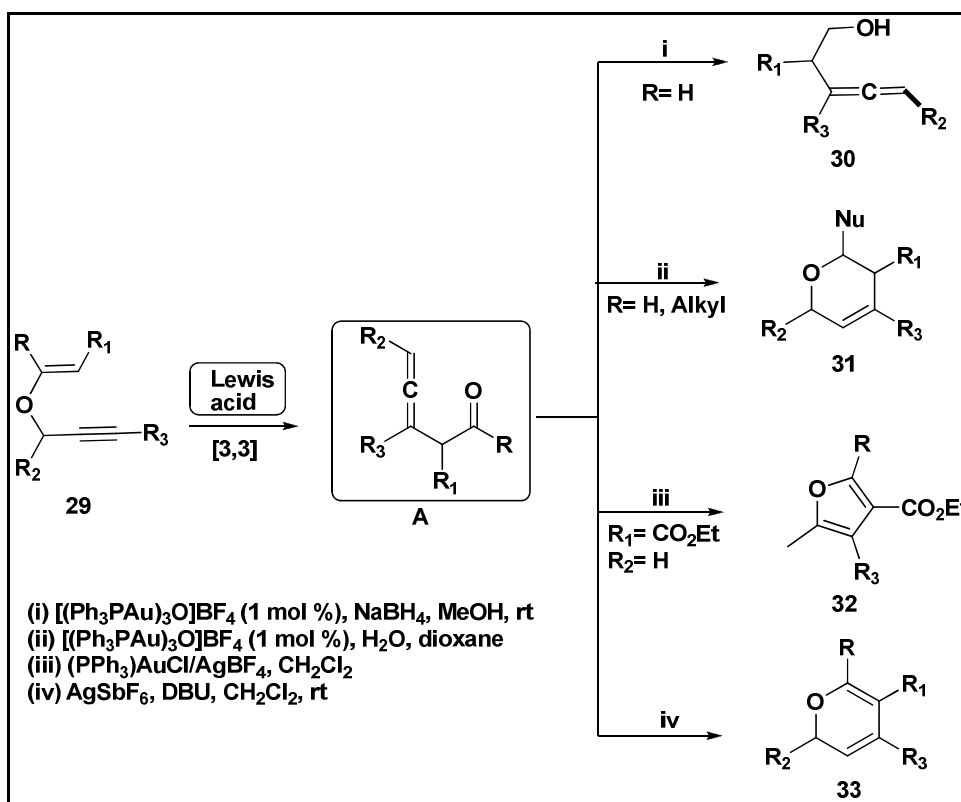
In general, the palladium catalyzed synthesis of medium-sized nitrogen heterocycles by the implementation of intramolecular Heck reactions are rare and require harsh reaction condition [Ribiere, P. *et al.* 2006; Declerck, V. *et al.* 2007; Vasudevan, A. *et al.* 2006]. Majumdar *et al.* have reported the synthesis of various 8-*exo*-azocine derivatives **28** via aza-Claisen rearrangement and followed by the intramolecular Heck reaction (Scheme 3.8) [Majumdar, K. C. *et al.* 2009]. This aza-Claisen rearrangement followed by intramolecular Heck reaction provided single azocine derivatives in a facile manner.



Scheme 3.8: Synthesis of 8-*exo*-azocine derivative.

3.2.7 Characteristic reactions of vinyl propargyl ether:

The vinyl propargyl ether **29** has been conveniently utilized as a precursor to construct various heterocyclic frameworks by a number of research groups [Binder, J. T. *et al.* 2006]. The pioneer work on vinyl propargyl ether has expanded *via* Claisen rearrangement by Toste and Kirsch and their co-workers separately. Toste *et al.* reported Au(I) catalyzed enatio-enriched synthesis of homoallenic alcohol **30** *via* Claisen rearrangement through oxocarbenium intermediate from racemic vinyl propargyl ether (Scheme 3.9) [Sherry, B. D. *et al.* 2004; 2006]. The same group utilized proposed oxocarbenium intermediate as precursor and reported dihydropyran derivative **31** *via* nucleophilic addition. Kirsch *et al.* have also utilized the vinyl propargyl ether **27** as starting material for the synthesis of dihydropyran **33** and tetra substituted furan derivative **32** *via* metal salt catalyzed Claisen rearrangement and base induced cyclization [Suhre, M. H. *et al.* 2005; Menz, H. *et al.* 2006].



Scheme 3.9: Synthetic utility of vinyl propargyl ether derivative **29**.

3.3 Objective of the work:

Literature survey reveals that the Claisen rearrangement is an important synthetic tool for the organized modification over the required chemical structures, new C-X bond formation, intramolecular cyclization and generating carbonyl and amine functionalities. Claisen rearrangement with vinyl propargyl ethers have furnished isolable, functionalized allene derivatives in a single mode of operation. The structure and reactivity of allenes are more attractive research area [Negishi, E. *et al.* 1996; Zimmer, R. *et al.* 2000; Smith, N. D. *et al.* 2000] which have been used as synthons due to its electronic nature towards a number of synthetic transformations [Joyasawal, S. S. *et al.* 2010; Shibata, T. *et al.* 2004]. Addressing these features, we selected Claisen rearrangement as a synthetic tool to make a highly functionalized allene appended oxindole frameworks from vinyl propargyl ether of oxindoles which in turn synthesized from MBH adduct of isatin. This chapter deals with the synthesis of vinyl propargyl ether, highly functionalized allene appended oxindole derivatives and dihydrofuran derivatives from propargyl isomerized MBH adducts of isatin *via* Claisen rearrangement and base mediated cyclization.

3.4 Synthesis of various MBH adduct of substituted isatin:

The starting material MBH adducts of isatin have been synthesized based on the literature [Garden, S. J. *et al.* 2002; Chung, Y. M. *et al.* 2002]. Detailed synthesis of MBH adducts from isatin derivatives have already been dealt in Chapter II. Following the literature procedure, a few more new MBH adducts **34-42** have been synthesized for the present studies (Figure 3.3). The synthesised MBH adducts have been purified by column chromatography and all the new compounds have been characterized by spectroscopic techniques.

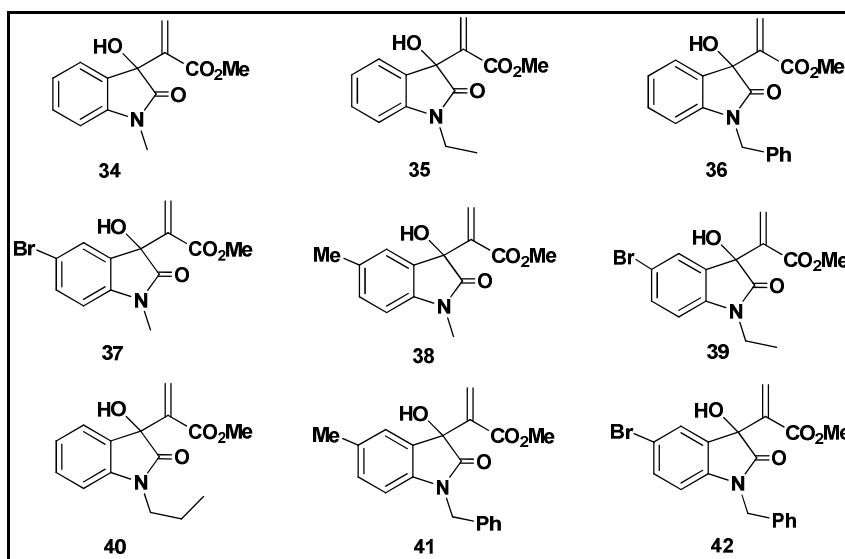
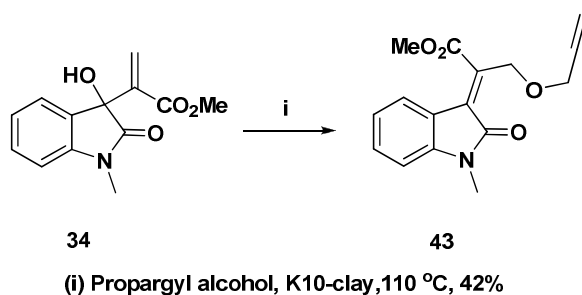


Figure 3.3: Various MBH adducts of substituted isatin.

3.4.1 Isomerization of MBH adduct of isatin with propargyl alcohol:

Initially for the propargyl isomerization studies, *N*-methyl MBH adduct **34** has been chosen as model substrate. Thus, the adduct **34** was treated with excess of propargyl alcohol and montmorillonite K10 clay as solid acid catalyst and heated at 110 °C (Scheme 3.10). The isomerization of MBH adduct by means of propargyl alcohol has already been known and reported by our group *via* conventional thermal method [Shanmugam, P. *et al.* 2004]. However, the overall yield of the conventional thermal reaction is only moderate (42% yield). In order to improve the yield of propargyl isomerization, the optimization of reaction has been carried out (Scheme 3.10).



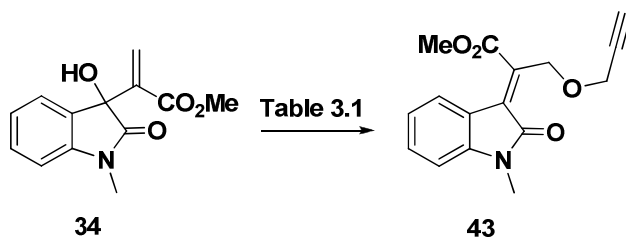
Scheme 3.10: Synthesis of allyl propargyl ether via conventional method.

Earlier from our group, we have demonstrated the synthesis of bromo isomerized MBH adduct of isatin *via* microwave irradiation which provided better yield than convention heating method [Shanmugam, P. *et al.* 2008]. Hence, in order to improve the

yield of propargyl isomerization, we utilized the microwave irradiation condition and the results are discussed in the following section.

3.4.2 Optimization of propargyl isomerization under microwave irradiation: Synthesis of allyl propargyl ether derivatives:

Preliminarily, we have chosen the *N*-methyl MBH adduct of isatin **34** as model substrate for optimization studies (Scheme 3.11). To increase the yield of compound **43**, the starting material was treated with propargyl alcohol and made as slurry in fume hood which then subjected to microwave irradiation for 5 min. at 50% power level. However, the reaction furnished the expected compound **43** only in 20% yield (Table 3.1, entry 1). In successive screening, the optimum microwave reaction condition was observed at 60% power level with 30 min. irradiation time offered 55% yield of product with remaining untreated starting material (Table 3.1, entry 5). Further increment of either the power level or the reaction time of microwave reaction resulted in decrease in the yield of the product **43** due to decomposition of starting material (Table 3.1, entries 6-7).



Scheme 3.11: Optimization of synthesis of allyl propargyl ether.

Table 3.1: Optimization of propargyl isomerization under microwave reaction condition.

Entry	Power level (%) (W)	Reaction time (min)	Yield (%)
1	50	5	20
2	50	10	15
3	50	25	36
4	50	30	42
5	60	30	55
6	70	30	45
7	60	40	40

The synthesized compound **43** have been characterized by spectroscopic techniques. In ^1H NMR spectrum, the characteristic MBH adduct terminal olefin proton disappeared and newly appeared two methylene group protons at δ 4.14 and 4.55 ppm, which correspond to two ether methylene groups (Figure 3.4). The terminal alkyne proton which appeared as a singlet at δ 2.31 ppm and the remaining protons were accounted and appeared in the expected region.

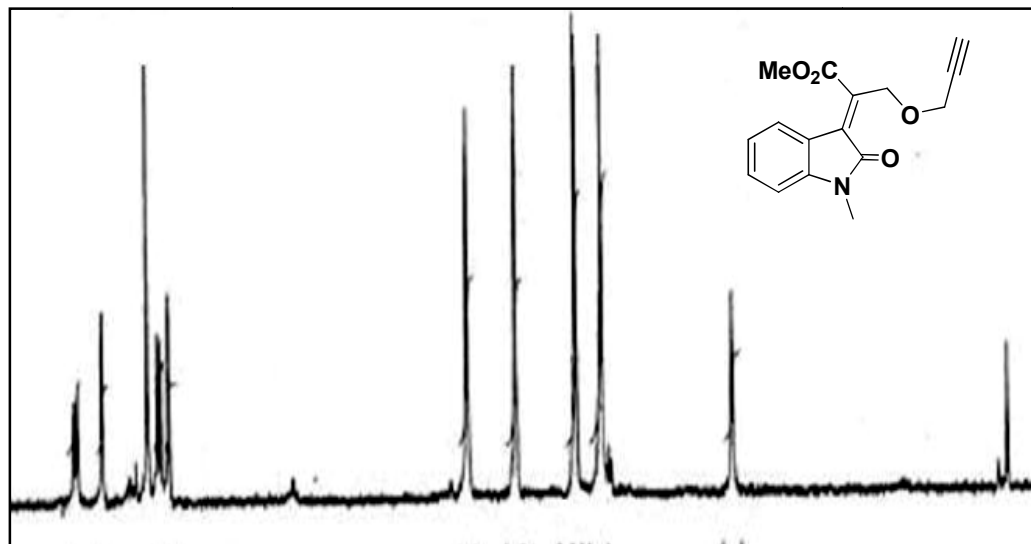


Figure 3.4: ^1H NMR Spectrum of propargyl isomerized compound **43**

The ^{13}C NMR spectrum further supported the assigned structure of compound **43** as it showed two characteristic methylene carbons appearing at δ 32.67 and 34.08 ppm, respectively. The propargyl acetylene carbons were resonated at δ 73.07 and 76.08 ppm (Figure 3.5). The remaining aromatic and carbonyl carbons appeared in the expected region with good agreement in isomerized structure **43**.

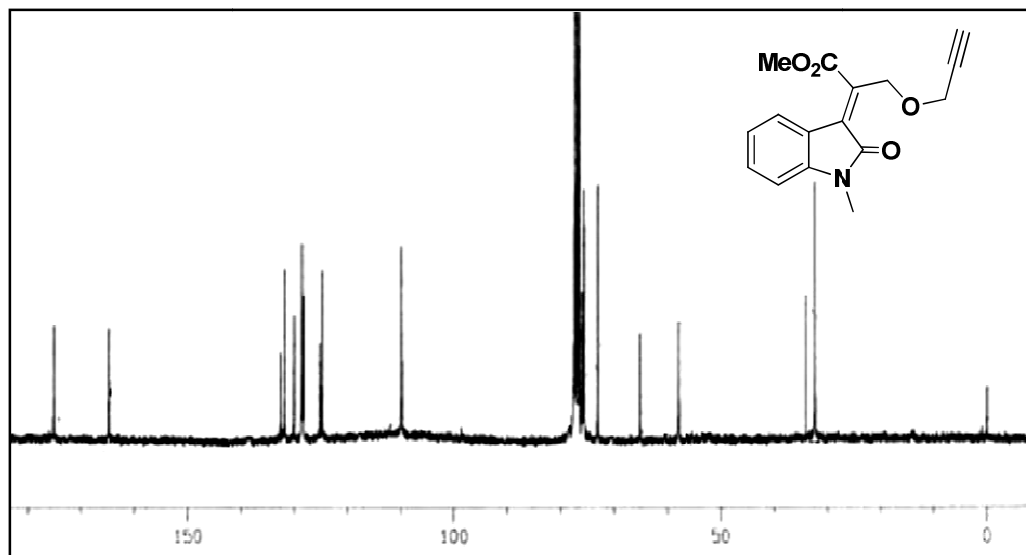
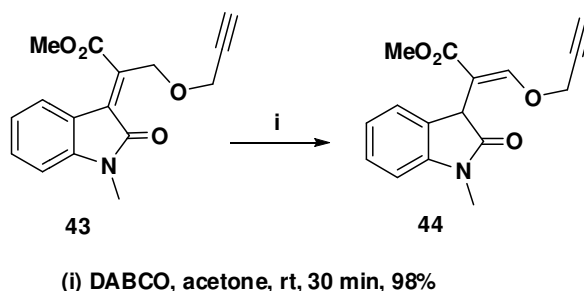


Figure 3.5: ^{13}C NMR Spectrum of propargyl isomerized compound **43**

With this optimized condition, we have synthesized a number of propargyl isomerized derivatives from MBH adducts for further synthetic manipulation (Scheme 3.12).

3.5 Synthesis of vinyl propargyl ethers from allyl propargyl ethers:

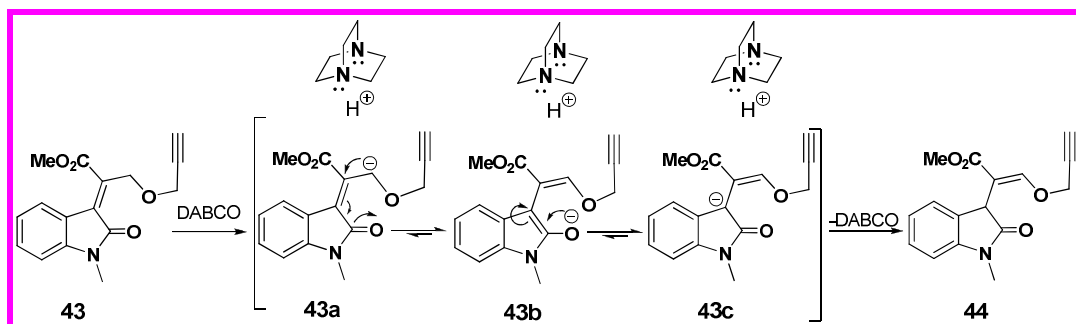
The synthesized allyl propargyl ether **43** needs to be converted to suitable substrate **44** for Claisen rearrangement reaction. In order to obtain suitable Claisen rearrangement substrate, the isomerized derivative **43** in acetone was reacted with a mild base such as DABCO for 30 min and provided the desired product **44** in excellent yield (98%) via [1,3]-hydride shift (Scheme 3.12).



Scheme 3.12: Synthesis of vinyl propargyl ether compound **44**

The base induced [1,3]-hydride shift of allyl propargyl ether is depicted in Scheme 3.13. Accordingly, the removal of allyl methylene proton in propargyl isomerized derivative **43** by DABCO can generate allyl anionic intermediate **43a** which undergoes resonance and form a stabilized enolate form **43b**. The stability of **43b** is more

than **43a** due to the inductive effect of amide carbonyl group. Finally, the intermediate **43c** retrieves a proton at C3 position from DABCO and triggers the base as well as vinyl propargyl ether **44**.



Scheme 3.13: *Mechanistic postulates of base induced [1,3]-allylic shift of allyl propargyl ether.*

The structure of the vinyl propargyl ether **44** was arrived on the basis of a detailed spectral analysis (FTIR, ^1H , ^{13}C NMR and FAB-mass). The FTIR spectrum of the compound **44** showed the presence of amide and ester carbonyl groups absorption at 1702 and 1712 cm^{-1} , respectively. The characteristic functionalities such as acetylene C-C triple bond absorption appeared at 2122 cm^{-1} .

In the ^1H NMR spectrum of compound **44**, one of the two methylene groups of allyl propargyl ether **43** disappeared and newly formed allylic sp^3 C-H methine proton appeared as a singlet at δ 3.81 ppm. The vinyl olefinic proton resonated as a singlet at δ 7.26 ppm (Figure 3.6). The entire aromatic protons were accounted and appeared in the region between δ 6.69-7.04 ppm. The remaining aliphatic protons appeared in good agreement with assigned structure of the compound **44**.

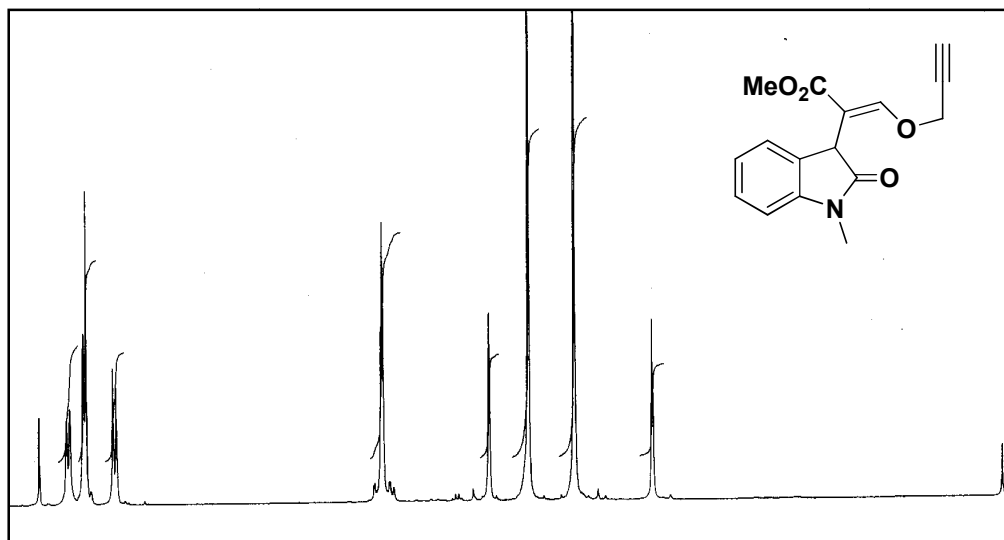


Figure 3.6: ^1H NMR Spectrum of compound **44**

Analysis of the ^{13}C NMR spectrum of compound **44** showed signals at δ 26.92 and 51.27 ppm corresponding to *N*-methyl and ester methyl carbons, respectively (Figure 3.7). Characteristically, the C3 carbon in the oxindole nucleus resonated at δ 60.10 ppm. The olefinic carbons appeared at δ 140.30 and 156.29 ppm. The terminal acetylene carbons were visible at δ 75.21 and 76.40 ppm, respectively. The entire aromatic and aliphatic carbons were in good agreement with assigned compound **44** and the aromatic carbons resonated between the range δ 107.90-129.80 ppm. The carbonyl carbons such as ester and amide appeared at δ 164.12 and 176.27 ppm, respectively.

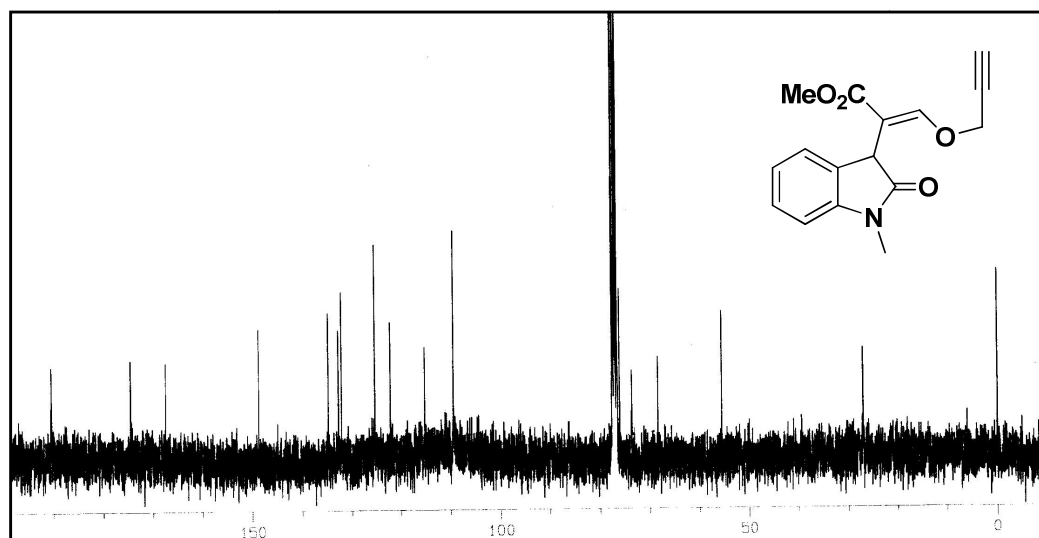


Figure 3.7: ^{13}C NMR Spectrum of compound **44**

Finally, the structure of the vinyl propargyl ether **44** was further supported by FAB mass spectrum as it showed a molecular ion $[M^+]$ peak at $m/z = 285.23$ against the calculated value $m/z = 285.10$ (Figure 3.8). The elemental analysis also supported the assigned structure **44**.

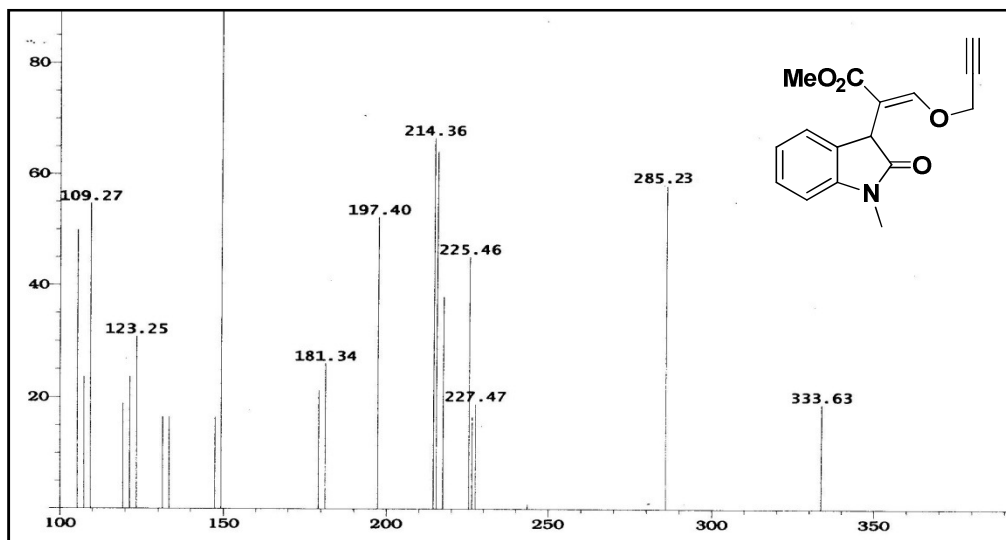


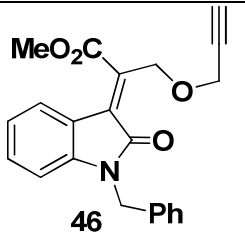
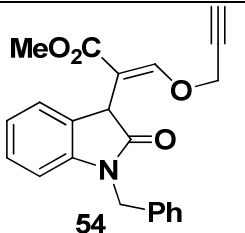
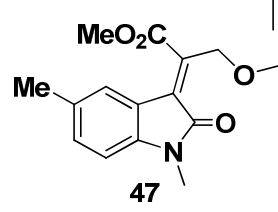
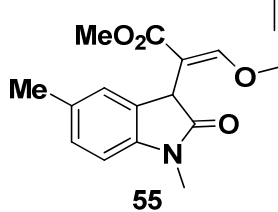
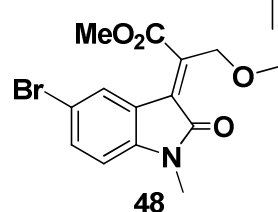
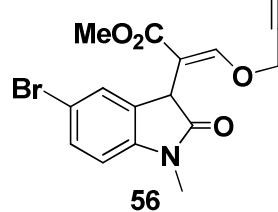
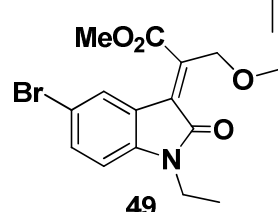
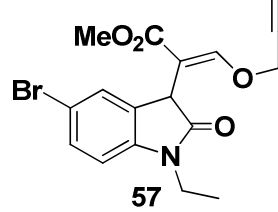
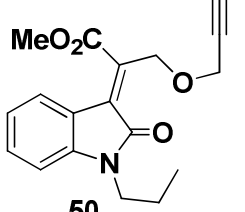
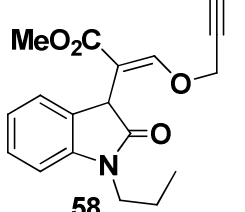
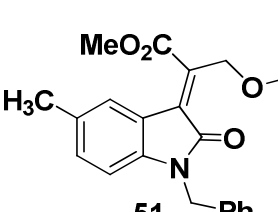
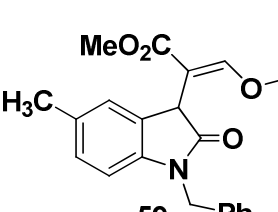
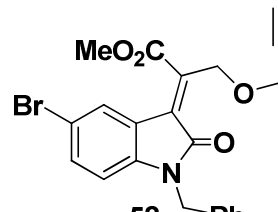
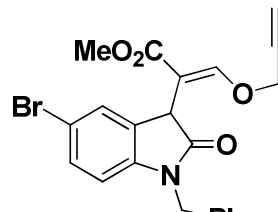
Figure 3.8: FAB mass spectrum of compound **44**

3.5.1 Generalization of [1,3]-hydride shift:

In order to exemplify the synthesis of diverse vinyl propargyl ethers from various allyl propargyl ether of oxindole, the compounds **45-52** were subjected to the DABCO mediated [1,3]-hydride shift reaction at room temperature. All the substrates underwent the isomerization smoothly and furnished the corresponding vinyl propargyl ether derivatives **53-60** in excellent yield. The results are shown in Table 3.2.

Table 3.2: Synthesis of vinyl propargyl ethers from allyl propargyl ethers.

Entry	Allyl propargyl ether 45-52	Vinyl propargyl ether 53-60	Yield (%) ^a 45-52	Yield (%) 53-60
1	<p>45</p>	<p>53</p>	56	97

2	 <p>46</p>	 <p>54</p>	52	99
3	 <p>47</p>	 <p>55</p>	56	75
4	 <p>48</p>	 <p>56</p>	51	99
5	 <p>49</p>	 <p>57</p>	52	97
6	 <p>50</p>	 <p>58</p>	50	99
7	 <p>51</p>	 <p>59</p>	51	81
8	 <p>52</p>	 <p>60</p>	54	97

^aYield of propargyl isomerized derivatives by microwave reaction.

The structure of the synthesized compound **55** was determined based on detailed spectroscopic analysis (IR, ^1H , ^{13}C NMR and FAB mass). From the FTIR spectrum, the presence of functional groups such as ester and amide carbonyl absorptions were seen at 1703 and 1721 cm^{-1} , respectively.

In the ^1H NMR spectrum, the characteristic allyl methylene proton of propargyl isomerized compound **55** disappeared and the allylic $\text{sp}^3\text{C-H}$ methine proton appeared as a singlet at δ 3.82 ppm (Figure 3.9). The 5-methyl group of aromatic oxindole resonated at δ 2.29 ppm. Characteristically, the newly appeared olefin proton resonated as a singlet at δ 7.26 ppm and all the aromatic protons appeared in the region δ 6.69 -7.04 ppm as multiplets. The *N*-methyl and ester methyl group protons were appeared as two singlets at δ 3.22 and 3.57 ppm, respectively.

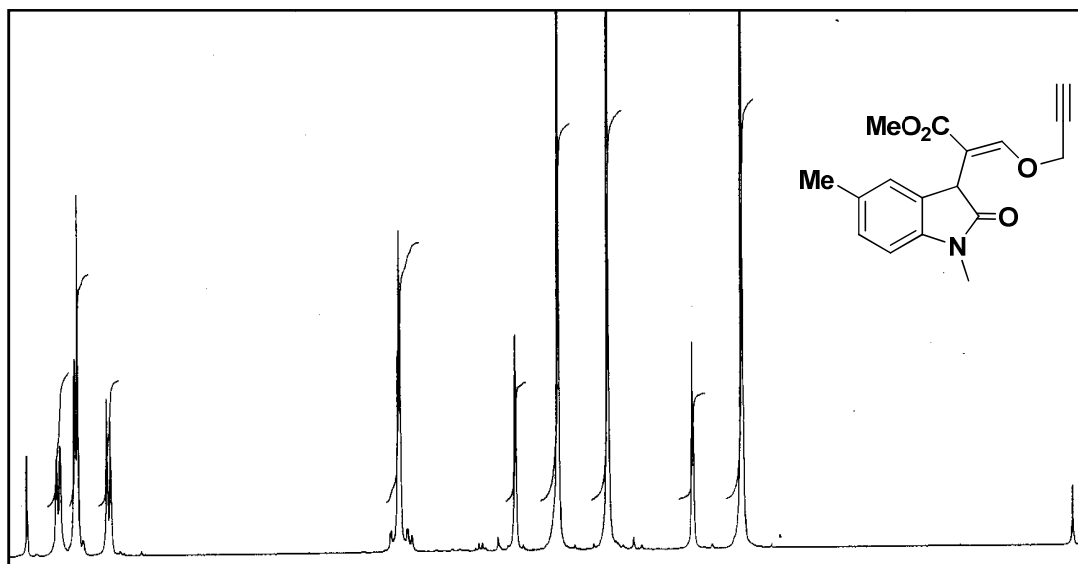


Figure 3.9: ^1H NMR spectrum of compound **55**

The ^{13}C NMR spectrum of compound **55** showed carbon peaks for 5-methyl, *N*-methyl and ester methyl groups at δ 21.09, 26.49 and 51.44 ppm, respectively (Figure 3.10). The methylene and acetylene carbons of propargyl part resonated at δ 47.89, 76.99 and 77.41 ppm, respectively. The characteristic C-H carbon at C3 position was visible at δ 61.26 ppm. The aromatic and olefin carbons appeared in the region δ 106.97-156.33 ppm. The ester and amide carbonyl carbons were visible at δ 164.65 ppm and 175.99 ppm, respectively.

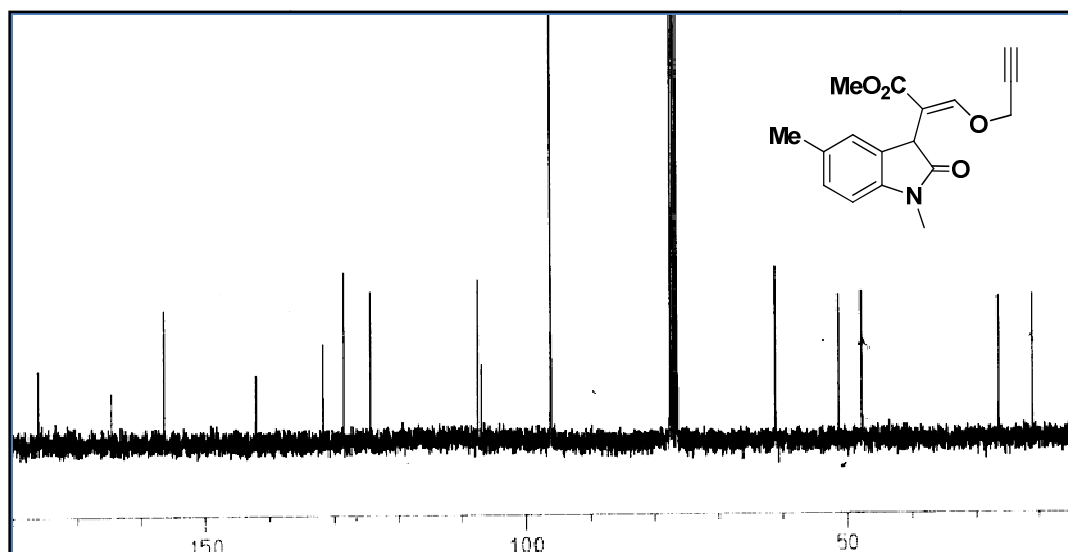


Figure 3.10: ^{13}C NMR spectrum of compound **55**

Finally, the structure of the compound **55** was supported by the FAB mass spectrum as it showed a $[\text{M}+1]$ peak at $m/z = 300.23$ against the calculated value $m/z = 299.12$ and with satisfied elemental analysis (Figure 3.11).

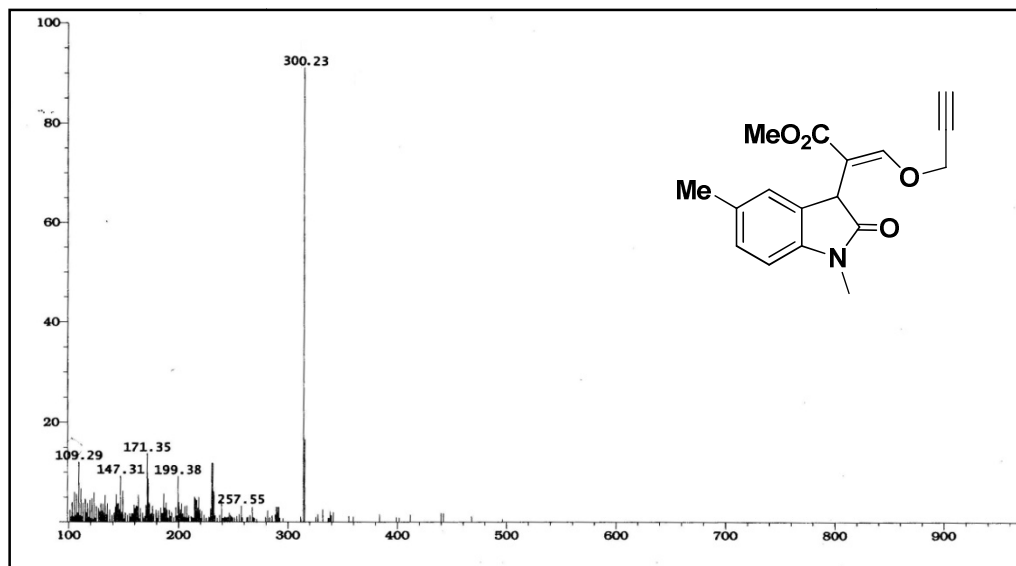
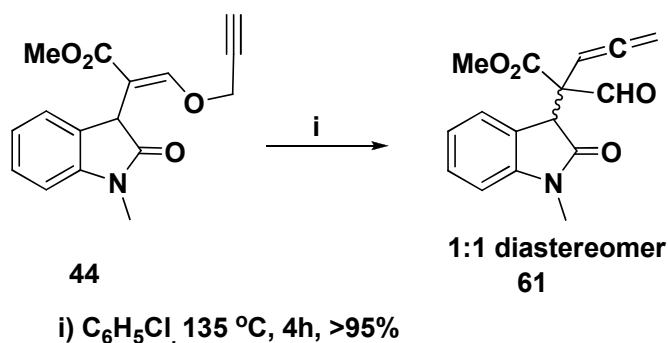


Figure 3.11: FAB mass spectrum of compound **55**

3.6 Synthesis of allene appended multi-functional oxindole derivatives *via* Claisen rearrangement:

The successful synthesis of suitable substrate for [3,3]-sigmatropic rearrangement prompted us to test the Claisen rearrangement under thermal condition. Initially, for this study, we have chosen the *N*-methyl vinyl propargyl ether **44** as a model substrate. Thus compound **44** in chlorobenzene as solvent was subjected to Claisen rearrangement under reflux condition. The reaction afforded a mixture of diastereomeric allene appended oxindole framework **61** in excellent yield (Scheme 3.14). The synthesized compound **61** is highly functionalized and encompasses quaternary stereogenic center with functional groups like allene, ester and aldehyde in oxindole moiety. The formation of diastereomeric mixture of products from the concerted reaction may be due to the racemic starting materials used in the reaction. The synthesized compound **61** had two stereogenic carbons in adjacent positions along with one quaternary stereogenic center. The compound **61** was obtained as a mixture of diastereomers (1:1) and inseparable by silica gel column chromatography. The ratio of compound **61** was established based on the integration of methine proton (-C-H) at C3 position of oxindole in the ^1H NMR spectrum.



Scheme 3.14: *Synthesis of oxindole appended allene derivatives via Claisen rearrangement.*

The structure of synthesized compound **61** was arrived on the basis of a detailed spectroscopic analysis (FTIR, ^1H , ^{13}C NMR and FAB mass). The FTIR spectrum of the compound **61** showed characteristic allene absorption at 2214 cm^{-1} . The carbonyl groups of aldehyde and ester showed absorptions at 1706 and 1720 cm^{-1} , respectively.

In the ^1H NMR spectrum, the characteristic allene terminal olefinic protons appeared as a multiplet of four protons due to other isomer centered at δ 4.88 ppm (Figure 3.12). The quaternary carbon bonded allene proton ($-\text{C}-\text{CH}=\text{C}=\text{C}$) of two isomers appeared as two separate triplets centered at δ 5.57 and 5.67 ppm with coupling constants $J = 7.1$ Hz and 7.2 Hz. The sp^3 methine proton at C3 position of oxindole frame work appeared as a singlet at δ 3.50 ppm for one isomer and that for the other isomer the proton merged with ester methyl groups centered at δ 3.55 ppm and appeared as a multiplet. Both the *N*-methyl groups merged and appeared as a singlet at δ 3.22 ppm. The ester methyl protons of two isomers also merged and appeared as a singlet at δ 3.55 ppm. The aromatic protons were accounted and appeared in the region at δ 6.69-7.23 (centered at 6.96) ppm. The two isomeric aldehyde protons resonated as two separate singlets at δ 9.59 and 9.73 ppm, respectively.

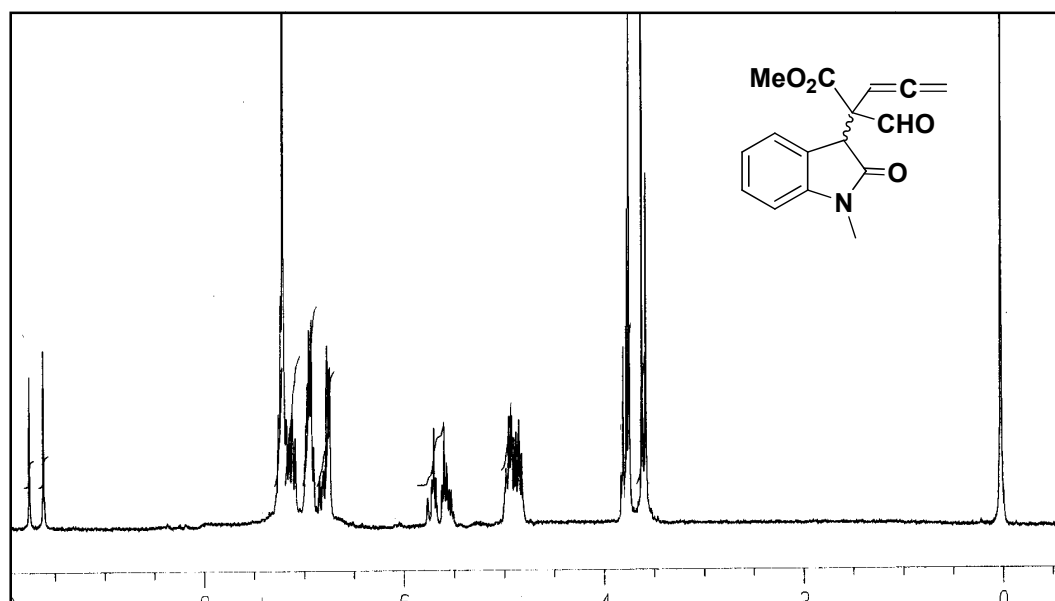


Figure 3.12: ^1H NMR Spectrum of compound **61**

Analysis of the ^{13}C NMR spectrum also supported the structure of compound **61** and showed mixture of diastereomer signals at δ 75.62, 76.01, 97.56 and 101.01 ppm corresponding to the characteristic terminal allene carbons. The central carbons of allene appeared at δ 209.18 and 211.65 ppm, respectively (Figure 3.13).

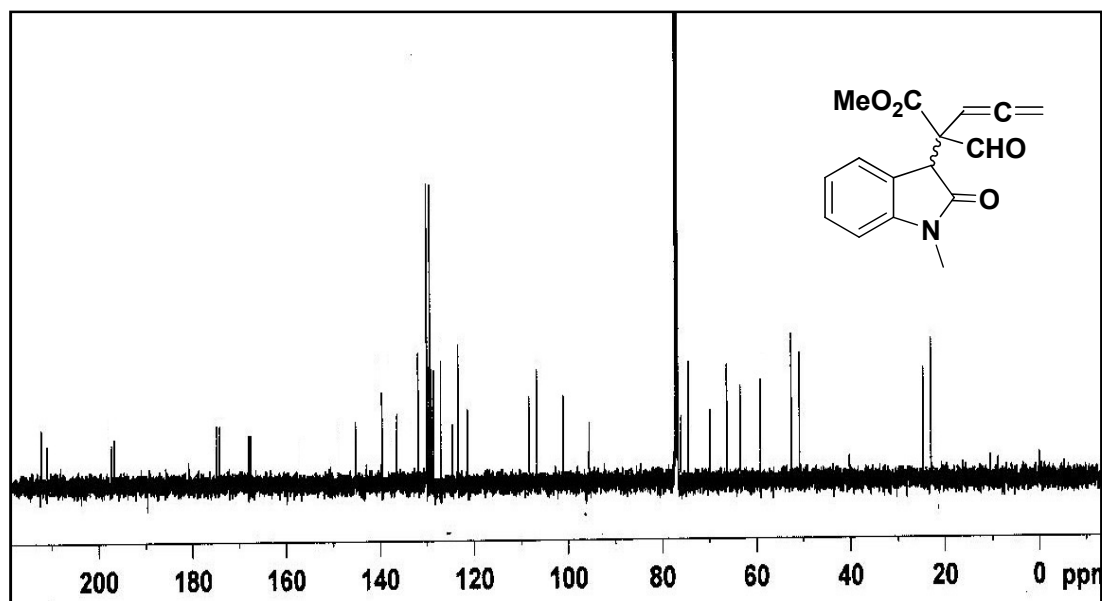


Figure 3.13: ^{13}C NMR Spectrum of compound **61**

The quaternary stereogenic carbons resonated at δ 63.41 and 69.71ppm. The oxindole C3 position carbon of two isomers resonated at δ 40.12 and 40.98 ppm. The *N*-methyl and ester methyl groups were visible at δ 23.89, 24.34 and 51.78, 52.34 ppm, due to two isomers. The two isomeric aldehyde carbonyl carbons resonated at δ 197.23 and 198.06 ppm. Remaining aromatic carbons of two isomers were accounted and appeared in the region δ 107.81- 144.91 ppm.

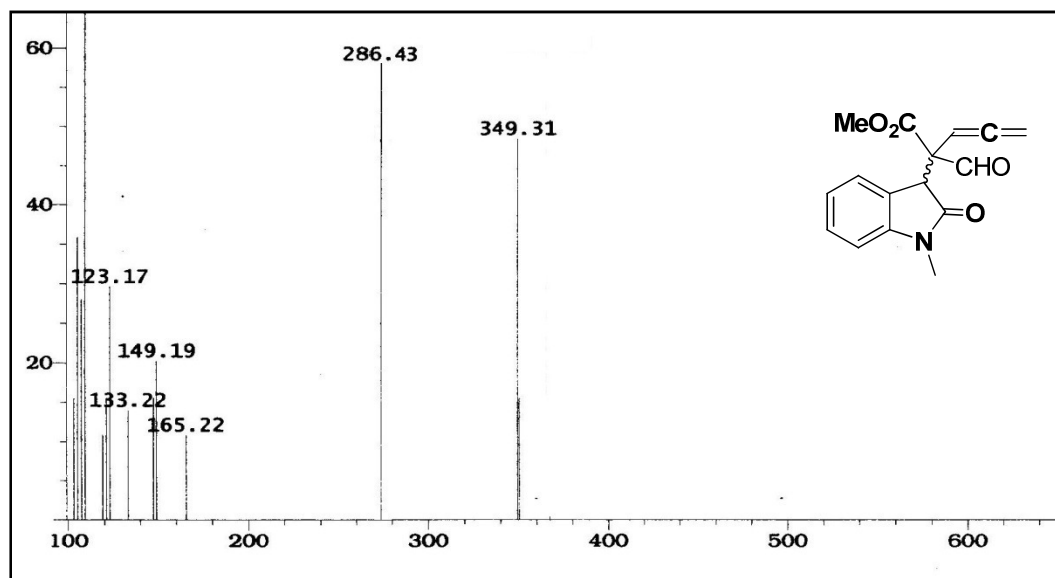


Figure 3.14: FAB mass spectrum of compound **61**

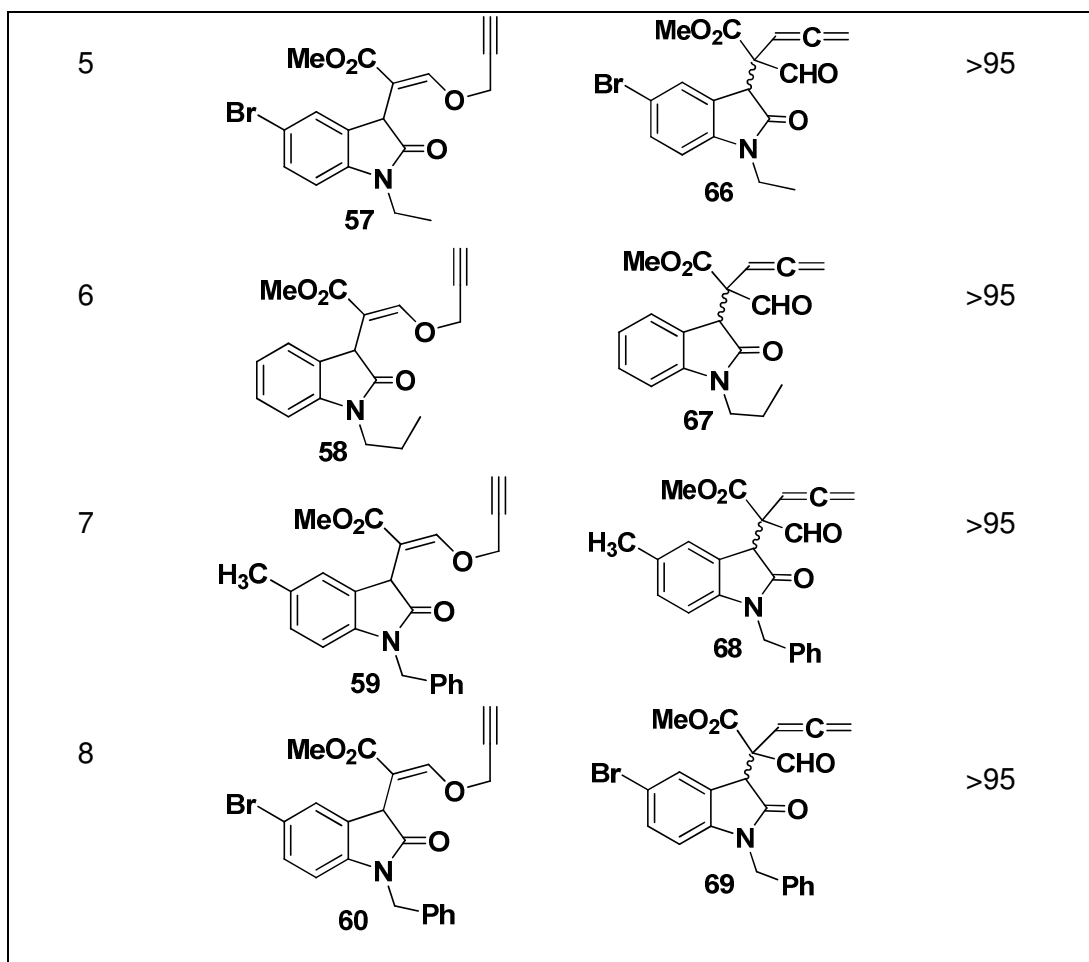
Finally, the FAB mass spectrum showed a molecular ion [M+1] peak at $m/z = 286.43$ against calculated value $m/z = 285.13$ which supported the assigned structure (Figure 3.14).

3.6.1 Generality of Claisen rearrangement reactions:

In order to synthesize diverse allene anchored oxindole frameworks, various vinyl propargyl ether of MBH adduct derivatives were subjected to [3,3]-sigmatropic rearrangement reaction. All the substrates underwent the Claisen rearrangement smoothly and afforded the corresponding diastereomeric mixture of highly functionalized allene appended oxindole derivatives in excellent yield.

Table 3.3: Generality of the Claisen rearrangement reactions.

Entry	Vinyl propargyl ether 53-60	Allene derivative 62-69	Yield (%)
1			>95
2			>95
3			94
4			>95

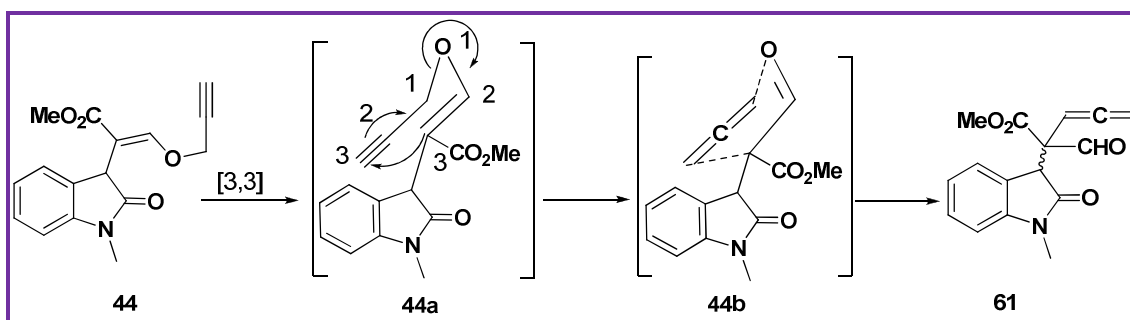


Notably, the substitution either at aromatic core or oxindole nitrogen did not alter the reaction time and yield.

3.6.2 Mechanistic postulates of Claisen rearrangements:

The formation of multi-functionalized allene appended oxindole derivative from vinyl propargyl ether has been rationalized through mechanistic postulates (Scheme 3.15). Initially, the reaction proceeded *via* the sequence of migration of π and σ bonds which provided half boat structure **44b**. Generally, Lewis acid (soft metal salts such as Pd and Hg salts) catalyzed the Claisen rearrangement of vinyl propargyl ethers precede through coordination to the allenic π -bonds and through a six member chair or boat transition states. But in the present case, due to the absence of coordination between metal salts and vinyl propargyl ether and also the linear structural nature of allene, the reaction proceeded *via* half boat transition state. A large number of theoretical

calculations aiming to predict the structures of transition states involved in the Claisen rearrangement concluded that the selective formation of product is completely related with either chair or boat like transition states. The outcome of the stereoselectivity of the product can also be controlled by the steric demand of the substrate and the catalytic system involved in that reaction. According to *Woodward-Hoffmann rule*, the concerted [3,3]-sigmatropic rearrangement processed *via supra-supra* mode orbital migration which is allowed under thermal condition.



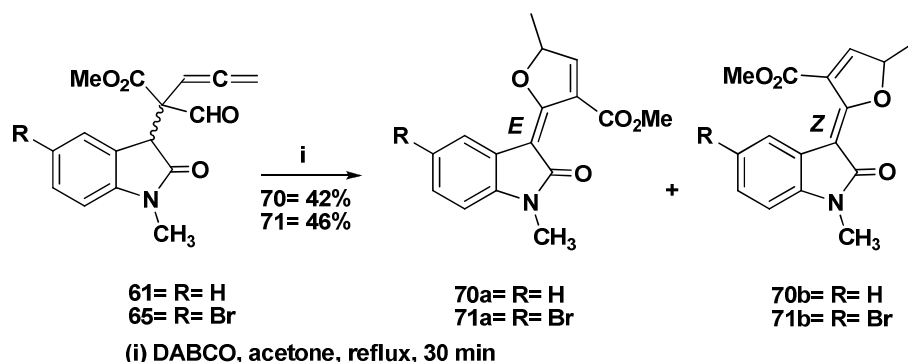
Scheme 3.15: Mechanistic postulate of Claisen rearrangement reaction.

The observed diastereomeric mixture of products from the concerted reaction can be explained due to racemic starting materials **44** were used.

3.7 Synthetic application of allene appended oxindole derivatives:

After successful synthesis of multi-functionalized allene appended oxindole frame work from vinyl propargyl ethers *via* Claisen rearrangement, we were interested in synthesizing dihydrofuran appended oxindole derivatives. The literature reports also revealed that the intramolecular cyclization between allene and carbonyl or imine afforded various heterocyclic frame works [Harrison, T. J. *et al.* 2006; Binder, J. T. *et al.* 2006]. Highly substituted furan derivatives play an important role as structural elements of many natural and pharmaceutically important substances (e.g., *ranitidine* or *zantac*) [Hou, X. L. *et al.* 2003; Keay, B. A. *et al.* 1997]. Moreover, they are useful intermediates to construct a variety of important organic compounds [Lipshutz, B. H. 1986]. In addition, the isatin C3 position contain olefin bond attached with heterocycles are important structural moiety and also found in a number of natural products [Wille, G. *et al.* 2001]. Hence, we were interested in synthesizing the furan appended oxindole

derivatives from the allene derivatives. In order to explore the reactivity of oxindole appended allene towards the synthesis of heterocyclic derivative, the *N*-methyl allene appended oxindole **61** was chosen as a model substrate. Thus, compound **61** in acetone was subject to DABCO mediated intramolecular cyclization at reflux condition provided C3 position bounded dihydrofuran oxindole derivative **70** in moderate yield (Scheme 3.16).



Scheme 3.16: Synthesis of dihydrofuran appended oxindole derivatives.

The cyclization reaction furnished two geometrical isomer mixtures of dihydrofuran derivatives in 1:1 ratio and is separable by silica gel column chromatography. The synthesized compounds were characterized on the basis of spectroscopic techniques (FTIR, NMR, and FAB-mass). The isomers **70a** and **70b** were distinguished by ^1H NMR and NOE irradiation experiments as explained in the following section.

The FTIR spectrum of the compound **70a** showed the two carbonyl absorptions at 1706 and 1718 cm^{-1} correspond to ester and amide groups, respectively.

In the ^1H NMR spectrum of compound **70a**, the characteristic olefin proton in the dihydrofuran ring appeared as a doublet centered at δ 8.14 ppm with a coupling constant $J = 16$ Hz (Figure 3.15). The methine proton from furan derivative **70a** resonated as a triplet of doublet centered at δ 6.11 ppm with coupling constants $J = 6.9$ and 16.0 Hz, respectively. The methyl proton in dihydrofuran moiety appeared as a doublet centered at δ 2.0 ppm with a coupling constant $J = 6.9$ Hz. The *N*-methyl and ester methyl protons resonated as two singlets at δ 3.23 and 3.98 ppm, respectively. All the aromatic protons appeared in the region δ 6.77 to 7.21 ppm as a multiplet.

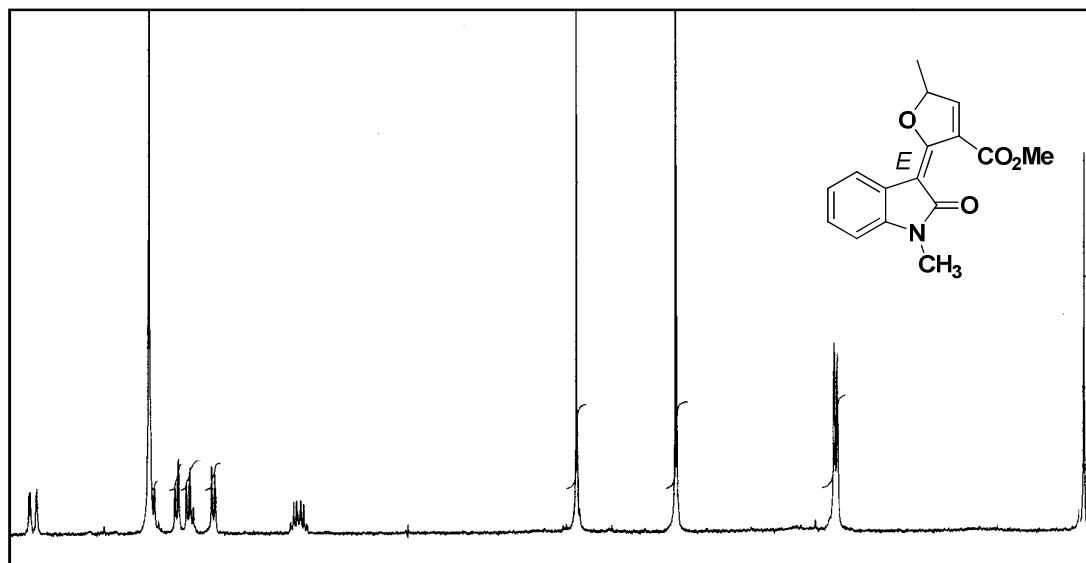


Figure 3.15: ^1H NMR spectrum of compound **70a**

Analysis of the ^{13}C NMR spectrum of compound **70a** supported the assigned structure and showed peaks at δ 19.51 and 52.48 ppm corresponding to methyl in dihydrofuran and ester methyl carbons, respectively (Figure 3.16). The *N*-methyl carbon of oxindole moiety resonated at δ 25.84 ppm. Methine carbon of dihydrofuran moiety was visible at δ 29.79 ppm. All the aromatic and olefinic carbons were in good agreement with the assigned structure and observed in the region δ 107.99-143.19 ppm.

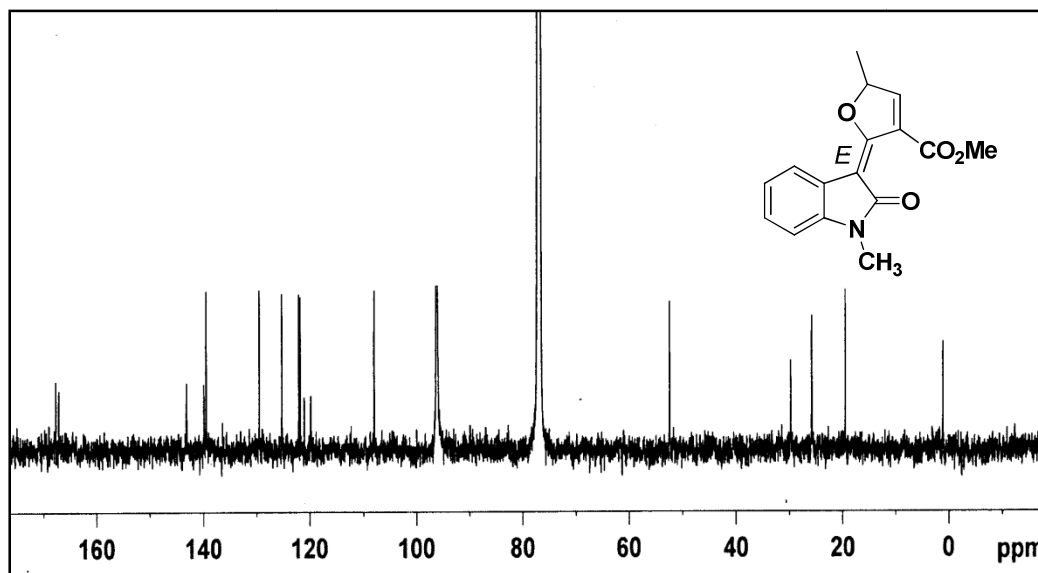


Figure 3.16: ^{13}C NMR spectrum of compound **70a**

The amide and ester carbonyl carbons were seen at δ 167.22 and 167.76 ppm, respectively.

Finally, the FAB mass spectrum further supported the assigned structure of compound **70a** as it showed a molecular ion $[M^+]$ peak at $m/z = 285.10$ as against the calculated mass $m/z = 285.21$ (Figure 3.17).

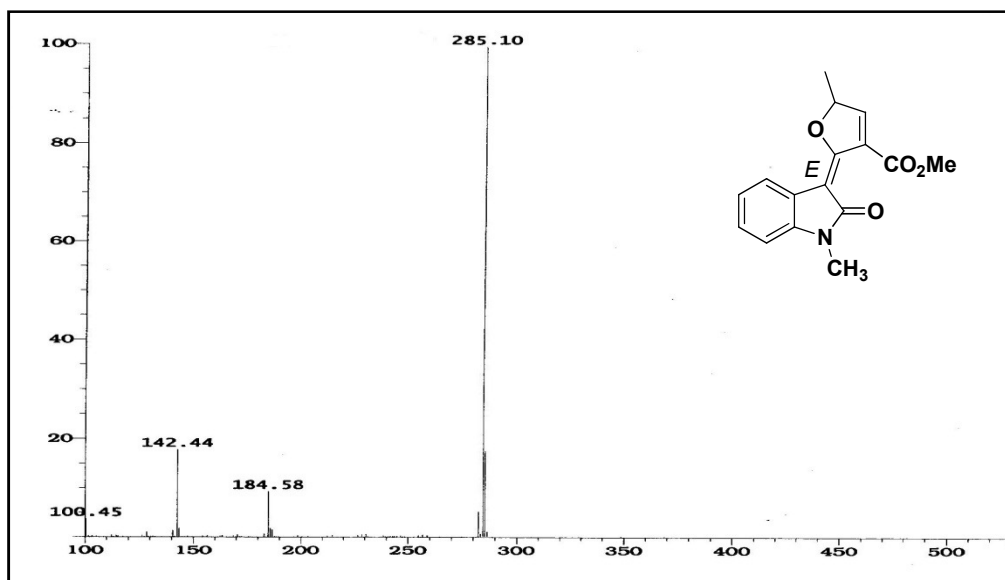


Figure 3.17: FAB mass spectrum of compound **70a**

The other isomer **70b** also showed similar pattern of 1H MNR spectrum except with two major characteristic changes in chemical shift values of ester methyl protons appeared at δ 3.89 ppm while in the case **70a** it was appeared at δ 3.98 ppm. Similarly, in the dihydrofuran derivative **70b**, the olefin proton appeared at δ 7.87 ppm and the corresponding proton of **70a** appeared at δ 8.14 ppm (Figure 3.18). The detailed spectroscopic values for both compounds are provided at the end of this chapter.

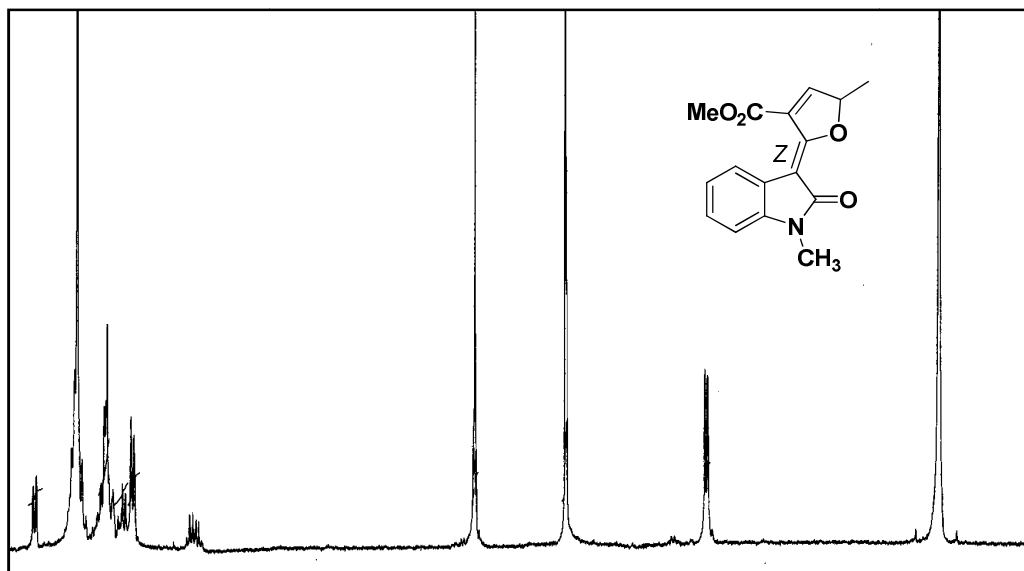


Figure 3.18: ^1H NMR Spectrum of compound **70b**

Similarly, in the ^{13}C NMR spectrum of compound **70b** the chemical shift value of ester methyl carbon slightly shifted from that of **70a** and the remaining carbons resonated as it is in **70a** (Figure 3.19).

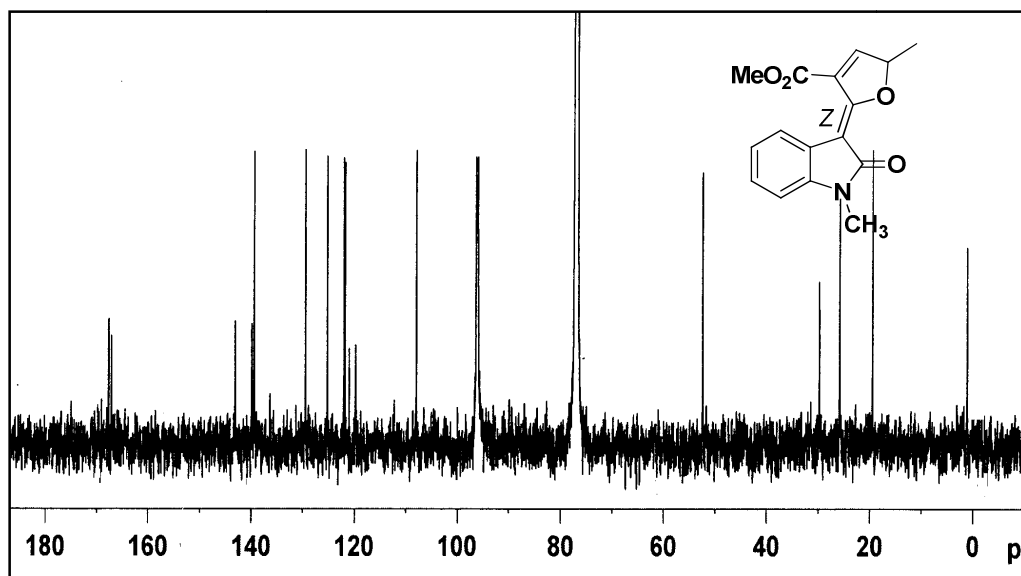


Figure 3.19: ^{13}C NMR Spectrum of compound **70b**

Finally, the FAB mass spectrum supported the assigned structure of **70b** as it showed molecular ion $[\text{M}+1]$ peak at $m/z = 286.07$ as against the calculated value $m/z = 285.21$.

3.7.1 Differentiation of two geometrical isomers 70a and 70b:

The relative stereochemistry of dihydrofuran derivatives **70a** and **70b** were distinguished based on the NMR spectroscopic technique. Remarkable change in the chemical shift value (δ) was observed between the two isomers **70a** and **70b** (Figure 3.20). The ^1H NMR was not sufficient to distinguish the isomers due to the absence of vicinal as well as allyl protons in olefinic bond. Hence, the geometry of these isomeric compounds **70a** and **70b** were distinguished by the NOE experiment.

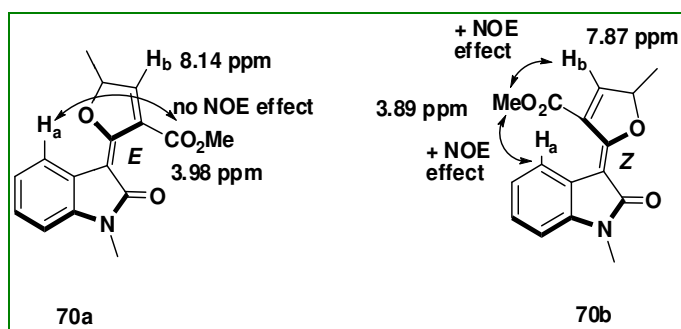


Figure 3.20: NOE correlation of compounds **70a** and **70b**

In the NOE spectrum, the irradiation of ester methyl group of the compound **70b** showed positive enhancement in aromatic proton H_a and also with H_b proton of furan ring (Figure 3.21). The compound **70a** did not give any NOE correlation between the H_a and ester methyl protons. Based on the NOE experiment, the geometry of the isomer **70a** was assigned as *E*-isomer and the **70b** isomer was assigned as *Z*-isomer.

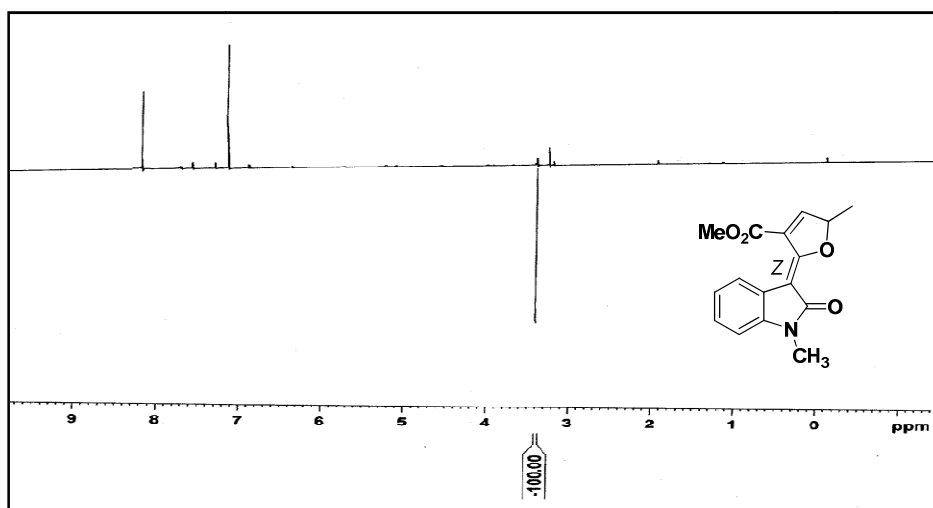
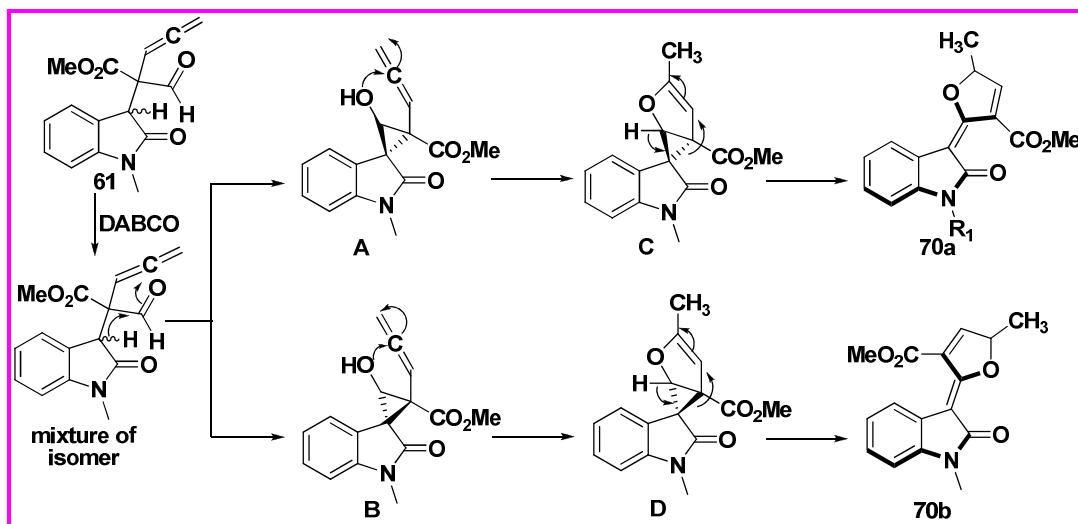


Figure 3.21: NOE spectrum of compound **70b**

3.8 Mechanistic postulate of base induced cyclization:

The formation of dihydrofuran appended oxindole derivatives **70a** and **70b** from allene derivatives can be explained by mechanistic postulates (Scheme 3.17). At first, abstraction of a proton at C3 position of oxindole derivative **61** by base take place followed by intramolecular nucleophilic addition with aldehyde generate diastereomeric cyclopropane intermediates **A** and **B**. The bicyclic intermediates **C** and **D** could be generated due to ring strain of cyclopropane derivatives in the initially formed intermediates **A** and **B** by the nucleophilic attack of hydroxyl group on allene. The bicyclic intermediate undergoes base induced proton shift and electron resettlement to yield dihydrofuran derivatives **70a** and **70b**. The reason for the formation of the two isomers **70a** and **70b** may be due to either racemic starting material or mode of nucleophilic addition with aldehyde.



Scheme 3.17: Mechanistic postulates of dihydrofuran derivatives.

3.9 Conclusions:

- ❖ Synthetic transformation of propargyl isomerized MBH of isatin has been demonstrated by Claisen rearrangement and afforded multi-functionalized allene appended oxindole derivatives.
- ❖ The Claisen rearrangement synthetic protocol provided two adjacent stereogenic centers with one quaternary carbon in the oxindole derivatives in one step.
- ❖ The synthetic utility of functionalized allene derivatives was further demonstrated in the formation of oxindole appended dihydrofuran derivatives *via* base mediated reaction.
- ❖ All the new compounds were thoroughly characterized by spectroscopic techniques and the stereochemistry of the dihydrofuran derivatives was assigned by NOE experiment.

3.10 Experimental section:

3.10.1 General considerations:

All the reactions were carried out in oven-dried glassware. Progress of reactions was monitored by Thin Layer Chromatography (TLC) while purification of crude compounds was done by column chromatography using silica gel (100-200 mesh). Melting points were recorded on a Buchi melting point apparatus and are uncorrected. NMR spectra were recorded at 500 and 300 MHz (based on availability of instruments) 125 and 75 MHz (for ^{13}C) respectively on Bruker Avance DPX-500 MHz. and Bruker Avance DPX-300 MHz. Chemical shifts are reported in δ (ppm) relative to TMS (^1H) or CDCl_3 (^{13}C) as internal standards. Mass spectra were recorded using JEOL JMS 600H mass spectrometer. IR spectra were recorded on Bomem MB series FT-IR spectrometer; absorbencies are reported in cm^{-1} . Yields refer to quantities obtained after chromatography.

3.10.2 Experimental procedure:

3.10.3 General experimental procedure for propargyl isomerization (Conventional heating):

A mixture of MBH adducts (100 mg) with w/w Mont. K10 clay and propargyl alcohol (1.5 mL) was refluxed for 1-4 h. The progress of the reaction was monitored by TLC. After completion of the reaction, the crude mixture was purified by silica gel column chromatography using gradient elution with Hexane/EtOAc to afford pure isomerized compounds.

3.10.4 Microwave irradiation:

A mixture of MBH adduct (100 mg) with w/w Mont K10 clay and propargyl alcohol was made as a paste and was irradiated (60% power level) in a microwave oven (30 min, SAMSUNG, Model: CE 118KF). The crude reaction mixture was purified by silica gel column chromatography.

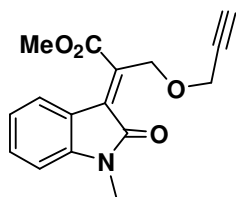
3.10.5 Characterization of new compounds:

Yellow viscous liquid;

R_f: 0.30 (25% EtOAc-Hexane);

IR (CH₂Cl₂) ν_{\max} : 1615, 1652, 1704, 1718, 2124, 3079, 3221 cm⁻¹;

¹H NMR (CDCl₃/TMS, 300.1 MHz): δ 2.31 (s, 1H), 3.44 (s, 3H), 3.64 (s, 3H), 4.14 (s, 2H), 4.55 (s, 2H), 6.69 (d, *J* = 7.8 Hz, 1H), 7.16 (t, *J* = 6.8 Hz, 1H), 7.63 (t, *J* = 7.8 Hz, 1H), 7.85 (d, *J* = 6.8 Hz, 1H);



Compound 43

¹³C NMR (CDCl₃/TMS, 75.4 MHz): δ 32.67, 34.08, 54.43, 65.17, 73.07, 76.08, 109.98, 125.24, 128.39, 128.56, 130.01, 130.05, 131.76, 132.54, 164.72, 175.16;

FAB mass: Calcd. for C₁₆H₁₅NO₄ *m/z* = 285.1; Found: 285.23 (M⁺);

Elemental Analysis: C₁₆H₁₅NO₄ Calcd. for C, 67.36; H, 5.30; N, 4.91; Found: C, 66.39; H, 5.12, N, 4.85.

3.10.6 General experimental procedure for preparation of allylic isomerization:

A mixture of propargyl ether of isomerized MBH adducts (100 mg) and DABCO (10 mol %) in acetone (3 mL) was allowed to stir at room temperature for 30 min. The progress of the reaction was monitored by TLC. After completion of the reaction, the crude mixture was purified by silica gel column chromatography using gradient elution with Hexane/EtOAc to afford pure compounds.

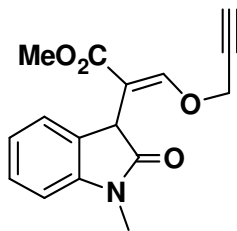
3.10.7 Characterization of new compounds:

Pale yellow viscous liquid;

R_f: 0.27 (20% EtOAc-Hexane);

IR (CH₂Cl₂) ν_{\max} : 1616, 1647, 1702, 1712, 2122, 3077, 3231 cm⁻¹;

¹H NMR (CDCl₃/TMS, 300.1 MHz): δ 2.64 (s, 1H), 3.22



Compound 44

(s, 3H), 3.57 (s, 3H), 3.81 (s, 1H), 4.67 (s, 2H), 6.69 (d, $J = 7.8$ Hz, 1H), 6.91 (m, 2H), 7.04 (d, $J = 7.6$ Hz, 1H), 7.26 (s, 1H);

^{13}C NMR (CDCl_3/TMS , 75.4 MHz): δ 26.92, 47.90, 51.27, 60.10, 75.21, 76.4, 107.90, 117.50, 127.80 (2C), 128.56, 129.80, 140.30, 156.29, 164.12, 176.27;

FAB mass: Calcd. for $\text{C}_{16}\text{H}_{15}\text{NO}_4$ $m/z = 285.10$; Found: 285.23 (M^+);

Elemental Analysis: $\text{C}_{16}\text{H}_{15}\text{NO}_4$ Calcd. for C, 67.36; H, 5.30; N, 4.91; Found: C, 67.38; H, 5.32, N, 4.93.

Pale yellow viscous liquid;

R_f: 0.29 (20% EtOAc-Hexane);

IR (CH_2Cl_2) ν_{max} : 1614, 1645, 1701, 1722, 2120, 3076, 3232 cm^{-1} ;

^1H NMR (CDCl_3/TMS , 300.1 MHz): δ 0.99 (t, $J = 6.7$ Hz, 3H), 2.64 (s, 1H), 3.56 (s, 3H), 3.81 (s, 1H), 4.35 (q, 2H), 4.66 (s, 2H), 6.68 (d, $J = 7.5$ Hz, 1H), 6.90 (m, 2H), 7.05 (d, $J = 7.6$ Hz, 1H), 7.27 (s, 1H);

^{13}C NMR (CDCl_3/TMS , 75.4 MHz): δ 11.86, 44.98, 47.91, 51.14, 60.23, 76.21, 77.4, 108.9, 117.6, 126.73, 127.8, 128.3, 129.7, 140.1, 156.34, 165.2, 174.3;

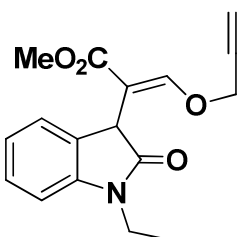
FAB mass: Calcd. for $\text{C}_{17}\text{H}_{17}\text{NO}_4$ $m/z = 299.12$; Found: 300.23 ($\text{M}+1$);

Elemental Analysis: $\text{C}_{17}\text{H}_{17}\text{NO}_4$ Calcd. for C, 68.21; H, 5.72; N, 4.68; Found: C, 68.25; H, 5.74, N, 4.66.

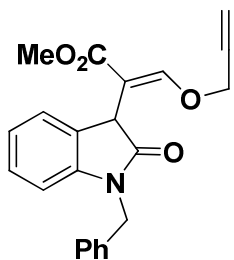
Pale yellow viscous liquid;

R_f: 0.28 (20% EtOAc-Hexane);

IR (CH_2Cl_2) ν_{max} : 1615, 1643, 1702, 1718, 2121, 3073, 3234 cm^{-1} ;



Compound 53



Compound 54

^1H NMR (CDCl_3/TMS , 300.1 MHz): δ 2.65 (s, 1H), 3.56 (s, 3H), 3.82 (s, 1H), 4.25 (m, 2H), 4.68 (s, 2H), 6.69 (t, $J = 7.6$ Hz, 1H), 6.93 (m, 2H), 6.97 (m, 3H), 7.03 (m, 3H), 7.27 (s, 1H);

^{13}C NMR (CDCl_3/TMS , 75.4 MHz): δ 44.1, 47.2, 51.3, 61.6, 74.2, 76.43, 107.34, 108.11, 123.23, 124.8 (2C), 126.31, 127.81 (2C), 128.14, 128.67, 129.36, 131.54, 141.74, 155.91, 164.32, 176.43;

FAB mass: Calcd. for $\text{C}_{22}\text{H}_{19}\text{NO}_4$ $m/z = 361.13$; Found: 361.34 (M^+);

Elemental Analysis: $\text{C}_{22}\text{H}_{19}\text{NO}_4$ Calcd. for C, 73.12; H, 5.30; N, 3.88; Found: C, 73.14; H, 5.32, N, 3.89.

Pale yellow viscous liquid;

R_f: 0.26 (20% EtOAc-Hexane);

IR (CH_2Cl_2) ν_{max} : 1616, 1645, 1703, 1721, 2124, 3077, 3231 cm^{-1} ;

^1H NMR(CDCl_3/TMS , 300.1 MHz): δ 2.29 (s, 3H), 3.22 (s, 3H), 3.57 (s, 3H), 3.82 (s, 1H), 4.66 (s, 2H), 6.69 (d, $J = 7.8$ Hz, 1H), 6.91 (m, 2H), 7.04 (d, $J = 7.6$ Hz, 1H), 7.26 (s, 1H);

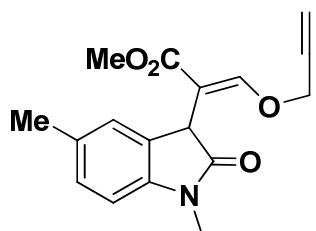
^{13}C NMR (CDCl_3/TMS , 75.4 MHz): δ 21.09, 26.49, 47.89, 51.44, 61.26, 76.99, 77.41, 106.97, 107.55, 124.23, 128.40, 128.44, 131.64, 142.02, 156.33, 164.65, 175.99;

FAB mass: Calcd. for $\text{C}_{17}\text{H}_{17}\text{NO}_4$ $m/z = 299.12$; Found: 300.23 ($\text{M}+1$);

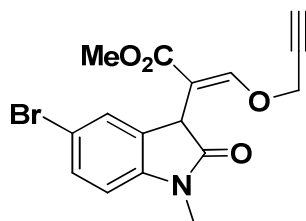
Elemental Analysis: $\text{C}_{17}\text{H}_{17}\text{NO}_4$ Calcd. for C, 68.21; H, 5.72; N, 4.68; Found: C, 68.24; H, 5.76, N, 4.66.

Pale yellow viscous liquid;

R_f: 0.27 (20% EtOAc-Hexane);



Compound 55



Compound 56

IR (CH₂Cl₂) ν_{\max} : 1124, 1615, 1645, 1704, 1724, 2125, 3077, 3231 cm⁻¹;

¹H NMR(CDCl₃/TMS, 300.1 MHz): δ 2.63 (s, 1H), 3.23 (s, 3H), 3.57 (s, 3H), 3.80 (s, 1H), 4.66 (s, 2H), 6.49 (d, J = 7.5 Hz, 1H), 6.79 (s, 1H), 6.92 (d, J = 7.5 Hz, 1H), 7.28 (s, 1H);

¹³C NMR (CDCl₃/TMS, 75.4 MHz): δ 26.45, 46.91, 52.27, 60.10, 74.20, 76.04, 108.26, 116.55, 124.43, 125.35, 127.56, 137.67, 147.31, 154.6, 164.21, 175.60;

FAB mass: Calcd. for C₁₆H₁₄BrNO₄ m/z = 363.02; Found: 365.43 (M+2);

Elemental Analysis: C₁₆H₁₄BrNO₄ Calcd. for C, 52.77; H, 3.87; N, 3.85; Found: C, 52.79; H, 3.89, N, 3.83.

Pale yellow viscous liquid;

R_f: 0.25 (20% EtOAc-Hexane);

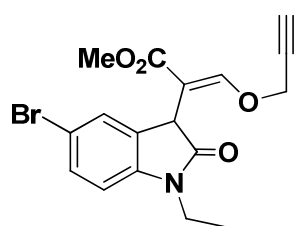
IR (CH₂Cl₂) ν_{\max} : 1123, 1614, 1643, 1701, 1713, 2123, 3078, 3232 cm⁻¹;

¹H NMR (CDCl₃/TMS, 300.1 MHz): δ 1.05 (m, 3H), 2.64 (s, 2H), 3.56 (s, 3H), 4.36 (q, J = 4.3 Hz, 2H), 4.67 (s, 2H), 6.48 (d, J = 7.6 Hz, 1H), 6.79 (m, 1H), 6.92 (d, J = 7.6 Hz, 1H), 7.25 (s, 1H);

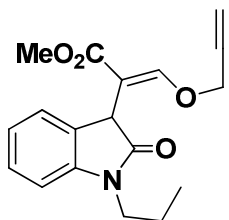
¹³C NMR (CDCl₃/TMS, 75.4 MHz): δ 12.87, 44.93, 46.92, 51.95, 61.23, 74.23, 76.40, 108.21, 117.80, 126.87, 128.33, 129.46, 129.73, 140.16, 154.31, 164.23, 176.53;

FAB mass: Calcd. for C₁₇H₁₆BrNO₄ m/z = 377.12; Found: 379.23 (M+2);

Elemental Analysis: C₁₇H₁₆BrNO₄ Calcd. for C, 53.99; H, 4.26; N, 3.70; Found: C, 53.97; H, 4.24, N, 3.72.



Compound 57



Compound 58

Pale yellow viscous liquid;

R_f: 0.26 (20% EtOAc-Hexane);

IR (CH₂Cl₂) ν_{\max} : 1616, 1647, 1705, 1718, 2122, 3077, 3231 cm⁻¹;

¹H NMR (CDCl₃/TMS, 300.1 MHz): δ 0.92 (t, *J* = 2.3 Hz, 3H), 1.78 (p, *J* = 2.3, 4.1 Hz, 2H), 2.64 (s, 1H), 3.54 (s, 3H), 3.68 (t, *J* = 4.1 Hz, 2H), 3.82 (s, 1H), 4.66 (s, 2H), 6.70 (d, *J* = 7.6 Hz, 1H), 7.01 (m, 2H), 7.03 (d, *J* = 7.6 Hz, 1H), 7.27 (s, 1H);

¹³C NMR (CDCl₃/TMS, 75.4 MHz): δ 10.22, 19.56, 44.96, 46.73, 51.46, 61.28, 74.28, 76.37, 108.92, 118.62, 126.80, 127.17, 128.32, 129.74, 140.24, 152.01, 166.46, 174.66;

FAB mass: Calcd. for C₁₈H₁₉NO₄ *m/z* = 313.13; Found: 313.23 (M⁺);

Elemental Analysis: C₁₈H₁₉NO₄ Calcd. for: C, 68.99; H, 6.11; N, 4.47; Found: C, 68.97; H, 6.11, N, 4.37.

Pale yellow viscous liquid;

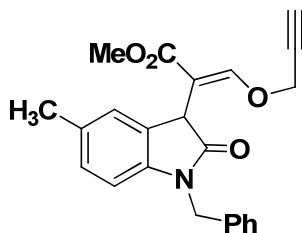
R_f: 0.35 (20% EtOAc-Hexane);

IR (CH₂Cl₂) ν_{\max} : 1614, 1645, 1702, 1722, 2120, 3076, 3232 cm⁻¹;

¹H NMR (CDCl₃/TMS, 300.1 MHz): δ 2.30 (s, 3H), 2.64 (s, 1H), 3.54 (s, 3H), 3.82 (s, 1H), 4.22 (m, 2H), 4.49 (m, 2H), 6.69 (d, *J* = 7.8 Hz, 1H), 6.94 (m, 2H), 7.03 (m, 2H), 7.28 (s, 1H), 7.36 (m, 3H);

¹³C NMR (CDCl₃/TMS, 75.4 MHz): δ 21.26, 42.17, 44.74, 51.36, 62.01, 75.27, 76.56, 108.41, 117.26, 123.20, 123.87, 124.21, 124.86 (2C), 127.81 (2C), 128.73, 129.35, 132.56, 142.23, 155.64, 164.34, 176.43;

FAB mass: Calcd. for C₂₃H₂₁NO₄ *m/z* = 375.15; Found:



Compound 59

376.23 (M+1);

Elemental Analysis: C₂₃H₂₁NO₄ Calcd. for: C, 73.58; H, 5.64; N, 3.73; Found: C, 72.56; H, 5.12, N, 3.11.

3.10.8 General experimental procedure for Claisen rearrangement:

A mixture of MBH adduct of propargyl vinyl ether (100 mg) in chlorobenzene (1 mL) was allowed to heat at 135 °C for 4 hours. The progress of reaction was monitored by TLC. After completion of the reaction, the solvent was removed under reduced pressure to afford allene-aldehyde functionalized product on silica gel column purification.

3.10.9 Characterization of new compounds:

Colourless viscous liquid;

R_f: 0.32 (20% EtOAc-Hexane);

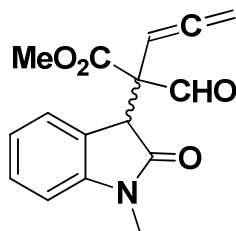
IR (CH₂Cl₂) ν_{\max} : 1623, 1706, 1720, 1974, 2214, 2823, 2934, 3049 cm⁻¹;

¹H NMR (CDCl₃/TMS, 300.1 MHz): δ 3.22 (s, 6H), 3.50 (s, 1H), 3.55 (m, 7H), 4.88 (m, 4H), 5.57 (t, *J* = 7.1 Hz, 1H), 5.67 (t, *J* = 7.2 Hz, 1H), 6.96 (m, 8H), 9.59 (s, 1H), 9.73 (s, 1H);

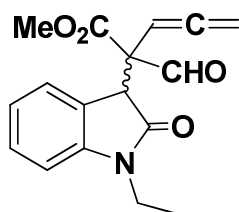
¹³C NMR (CDCl₃/TMS, 75.4 MHz): δ 23.89, 24.34, 40.12, 40.98, 51.78, 52.34, 63.41, 69.71, 75.62, 76.01, 97.56, 101.01, 107.81, 108.45, 123.81, 124.80, 125.03 (2C), 125.81, 126.24, 127.81 (2C), 143.23, 144.91, 164.98, 165.76, 175.54, 176.13, 197.23, 198.06, 209.18, 211.65;

FAB mass: Calcd. for C₁₆H₁₅NO₄ *m/z* = 285.13; Found: 286.43 (M+1);

Elemental Analysis: C₁₆H₁₅NO₄ Calcd. for C, 67.36; H, 5.30; N, 4.91; Found: C, 66.12; H, 4.34, N, 3.71.



Compound 61



Compound 62

Colourless viscous liquid;

R_f: 0.30 (20% EtOAc-Hexane);

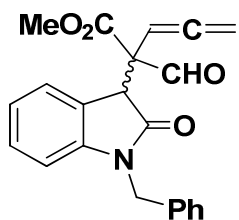
IR (CH₂Cl₂) ν_{\max} : 1621, 1704, 1720, 1975, 2215, 2824, 2933, 3047 cm⁻¹;

¹H NMR (CDCl₃/TMS, 300.1 MHz): δ 1.47 (m, 6H), 3.52 (m, 7H), 3.56 (s, 1H), 4.36 (m, 4H), 4.88 (m, 4H), 5.57 (m, 1H), 5.67 (m, 1H), 6.87 (m, 3H), 7.19 (m, 5H), 9.67 (s, 1H), 9.71 (s, 1H);

¹³C NMR (CDCl₃/TMS, 75.4 MHz): δ 11.86, 11.92, 40.13, 40.87, 44.98, 45.03, 53.45, 54.56, 67.91, 69.71, 75.64, 75.78, 94.56, 101.23, 109.26, 109.67, 123.26, 124.56, 124.89, 124.97, 125.63, 127.23, 127.81, 128.01, 144.21, 144.91, 164.76, 164.87, 174.52, 176.67, 199.05, 199.27, 207.03, 209.67;

FAB mass: Calcd. for C₁₇H₁₇NO₄ m/z = 299.12; Found: 300.43 (M+1);

Elemental Analysis: C₁₇H₁₇NO₄ Calcd. for C, 68.21; H, 5.72; N, 4.68; Found: C, 67.25; H, 4.74, N, 3.64.



Compound 63

Colourless viscous liquid;

R_f: 0.30 (20% EtOAc-Hexane);

IR (CH₂Cl₂) ν_{\max} : 1623, 1702, 1719, 1975, 2218, 2827, 2931, 3045 cm⁻¹;

¹H NMR (CDCl₃/TMS, 300.1 MHz): δ 3.53 (m, 7H), 3.55 (s, 1H), 4.35 (m, 4H), 4.76 (m, 4H), 5.61 (m, 1H), 5.63 (m, 1H), 6.96 (m, 16H), 7.79 (m, 2H), 9.63 (s, 1H), 9.83 (s, 1H);

¹³C NMR (CDCl₃/TMS, 75.4 MHz): δ 40.13, 40.89, 42.23, 44.98, 52.34, 54.40, 67.28, 69.83, 74.54, 75.68, 92.46, 99.58, 107.21, 110.62, 110.78, 115.43, 117.62, 122.43, 125.41, 126.91, 126.94, 127.15, 127.88, 128.04

(2C), 128.15, 128.51, 128.99, 129.05, 129.12, 129.64, 132.08, 132.16, 134.09, 143.58, 144.43, 164.37, 165.41, 174.38, 176.31, 197.12, 198.65, 206.5, 211.01;

FAB mass: Calcd. for $C_{22}H_{19}NO_4$ m/z = 361.13; Found: 362.43 (M+1);

Elemental Analysis: $C_{22}H_{19}NO_4$ Calcd. for C, 73.12; H, 5.30; N, 3.88; Found: C, 71.14; H, 5.22, N, 3.84.

Colourless viscous liquid;

R_f: 0.35 (20% EtOAc-Hexane);

IR (CH_2Cl_2) ν_{max} : 1623, 1703, 1718, 1953, 2217, 2821, 2953, 3046 cm^{-1} ;

¹H NMR ($CDCl_3/TMS$, 300.1 MHz): δ 2.29 (s, 3H), 2.30 (s, 3H), 3.21 (s, 6H), 3.52 (m, 7H), 3.55 (s, 1H), 4.89 (m, 4H), 5.55 (m, 1H), 5.65 (m, 1H), 6.99 (m, 6H), 9.62 (s, 1H), 9.75 (s, 1H);

¹³C NMR ($CDCl_3/TMS$, 75.4 MHz): δ 21.64, 21.75, 24.34, 24.37, 40.14, 40.97, 52.34, 54.45, 69.73, 69.79, 74.34, 75.62, 94.56, 98.57, 108.45, 109.02, 124.80, 124.87, 125.03, 125.34, 126.24, 127.12, 127.54, 127.81, 139.85, 144.91, 165.76, 165.87, 176.54, 177.86, 198.06, 199.02, 206.53, 207.65;

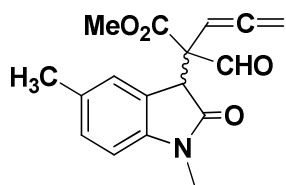
FAB mass: Calcd. for $C_{17}H_{17}NO_4$ m/z = 299.12; Found: 300.73 (M+1);

Elemental Analysis: $C_{17}H_{17}NO_4$ Calcd. for C, 68.21; H, 5.72; N, 4.68; Found: C, 68.03; H, 5.44, N, 4.46.

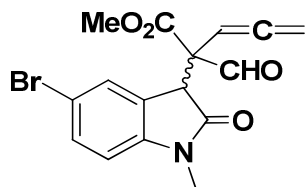
Colourless viscous liquid;

R_f: 0.34 (20% EtOAc-Hexane);

IR (CH_2Cl_2) ν_{max} : 1177, 1620, 1703, 1722, 1956, 2216, 2826, 2933, 3045 cm^{-1} ;



Compound 64



Compound 65

$^1\text{H NMR}$ (CDCl_3/TMS , 300.1 MHz): δ 3.23 (s, 6H), 3.52 (m, 7H), 3.56 (s, 1H), 4.80 (m, 4H), 5.55 (t, $J = 7.0$ Hz, 1H), 5.65 (t, $J = 7.2$ Hz, 1H), 6.65 (m, 3H), 7.45 (m, 3H), 9.69 (s, 1H), 9.75 (s, 1H);

$^{13}\text{C NMR}$ (CDCl_3/TMS , 75.4 MHz): δ 23.31, 23.33, 40.12, 40.78, 52.34, 54.39, 68.98, 69.23, 74.73, 75.62, 93.73, 99.76, 108.45, 109.12, 119.86, 119.99, 124.87, 125.34, 126.61, 127.52, 127.54, 127.91, 139.86, 144.99, 164.77, 165.77, 176.17, 177.86, 198.18, 199.16, 204.57, 208.61;

FAB mass: Calcd. for $\text{C}_{16}\text{H}_{14}\text{BrNO}_4$ $m/z = 363.01$; Found: 365.43 (M+2);

Elemental Analysis: $\text{C}_{16}\text{H}_{14}\text{BrNO}_4$ Calcd. for C, 52.77; H, 3.87; N, 3.85; Found C, 51.99; H, 3.29, N, 3.18.

Colourless viscous liquid;

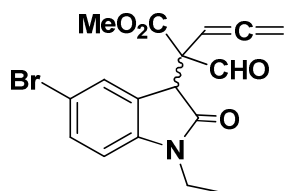
R_f: 0.35 (20% EtOAc-Hexane);

IR (CH_2Cl_2) ν_{max} : 1176, 1622, 1702, 1719, 1986, 2216, 2827, 2932, 3046 cm^{-1} ;

$^1\text{H NMR}$ (CDCl_3/TMS , 300.1 MHz): δ 1.46 (m, 6H), 3.53 (m, 7H), 3.56 (s, 1H), 4.35 (m, 4H), 4.89 (m, 4H), 5.57 (m, 1H), 5.67 (m, 1H), 6.83 (m, 6H), 9.67 (s, 1H), 9.71 (s, 1H);

$^{13}\text{C NMR}$ (CDCl_3/TMS , 75.4 MHz): δ 10.23, 10.92, 40.19, 40.89, 44.98, 45.03, 53.46, 54.56, 67.91, 69.71, 75.64, 75.78, 94.56, 101.23, 109.26, 109.67, 119.28, 123.26, 124.56, 124.89, 124.97, 125.63, 127.23, 128.01, 144.21, 144.91, 164.77, 165.87, 174.52, 176.67, 198.15, 199.37, 204.21, 207.61;

FAB mass: Calcd. for $\text{C}_{17}\text{H}_{16}\text{BrNO}_4$ $m/z = 377.03$; Found: 379.43 (M+2);



Compound 66

Elemental Analysis: C₁₇H₁₆BrNO₄ Calcd. for C, 53.99; H, 4.26; N, 3.70; Found: C, 51.97; H, 4.24, N, 3.61.

Colourless viscous liquid;

R_f: 0.32 (20% EtOAc-Hexane);

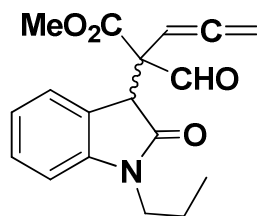
IR (CH₂Cl₂) ν_{\max} : 1623, 1703, 1717, 1976, 2218, 2829, 2931, 3045 cm⁻¹;

¹H NMR (CDCl₃/TMS, 300.1 MHz): δ 0.95 (m, 6H), 1.69 (m, 4H), 3.48 (m, 4H), 3.52 (m, 7H), 3.56 (s, 1H), 4.80 (m, 4H), 5.57 (t, *J* = 7.0 Hz, 1H), 5.65 (t, *J* = 7.2 Hz, 1H), 6.56 (m, 3H), 7.22 (m, 5H), 9.71 (s, 1H), 9.75 (s, 1H);

¹³C NMR (CDCl₃/TMS, 75.4 MHz): δ 11.53, 11.78, 19.01, 19.51, 40.17, 40.83, 43.29, 43.91, 52.34, 54.39, 68.98, 69.23, 74.73, 75.62, 93.73, 99.76, 108.45, 109.12, 119.86, 119.99, 124.97, 125.63, 127.23, 127.31, 127.54, 127.91, 139.86, 144.99, 164.26, 165.77, 175.17, 176.86, 197.18, 199.16, 204.57, 207.61;

FAB mass: Calcd. for C₁₈H₁₉NO₄ *m/z* = 313.13; Found: 314.72 (M+1);

Elemental Analysis: C₁₈H₁₉NO₄ Calcd. for C, 68.99; H, 6.11; N, 4.47; Found: C, 67.95; H, 5.83, N, 4.12.



Compound 67

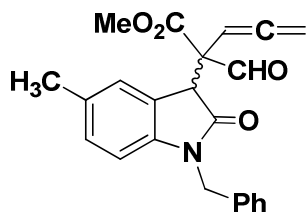
Colourless viscous liquid;

R_f: 0.30 (20% EtOAc-Hexane);

IR (CH₂Cl₂) ν_{\max} : 1623, 1705, 1716, 1984, 2215, 2827, 2921, 3025 cm⁻¹;

¹H NMR (CDCl₃/TMS, 300.1 MHz): δ 2.29 (m, 6H), 3.53 (m, 7H), 3.56 (s, 1H), 4.35 (m, 4H), 4.78 (m, 4H), 5.61 (m, 1H), 5.61 (m, 1H), 6.71 (m, 14H), 7.80 (m, 2H), 9.61 (s, 1H), 9.81 (s, 1H);

¹³C NMR (CDCl₃/TMS, 75.4 MHz): δ 21.67, 21.98,



Compound 68

40.18, 40.89, 42.73, 44.98, 45.53, 52.56, 54.41, 69.71, 69.81, 74.34, 75.68, 92.16, 101.51, 107.27, 109.62, 110.78, 115.43, 118.62, 122.43, 125.41, 126.51, 126.95, 127.15, 127.88, 128.03 (2C), 128.16, 128.52, 128.91, 129.02, 129.11, 129.61, 132.08, 132.16, 134.31, 143.58, 144.25, 164.23, 165.42, 174.39, 176.82, 197.21, 198.67, 202.51, 209.12;

FAB mass: Calcd. for $C_{23}H_{21}NO_4$ $m/z = 375.15$; Found: 376.43 (M+1);

Elemental Analysis: $C_{22}H_{21}NO_4$ Calcd. for C, 73.58; H, 5.64; N, 3.73; Found: C, 72.76; H, 4.82, N, 2.98.

Colourless viscous liquid;

R_f: 0.35 (20% EtOAc-Hexane);

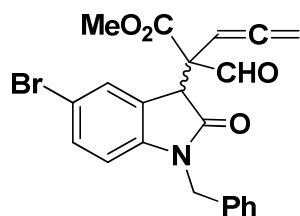
IR (CH_2Cl_2) ν_{max} : 1623, 1703, 1720, 1953, 2217, 2821, 2953, 3046 cm^{-1} ;

¹H NMR ($CDCl_3/TMS$, 300.1 MHz): δ 2.29 (s, 3H), 2.30 (s, 3H), 3.21 (s, 6H), 3.52 (m, 7H), 3.55 (s, 1H), 4.92 (m, 4H), 5.55 (m, 2H), 5.65 (m, 2H), 6.99 (m, 6H), 9.62 (s, 1H), 9.75 (s, 1H);

¹³C NMR ($CDCl_3/TMS$, 75.4 MHz): δ 21.64, 21.75, 24.34, 24.37, 40.14, 40.97, 52.34, 54.45, 69.73, 69.79, 74.34, 75.62, 94.56, 98.57, 108.45, 109.02, 124.80, 124.87, 125.03, 125.34, 126.24, 127.12, 127.54, 127.81, 139.85, 144.91, 165.76, 165.87, 176.54, 177.86, 198.06, 199.02, 206.53, 207.65;

FAB mass: Calcd. for $C_{22}H_{18}BrNO_4$ $m/z = 440.19$; Found: 442.13 (M+2);

Elemental Analysis: $C_{22}H_{18}BrNO_4$ Calcd. for C, 60.01; H, 4.12; N, 3.18; Found: C, 59.83; H, 3.87, N, 3.10.

**Compound 69****3.10.10 Synthesis of dihydrofuran derivatives:**

A mixture of MBH adduct of allene (100 mg) in acetone (1 mL) with DABCO (10 mol %) was allowed to reflux for 4 hours. The progress of the reaction was monitored by TLC. After completion of the reaction, the solvent was removed under reduced pressure to afford oxindole appended dihydrofuran derivatives in moderate yield (42-48%) by silica gel column purification.

3.10.11 Characterization of new compounds:

Yellow viscous liquid;

R_f: 0.30 (20% EtOAc-Hexane);

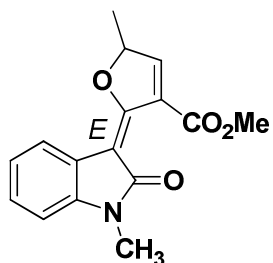
IR (CH₂Cl₂) ν_{\max} : 1123, 1642, 1706, 1718, 2976, 3078 cm⁻¹;

¹H NMR (CDCl₃/TMS, 300.1 MHz): δ 2.0 (d, J = 6.9 Hz, 3H), 3.23 (s, 3H), 3.98 (s, 3H), 6.11 (td, J = 6.9, 16 Hz, 1H), 6.77 (d, J = 7.8 Hz, 1H), 6.94 (t, J = 7.7 Hz, 1H), 7.04 (d, J = 7.7 Hz, 1H), 7.21 (t, J = 7.7 Hz, 1H), 8.14 (d, J = 16 Hz, 1H);

¹³C NMR (CDCl₃/TMS, 75.4 MHz): δ 19.51, 25.84, 29.79, 52.48, 107.99, 119.86, 121.04, 121.83, 122.07, 125.27, 129.49, 139.52, 139.98, 143.19, 167.22, 167.76;

FAB mass: Calcd. for C₁₆H₁₅NO₄ m/z = 285.21; Found: 286.10 (M+1);

Elemental Analysis: C₁₆H₁₄NO₄ Calcd. for C, 52.77; H, 3.87; N, 3.85; Found: C, 51.95; H, 3.69, N, 3.55.



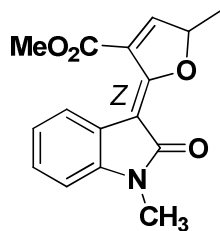
Compound 70a
(*E*-isomer)

Yellow viscous liquid;

R_f: 0.26 (20% EtOAc-Hexane);

IR (CH₂Cl₂) ν_{\max} : 1122, 1641, 1702, 1718, 2971, 3100 cm⁻¹;

¹H NMR (CDCl₃/TMS, 300.1 MHz): δ 1.98 (d, J = 6.9 Hz, 3H), 3.23 (s, 3H), 3.89 (s, 3H), 6.21 (td, J = 6.87, 16.3 Hz, 1H), 6.73 (d, J = 7.8 Hz, 1H), 6.94 (t, J = 7.5 Hz, 1H), 7.21 (t, J = 7.7 Hz, 1H), 7.54 (d, J = 6.9 Hz, 1H), 7.87 (d,



Compound 70b

(Z-isomer)

$J = 16.3$ Hz, 1H);

^{13}C NMR (CDCl_3/TMS , 75.4 MHz): δ 19.46, 25.84, 29.78, 52.38, 107.73, 120.12, 121.06, 122.67, 125.32, 129.93, 131.16, 139.14, 139.63, 141.10, 167.26, 167.82;

FAB mass: Calcd. for $\text{C}_{16}\text{H}_{15}\text{NO}_4$ $m/z = 285.21$; Found: 286.07 (M+1);

Elemental Analysis: $\text{C}_{16}\text{H}_{14}\text{BrNO}_4$ Calcd. for C, 52.77; H, 3.87; N, 3.85; Found: C, 52.35; H, 3.29, N, 3.67.

Yellow viscous liquid;

R_f : 0.28 (20% EtOAc-Hexane);

IR (CH_2Cl_2) ν_{max} : 1124, 1642, 1702, 1720, 2975, 3081 cm^{-1} ;

^1H NMR (CDCl_3/TMS , 300.1 MHz): δ 2.01 (d, $J = 6.8$ Hz, 3H), 3.23 (s, 3H), 3.99 (s, 3H), 6.12 (td, $J = 6.8, 16.3$ Hz, 1H), 6.78 (d, $J = 7.8$ Hz, 1H), 6.94 (d, $J = 7.8$ Hz, 1H), 7.04 (d, $J = 7.8$ Hz, 1H), 8.98 (d, $J = 16.3$ Hz, 1H);

^{13}C NMR (CDCl_3/TMS , 75.4 MHz): δ 19.47, 25.54, 29.67, 52.54, 107.87, 118.86, 121.64, 121.83, 122.37, 125.73, 129.32, 139.18, 139.53, 143.19, 167.23, 167.45;

FAB mass: Calcd. for $\text{C}_{16}\text{H}_{14}\text{BrNO}_4$ $m/z = 363.01$; Found: 365.21 (M+2);

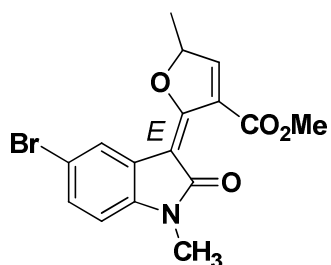
Elemental Analysis: $\text{C}_{16}\text{H}_{14}\text{BrNO}_4$ Calcd. for C, 52.77; H, 3.87; N, 3.85; Found: C, 51.95; H, 3.43, N, 3.19.

Yellow viscous liquid;

R_f : 0.32 (20% EtOAc-Hexane);

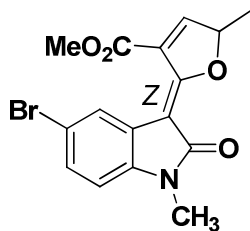
IR (CH_2Cl_2): 1123, 1640, 1726, 2976, 3120 cm^{-1} ;

^1H NMR (CDCl_3/TMS , 300.1 MHz): δ 1.98 (d, $J = 6.9$ Hz, 3H), 3.23 (s, 3H), 3.89 (s, 3H), 6.21 (td, $J = 6.87, 16$ Hz, 1H), 6.73 (d, $J = 7.8$ Hz, 1H), 6.94 (t, $J = 7.5$ Hz, 1H),



Compound 71a

(E-isomer)



Compound 71b

(Z-isomer)

7.54 (d, $J = 6.9$ Hz, 1H), 7.87 (d, $J = 16.1$ Hz, 1H);

^{13}C NMR (CDCl_3/TMS , 75.4 MHz): δ 19.46, 25.54, 29.66, 52.48, 107.89, 119.36, 121.64, 121.83, 122.37, 125.62, 128.34, 138.51, 139.98, 142.13, 167.29, 168.76;

FAB mass: Calcd. for $\text{C}_{16}\text{H}_{14}\text{BrNO}_4$ $m/z = 363.01$;

Found: 365.07 (M+2);

Elemental Analysis: $\text{C}_{16}\text{H}_{14}\text{BrNO}_4$ Calcd. for C, 52.77;

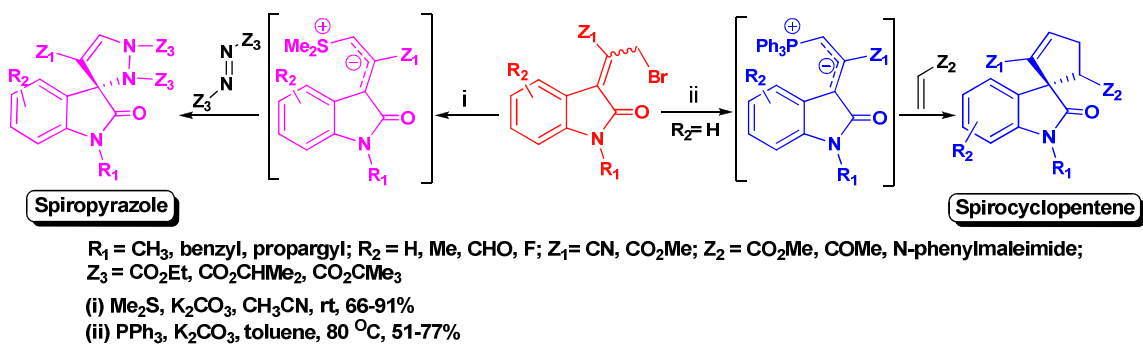
H, 3.87; N, 3.85; Found: C, 52.75; H, 3.85, N, 3.87.

Chapter IV

Diastereoselective Synthesis of 3-Spirocyclopentene and 3-Spiropyrazole-2-Oxindole Derivatives *via* [3+2]-Annulation Reaction

Abstract:

The chemistry phosphorus and sulphur ylides have been exploited for a facile, short and efficient synthesis of 3-spirocyclopentene- and 3-spiropyrazole-2-oxindoles from *E*- and *Z*-isomers of bromo derivatives of Morita-Baylis-Hillman adducts of isatin with Ph_3P /activated alkene/ K_2CO_3 and Me_2S /DEAD/ K_2CO_3 *via* [3+2]-annulation strategy, respectively.



Shanmugam, P. *et al. Chem. Commun.*, 2010, 46, 2826–2828.

Chapter IV

Diastereoselective Synthesis of 3-Spirocyclopentene and 3-Spiropyrazole-2-Oxindole Derivatives via [3+2]-Annulation Reaction

4.1 Introduction:

Spirocyclic compounds have attracted the attention of organic chemists due to their unique structural and reactivity pattern. Many natural products such as fredericamycin [Kelly, T. R. *et al.* 1986], spirovetivanes, acroanes, chamigrenes [Heathcock, C. K. *et al.* 1983], angularly fused cyclopentanoids (e.g. crinipellin-A, laurenene) [Mehta, G. *et al.* 1997], non-natural products [5.5.5.5] fenestrane [Thommen, M. *et al.* 1997], spiranes [Fitjer, L. *et al.* 1988] and coronane possess the spiro-linkages [Krapcho, A. P. 1987; Sannigrahi, M. 1999] as crucial structural units [Figure 4.1].

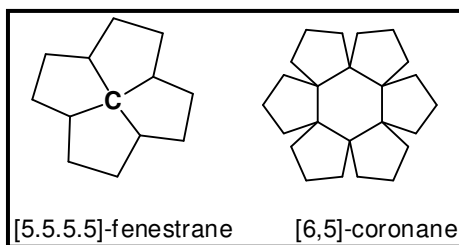


Figure 4.1: Structurally unique spirocyclic frameworks.

Among them, spirooxindoles are commonly occurring heterocyclic ring systems found in many natural products and pharmaceuticals [Galliford, C.V. *et al.* 2007]. A range of biologically active compounds possessing the spiropyrrolidine framework is well displayed in the literature (Figure 4.2) [Stylianakis, I. *et al.* 1999]. Various approaches to prepare spirocyclic systems have encountered problems associated with functional group incompatibility at one or more stages and restricted to a single substitution pattern. In a few instances, the newly generated ring system left with a useful functionality for further synthetic transformations.

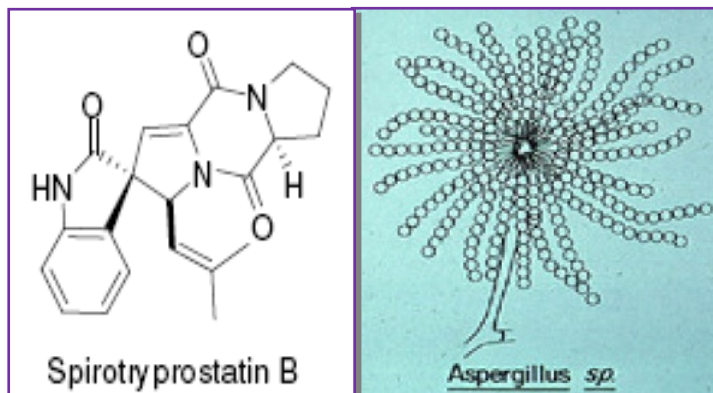


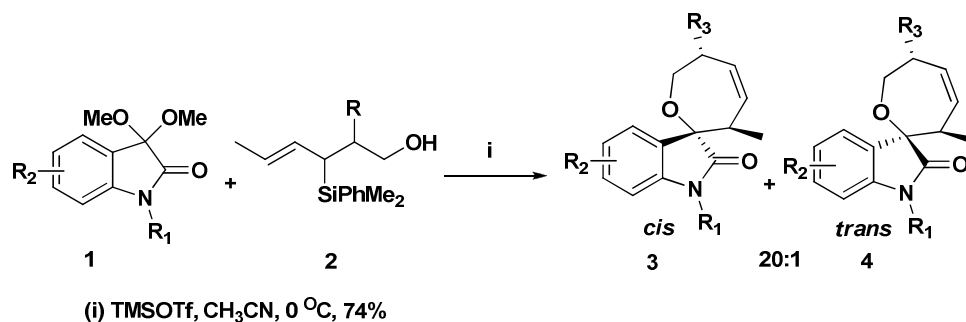
Figure 4.2: Spirooxindole natural product isolated from *Aspergillus fumigates*.

Owing to its advantage, we were interested to synthesise 3-spiro cyclopentene- and 3-spiropyrazole-2-oxindole derivatives from 3-allyl bromides of oxindole *via* phosphorous and sulphur ylides [3+2]-annulation reaction. To familiarise the chemistry of phosphorous and sulphur ylides, the following section outlines a brief account on the generation and some literature known annulation reactions of phosphorous and sulphur ylides.

4.2 Synthesis of cyclic and spirocyclic derivatives *via* annulation strategy:

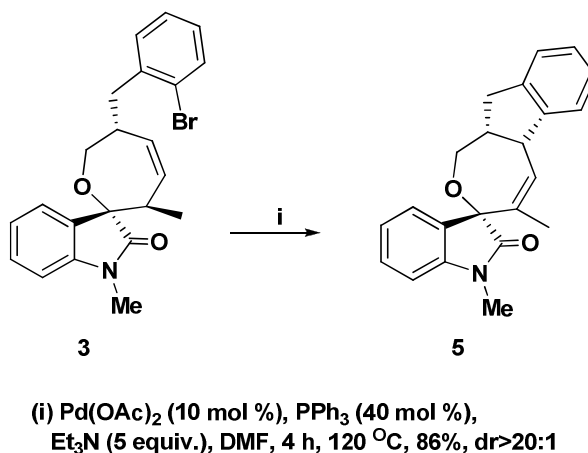
4.2.1 Lewis acids promoted [5+2]-annulation:

The stereoselective 3-oxepene appended 2-oxindole derivatives were synthesized from the chiral crotylsilane **2** with *N*-methylisatin dimethyl ketal **1** *via* Lewis acid promoted [5+2]-annulation (Scheme 4.1). The diastereoselective formation *cis*-spiro oxepene **3** was controlled by kinetic means, can undergo epimerization and furnish *trans* isomer **4** *via* $\text{BF}_3 \cdot \text{OEt}_2$ induced ring opening mechanism [Zhang, Y. *et al.* 2009].



Scheme 4.1: Synthesis of spirooxapene oxindole derivatives.

The annulation products **3** and **4** were further elaborated for the preparation of a complex molecular framework **5** through intramolecular Heck reaction of keeping substituent **R**₃ as aryl halide and oxepene olefin (Scheme 4.2).

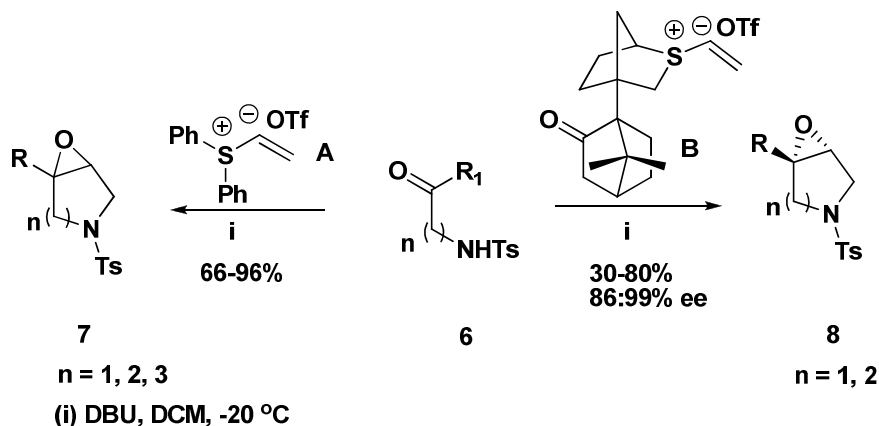


Scheme 4.2: Synthesis of complex spirooxepene oxindole derivatives.

4.2.2 Epoxy annulation: reagent vs. kinetic resolution of substrate controlled reaction:

Unthank *et al.* reported a substrate and reagent controlled stereoselective epoxy annulation reaction between α -aminoketone **6** and vinyl sulfonium salt [Unthank *et al.* 2008] (Scheme 4.3). The diastereoselective *syn*-epoxy pyrrolidine derivative **7** has been synthesised from α -aminoketone **6** and achiral vinyl sulfonium salt **A** via substrate controlled mode of synthesis. The enantiomerically enriched *anti*-epoxy pyrrolidine derivative **8** have also been achieved from chiral vinyl sulfonium salt **B** via reagent controlled mode of synthesis. The enatio enriched stereoisomer **8** synthesised from

racemic mixture of starting material by kinetic resolution as a key step using the chiral vinyl sulfonium salt **B** as a catalyst.

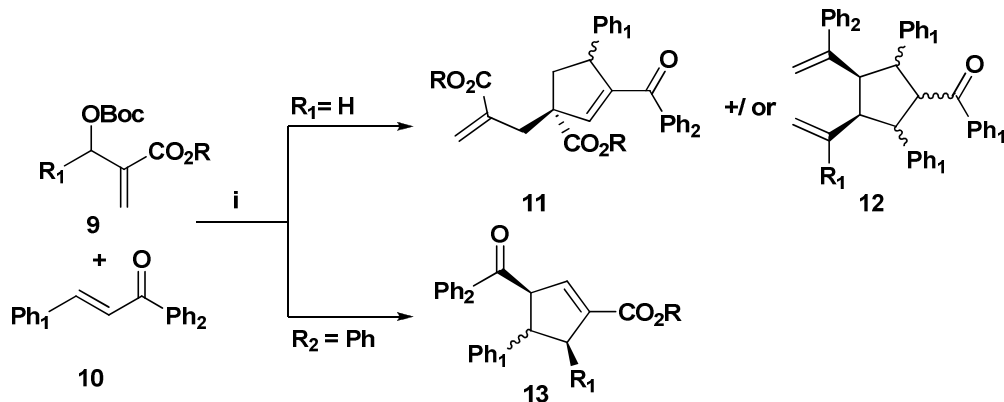


Scheme 4.3: Synthesis of epoxy pyrrolidines derivatives via sulphur ylide annulation.

4.3 Recent reports on phosphorous and sulphur ylide annulation reactions using MBH adducts and their derivatives:

4.3.1 Phosphine catalyzed cascade [3+2]-cyclization-allylic alkylation and [2+2+1]-annulation:

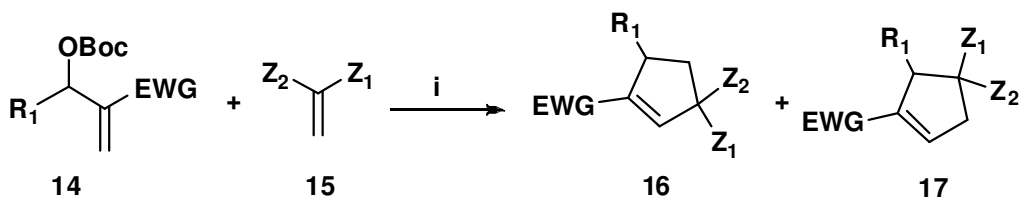
Recently, Zhou *et al.* have reported the synthesis of a variety of cyclopentenes **11**, **13** and cyclopentane derivative **12** via PBU_3 catalyzed chemoselective cascade [3+2]-cyclization-allylic alkylation, [2+2+1]-annulation, and [3+2]-cyclization reactions, respectively (Scheme 4.4). The mode of cyclization depends on the substitution on carbonate **9** and enone **10**. The formation of product **11** has been rationalised by the three components involving cascade/tandem [3+2]-cyclization-allylic alkylation reaction between the two molecules of carbonate **9** and one molecule of chalcones **10** [Zhou *et al.* 2011]. The aryl group substituted at R_1 position of allylic carbonate selectively provided single diastereomer of cyclopentene derivative **13** via [3+2]-cycloaddition. The electron-deficient chalcones bearing a 4-nitrophenyl group at Ph_2 position afforded selectively the [2+2+1]-annulation product **12** along with allylic carbonate **9**.



Scheme 4.4: Synthesis of cyclopentene and cyclopentane derivatives via phosphine ylide.

4.3.2 Phosphine catalysed [3+N]-annulation reaction:

The catalytic version of phosphorus mediated C-C bond forming reactions is scarce due to the higher oxophilicity of phosphine [Maryanoff, B. E.]. In 2003, Du *et al.* first reported the phosphine catalysed C-C bond forming reaction between the modified MBH carbonate derivative **14** and various activated olefins **15** [Du, *et al.* 2003]. The allyl-phosphorous ylide is generated *in-situ* from K_2CO_3 and allyl phosphonium salt by the reaction between modified MBH adducts **14** and triphenylphosphine (PPh_3). The ylide provided regioisomeric mixture of cyclopentenes **16** and **17** via dipolar cycloaddition with activated olefin (Scheme 4.5).

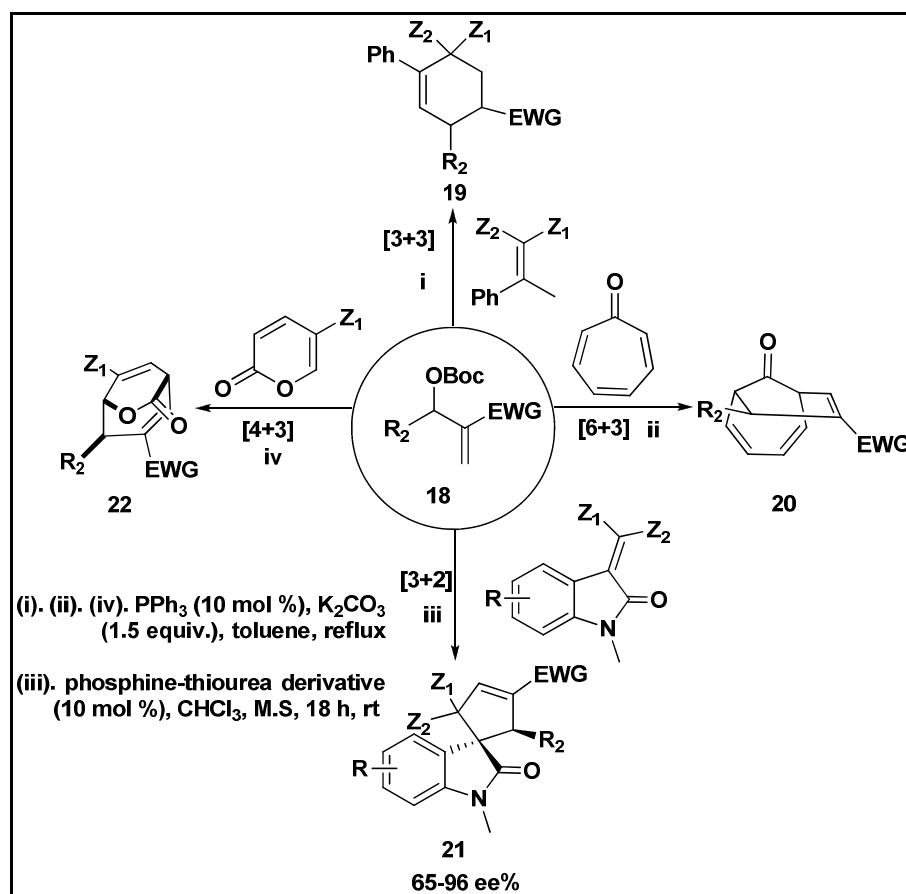


(i) PPh_3 , K_2CO_3 , toluene, $120\text{ }^\circ\text{C}$

Scheme 4.5: Synthesis of cyclopentene derivatives.

Pioneer work on the phosphine catalyst has been extended to a number of activated alkenes with MHB adduct and led to a variety [3+6], [3+2], [4+3] and [3+3]

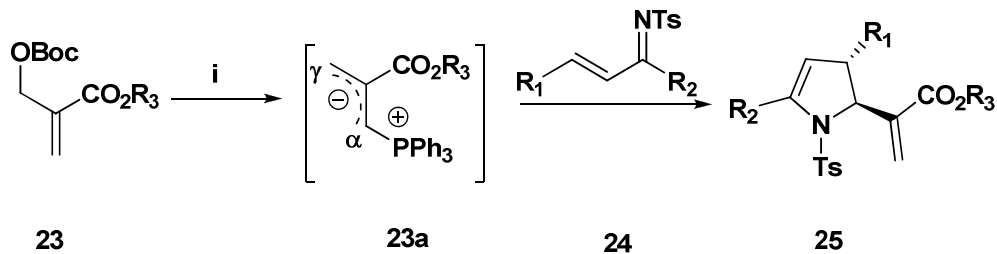
annulated products (Scheme 4.6) [Du, Y. *et al.* 2005; Zheng, S. *et al.* 2009^a; Zheng, S. *et al.* 2009^b; Zhong, F. *et al.* 2011].



Scheme 4.6: Phosphine catalyzed $[3+N]$ -annulation reactions.

4.3.3 Phosphine-catalyzed $[4+1]$ -annulation:

The sulphur and nitrogen mediated synthesis of pyrroline derivatives *via* $[4+1]$ -annulation reaction have been well explored [Zheng, J.-C. *et al.* 2008]. In 2011, Tian *et al.* have reported diastereoselective synthesis of pyrroline derivatives **16** *via* phosphine catalyzed annulation reaction of α,β -unsaturated imine **24** and allylic carbonate of MBH adduct **23** [Tian, J. *et al.* 2011]. The catalytic cycle was initiated from *in-situ* generated allylic phosphorus ylide. The ylide **23a** generated by the addition-elimination-deprotonation process and undergoes either γ - or α -addition with α,β -unsaturated imine followed by intramolecular cyclization provided the pyrroline derivative **25** (Scheme 4.7).

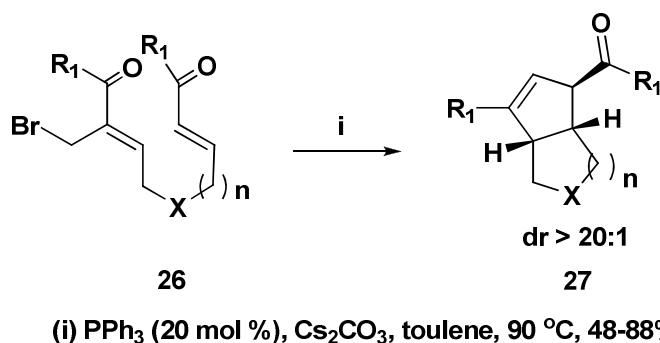


(i) PPh₃ (20 mol %), CH₂Cl₂, rt, 24 h, 83-99%, dr >20:1

Scheme 4.7: Synthesis of diastereoselective pyrrolidine derivatives.

4.3.4 Phosphine-catalyzed intramolecular [3+2]-cycloaddition:

Lu *et al.* have reported a catalytic phosphine version C-C bond formation that have subsequently been explored by a number of groups and also synthesised a variety of carbo- and heterocyclic frame works [Wurz, R. P. *et al.* 2005; Wilson, J. E. *et al.* 2006]. Interestingly, Ye *et al.* have reported the phosphine catalyzed diastereoselective synthesis of a number of bicyclic carbo- and heterocycle derivatives **27** from diketone derivative **26** via tandem intramolecular annulation reaction (Scheme 4.8) [Ye. L.-W. *et al.* 2007].



Scheme 4.8: Synthesis of bicyclic carbo- and heterocycle derivatives.

4.3.5 Sulphide induced [3+2]-annulation strategy:

The catalytic sulphur mediated olefination [Choi, J. *et al.* 2003], epoxidation [Edwards, D. R. *et al.* 2007], aziridination [Kokotos, C. G. *et al.* 2007] and cyclopropanation [Appel, R. *et al.* 2010; Zhang, R. *et al.* 1999] have been well explored. Basavaiah and co-workers first reported the synthesis of pyrazole derivatives **30** from

bromide of oxindole prepared from MBH adduct of isatin with various dipolarophiles utilizing catalytic phosphorous and sulphur ylide chemistry. In this context, phosphorous and sulphur catalyzed diastereoselective spirocyclopentene and spiropyrazole derivatives synthesised from the mixture of *E*- and *Z*-isomerised allyl bromide of oxindole *via* [3+2]-annulation are subject matter of this chapter. The results of the investigations are presented as follows.

4.5 Retrosynthetic analysis:

According to the proposal, a retrosynthetic strategy is shown in Figure 4.3. The structurally and synthetically important derivatives of 3-spirocyclopentene **C** and 3-spiropyrazole-2-oxindole **D** can be synthesised from a common starting material such as allyl bromide of oxindole **B** *via* [3+2]-annulation strategy by utilizing phosphorus and sulphur ylide chemistry. The MBH adduct and allyl bromide derivative **B** could be prepared as per literature procedure.²³ The formation of spirocyclic products **C** or **D** would depend on the basis of dipolarophile component as well as reagent selection.

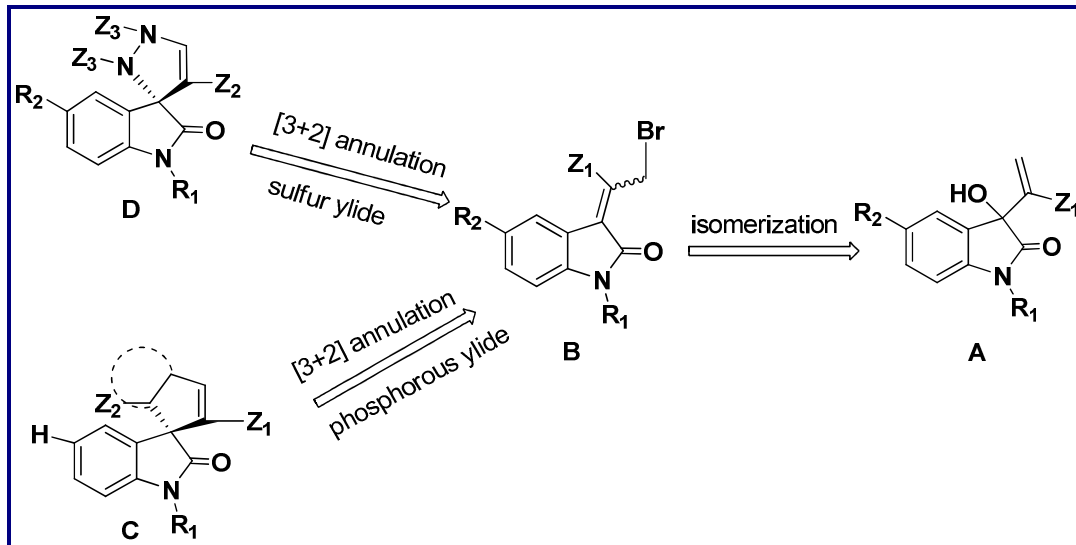


Figure 4.3: Retrosynthetic strategy for spirocyclic oxindole derivatives.

4.6 Results and Discussion:

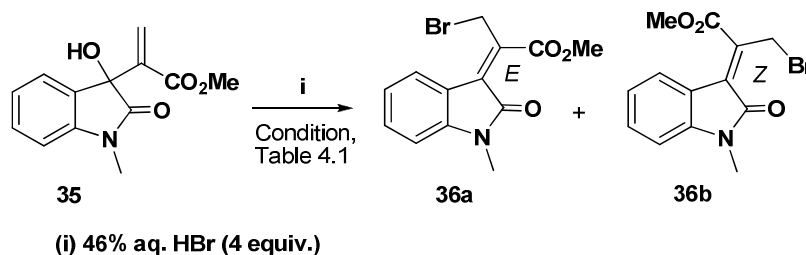
4.6.1 Preparation of allyl bromide from MBH adduct of isatin:

Before entering into isomerization study, we first screened the methods known for the synthesis of bromo isomerized derivative of simple MBH adducts. It has been

reported in the literature that for the isomerization of MBH adducts derived from benzaldehyde, aqueous HBr is a facile reagent under various conditions such as room temperature stirring in CH₂Cl₂/HBr, CH₂Cl₂/HBr/cat.H₂SO₄. Hence, we utilized aqueous HBr as a reagent for the isomerization of MBH adduct of isatin.

4.6.2 Optimization study for the isomerization reaction of MBH adduct with aqueous HBr:

The isomerization study was initiated with MBH adduct of isatin **35** with 46% aqueous HBr. However, to our surprise the isomerization procedure reported for simple MBH adduct with aqueous HBr failed for isatin derived MBH adduct **35** under various conditions such as stirring in CH₂Cl₂/HBr at room temperature, CH₂Cl₂/HBr/cat.H₂SO₄. Stirring the adduct **35** in CH₂Cl₂/HBr for a long period (overnight) at room temperature afforded the unaltered starting material quantitatively (Table 1, entry 1), while the reaction by stirring the adduct **35** in CH₂Cl₂/HBr/cat.H₂SO₄ resulted in decomposition of MBH adduct of isatin (Table 1, entry 2). The reaction of adduct **35** in CHCl₃/HBr under reflux condition showed a trace of desired isomerized product formation (Table 1, entry 4). The trace of product formation under chloroform reflux condition prompted us to carry out a reaction under microwave irradiation. Thus, the MBH adduct **35** with 46% aqueous HBr (4 equiv.) embedded on silica gel (200 mg) was irradiated in a microwave oven for 5 minutes afforded a 1:1 mixture of *E*:*Z* isomers of allyl bromide derivative **36a** and **36b** in 65% combined yield after purification by silica gel column chromatography (Scheme 4.11) (Table 1, entry 5). The geometrical isomers **36a** and **36b** were separated by column chromatography. The proton NMR spectra of the purified individual isomers were used as a tool to distinguish and assign the geometries of the products as discussed in the following section.



Scheme 4.11: Synthesis of allyl bromide of oxindole compounds **36a/b**

Table 4.1: Optimization of allyl bromide of oxindole derivative synthesis.

Entry	Reaction condition	Product(s)	Yield (%)
1	CH ₂ Cl ₂ /HBr, 12h, rt	-	-
2	CH ₂ Cl ₂ /HBr/cat.H ₂ SO ₄ , 12h, rt	decomposed	-
3	CH ₂ Cl ₂ /HBr, 1h, reflux	-	-
4	CHCl ₃ /HBr, 1h, reflux	36a/b	Trace
5	46% aq. HBr, MW, 750W, 5 min.	36a/b	65

4.6.3 Distinction of *E/Z*-isomers **36a/b** by ¹H NMR:

The geometries of allyl bromide of oxindole **36a** and **36b** were arrived on the basis of correlation of proton NMR chemical shifts. The *E*- **36a** and *Z*-isomers **36b** were distinguished by ¹H NMR unambiguously using chemical shift differences of methylene proton attached with bromine atom (Figure 4.4). Thus, the compound **36a** showed a peak at δ 5.23 ppm which explains the electronic environment and influence of shielding effect by aromatic ring current (Figure 4.4). On the other hand, the other isomer **36b** showed a peak corresponds to methylene protons attached with bromine atom at usual chemical shift at δ 4.49 ppm as shown in Figure 4.4.

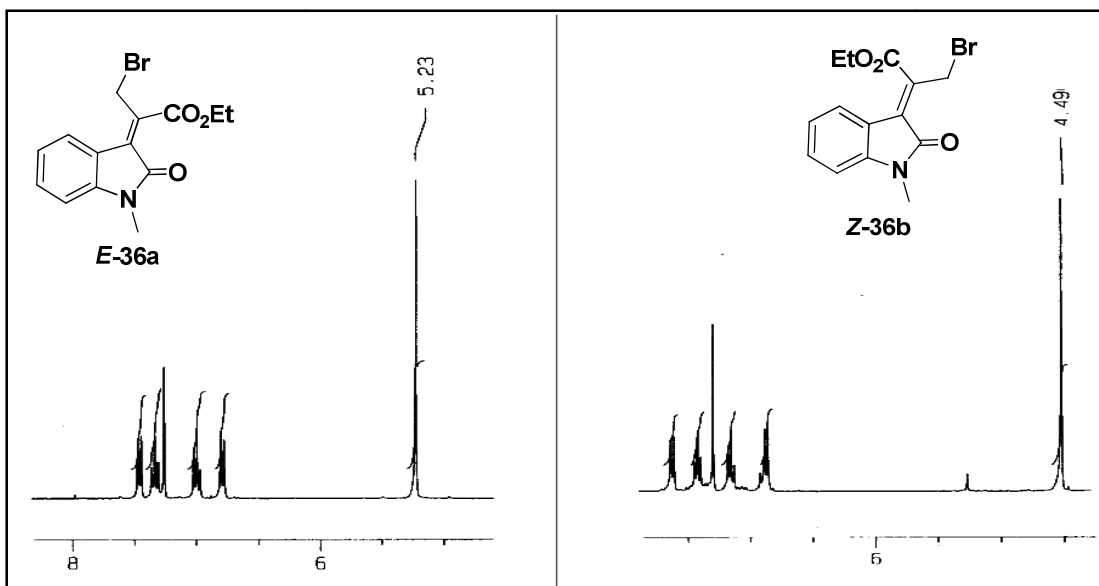
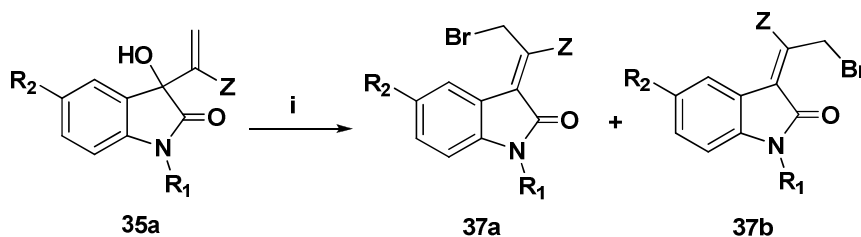


Figure 4.4: Differentiation of *E*- and *Z*-isomers **36 a/b** by ¹H NMR spectrum.

4.6.4 Isomerization of MBH adduct: Generality of the reaction:

In order to synthesise several allyl bromide derivatives for the subsequent [3+2]-annulation reactions, we have carried out the isomerization under the optimized reaction condition for a number of adducts. All the MBH adduct of isatin **35a** afforded the corresponding *E/Z*-isomeric mixture **37a** and **37b** in almost same yield and ratio of the isomeric product, except the 5-formyl MBH adduct (Scheme 4.12). The 5-formyl MBH adduct provided the expected product in low yield (30%) with prolonged microwave irradiation time (15 min). All the compounds were purified through silica gel column chromatography and completely characterized by standard spectroscopic analysis.



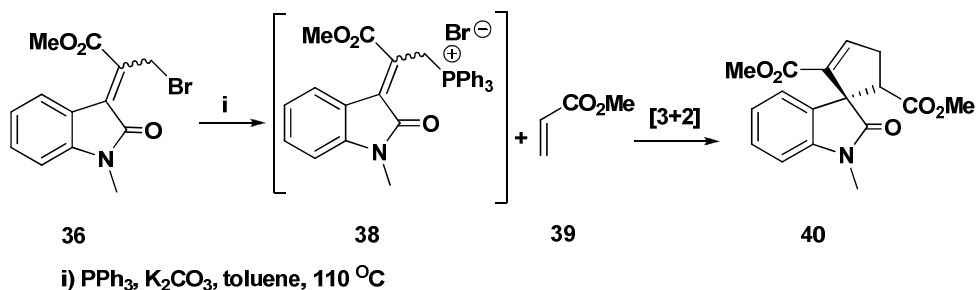
$R_1 = \text{Me, CH}_2\text{Ph, Propargyl}; R_2 = \text{H, Br, CHO, CH}_3, \text{F}$
 $Z = \text{CO}_2\text{Et, CN.}$

(i) 46% HBr (4 equiv.), silica gel, MW 750 W, 5-15 min, 30-66%

Scheme 4.12: Generalization of isomerization.

4.6.5 Synthesis of 3-spirocyclopentene oxindole derivative from allyl bromide of oxindole via phosphine mediated [3+2]-annulation strategy:

The successful synthesis of allyl bromide of oxindole intrigued us to carry out the [3+2]-annulation reactions with dipolarophiles. A prototype experiment has been conducted using a mixture of allyl bromide of oxindole **36** in toluene, with methyl acrylate **39**, triphenylphosphine (PPh_3) and K_2CO_3 was refluxed for 7 hours (Scheme 4.13). This annulation reaction proceeded smoothly and has led to the expected diastereoselective spirocyclic compound **40** in 47% yields after silica gel column chromatography purification.



Scheme 4.13: *Synthesis of spirocyclopentene compound 40.*

The structure of synthesized compound **40** was arrived on the basis of detailed spectroscopic data analysis (FTIR, ^1H NMR, ^{13}C NMR and FAB-MS). The FTIR spectrum of the compound **40** showed the presence of key functional groups such as amide and ester carbonyl group absorptions at 1704 and 1726 cm^{-1} , respectively.

In the ^1H NMR spectrum, the characteristic spirocyclopentene olefin proton appeared as a doublet of doublet centered at δ 7.11 ppm with coupling constant $J = 2.5, 3.0$ Hz (Figure 4.5). The spirocyclopentene methylene protons were resonated as well separated doublet of doublet of doublet (ddd) centered at δ 2.93 and 3.33 ppm, and mutually coupled with olefin and methine protons with coupling constant $J = 3, 9$ and 12 Hz and $J = 2.5, 9.5$ and 11.5 Hz, respectively. The methine proton from spirocyclopentene appeared as a doublet of doublet (dd) centered at δ 3.89 ppm with coupling constants $J = 9.5$ and 9.0 Hz.

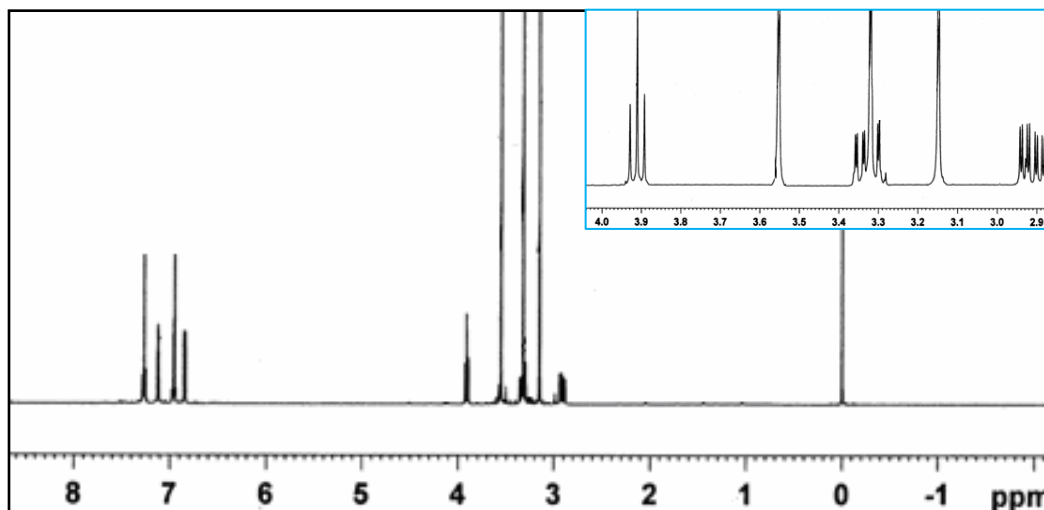


Figure 4.5: ^1H NMR Spectrum of spirocyclopentene derivative **40**

The *N*-methyl and two ester methyl protons were resonated as three sharp singlets at δ 3.14, 3.35 and 3.55 ppm, respectively. The entire aromatic protons were visible in the region from δ 6.84 to 7.27 ppm.

The structure assigned to spirocyclopentene compound **40** adjacent proton coupling pattern was further supported by 2D-HOMOCOSY spectrum and showed various cross peaks between the cyclopentene ring protons (Figure 4.6).

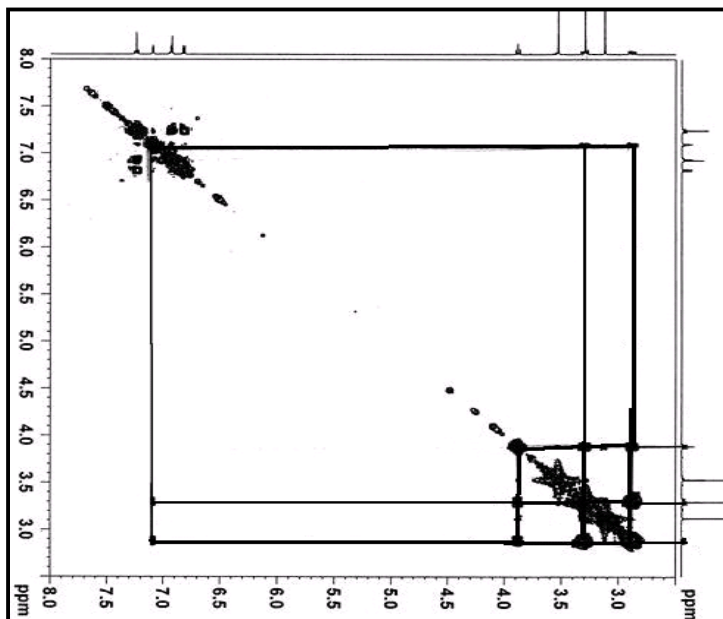


Figure 4.6: ^1H - ^1H -COSY Spectrum of spirocyclopentene derivative **40**

Analysis of ^{13}C NMR spectrum of compound **40** showed signals at δ 26.72, 51.53 and 51.72 ppm which correspond to *N*-methyl and two ester methyl groups carbon, respectively (Figure 4.7). The cyclopentene ring carbons *viz.* methylene, methine and spiro centre were visible at δ 33.71, 52.80 and 61.60, respectively. All the aromatic carbons were in good agreement with assigned structure and resonated in the region at δ 107.78-145.84. The three carbonyl carbons were appeared at δ 162.51, 170.69 and 177.92, respectively.

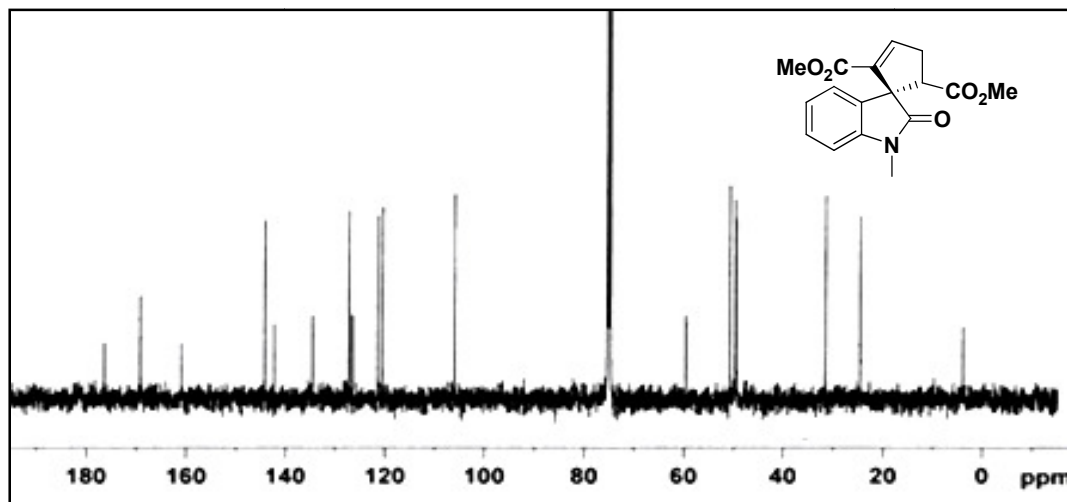


Figure 4.7: ^{13}C NMR Spectrum of spirocyclopentene derivative **40**

The presence of quaternary carbon was confirmed by ^1H - ^{13}C correlation spectrum and the same at δ 61.60 disappeared in the DEPT-135 spectrum (Figure 4.8).

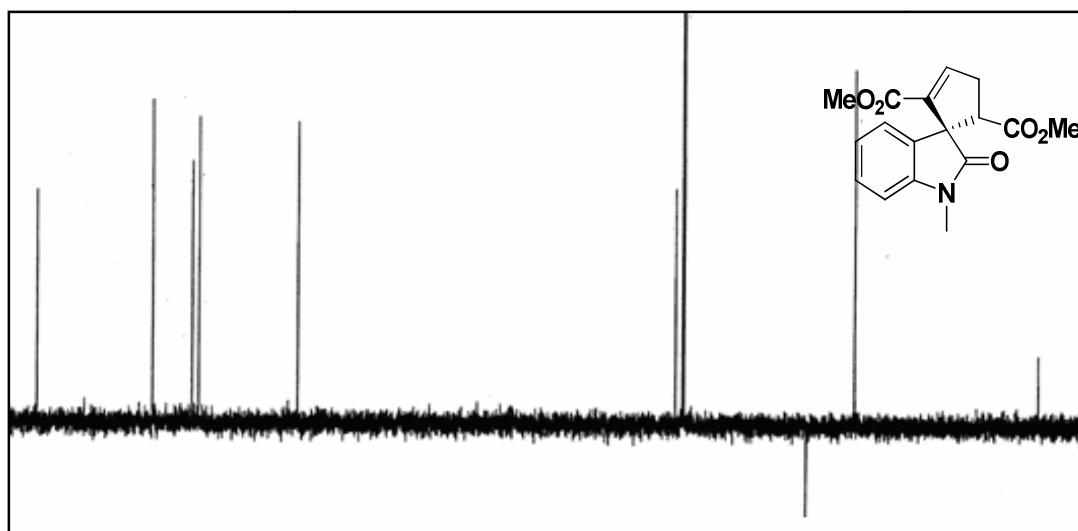


Figure 4.8: DEPT-135 Spectrum of spirocyclopentene derivative **40**

Finally, the FAB-MS supported the assigned structure as it showed a molecular ion $[\text{M}+1]$ peak at $m/z = 316.54$ as against the calculated value $m/z = 315.32$ (Figure 4.9).

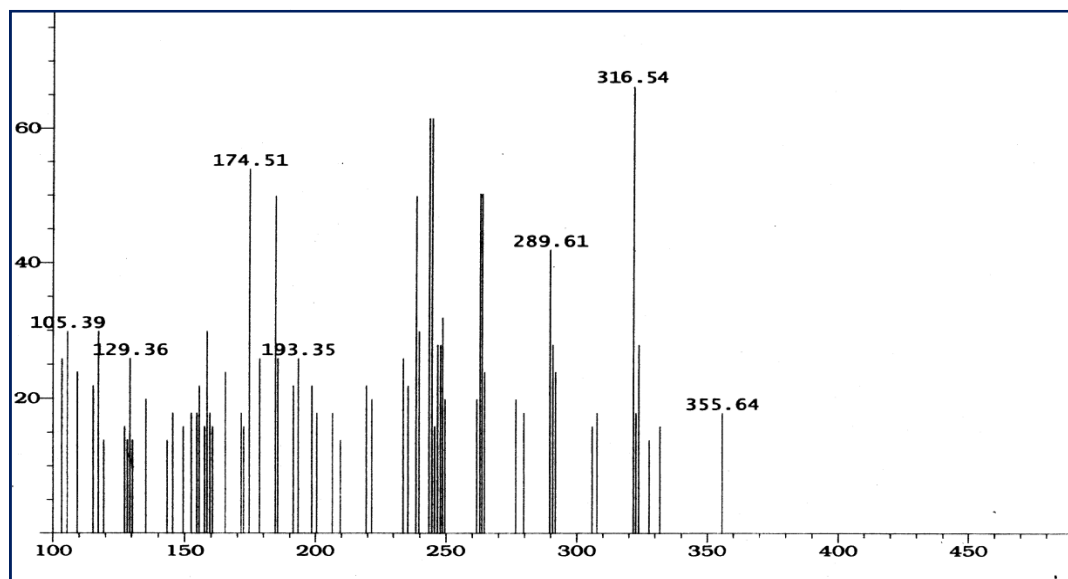
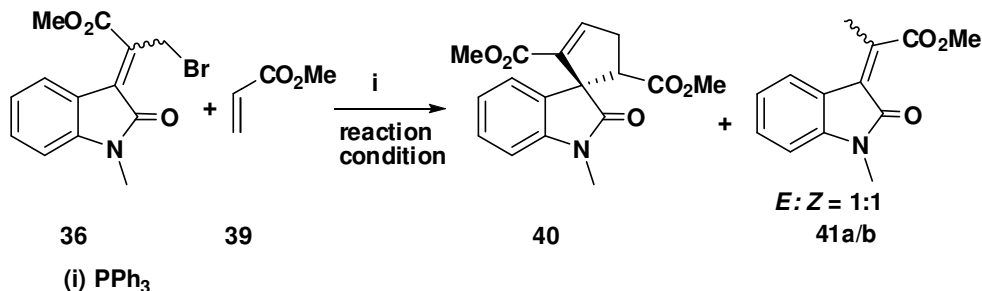


Figure 4.9: Mass spectrum of spirocyclic compound **40**

4.6.6 Optimization study: Effect of solvent and base:

After the successful structural elucidation of spirocyclopentene compound **40**, we have turned our attention towards optimization of the reaction. In order to increase the reaction yield, the effect of solvent and base was evaluated and the results are shown in the Table 4.2.



Scheme 4.14: Optimization of phosphine mediated [3+2]-annulation reaction.

For optimization studies, *N*-methyl allyl bromide of oxindole **36** was chosen as model substrate (Scheme 4.14). Among the several test reactions, a combination of toluene in K_2CO_3 at 80°C was found to be the best condition which provided 65% yield of the product (Table 4.2, entry 2). In presence of Na_2CO_3 , the reaction mixture furnished *E*- and *Z*- mixture of α -methylene reduced alkenes **41a/b** which was separable by silica gel column chromatography (Table 4.2, entry 4). The structures of the α -methylene

reduced compounds **41a/b** were assigned by spectral analysis and discussed in the subsequent section. In the optimization of phosphine catalyzed annulation of allyl bromide of oxindole exposed, a small change in the reaction condition resulted in to marginal difference in the yield (Table 4.2, entries 1 and 2). Except the optimized reaction condition (Table 4.2, entry 2), remaining all were furnished either low yield of the product, reduced product or decomposition of starting materials. Specifically, solvents like benzene gave relatively better yield than other solvents however lesser than in toluene (Table 4.2, entry 3). Polar solvents preferably furnished α -methylene reduced alkene compounds (Table 4.2, entries 8-11).

Table 4.2: Optimization of phosphine catalyzed [3+2]-annulation reaction.

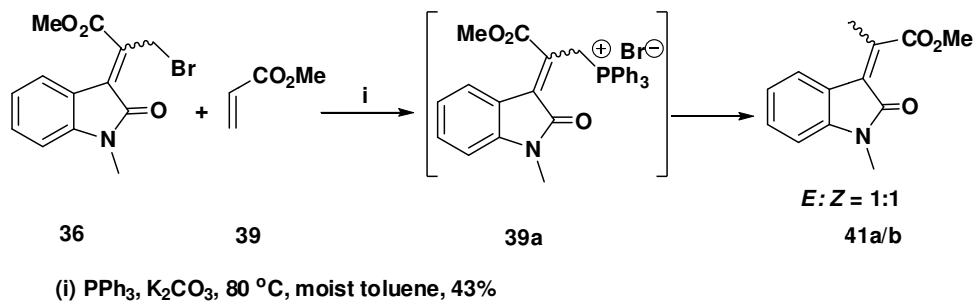
Entry	Solvent	Base	Temp (°C)	Time (h)	Yield (%)	
					41	42
1	toluene	K ₂ CO ₃	120	8	47	-
2	toluene	K₂CO₃	80	12	65	-
3	benzene	K ₂ CO ₃	80	16	55	-
4	toluene	Na ₂ CO ₃	80	3	-	46
5	toluene	NaOH	80	3	decomposed	
6	toluene	KOH	80	3	decomposed	
7	toluene	CsCO ₃	80	3	decomposed	
8	DMF	K ₂ CO ₃	110	1	-	51
9	THF	K ₂ CO ₃	60	3	-	45
10	MeOH	K ₂ CO ₃	60	2	-	61
11	CH ₃ CN	K ₂ CO ₃	60	2	-	34
12	toluene	K ₂ CO ₃	80	3	-	43 ^a

^aMoist toluene was used as a solvent.

4.6.7 Formation of α -methylene reduced alkene compounds **41a/b**:

The α -methylene reduced alkene compounds were formed whenever annulation reaction conducted in polar solvents. The formation of α -methylene reduced alkene compounds can be explained by mechanistic postulates. Accordingly, phosphonium salt **39a** formed from allyl bromide of oxindole and PPh₃, undergoes oxygenation with either water or air. The oxophilicity of phosphorous and higher reactivity of allyl derivatives of

oxindole **36** were assisted the formation of triphenylphosphine oxide ($\text{Ph}_3\text{P}=\text{O}$) and thus thereby reduced compounds **41a/b** (Scheme 4.15).



Scheme 4.15: Synthesis of α -methylene reduced alkene derivatives **41a/b**

These two contentions were further confirmed based on the experimental results. Even under optimized condition, the moist toluene provided only the reduced product (Table 2, entry 12) and also the allyl bromide derivatives from MBH adduct of aldehyde did not give any reduced products.

The structure of reduced compound **41a** was established based on the NMR and the mass spectral analysis (Figure 4.10). In ^1H NMR spectrum of compound **41a** (*E*-isomer) the methyl group attached to the alkene observed as a singlet at δ 2.65 ppm and *N*-methyl, ester methyl proton were resonated as two singlets at δ 3.20 and 3.90 ppm, respectively. The entire aromatic protons were visible at δ 6.80-7.28 ppm as multiplets.

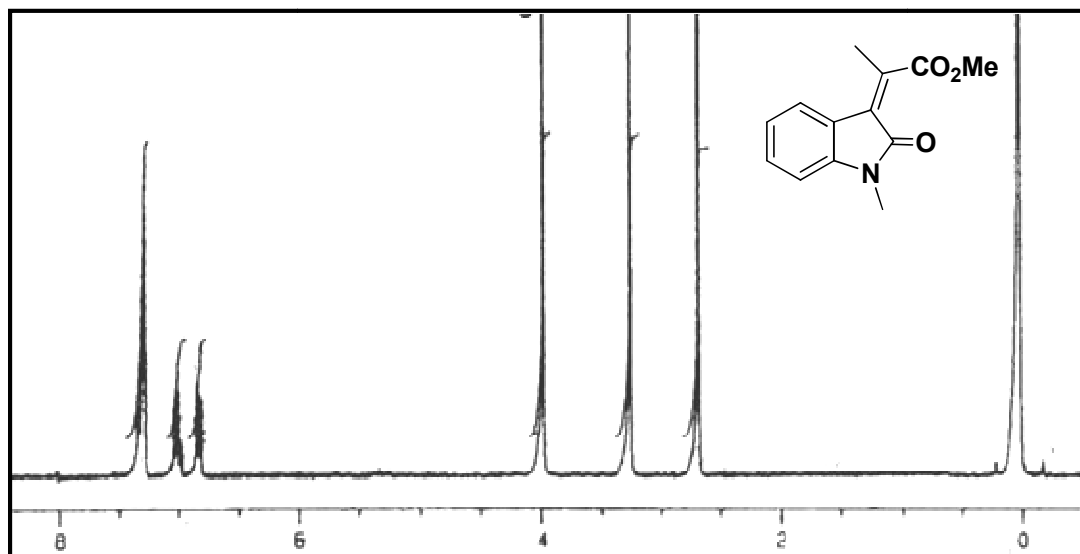


Figure 4.10: ^1H NMR Spectrum of compound **41a** *E*-isomer.

Similarly, in the ^1H NMR spectrum of compound **41b** (*Z*-isomer) the olefin methyl group appeared as a singlet at δ 2.44 ppm. Two singlets at δ 3.23 and δ 3.96 ppm

were discernable to the methyl groups of the amide nitrogen and the ester, respectively (Figure 4.11). The down field signals in the chemical shift range from δ 6.83-7.52 were discernable to the aromatic protons of the oxindole moiety.

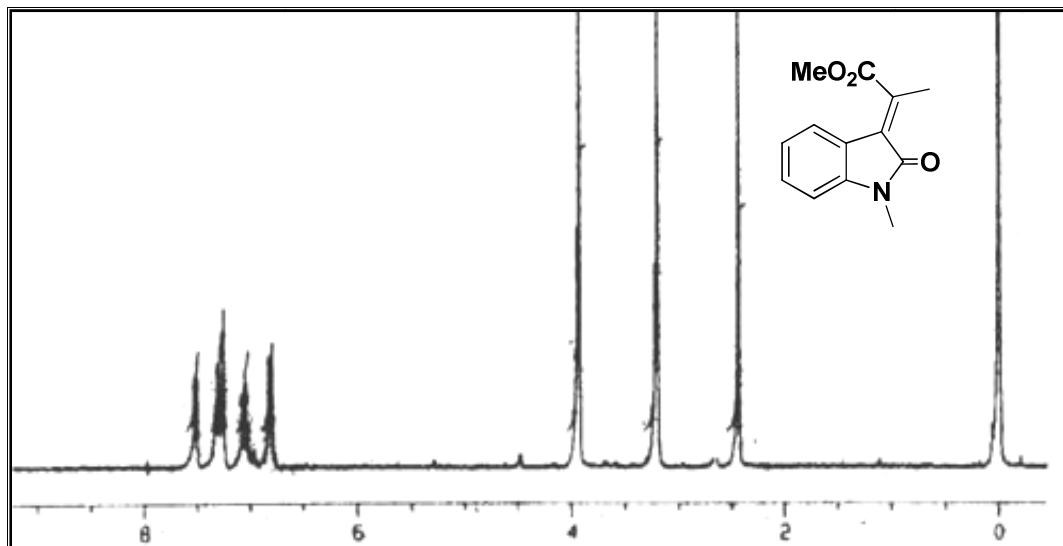


Figure 4.11: ^1H NMR Spectrum of compound **41b** Z- isomer.

The ^{13}C spectrum showed three carbon signals at δ 17.90, 25.86 and at 52.71 which correspond to methyl carbons attached in alkene, nitrogen and ester, respectively. The ester carbonyl was observed at δ 170.60 and the amide carbonyl of the oxindole moiety appeared at δ 165.70 (Figure 4.12).

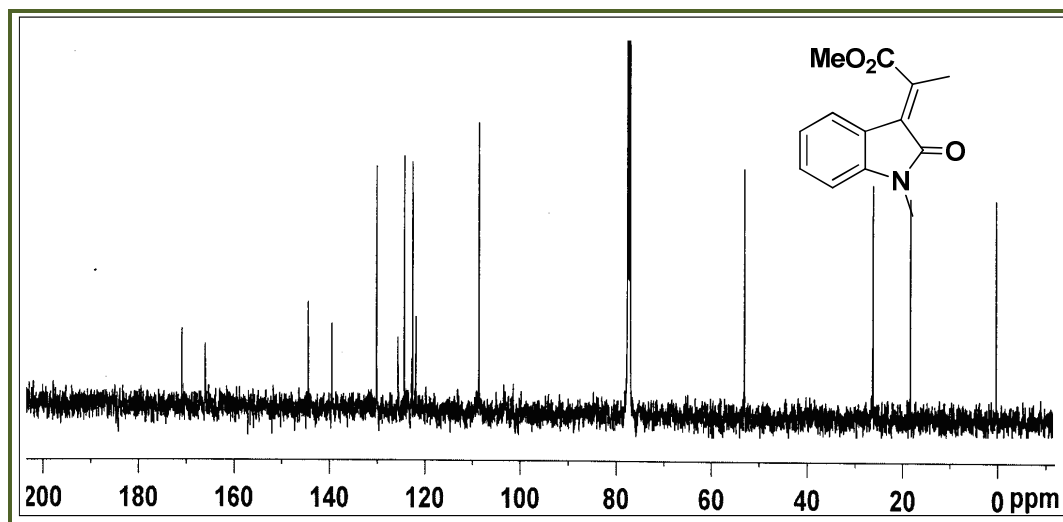


Figure 4.12: ^{13}C NMR Spectrum of compound **41b** Z- isomer.

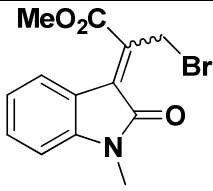
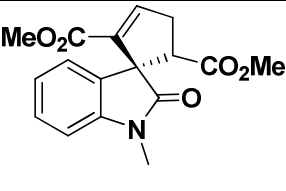
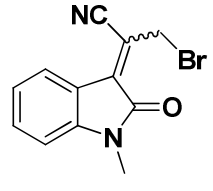
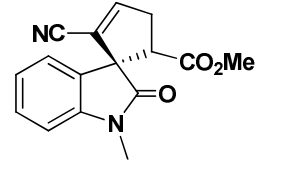
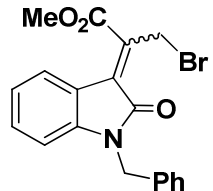
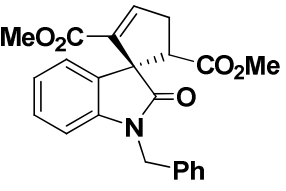
The analyzed structure of **41b** was supported by the mass spectral analysis as it showed a molecular ion $[\text{M}+1]$ peak at $m/z = 232.35$ against the calculated value of $m/z = 231.24$.

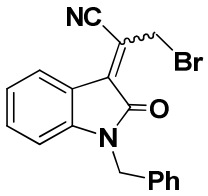
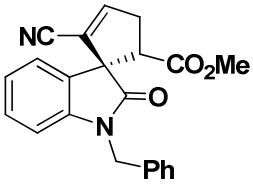
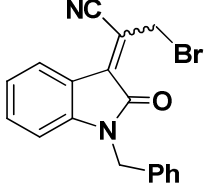
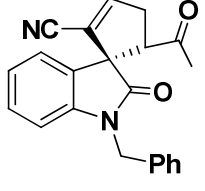
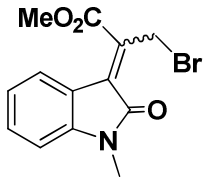
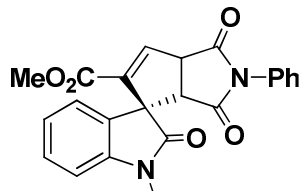
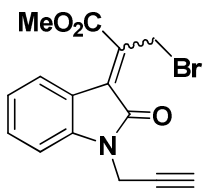
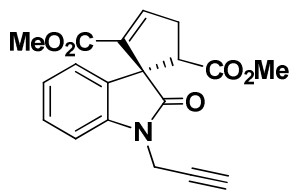
4.6.8 Synthesis of spirocyclopentene derivatives *via* [3+2]-annulation:

Generality of the reaction:

The successful synthesis of 3-spirocyclopentane-2-oxindole derivative **40** prompted us to explore the phosphine catalyzed [3+2]-annulation reaction with a number of allyl derivatives and activated olefins under optimized condition. All the substrates underwent the annulation reaction smoothly and provided the corresponding diastereoselective spiro cyclopentene derivatives in good yield. The results are shown in Table 4.3.

Table 4.3: Generality of phosphine catalyzed [3+2] annulation.

Entry	Substrate	Product	Temp (°C) /Time (h)	Yield (%)
1	 36	 40	80/12	65
2	 42	 46	60/5	74
3	 43	 47	80/12	63

4	 44	 48	60/6	77
5	 44	 49	60/2	65
6	 36	 50	60/4	51
7	 45	 51	60/6	66

The functional groups such as benzyl and propargyl substitution in allyl bromide of oxindole furnished the spirocyclic product in good yield (Table 4.3, entries 3-5 and 7). The nitrile appended allyl bromide derivatives provided the desired spiro cyclic products in good yield with a shorter reaction time than ester derivatives (Table 4.3 entries 2 and 4-5). The methyl vinyl ketone (MVK) also acts as dipolarophile and delivered the spirocyclic **49**, however, in low yield. The reason may be due the higher reactivity MVK for dimerization in presence of PPh_3 [Ma, G.-N. *et al.* 2009], while the excess addition of MVK (2.5 equivalent) to the reaction gave the spirocyclopentene **49** in good yield 65% (Table 4.3, entry 5). Finally, the *N*-phenyl maleimide furnished the spirotetra-cyclic product **50**, where three consecutive stereogenic centers generated in a one-pot reaction

(Table 4.3, entry 6). It should be noted that phosphine catalyzed [3+2]-annulation reaction of allyl bromide of MBH adduct was selective toward the functional groups substituted on isatin aromatic core. Electron withdrawing or releasing group on aromatic ring of oxindole provided only reduced products. The entire tabulated compounds were completely characterized by standard spectroscopic techniques and complete characterization data is given at the end of the chapter. For instance, unambiguous structural evidence and stereochemistry of one the product **46** was obtained by single crystal X-ray analysis (Figure 4.13).

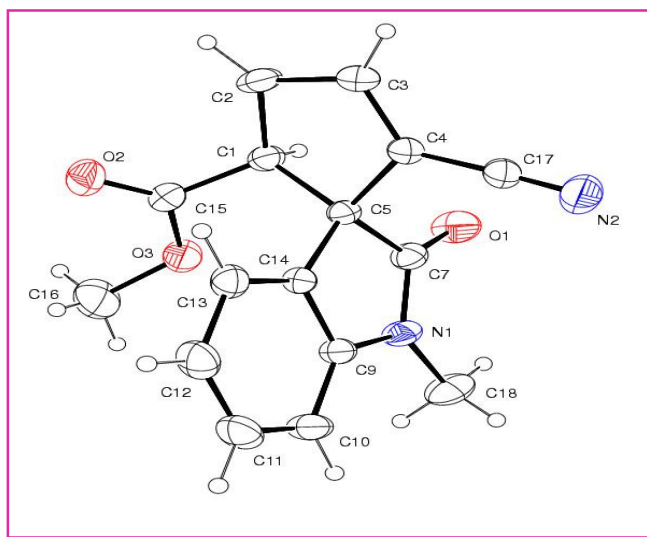
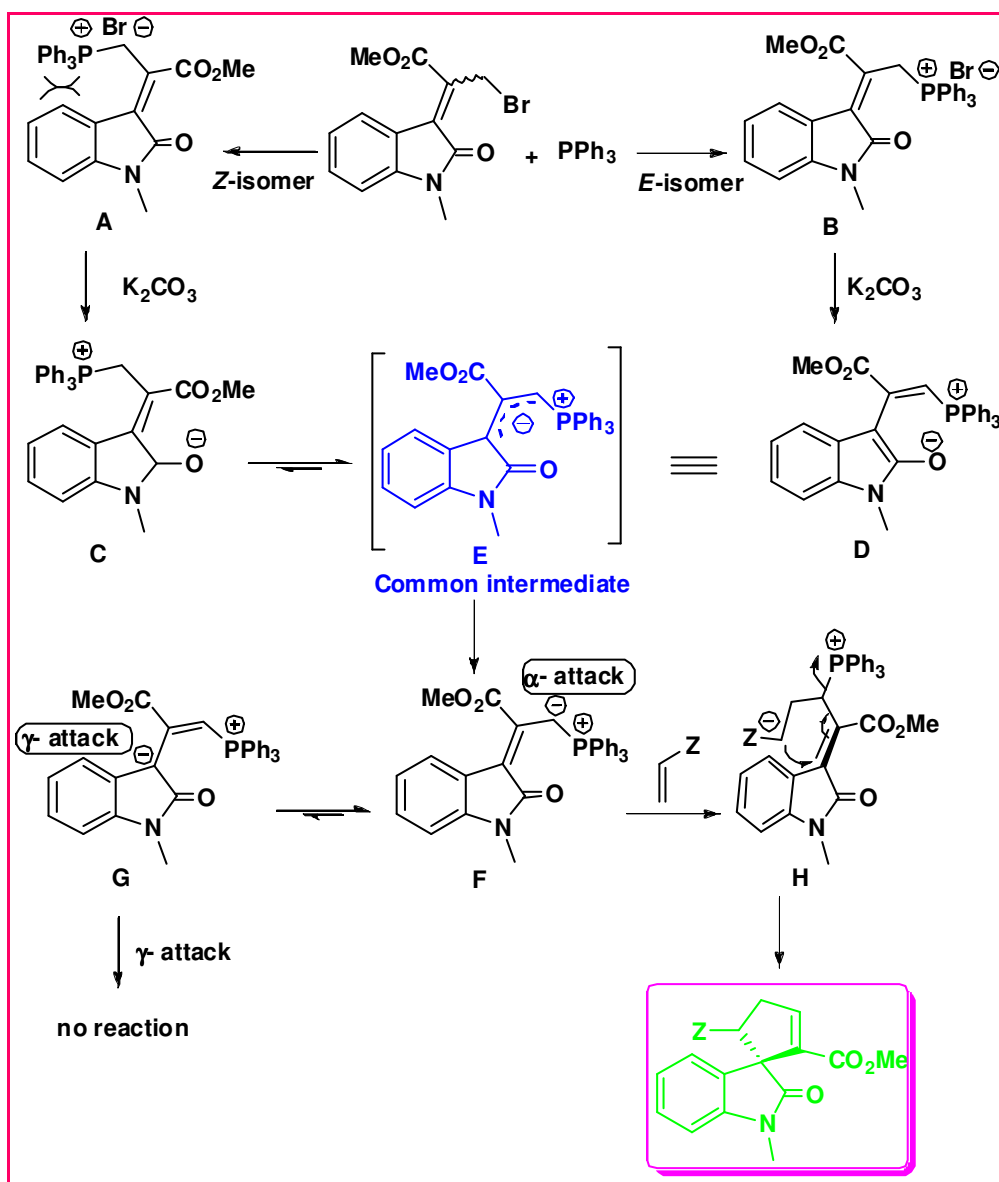


Figure 4.13: ORTEP diagram of spirocyclopentene compound **46**

4.6.9 A diastereoselective synthesis of spirocyclopentene: Plausible reaction mechanism:

The formation of a diastereoselective compound from a mixture of starting material is considered to be the significance of this work. The observed diastereoselective formation spirocyclopentene derivative from mixture of *E*- and *Z*-isomer was accounted and explained through the two important transition states. Initially, a mixture of *E*- and *Z*-ylides **C** and **D** were generated *in-situ* by the deprotonation of phosphonium salt (**A** and **B**) by K_2CO_3 . The generated ylides **C** and **D** underwent resonance with amide carbonyl of isatin core to form common intermediate **E**. Among the two possible ylide structures, ylide **D** is probably more stable due to the intramolecular electrostatic interaction between the two terminals of dipole. The structure **C** is destabilized due to the steric

repulsion between the bulky PPh_3 with aromatic core of oxindole which assisted the formation of common intermediate **E**. Among the two possible mode of addition (α - and γ -attack) with dipolarophile, the intermediate **E** regioselectively underwent α -addition with Michael acceptors and furnished the single regioisomer as a sole product (Scheme 4.16).



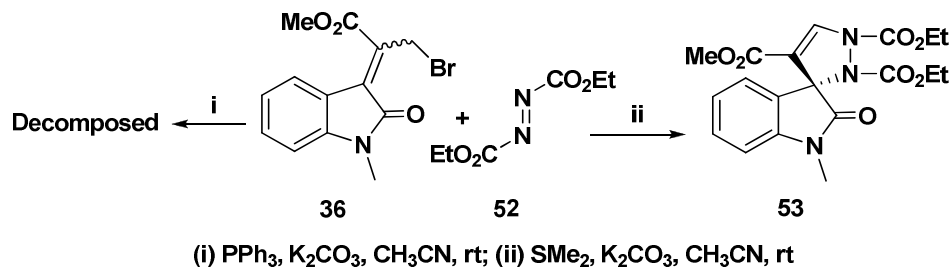
Scheme 4.16: Mechanistic postulate for the stereoselective synthesis of spirocyclopentene.

The reason may be the less stabilization of tertiary carbanion **G** than secondary carbanion **F**, which controls the mode of attack. Hence, the α -carbanion undergone addition predominantly with dipolarophile and furnished only the isolated diastereoisomer. In conclusion, the regio- and stereoselectivity of the reaction is controlled by the formation of common intermediate **E** and the stability of generated carbanion **F**, respectively.

4.6.10 Synthesis of 3-spiropyrazole-2-oxindole derivatives from allyl bromide of oxindole via sulphur ylide [3+2]-annulation reaction:

Sulphur ylide chemistry has been well explored for the synthesis of diverse and highly strained ring systems like epoxides¹⁹, aziridines²⁰ and cyclopropanes²¹ with activated ketones. In a very few occasion the sulphur ylide reactions have been explored towards the synthesis of five and medium ring size compounds. The pyrazole framework belongs to an important class of heterocyclic compounds possessing pronounced pharmacological properties such as antiviral, antitumor, anti-inflammatory, and antimicrobial activities. Certain, 1*H*-pyrazole-4-carboxylic esters are known to exhibit antimicrobial activity and are also found to act as intermediates for synthesis of agrochemical microbicides and herbicides [Sridhar, R. *et al.* 2004; Manna, F. *et al.* 2005]. The synthesis of five member heterocycles utilising sulphur ylide chemistry is seldom explored. Because of the remarkable medicinal and pharmacological potential of pyrazole derivatives, development of simple and efficient methodologies for synthesis of these compounds was highly warranted. With this intention, we were interested to synthesize 3-spiropyrazole-2-oxindole derivatives using allyl bromide of oxindole as starting materials via sulphur ylide cycloaddition reaction. To realize the current needfulness, we carried out an initial reaction with allyl bromide of oxindole **36** in acetonitrile with PPh₃ as catalyst and diethyl azodicarboxylate (DEAD) **52** at room temperature. To our dismay, the reaction resulted in decomposition of starting material. This may be due to unavailability of DEAD which undergoes self dimerization in presence of PPh₃ [Nair, V. *et al.* 2007^b] and the starting material also decomposed in the presence of K₂CO₃. However, when dimethyl sulfide (Me₂S) was used instead of PPh₃ at room temperature, the reaction furnished the desired diastereoselective spiropyrazole compound **53** in good

yield as the only product (Scheme 4.17). Thus, dimethyl sulphide is considered to be a suitable reagent for this transformation.



Scheme 4.17: Synthesis of spiropyrazole compound **53**

The structure of newly synthesized compound **53** was elucidated on the basis of detailed spectroscopic data analysis (FTIR, ^1H , ^{13}C NMR and FAB-Mass). The FTIR spectrum of the compound **53** showed the characteristic carbonyl absorptions for amide and ester groups at 1702, 1719 and 1742 cm^{-1} , respectively.

In ^1H NMR spectrum, the characteristic pyrazole olefin proton appeared as a singlet at δ 7.77 ppm and the remaining aromatic protons were accounted and visible at δ 6.84-7.33 ppm (Figure 4.14). In the *N*-ester ($-\text{N}-\text{CO}_2\text{CH}_2\text{CH}_3$) two methylene group protons were resonated as a multiplet centered at δ 4.25, 4.36 ppm and two methyl protons appeared as a multiplet centered at δ 1.30, 1.37. The *N*-methyl and pyrazole ring ester methyl protons resonated as two separate singlets at δ 3.27 and 3.57, respectively.

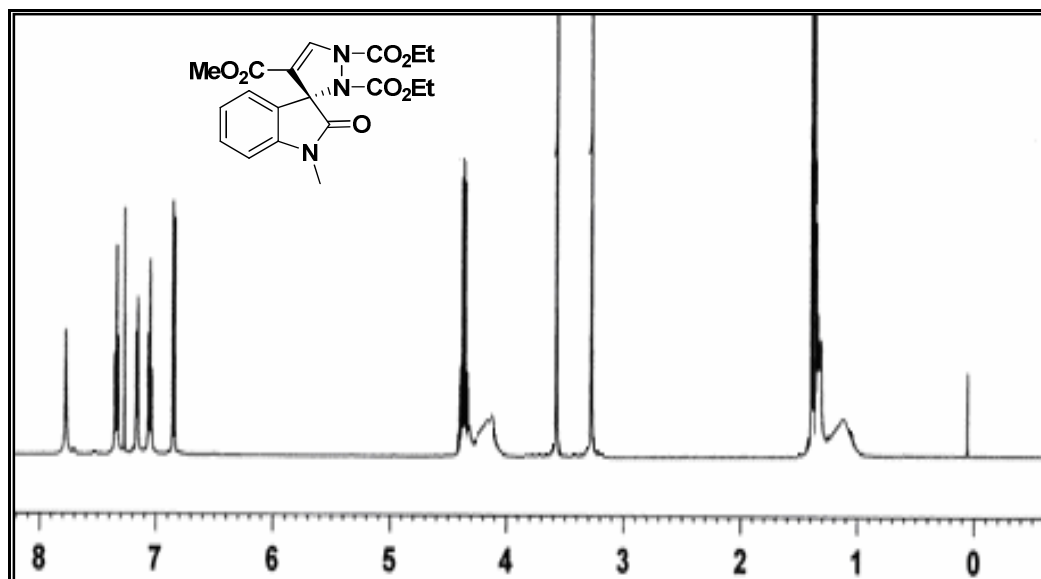


Figure 4.14: ^1H NMR Spectrum of spiropyrazole compound **53**

In ^{13}C NMR spectrum of compound **53** showed a signal at δ 51.07 assigned to methoxy carbon (-OMe) of the ester (Figure 4.15). The characteristic DEAD ester methylene carbons were appeared at δ 62.22 and 62.88 and the corresponding methyl carbons were visible at δ 14.02 and 14.43, respectively. The other aliphatic carbons *N*-methyl and spirocarbon were resonated at δ 26.76 and 74.18, respectively. Remaining all aromatic carbons were accounted and appeared in the region at δ 107.92-141.92 ppm. The functionalities such as DEAD ester, amide and ester carbonyl carbons were appeared at δ 153.64, 156.54, 161.24 and 172.21, respectively.

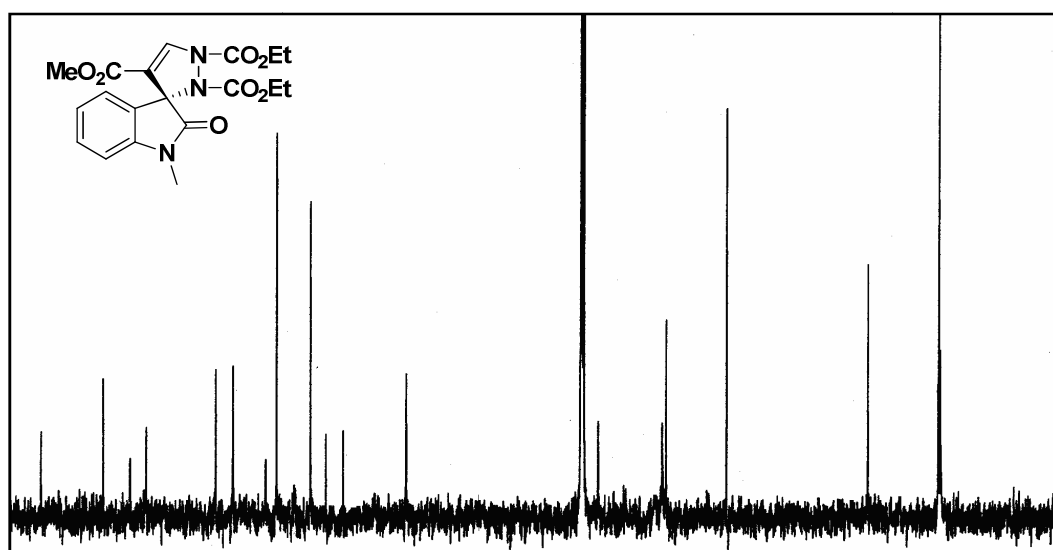


Figure 4.15: ^{13}C NMR Spectrum of spiropyrazole compound **53**

Finally, the assigned structure of compound **53** was supported by FAB mass spectrum as it showed a molecular ion peak [M+1] at $m/z = 404.28$ as against calculated value $m/z = 403.38$ (Figure 4.16).

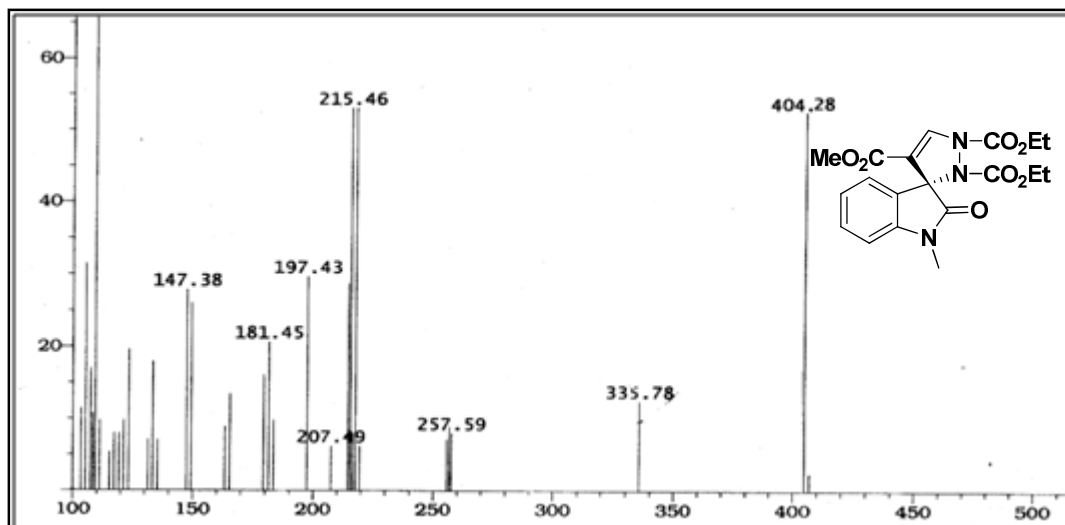
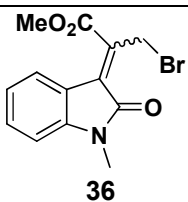
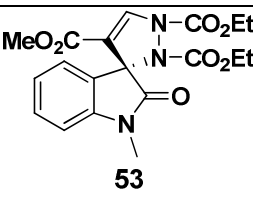
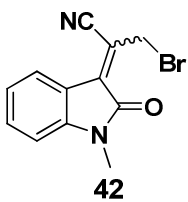
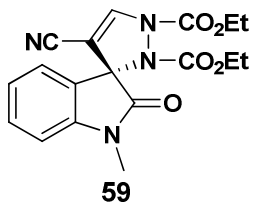
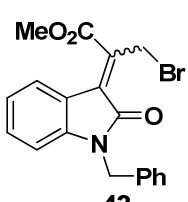
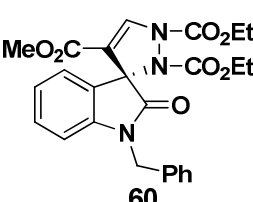
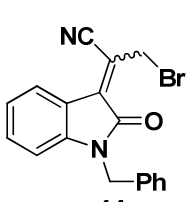
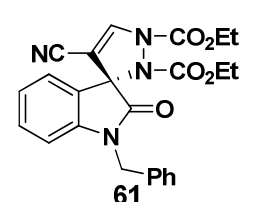
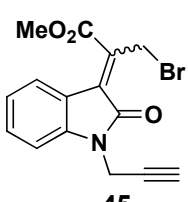
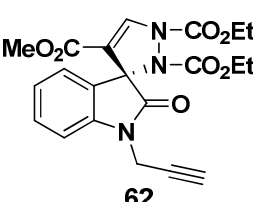
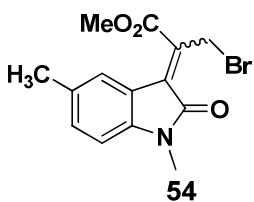
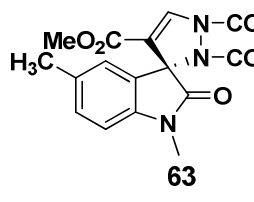


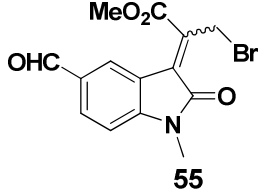
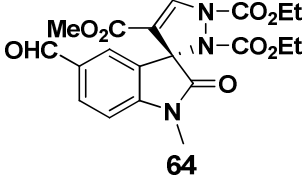
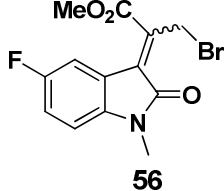
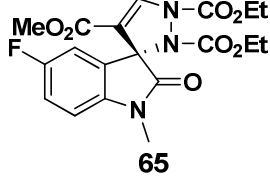
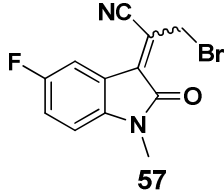
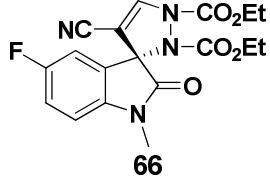
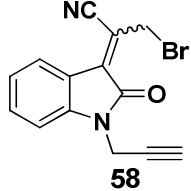
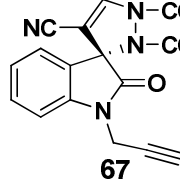
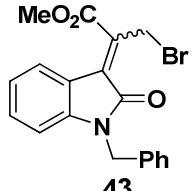
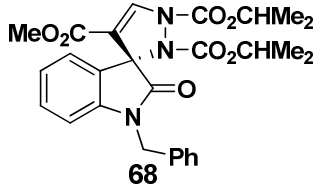
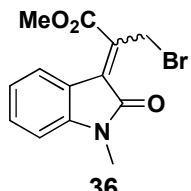
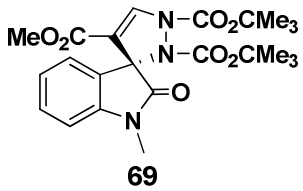
Figure 4.16: Mass spectrum of compound 53

4.6.11 Diastereoselective synthesis of 3-spiropyrazole-2-oxindole derivatives *via* [3+2]-annulation: Generality of the reaction:

In order to synthesise a potential and diverse spiropyrazole derivatives, under optimized reaction condition, we have carried out [3+2]-annulation reactions with a number of allyl bromides of MBH oxindole with dimethyl sulphide and DEAD. The synthesis of various spiropyrazole derivatives is important to succeed the molecule to further functionalization and synthetic transformation to attain a number of bio-active molecule syntheses. Fortunately, all the allyl bromo isomerized MBH derivatives underwent the annulation reaction smoothly to afford the corresponding spiropyrazole derivatives in good to excellent yield. The results are shown in Table 4.4. Electron withdrawing group substituted on isatin aromatic core gave better yield than electron releasing groups (Table 4.4, entries 7-9). Interestingly, the nitrile MBH derivatives need lesser reaction time than ester derivatives for the completion of reaction (Table 4.4, entries 2, 4, 9-10). Generally, the propargyl substituent at oxindole nitrogen have played crucial role in the dipolar addition reaction through secondary orbital interaction and afforded mixture of isomers. While, [3+2]-annulation reaction of propargyl substituted allyl derivatives of oxindole **62** and **67** afforded a single diastereomer without any compensation of yield (Table 4.4, entries 5 and 10).

Table 4.4: Diastereoselective synthesis of 3-spiropyrazole-2-oxindole derivatives.

Entry	Substrate	Product	Time (h)	Yield (%)
1	 <p>36</p>	 <p>53</p>	9	76
2	 <p>42</p>	 <p>59</p>	6	74
3	 <p>43</p>	 <p>60</p>	8	87
4	 <p>44</p>	 <p>61</p>	4	91
5	 <p>45</p>	 <p>62</p>	8	76
6	 <p>54</p>	 <p>63</p>	26	63

7	 55	 64	4	77
8	 56	 65	4	79
9	 57	 66	2	74
10	 58	 67	5	79
11	 43	 68	9	83
12	 36	 69	8	86

Notably, all the *N*-substituted oxindole derivatives furnished the desired products without any impact on the reaction time and yield. The annulation reaction was also carried out with diisopropyl azodicarboxylates and di-*tert*-butyl azodicarboxylates successfully and afforded corresponding spiropyrazole derivatives **68** and **69** in good yield (Table 4.4, entries 11-12).

The structure of synthesized compound **61** was elucidated based on the detailed spectroscopic analysis (FTIR, ^1H , ^{13}C NMR and FAB-mass). Thus, FTIR of compound **61** showed the presence of key carbonyl functional groups of ester, amide and nitrile group absorption bands at 1732, 1706 and 2240 cm^{-1} , respectively.

In ^1H NMR spectrum of compound **61**, the pyrazole ring *N*-ester methylene and methyl group proton were appeared as two multiplets centered at δ 0.99, 1.31 and 4.03, 4.31 ppm, respectively (Figure 4.17).

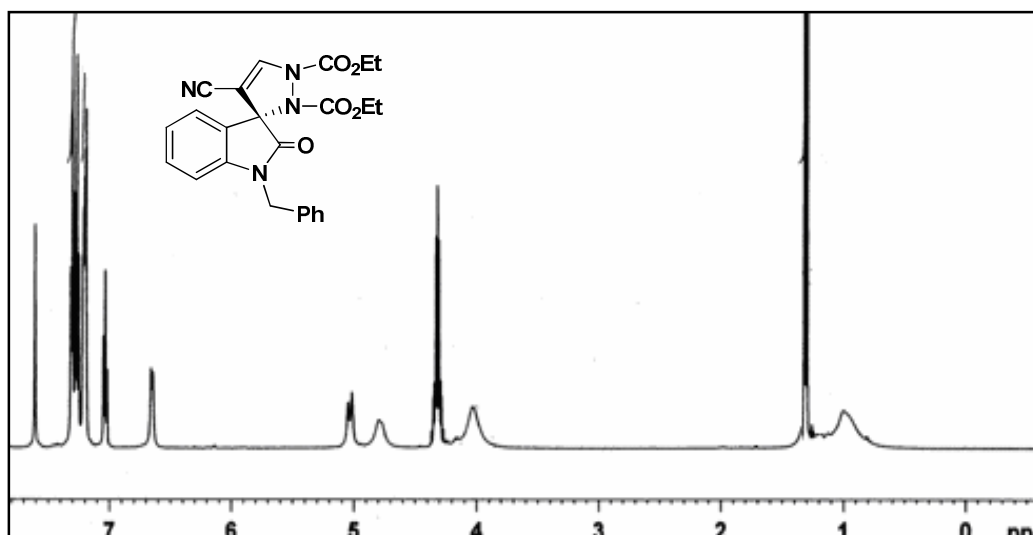


Figure 4.17: ^1H NMR Spectrum of spiropyrazole compound **61**

The *N*-benzyl methylene group resonated as two separate multiplets centered at δ 4.79 and 5.02 ppm. All the aromatic protons were visible between δ 6.64-7.27 ppm. The characteristic spiropyrazole olefin proton appeared as a singlet at δ 7.51 ppm.

The ^{13}C NMR spectrum of compound **61** showed signals at δ 62.90, 63.59, 14.26 and 14.49 due to pyrazole ring *N*-ester methylene and methyl carbons, respectively (Figure 4.18). The characteristic spiro carbon centre was visible at δ 74.87. All the aromatic and olefin carbons were accounted and resonated in the region δ 110.22 - 142.05. The three carbonyl carbons of two esters and one amide were seen at δ 153.57, 155.23 and 171.21, respectively.

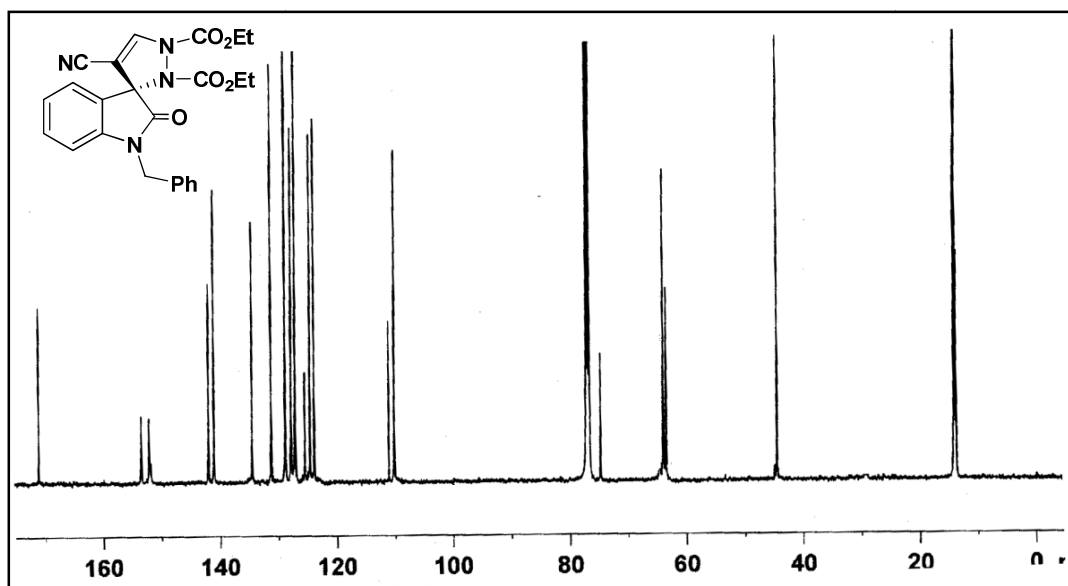


Figure 4.18: ^{13}C NMR Spectrum of pyrazole compound **61**

The structure of synthesized compound **61** was further supported by the FAB mass spectrum and it showed a molecular ion peak $[\text{M}+1]$ at $m/z = 447.19$ against the calculated value at $m/z = 446.12$ (Figure 4.19).

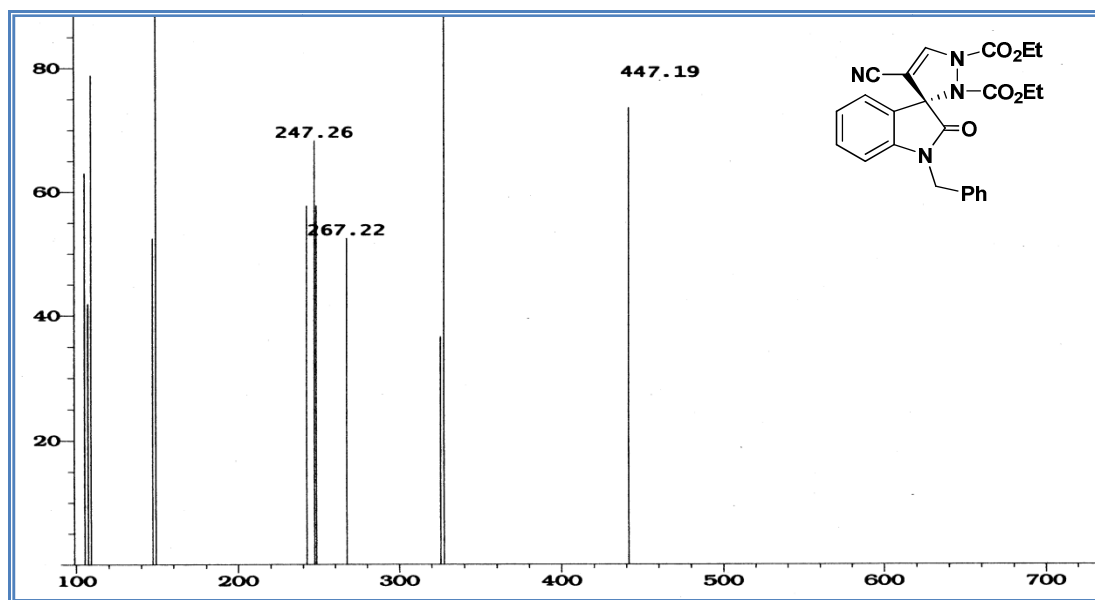


Figure 4.19: Mass spectrum compound **61**

Finally, unambiguous structural evidence and stereochemistry of the spirocyclic compound **61** was obtained by single crystal X-ray analysis (Figure 4.20).

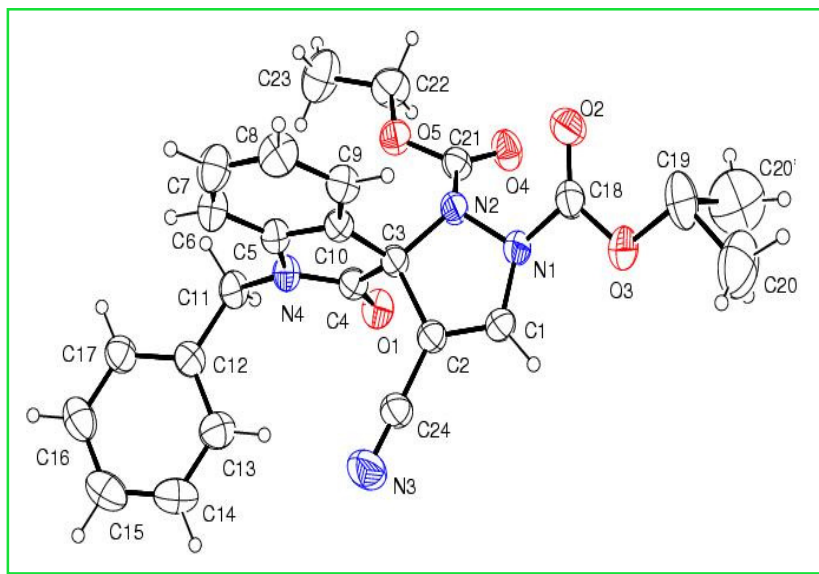


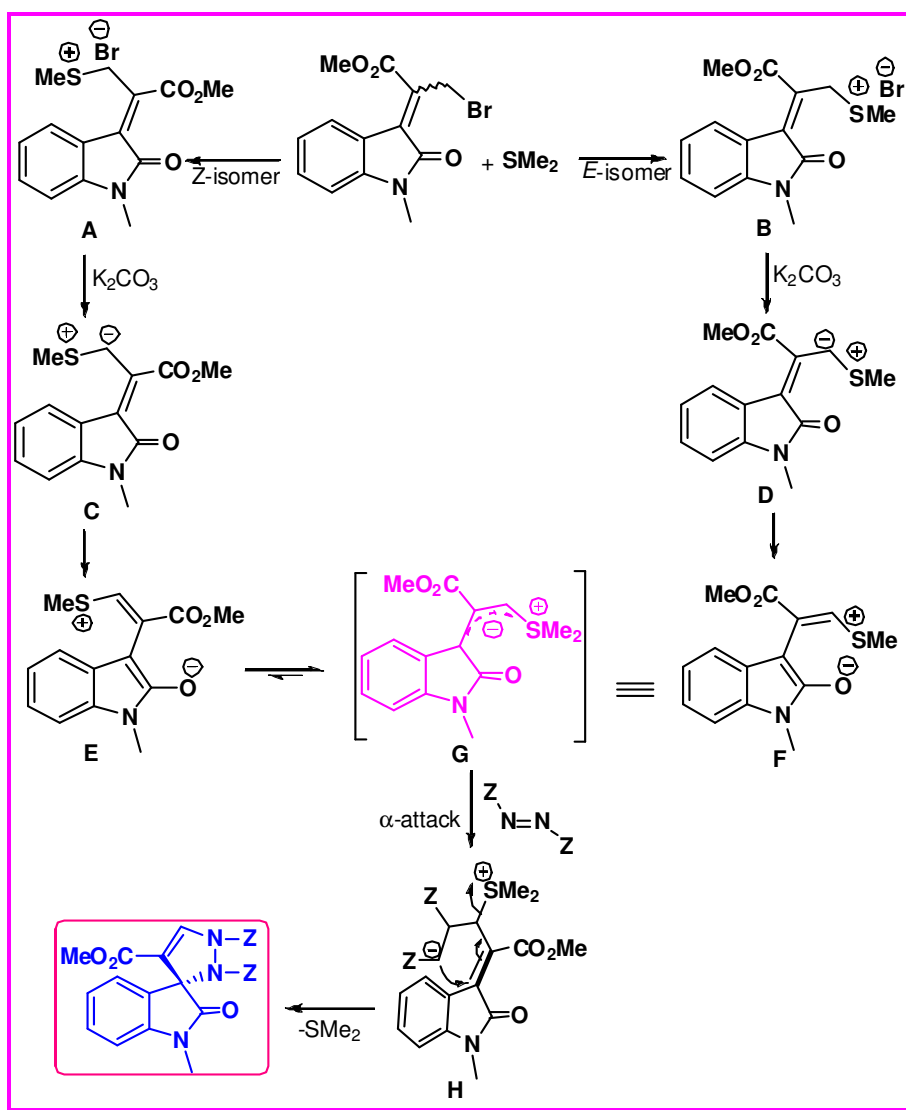
Figure 4.20: ORTEP diagram of compound **61**

It should be mentioned that the experiments carried out with mutual exchange of either catalyst ($\text{Ph}_3\text{P}/\text{Me}_2\text{S}$) or dipolarophile (activated alkene/DEAD) did not provide any desired spirocyclic products for the both strategies described above. The sulphur mediated ylide reaction with allyl derivatives of oxindole showed good substrate tolerance than phosphorous catalyzed annulation reaction. All the new compounds were completely characterized by spectroscopic means and detailed data are provided in the experimental section.

4.6.12 Reaction mechanism of the formation of diastereoselective 3-spiropyrazoles-2-oxindole:

Diastereoselective formation of spiropyrazole from the mixture of (*E*- and *Z*) allyl bromide of oxindole can be explained through a plausible reaction mechanism (Scheme 4.18). Initially, a mixture of sulphonium salts **A** and **B** (*E*- and *Z*-isomeric salts) are formed from allyl bromide of oxindole with dimethyl sulphide. The salts **A** and **B** underwent *in-situ* deprotonation with K_2CO_3 and generate mixture of dipoles **C** and **D**. The generated dipoles **C** and **D** undergo resonance with amide carbonyl of isatin provide

two intermediates **E** and **F**. Among the two resonance structures, the formation of common intermediate **G** was assisted by the steric interaction between the bulky Me_2S with aromatic core of oxindole **E** and the stability arose due to the intramolecular electrostatic interaction in the dipole **F**. The formation of common intermediate **G** is important factors which lead to the diastereoselective synthesis of spiropyrazole derivatives. In contrast to phosphine catalyzed annulation reaction, the sulphur ylide reaction with either mode of addition (α - or γ -attack) with DEAD afforded single spiropyrazole regioisomer.



Scheme 4.18: Mechanistic postulate of the diastereoselective synthesis of 3-spiropyrazoles-2-oxindole.

4.7 Conclusions:

- We have synthesized a number of 3-spirocyclopentene- and 3-spiropyrazole-2-oxindole derivatives from a common starting material *via* [3+2]-annulation strategy utilizing phosphorous and sulphur ylide chemistry.
- Plausible reaction mechanisms have been proposed on the basis of observed diastereoselective products.
- The synthesized spirocyclopentene is having adjacent three stereogenic centres among them one is quaternary and all of them have been constructed in a single mode of operation.
- The 3-spiropyrazole-2-oxindoles were synthesized for the first time with isatin core in a diastereoselective manner.
- According to the literature analogy, the spirocyclic compounds synthesized herein are expected to display significant biological activities.
- All reported compounds were completely characterized by spectroscopic techniques and the stereochemistry of the spiro derivatives was assigned based on the X- ray single crystal analysis.

4.8 Experimental part:

4.8.1 General considerations:

All the reactions were carried out in oven-dried glassware. Progress of reactions was monitored by Thin Layer Chromatography (TLC) while purification of crude compounds was done by column chromatography using silica gel (100-200 mesh). Melting points were recorded on a Buchi melting point apparatus and are uncorrected. NMR spectra were recorded at 500 and 300 MHz (based on availability of instruments) 125 and 75 MHz (for ^{13}C) respectively on Bruker Avance DPX-500 MHz. and Bruker Avance DPX-300 MHz. Chemical shifts are reported in δ (ppm) relative to TMS (^1H) or CDCl_3 (^{13}C) as internal standards. Mass spectra were recorded using JEOL JMS 600H mass spectrometer. IR spectra were recorded on Bomem MB series FT-IR spectrometer, absorbencies are reported in cm^{-1} . Yields refer to quantities obtained after chromatography.

4.9 General experimental procedure:

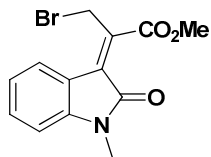
4.9.1 General experimental procedure for the preparation of Morita-Baylis-Hillman adducts of isatin:

The detailed experimental procedure for synthesis of MBH adduct of isatin was given in the experimental section of Chapter II at 2.92 and 2.93.

4.9.2 General experimental procedure for the preparation of bromo isomerized Morita-Baylis-Hillman adducts of isatin:

A mixture of MBH adduct of isatin derivatives (100 mg) was added with 46% HBr (4 equiv.) and silica gel (200 mg) and made as slurry. The slurry was subjected to microwave irradiation (750 W) over a period of 5-15 min. The mixture was cooled to room temperature and then extracted with CH_2Cl_2 and the organic phase was washed with water. The organic layer was separated and dried over Na_2SO_4 and concentrated in *vacuo*. The crude mixture was purified by silica gel column chromatography using a gradient elution with hexane and EtOAc as eluent to afford pure isomerized bromo derivatives in 30-65% combined yield.

4.9.3 Spectral data for isomerized MBH adducts:



Compound 36a

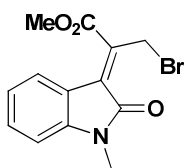
Red crystalline solid, mp: 127-129 °C;

IR (CH₂Cl₂) ν_{\max} : 1746, 1722, 1617 cm⁻¹;

R_f: 0.30 (EtOH-Hexane 50 %);

¹H NMR (CDCl₃/TMS, 300.1 MHz) : δ 1.20 (t, *J* = 6.9 Hz, 3H), 3.28 (s, 3H), 4.13 (q, *J* = 6.9 Hz, 2H), 5.23 (s, 2H), 6.90 (d, *J* = 7.8 Hz, 1H), 7.02 (t, *J* = 7.8 Hz, 1H), 7.29 (t, *J* = 7.8 Hz, 1H), 7.36 (d, *J* = 7.8 Hz, 1H);

FAB mass: Calcd. for C₁₄H₁₄BrNO₃ *m/z* = 323.02; Found: 325.35(M+2).



Compound 36b

Yellow crystalline solid, mp: 127-129 °C;

IR (CH₂Cl₂) ν_{\max} : 1739, 1709, 1611 cm⁻¹;

R_f: 0.26 (EtOH-Hexane 20 %);

¹H NMR (CDCl₃/TMS, 300.1 MHz): δ 1.21 (t, *J* = 6.9 Hz, 3H), 3.19 (s, 3H), 4.14 (q, *J* = 6.9 Hz, 2H), 4.49 (s, 2H), 6.77 (d, *J* = 7.2 Hz, 1H), 6.82 (d, *J* = 7.8 Hz, 1H), 6.98 (t, *J* = 7.5 Hz, 1H), 7.22 (t, *J* = 7.8 Hz, 1H);

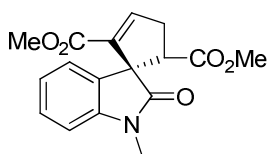
FAB mass: Calcd. for C₁₄H₁₄BrNO₃ *m/z* = 323.02; Found: 325.35(M+2).

4.9.4 General experimental procedure for the preparation of spirocyclopentene derivatives via [3+2]-annulation strategy:

Under argon atmosphere, a mixture of bromo isomerized MBH adducts (100 mg) and variety of dipolarophile (1.2 equiv.) in dry toluene (1.0 mL) was added over mixture of triphenylphosphine (10 mol %) and K₂CO₃ (1.2 equiv.) at the indicated temperature and the reaction was continuously monitored until complete conversion of starting materials. After the reaction completed (monitored by TLC), the crude mixture was filtered through a pad of celite and then purified by a silica gel column chromatography

using EtOAc: Hexane (25:75) as eluent to afford products in moderate to good yields (44-77%).

4.9.5 Characterization of new compounds:



Compound 40

White crystalline solid, mp: 157-159 °C;

R_f: 0.27 (35% EtOAc-Hexane);

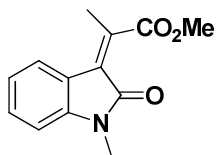
IR (KBr) ν_{\max} : 3025, 2921, 1742, 1726, 1704, 1623 cm^{-1} ;

¹H NMR(CDCl₃/TMS, 500.1 MHz): δ 2.93 (ddd, $J = 3, 9, 12$ Hz, 1H), 3.14 (s, 3H), 3.33 (ddd, $J = 2.5, 9.5, 11.5$ Hz, 4H), 3.35 (s, 3H), 3.55 (s, 3H), 3.89 (dd, $J = 9.5, 9.0$ Hz, 1H), 6.84 (d, $J = 7.5$ Hz, 1H), 6.95 (m, 2H), 7.11 (dd, $J = 2.5, 3.0$ Hz, 1 H), 7.27 (m, 1H);

¹³C NMR (CDCl₃/TMS, 125.7 MHz): δ 26.72, 33.71, 51.53, 51.72, 52.80, 61.60, 107.78, 122.26, 123.22, 128.29, 129.00, 136.24, 143.98, 145.84, 162.51, 170.69, 177.92;

FAB mass: Calcd. for C₁₇H₁₇NO₅ $m/z = 315.32$; Found: 316.54 (M+1);

Elemental Analysis: Calcd. for C₁₇H₁₇NO₅: C, 64.75; H, 5.43; N, 4.44; Found: C, 64.77; H, 5.45; N, 4.42.



Compound 41a

Yellow viscous liquid, mp: 165-167;

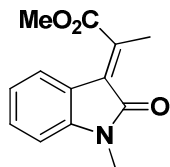
R_f: 0.26 (25% EtOAc-Hexane);

IR (CHCl₃) ν_{\max} : 1615, 1716, 2998 cm^{-1} ;

¹H NMR(CDCl₃/TMS, 500.1 MHz): δ 2.65 (s, 3H), 3.20 (s, 3H), 3.90 (s, 3H), 6.80 (d, $J = 7.8$ Hz, 1H), 6.98 (d, $J = 7.8$ Hz, 1H), 7.28 (d, $J = 7.8$ Hz, 2H).

¹³C NMR(CDCl₃/TMS, 125.7 MHz): δ 15.2, 30.5, 52.3, 121.5, 122.7, 124.3, 126.6, 128.2, 134.6, 141.4, 167.2, 168.7;

FAB mass: Calcd. for C₁₃H₁₃NO₃ $m/z = 231.24$; Found: 232.35 (M+1).



Compound 41b

Yellow viscous liquid, mp: 157-159 °C;

R_f: 0.25 (30% EtOAc-Hexane);

IR (CHCl₃) ν_{max} : 1613, 1715, 2995 cm⁻¹;

¹H NMR(CDCl₃/TMS, 500.1 MHz): δ 2.44 (s, 3H), 3.23 (s, 3H), 3.96 (s, 3H), 6.83 (d, *J* = 7.8 Hz, 1H), 7.06 (t, *J* = 7.8 Hz, 1H), 7.22 (t, *J* = 7.8 Hz, 1H), 7.52 (d, *J* = 7.8 Hz, 1H);

¹³C NMR(CDCl₃/TMS, 125.7 MHz): δ 17.90, 25.86, 52.71, 108.20, 121.50, 122.20, 124.0, 125.30, 129.80, 139.10, 144.10, 165.70, 170.60;

FAB mass: Calcd. for C₁₃H₁₃NO₃ *m/z* = 231.24; Found: 232.35 (M+1).

White crystalline solid, mp: 142-144 °C;

R_f: 0.25 (35 % EtOAc-Hexane);

IR (KBr) ν_{max} : 3104, 2851, 2224, 1735, 1717, 1702, 1621 cm⁻¹;

¹H NMR (CDCl₃/TMS, 500.1 MHz): δ 3.03 (ddd, *J* = 2.8, 9.1, 12.0 Hz, 1H), 3.19 (s, 3H), 3.37 (m, 4H), 3.93 (dd, *J* = 8.8, 8.8 Hz, 1H), 6.89 (d, *J* = 7.8 Hz, 1H), 6.97 (dd, *J* = 2.5, 2.6 Hz, 1H), 6.72 (m, 2H), 7.34 (m, 1H);

¹³C NMR (CDCl₃/TMS, 125.7 MHz): δ 27.39, 34.74, 51.39, 51.83, 63.40, 108.3, 113.53, 115.89, 123.14, 123.89, 126.04, 130.06, 143.53, 150.20, 170.12, 175.47;

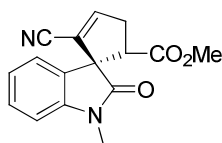
FAB mass: Calcd. for C₁₆H₁₄N₂O₃ *m/z* = 282.29; Found: 283.93 (M+1);

Elemental Analysis: Calcd. for C₁₆H₁₄N₂O₃: C, 68.07; H, 5.00; N, 9.92; Found: C, 68.05; H, 5.03; N, 9.94.

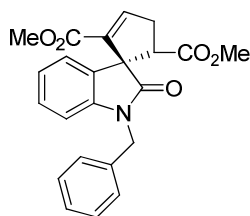
White crystalline solid, mp: 138-140 °C;

R_f: 0.25 (30% EtOAc-Hexane);

IR (KBr) ν_{max} : 3023, 2917, 2848, 1731, 1720, 1704, 1627



Compound 46



Compound 47

cm⁻¹;

¹H NMR (CDCl₃/TMS, 500.1 MHz): δ 2.98 (ddd, *J* = 2.9, 9.0, 12.0 Hz, 1H), 3.05 (s, 3H), 3.35 (ddd, *J* = 2.5, 9.1, 11.2 Hz, 1H), 3.58 (s, 3H), 3.96 (dd, *J* = 9.1, 9.0 Hz, 1H), 4.96 (dd, *J* = 15.20, 11.12 Hz, 2H), 6.71 (d, *J* = 7.8 Hz, 1H), 6.94 (m, 2H), 7.15 (m, 2H), 7.33 (m, 3H), 7.47 (m, 2H);

¹³C NMR (CDCl₃/TMS, 125.7 MHz): δ 33.91, 44.56, 51.32, 51.59, 53.21, 61.80, 108.84, 113.75, 117.64, 119.09, 122.25, 123.50, 127.59, 127.72, 128.69, 128.88, 136.31, 136.71, 143.51, 145.66, 162.42, 170.59, 177.95;

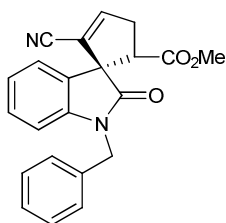
FAB mass: Calcd. for C₂₃H₂₁NO₅ *m/z* = 391.42; Found: 392.23 (M+1);

Elemental Analysis: Calcd. for C₂₃H₂₁NO₅: C, 70.58; H, 5.41; N, 3.58; Found: C, 70.58; H, 5.45; N, 3.56.

White crystalline solid, mp: 135-137 °C;

R_f: 0.27 (30% EtOAc-Hexane);

IR (KBr) ν_{max}: 3046, 2953, 2228, 1731, 1719, 1704, 1642 cm⁻¹;



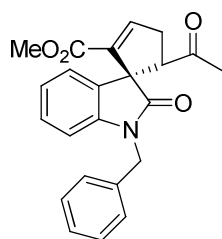
Compound 48

¹H NMR (CDCl₃/TMS, 500.1 MHz): δ 2.02 (ddd, *J* = 3.0, 9.0, 12.0 Hz, 1H), 3.08 (s, 3H), 3.43 (ddd, *J* = 2.5, 9.0, 11.0 Hz, 1H), 4.13 (m, 1H), 5.13 (dd, *J* = 16, 15.5 Hz, 2H), 6.78 (d, *J* = 8.0 Hz, 1H), 7.13 (t, *J* = 7.5, Hz 1H), 7.31 (m, 8H);

¹³C NMR (CDCl₃/TMS, 125.7 MHz): δ 34.76, 44.36, 51.53, 51.76, 63.45, 110.37, 115.67, 124.75, 127.02, 127.17, 127.33, 127.82, 128.80, 142.61, 170.11, 174.46;

FAB mass: Calcd. for C₂₂H₁₈N₂O₃ *m/z* = 358.13; Found: 359.23 (M+1);

Elemental Analysis: Calcd. for C₂₂H₁₈N₂O₃: C, 73.73; H, 5.06; N, 7.82; Found: C, 73.75; H, 5.08; N, 7.80.



Compound 49

White crystalline solid, mp: 126-128 °C;

R_f: 0.25 (30% EtOAc-Hexane);

IR (KBr) ν_{\max} : 3013, 2989, 1742, 1725, 1718, 1703, 1623 cm^{-1} ;

¹H NMR (CDCl_3/TMS , 500.1 MHz): δ 1.53 (s, 3H); 2.75 (ddd, $J = 3, 8.5, 11.5$ Hz, 1H), 3.43 (ddd, $J = 2.5, 9.0, 11.5$ Hz, 1H), 3.53 (s, 3H), 4.03 (dd, $J = 8.5, 9.0$ Hz, 1H), 4.06 (dd, $J = 15.5, 11.15$ Hz, 2H), 6.79 (d, $J = 8.05$ Hz, 1H), 6.86 (d, $J = 7.5$ Hz, 1H), 6.95 (t, $J = 8.05$ Hz, 1H), 7.17 (m, 2H), 7.28 (m, 1H), 7.35 (m, 2H), 7.48 (m, 2H);

¹³C NMR (CDCl_3/TMS , 125.7 MHz): δ 28.86, 32.77, 44.75, 51.68, 60.79, 61.08, 109.15, 122.87, 124.31, 127.75 (2C), 127.85, 127.94, 128.74 (2C), 129.05, 135.77, 136.01, 142.82, 146.31, 162.35, 178.35, 203.65;

FAB mass: Calcd. for $\text{C}_{23}\text{H}_{21}\text{NO}_4$ $m/z = 375.15$; Found: 375.85 (M^+);

Elemental Analysis: Calcd. for $\text{C}_{23}\text{H}_{21}\text{NO}_4$: C, 73.58; H, 5.64; N, 3.73. Found: C, 73.75; H, 5.08; N, 7.80.

White crystalline solid, mp: 161-163 °C;

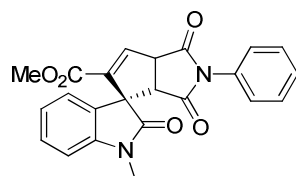
R_f: 0.27 (30% EtOAc-Hexane);

IR (KBr) ν_{\max} : 3021, 2989, 1742, 1728, 1706, 1618 cm^{-1} ;

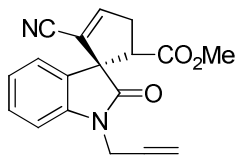
¹H NMR (CDCl_3/TMS , 500.1 MHz): δ 3.28 (s, 3H), 3.68 (s, 3H), 3.74 (d, $J = 8.5$ Hz, 1H), 4.38 (dd, $J = 3.5, 8.5$ Hz, 1H), 6.89 (d, $J = 7.5$ Hz, 1H), 7.06 (m, 2H), 7.18 (m, 1H), 7.35 (m, 6H);

¹³C NMR (CDCl_3/TMS , 125.7 MHz): δ 26.87, 52.12, 52.84, 53.65, 63.11, 108.77, 122.27, 122.99, 127.09, 128.89 (2C), 129.20, 129.55 (2C), 131.51, 131.74, 139.52, 140.61, 144.37, 161.81, 173.07, 174.26, 174.83;

FAB mass: Calcd. for $\text{C}_{23}\text{H}_{18}\text{N}_2\text{O}_5$ $m/z = 402.32$; Found:



Compound 50



Compound 51

403.85 (M+1);

Elemental Analysis: Calcd. for C₂₃H₁₈N₂O₅: C, 68.65; H, 4.51; N, 6.96; Found: C, 68.67; H, 4.53; N, 6.98.

White crystalline solid, mp: 133-135 °C;

R_f : 0.34 (35% EtOAc-Hexane);

IR (KBr) ν_{max} : 3269, 3016, 2923, 2226, 2135, 1742, 1717, 1703, 1676 cm⁻¹;

¹H NMR (CDCl₃/TMS, 500.1 MHz): δ 2.18 (s, 1H), 2.93 (ddd, $J = 2.7, 9.1, 11.8$ Hz, 1H), 3.11 (s, 3H), 3.26 (ddd, $J = 1.9, 8.7, 10.7$ Hz, 1H), 3.86 (dd, $J = 8.7, 9.1$ Hz, 1H), 4.75 (m, 2H), 6.90 (m, 2H), 7.16 (m, 1H), 7.31 (m, 1H), 7.63 (m, 1H);

¹³C NMR (CDCl₃/TMS, 125.7 MHz): δ 33.69, 35.30, 51.85, 58.17, 62.27, 63.31, 72.34, 109.60, 112.93, 116.16, 122.86, 123.12, 123.70, 126.09, 141.75, 149.73, 169.79, 174.56;

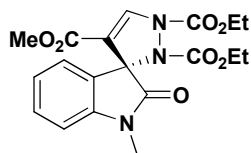
FAB mass: Calcd. for C₁₈H₁₄N₂O₃: 306.1; Found: 307.54 (M+1);

Elemental Analysis: Calcd. for C₁₈H₁₄N₂O₃: C, 70.58; H, 4.61; N, 9.15; Found: C, 70.56; H, 4.63; N, 9.13.

4.9.6 General experimental procedure for the preparation of spiro pyrazole derivatives:

A mixture bromo isomerized MBH adduct (100 mg), dimethyl sulfide (1.2 equiv.), K₂CO₃ (1.2 equiv.) in CH₃CN (1.0 mL) and dialkyl azodicarboxylate (1.2 equiv.) were added successively at room temperature. After completion of the reaction (monitored by TLC), solvent was removed under vacuum. Water (5.0 mL) was added to the residue and extracted with ether (3×5.0 mL). Combined organic layer was dried over anhyd. Na₂SO₄ and solvent was evaporated. The crude product obtained was purified by silica gel column chromatography using EtOAc: Hexane (20: 80) as eluent to afford the product in good yields (66-91%).

4.9.7 Characterization of new compounds:



Compound 53

White crystalline solid, mp: 141-143 °C;

R_f: 0.29 (35% EtOAc-Hexane);

IR (KBr) ν_{\max} : 2984, 1742, 1719, 1702, 1628 cm^{-1} ;

¹H NMR (CDCl_3/TMS , 500.1 MHz): δ 1.30 (m, 3H), 1.37 (m, 3H), 3.27 (s, 3H), 3.57 (s, 3H), 4.25 (m, 2H), 4.36 (m, 2H), 6.84 (d, $J = 7.5$ Hz, 1H); 7.04 (t, $J = 7.0$, Hz, 1H), 7.16 (d, $J = 7.0$ Hz, 1H), 7.33 (t, $J = 7.5$, Hz, 1H), 7.77 (s, 1H);

¹³C NMR (CDCl_3/TMS , 125.7 MHz): δ 14.02, 14.43, 26.76, 51.07, 62.22, 62.88, 74.18, 107.92, 119.96, 122.20, 124.82, 130.73, 132.64, 138.39, 141.92, 153.64, 156.54, 161.24, 172.21;

FAB mass: Calcd. for $\text{C}_{19}\text{H}_{21}\text{N}_3\text{O}_7$ $m/z = 403.38$;
Found: 404.28 (M+1);

Elemental Analysis: Calcd. for $\text{C}_{19}\text{H}_{21}\text{N}_3\text{O}_7$: C, 56.57; H, 5.25; N, 10.42; Found: C, 56.56; H, 4.63; N, 9.13.

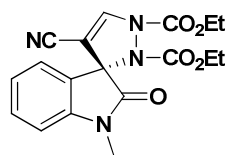
White crystalline solid, mp: 135-137 °C;

R_f: 0.30 (35% EtOAc-Hexane);

IR (KBr) ν_{\max} : 2984, 2234, 1745, 1718, 1703, 1613, 1487 cm^{-1} ;

¹H NMR (CDCl_3/TMS , 500.1 MHz): δ 1.27 (m, 3H), 1.34 (m, 3H), 3.28 (s, 3H), 4.12 (m, 2H), 4.30 (m, 2H), 6.90 (d, $J = 7.8$ Hz, 1H), 7.14 (t, $J = 7.4, 7.5$ Hz, 1H), 7.27 (m, 1H), 7.41 (t, $J = 8.0, 9.0$ Hz, 1H), 7.64 (s, 1H);

¹³C NMR (CDCl_3/TMS , 125.7 MHz): δ 14.13, 14.26, 26.89, 63.29, 63.98, 74.79, 108.90, 110.86, 115.36, 123.89, 124.73, 125.53, 131.35, 140.42, 142.90, 153.42, 156.69, 171.03;



Compound 59

FAB mass: Calcd. for $C_{18}H_{18}N_4O_5$ $m/z = 370.13$;
Found: 370.51 (M^+);

Elemental Analysis: Calcd. for $C_{18}H_{18}N_4O_5$: C, 58.37;
H, 4.90; N, 15.13; Found: C, 58.35; H, 4.92; N, 15.15;

White crystalline solid, mp: 149-151 °C;

R_f: 0.36 (35% EtOAc-Hexane);

IR (KBr) ν_{max} : 3059, 2958, 1734, 1719, 1702, 1628,
1612 cm^{-1} ;

¹H NMR ($CDCl_3/TMS$, 500.1 MHz): δ 1.31 (m, 3H),
1.37 (m, 3H), 3.57 (s, 3H), 4.18 (m, 2H), 4.29 (m, 2H),
4.36 (m, 2H), 6.99 (m, 2H), 7.19 (m, 3H), 7.31 (m, 2H),
7.43 (m, 2H), 7.81 (s, 1H);

¹³C NMR ($CDCl_3/TMS$, 125.7 MHz): δ 14.32, 14.42,
44.65, 51.65, 63.01, 63.98, 73.88, 109.39, 120.66,
123.10, 123.81, 127.44, 127.55 (2C), 128.66 (2C),
130.22, 132.20, 135.41, 138.85, 142.97, 152.16, 156.68,
161.19, 172.35;

FAB mass: Calcd. for $C_{25}H_{25}N_3O_7$ $m/z = 479.17$;
Found: 480.36 ($M+1$);

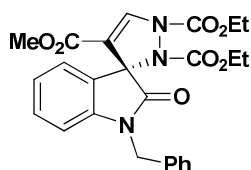
Elemental Analysis: Calcd. for $C_{25}H_{25}N_3O_7$: C, 62.62;
H, 5.26; N, 8.76; Found: C, 62.61; H, 5.18; N, 8.54.

White crystalline solid, mp: 156-158 °C;

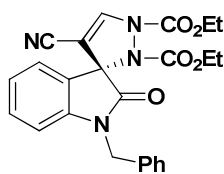
R_f: 0.34 (35% EtOAc-Hexane);

IR (KBr) ν_{max} : 3046, 2954, 2240, 1732, 1722, 1706,
1632 cm^{-1} ;

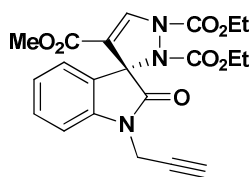
¹H NMR ($CDCl_3/TMS$, 500.1 MHz): δ 0.99 (m, 3H),
1.31 (m, 3H), 4.03 (m, 2H), 4.31 (m, 2H), 4.79 (m, 1H),
5.02 (m, 1H), 6.64 (d, $J = 7.0$ Hz, 1H), 7.02 (t, $J = 7.0$,
Hz, 1H), 7.19 (m, 3H), 7.27 (m, 4H), 7.51 (s, 1H);



Compound 60



Compound 61



Compound 62

^{13}C NMR (CDCl_3/TMS , 125.7 MHz): δ 14.26, 14.39, 44.63, 62.90, 63.59, 74.87, 110.22, 111.18, 123.95, 124.68, 125.54, 127.18 (2C), 127.87, 128.69 (2C), 128.89, 131.28, 134.58, 141.13, 142.05, 153.57, 155.23, 171.21;

FAB mass: Calcd. for $\text{C}_{24}\text{H}_{22}\text{N}_4\text{O}_5$ m/z = 446.12;
Found: 447.19 (M+1);

Elemental Analysis: Calcd. for $\text{C}_{24}\text{H}_{22}\text{N}_4\text{O}_5$: C, 64.57; H, 4.97; N, 12.55; Found: C, 64.53; H, 4.91; N, 12.52.

White crystalline solid, mp: 120-122 °C;

R_f: 0.32 (35% EtOAc-Hexane);

IR (KBr) ν_{max} : 3272, 3010, 2923, 2246, 1730, 1717, 1704, 1676 cm^{-1} ;

^1H NMR (CDCl_3/TMS , 500.1 MHz): δ 1.27 (m, 3H), 1.37 (m, 3H), 2.26 (m, 1H), 3.55 (s, 3H), 4.19 (m, 1H), 4.36 (m, 4H), 7.07 (m, 2H) 7.17 (d, J = 7.0 Hz, 1H), 7.35 (m, 1H), 7.79 (s, 1H);

^{13}C NMR (CDCl_3/TMS , 125.7 MHz): δ 14.04, 14.37, 29.82, 51.75, 62.19, 63.11, 64.18, 72.60, 73.79, 109.30, 120.82, 123.52, 124.01, 127.43, 130.34, 138.77, 141.79, 153.43, 157.75, 161.18, 171.36;

FAB mass: Calcd. for $\text{C}_{21}\text{H}_{21}\text{N}_3\text{O}_7$ m/z = 427.14;
Found: 428.51 (M+1);

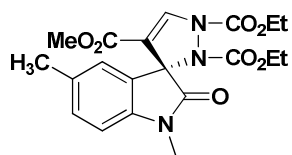
Elemental Analysis: Calcd. for $\text{C}_{21}\text{H}_{21}\text{N}_3\text{O}_7$: C, 59.01; H, 4.95; N, 9.83; Found: C, 59.03; H, 4.97; N, 9.87.

White crystalline solid, mp: 146-148 °C;

R_f: 0.27 (30% EtOAc-Hexane);

IR (KBr) ν_{max} : 3269, 2923, 1742, 1719, 1701, 1676, 1612 cm^{-1} ;

^1H NMR (CDCl_3/TMS , 500.1 MHz): δ 1.23 (m, 3H),



Compound 63

1.32 (m, 3H), 2.44 (s, 3H), 3.18 (s, 3H), 3.51 (s, 3H),
4.14 (m, 2H), 4.30 (m, 2H), 6.66 (d, $J = 7.5$ Hz, 1H),
6.90 (s, 1H), 7.05 (d, $J = 7.0$ Hz, 1H), 7.70 (s, 1H);

^{13}C NMR (CDCl_3/TMS , 125.7 MHz): δ 14.23, 14.33,
21.03, 26.77, 51.74, 62.91, 63.39, 74.20, 108.00,
124.75, 127.46, 130.77, 132.75, 133.36, 138.49, 141.35,
151.85, 153.76, 163.60, 172.30;

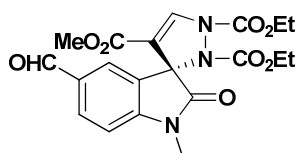
FAB mass: Calcd. for $\text{C}_{20}\text{H}_{23}\text{N}_3\text{O}_7$ $m/z = 417.15$;
Found: 418.56 (M+1);

Elemental Analysis: Calcd. for $\text{C}_{20}\text{H}_{23}\text{N}_3\text{O}_7$: C, 57.55;
H, 5.55; N, 10.07; **Found:** C, 56.51; H, 4.87; N, 9.09.

White crystalline solid, mp: 130-132 °C;

R_f: 0.31 (35% EtOAc-Hexane);

IR (KBr) ν_{max} : 3023, 2923, 2846, 2754, 1734, 1716,
1703, 1654, 1635 cm^{-1} ;



Compound 64

^1H NMR (CDCl_3/TMS , 500.1 MHz): δ 1.34 (m, 3H),
1.40 (m, 3H), 3.32 (s, 3H), 3.58 (s, 3H), 4.28 (m, 2H),
4.39 (m, 2H), 6.98 (d, $J = 8.0$ Hz, 1H); 7.74 (m, 2H),
7.87 (d, $J = 8.0$ Hz, 1H), 9.86 (s, 1H);

^{13}C NMR (CDCl_3/TMS , 125.7 MHz): δ 12.54, 12.82,
25.57, 50.38, 61.77, 63.01, 71.85, 107.43, 117.18,
122.70, 127.07, 130.83, 132.47, 137.57, 147.56, 152.30,
154.73, 161.27, 171.82, 189.05;

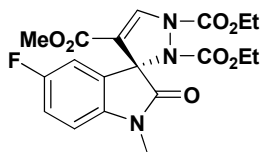
FAB mass: Calcd. for $\text{C}_{20}\text{H}_{21}\text{N}_3\text{O}_8$ $m/z = 431.13$;
Found: 432.56 (M+1);

Elemental Analysis: Calcd. for $\text{C}_{20}\text{H}_{21}\text{N}_3\text{O}_8$: C, 55.68;
H, 4.91; N, 9.74; **Found:** C, 54.51; H, 3.87; N, 9.09.

White crystalline solid, mp: 139-141 °C;

R_f: 0.27 (30% EtOAc-Hexane);

IR (KBr) ν_{max} : 3011, 2956, 2845, 1746, 1718, 1705,



Compound 65

1628 cm^{-1} ;

$^1\text{H NMR}$ (CDCl_3/TMS , 500.1 MHz): δ 1.19 (m, 3H), 1.37 (m, 3H), 3.27 (s, 3H), 3.59 (s, 3H), 4.22 (m, 2H), 4.37 (m, 2H), 6.79 (m, 1H); 6.93 (m, 1H), 7.05 (m, 1H), 7.79 (s, 1H) ;

$^{13}\text{C NMR}$ (CDCl_3/TMS , 125.7 MHz): δ 13.95, 14.26, 26.85, 51.80, 63.60, 64.35, 73.94, 108.84, 112.13, 112.33, 116.57, 116.76, 128.85, 138.86, 139.61, 153.47, 158.49, 160.41, 172.18;

FAB mass: Calcd. for $\text{C}_{19}\text{H}_{20}\text{FN}_3\text{O}_7$ m/z = 421.13; Found: 422.14 (M+1);

Elemental Analysis: Calcd. for $\text{C}_{19}\text{H}_{20}\text{FN}_3\text{O}_7$: C, 54.16; H, 4.78; N, 9.97; Found: C, 54.13; H, 4.78; N, 9.92.

White crystalline solid, mp: 128-130 $^\circ\text{C}$;

R_f: 0.32 (35% EtOAc-Hexane);

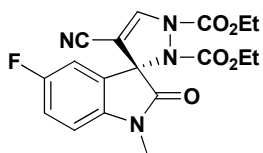
IR (KBr) ν_{max} : 3054, 2986, 2232, 1742, 1719, 1702, 1631, 1616 cm^{-1} ;

$^1\text{H NMR}$ (CDCl_3/TMS , 500.1 MHz): δ 1.12 (m, 3H), 1.26 (m, 3H), 3.27 (s, 3H), 4.19 (m, 2H), 4.37 (m, 2H), 6.85 (m, 1H); 7.04 (m, 1H), 7.13 (m, 1H), 7.66 (s, 1H);

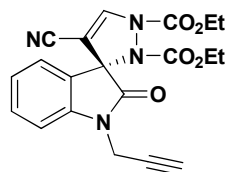
$^{13}\text{C NMR}$ (CDCl_3/TMS , 125.7 MHz): δ 14.20, 14.35, 26.82, 63.60, 64.84, 74.79, 110.00, 113.04, 115.30, 122.64, 123.88, 128.63, 131.73, 138.81, 141.43, 158.79, 160.73, 171.01;

FAB mass: Calcd. for $\text{C}_{18}\text{H}_{17}\text{FN}_4\text{O}_5$ m/z = 388.12; Found: 389.56 (M+1);

Elemental Analysis: Calcd. for $\text{C}_{18}\text{H}_{17}\text{FN}_4\text{O}_5$: C, 55.67; H, 4.41; N, 14.43; Found: C, 55.61; H, 4.45; N, 14.42.



Compound 66



Compound 67

White crystalline solid, mp: 122-124 °C;

R_f: 0.30 (35% EtOAc-Hexane);

IR (KBr) ν_{max} : 3293, 3023, 2911, 2231, 2143, 1738, 1716, 1701, 1654 cm^{-1} ;

¹H NMR (CDCl_3/TMS , 300.1 MHz): δ 1.27 (m, 6H), 2.22 (s, 1H), 4.23 (m, 6H), 7.09 (m, 2H) 7.22 (m, 1H), 7.38 (m, 1H), 7.57 (s, 1H);

¹³C NMR (CDCl_3/TMS , 75.4 MHz): δ 14.20, 14.32, 29.73, 63.56, 64.06, 64.63, 73.22, 76.00, 110.12, 110.68, 118.19, 124.28, 124.79, 125.61, 131.31, 132.19, 140.19, 152.15, 155.11, 170.24;

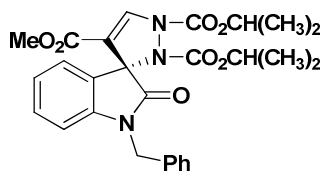
FAB mass: Calcd. for $\text{C}_{20}\text{H}_{18}\text{N}_4\text{O}_5$ m/z = 394.13; Found: 395.51 (M+1);

Elemental Analysis: Calcd. for $\text{C}_{20}\text{H}_{18}\text{N}_4\text{O}_5$: C, 60.91; H, 4.60; N, 14.21; Found: C, 60.83; H, 4.42; N, 14.23.

White crystalline solid, mp: 146-148 °C;

R_f: 0.30 (35% EtOAc-Hexane);

IR (KBr) ν_{max} : 3039, 2945, 1742, 1722, 1706, 1623, 1474 cm^{-1} ;



Compound 68

¹H NMR (CDCl_3/TMS , 300.1 MHz): δ 1.05 (m, 6H), 1.31 (m, 6H), 3.49 (s, 3H), 5.03 (s, 4H) 6.67 (d, J = 7.41 Hz, 1H), 7.01 (d, J = 7.41 Hz, 1H), 7.28 (m, 7H), 7.82 (s, 1H);

¹³C NMR (CDCl_3/TMS , 75.4 MHz): δ 21.84, 21.94, 29.69, 29.99, 44.74, 51.69, 72.28, 72.72, 73.81, 109.34, 121.84, 121.99, 123.10, 123.83, 127.58 (2C), 128.70 (2C), 130.20, 135.46, 138.70, 139.26, 140.99, 153.3, 156.33, 161.43, 174.61;

FAB mass: Calcd. for $\text{C}_{27}\text{H}_{29}\text{N}_3\text{O}_7$ m/z = 507.2; Found: 508.36 (M+1);

Elemental Analysis: Calcd. for C₂₇H₂₉N₃O₇: C, 63.89; H, 5.76; N, 8.28; Found: C, 64.55; H, 4.95; N, 12.57.

White crystalline solid, mp: 192-194 °C;

R_f: 0.32 (35% EtOAc-Hexane);

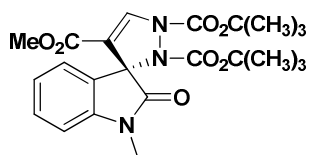
IR (KBr) ν_{\max} : 3011, 2986, 1741, 1719, 1702, 1624, 1471 cm⁻¹;

¹H NMR (CDCl₃/TMS, 500.1 MHz): δ 1.42 (m, 9H), 1.56 (m, 9H), 3.27 (s, 3H), 3.56 (s, 3H), 6.81 (d, *J* = 7.5 Hz, 1H), 7.05 (t, *J* = 9.5 Hz, 1H), 7.15 (d, *J* = 9.5 Hz, 1H), 7.32 (t, *J* = 7.5 Hz, 1H), 7.39 (s, 1H);

¹³C NMR (CDCl₃/TMS, 125.7 MHz): δ 12.03, 18.77, 24.42, 25.43 (2C), 25.83, 49.31, 58.06, 71.64, 80.45, 82.25, 105.58, 120.75, 121.64, 126.00, 126.08, 127.89, 137.02, 141.54, 150.26, 159.29, 168.60, 170.36;

FAB mass: Calcd. for C₂₃H₂₉N₃O₇ *m/z* = 459.29; Found: 460.65 (M+1);

Elemental Analysis: Calcd. for C₂₃H₂₉N₃O₇: C, 60.12; H, 6.36; N, 9.14; Found: C, 60.13; H, 6.38; N, 9.11.



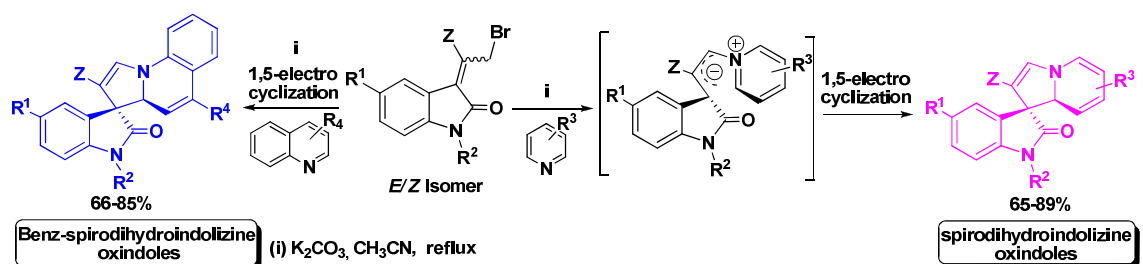
Compound 69

Chapter V

Pyridine Core Activation *via* 1, 5-Electrocyclization of Vinyl Pyridinium Ylide Generated from Bromo Isomerized Morita-Baylis-Hillman Adduct of Isatin: Synthesis of 3-Spirodihydroindolizine-2-Oxindoles

Abstract:

An activation of the pyridine nucleus has been achieved *via* 1,5-electrocyclization of vinyl pyridinium ylides generated from bromo isomerized Morita-Baylis-Hillman adducts of isatin and pyridine under basic conditions. The method has been successfully applied for an efficient synthesis of a number of 3-spirodihydroindolizine-2-oxindoles, which have been found as core structure of secoyohimbane and heteroyohimbane alkaloid natural products.



Shanmugam, P. *et al. Org. Lett.*, 2010, 12, 2108-2111.

Pyridine Core Activation *via* 1, 5-Electrocyclization of Vinyl Pyridinium Ylide Generated from Bromo Isomerized Morita-Baylis-Hillman Adduct of Isatin: Synthesis of 3-Spirohydroindolizine-2-Oxindoles

5.1 Introduction:

Pyridine core activation is an important and challenging synthetic transformation in contemporary organic synthesis, which has been utilised to synthesise a variety of bioactive natural products [Katrizky, A. R. *et al.* 1984; Michael, J. P. 2001; Shipman, M. 2001], pharmaceutical cores [Micheal, J. P. 2002] and also used as high level fluorescent providers [Vlahovici, A. *et al.* 1999; Vlahovici, A. *et al.* 2002; Sonnenschein, H. 2000]. The most common and well known method for pyridine core activation is the use of transition metal catalyzed intramolecular cyclization categories. The major disadvantage of such type of transition metal catalyzed pyridine core activation reaction is an easy formation metal complexes with pyridine, which underplay the formation of the expected product and low yields [Togni, A. *et al.* 1994; Joule, J. A. 2000; Gibson, V. C. *et al.* 2007]. However, a very few of the literature reports have been known to overcome the above limitation in a metal free reaction which provided selective functionalization at C2 position of pyridine core [Bennasar, M.-L. *et al.* 2003; Comins, D. L. *et al.* 2002; Charette, A. B. *et al.* 2001]. To rectify these problems, a number groups have been utilized annulation reaction as an alternative method to activate the pyridine core either by the *N*-alkylation [Sadana A. K. *et al.* 2003] or nucleophilic cyclization at C2 position of pyridinium ylides [Seregin, I. V. *et al.* 2008; Chernyak, D. *et al.* 2008; Schwier, T. *et al.* 2007; Seregin, I. V. *et al.* 2006]. Like that, the inter and intramolecular 1,5-electrocyclization *via* aza vinyl azomethine ylide strategy have also been used for the construction of heterocycles or pyridine core activation [Pohjala, E. 1972; Tamura, Y. *et al.* 1972]. Even though, the efficient functionalization of pyridine ring and their core derivatives in metal free condition is yet to be explored and also remains an important

issue in front of synthetic organic chemists. Hence, in the present chapter, we focused our attention in the synthesis of bioactive molecules of 3-spiroindolizine-2-oxindole derivatives starting from allyl bromide of oxindole *via* 1,5-electrocyclization as a key reaction. Since, the electrocyclization reaction is the key reaction applied for the present study, a general introduction on the concept of electrocyclization is discussed in the following section.

5.1.1 Electrocyclization reactions:

Electrocyclization is one of the pericyclic reaction which involve either the formation of a ring, by the generation of one new σ -bond and the consumption of one π -bond or the converse [Hoffmann, R. *et al.* 1968; Fleming, I. 1976; Morrison, R. T. *et al.* 1992]. These intramolecular ring closing or ring opening reactions follow concerted pathway by the molecular orbital interaction between the highest occupied molecular orbital (HOMO) and the lowest unoccupied molecular orbital (LUMO) of the reactants in a particular reaction condition. Thus, the HOMO of the reactant exclusively depends on the reaction condition (thermal or photochemical) and the outcome would provide well defined stereo specified products. The exact stereochemistry depends upon two things: (a) The number of double bonds in the polyene and (b) the reaction condition i.e., either thermal or photochemical. The mode of ring closing or ring opening electrocyclic reactions are predicted by *Woodward-Hoffmann rules* based on the number of π -electrons involved and mode of orbital rotation in the electrocyclization (Table 5.1).

Table 5.1: Woodward-Hoffmann rule for electrocyclization reaction.

Number of π -electrons	Reaction condition	Allowed orbital rotation	Disallowed orbital rotation
4n	Thermal	Conrotatory	Disrotatory
4n	Photochemical	Disrotatory	Conrotatory
4n+2	Thermal	Disrotatory	Conrotatory
4n+2	Photochemical	Conrotatory	Disrotatory

For example, the thermal and photochemical electrocyclization of 1,4-disubstituted butadienes ($4n$ π -electrons) provided *cis* and *trans* 3,4-dimethyl cyclobutene, respectively (Figure 5.1). According to the *Woodward-Hoffmann rule*,

either the ring closing or ring opening of the reaction depends on the condition and the reaction progress only symmetry allowed process. In the case of 1,3-butadiene, ψ_2 -orbital is the HOMO can undergo symmetry allowed *dis* rotation under photochemical reaction condition, while the thermal reaction condition ψ_3 -orbital is HOMO of the 1,3-butadiene provide only *con* rotation and affords the corresponding stereo defined products.

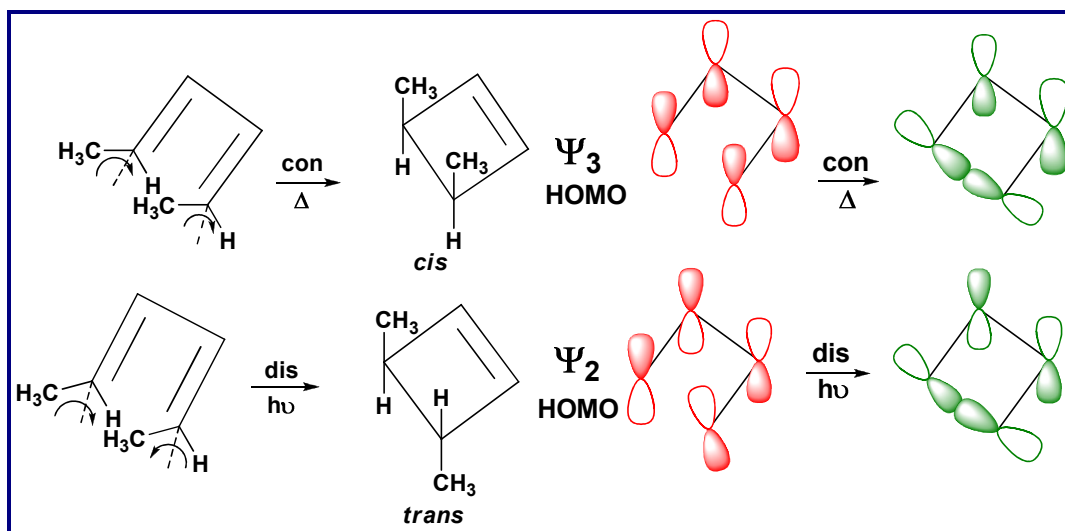


Figure 5.1: Thermal and photochemical electrocyclization of 1,3-disubstituted butadiene with molecular orbital energy diagram ($4n$ system).

Similarly, the 5,6-dimethylcyclohexa-1,3-diene ($4n+2$ π -electrons) follows the Woodward-Hoffmann rule and provides the stereo-defined product with respect to the reaction condition. The pictorial representation of HOMO of 5,6-dimethylcyclohexa-1,3-diene under thermal (ψ_3) and photochemical (ψ_4) reactions and the mode of ring closing and ring opening are depicted in Figure 5.2.

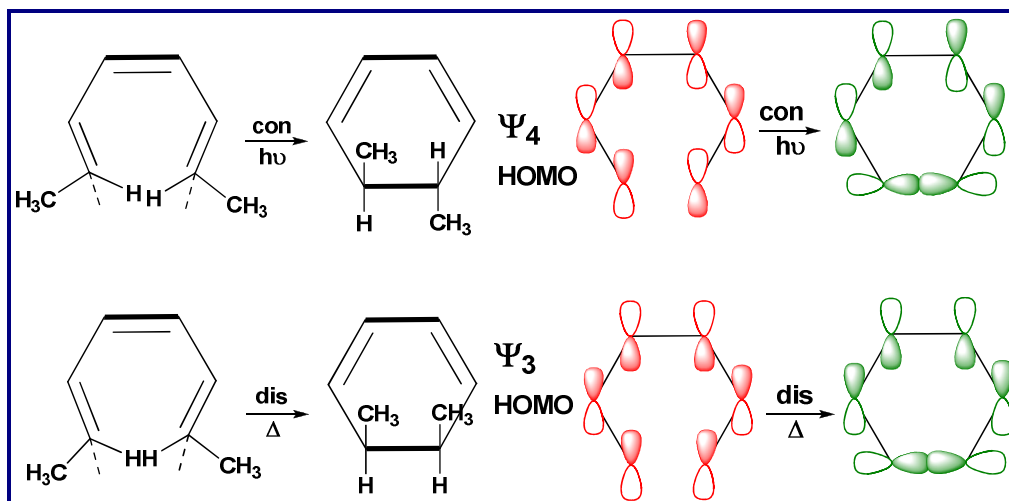


Figure 5.2: Thermal and photochemical cyclization of 5,6-dimethylcyclohexa-1,3-diene with molecular orbital energy diagram ($4n+2$ system).

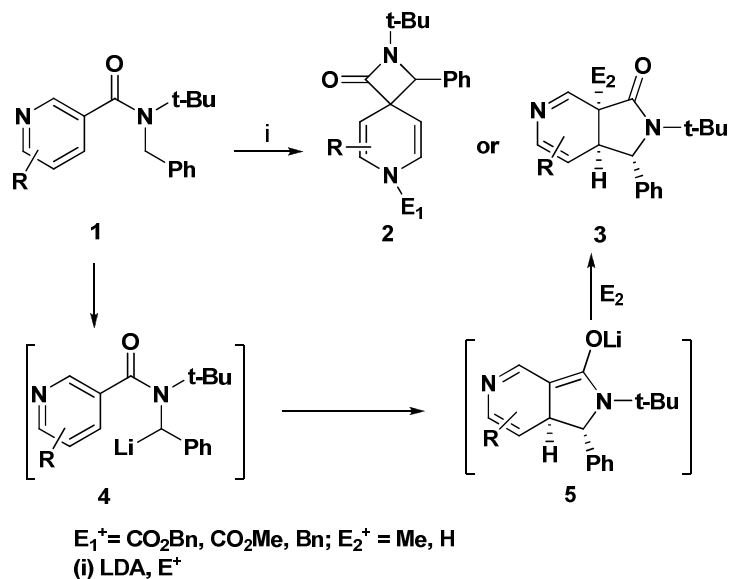
However, it would be better and is relevant to understand the literature known methods for the synthesis of nitrogen heterocycles either *via* 1,5-electrocyclization or the pyridine core activation as described in the following section.

5.2 A literature review on the synthesis of nitrogen heterocyclics and pyridine core activation:

5.2.1 Synthesis of partially saturated pyrrolopyridines and spiro- β -lactams *via* pyridine core activation:

Clayden and co-workers have reported a range of poly heterocyclic compounds such as pyrrolopyridines, pyrroloquinolines, benzonaphthyridines and aza spirocyclic β -lactam **2** from pyridine derivative **1** *via* lithium stabilized nucleophilic pyridinium core activation as a key step (Scheme 5.1). Mechanistically, the *N*-benzyl pyridine and quinoline carboxamide α -methylene proton was deprotonated by the base and lithium stabilized nucleophile upon intramolecular attack on the pyridine or quinoline ring, either directly or on activation of the ring by *N*-acylation. Thus, a range of poly heterocyclic compounds have been synthesized from four and five member-ring compounds by either one of the chemical process such as oxidization, protonation, alkylation, or acylation. The formation of spiro cyclic product **2** was assisted by the prior electrophilic attack on the

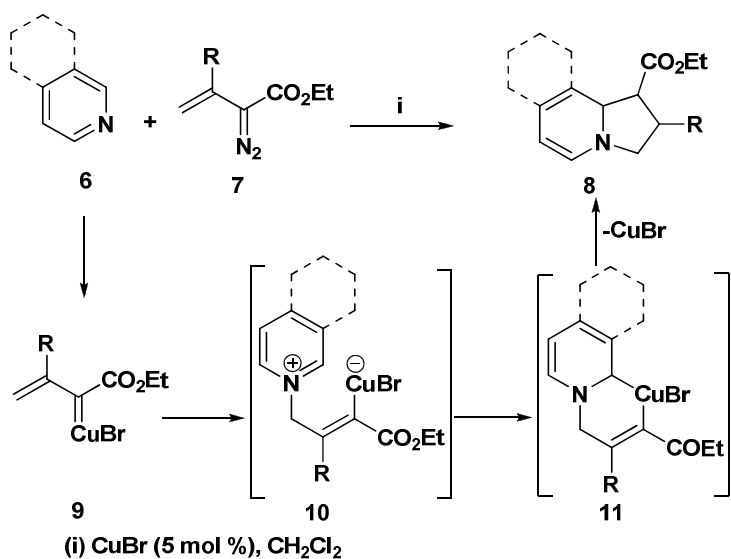
lithiated amide **4** at the pyridine nitrogen and more basic organolithium center [Clayden, J. *et al.* 2005].



Scheme 5.1: Synthesis of partially saturated and spiro poly *N*-heterocycle compounds.

5.2.2 Copper catalyzed [3+2]-annulation *via* pyridine activation:

In 2010, Barluenga and co-workers have reported a copper (I) catalyzed synthesis of indolizine derivative **8** from the reaction between pyridine derivative **6** and alkenyldiazo compound **7** *via* pyridine core activation as a key step (Scheme 5.2).

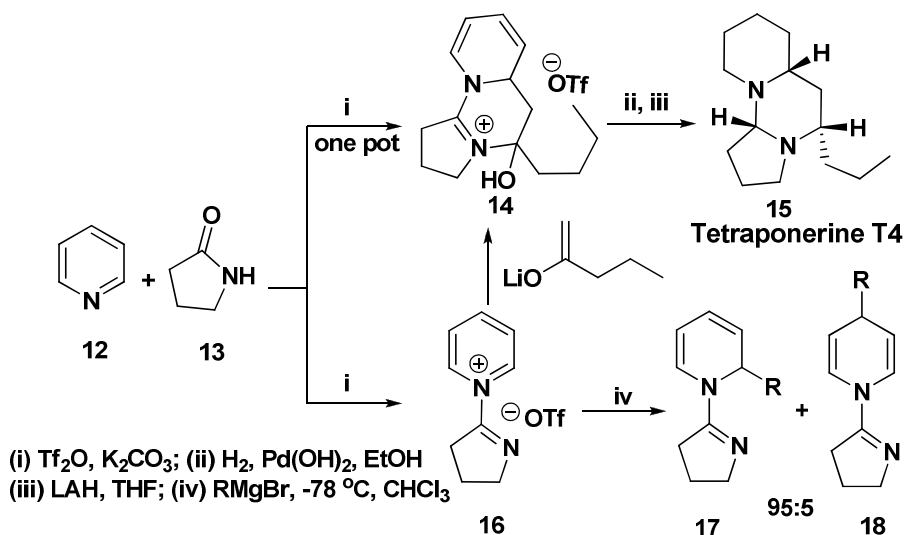


Scheme 5.2: Copper(I) catalyzed pyridine core activation.

The synthesized compound **8** was accounted by the intermediate copper (III) metallacyclization **11** generated from Michael addition between pyridine nitrogen **10** and alkenyldiazo compound olefin **7** followed by reductive elimination furnished the compounds **8** [Barluenga, J. *et al.* 2010].

5.2.3 Electrophilic activation of lactam with pyridine:

Tetraponerines were isolated from the venom of the New Guinean ant *Tetraponera sp.* These alkaloids represent the major constituents of the contact poison [Merlin, P. *et al.* 1988]. The (\pm)-Tetraponerine T4 **15** was enabled from pyridine **12** and 2-pyrrolidone **13** with triflic anhydride *via* nucleophilic pyridine ring substitution as a key step (Scheme 5.3). The proposed cyclic pyridinium salt **16** was isolated at room temperature and subjected to various nucleophilic additions with Grignard reagents at C2 and C4 positions of pyridine ring to afford compounds **17** and **18** [Charette, A. B. *et al.* 2005].

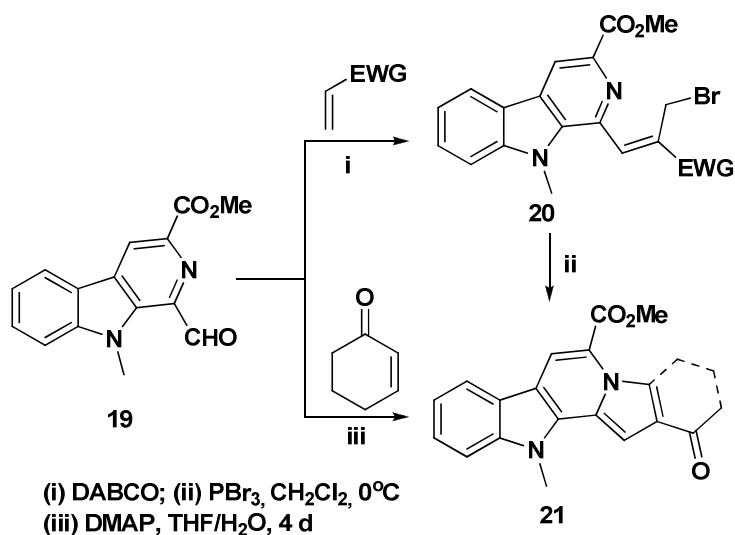


Scheme 5.3: Synthesis of (\pm)-Tetraponerine T4 derivative via pyridine core activation.

5.2.4 Pyridine core activation *via* MBH adduct/*N*-alkylation:

The natural product mimic structures such as harmicine and homofascaplysin alkaloid cores have been synthesised from 1- formyl- β -carbolines **19** with activated alkene *via* MBH adduct formation as a key step. The formations of indolizino-indole

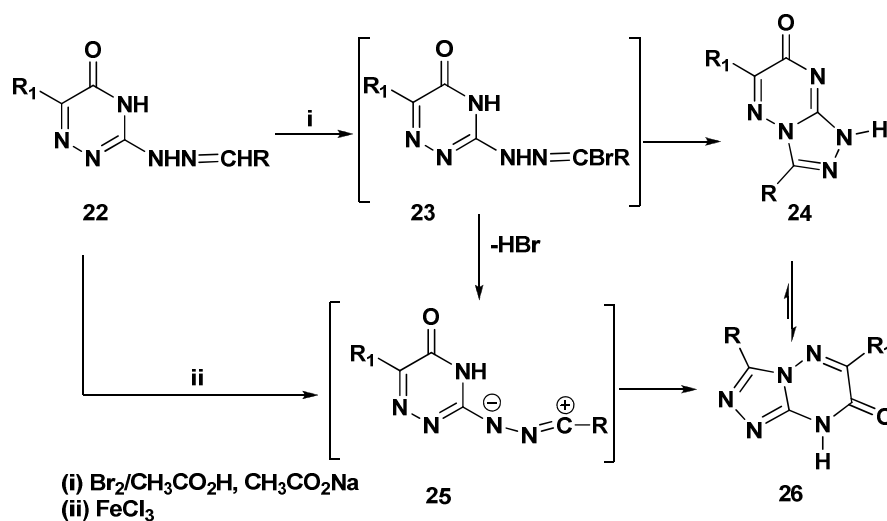
derivative **21** is explained either by nucleophilic substitution of allyl bromide of MBH derivative **20** to the β -carbolines derivative or by intramolecular cyclization of cyclic olefin provided pyridine core nitrogen activation product (Scheme 5.4). However, in the presence of DMAP, cycloalkenes directly provided the ring closed product in a one-pot manner [Singh, V. *et al.* 2010].



Scheme 5.4: Synthesis of indolizino-indole derivative.

5.2.5 Regioselective *N*-heterocycle activation via 1,5-electrocyclization:

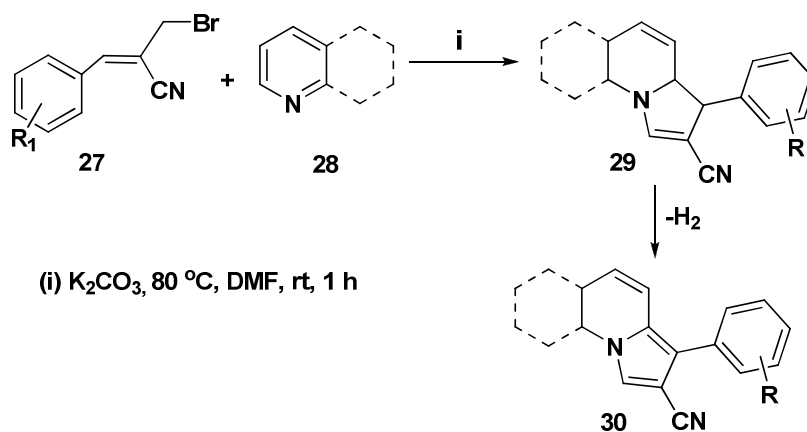
The regioselective synthesis of S-triazolo-triazinone derivative **26** have been reported from the reaction of 6-benzyl-3-(arylmethylidenehydrazino)-as-triazin-5(4H)-one **22** with either bromine in acetic acid containing sodium acetate or with ferric chloride *via* 1,5-electrocyclization (Scheme 5.5) [Shawali, A. S. *et al.* 2002].



Scheme 5.5: Synthesis of *S*-triazolo-triazinone derivative via 1,5-electrocyclization.

5.2.6 Pyridine core activation via *N*-alkylation/nucleophilic substitution:

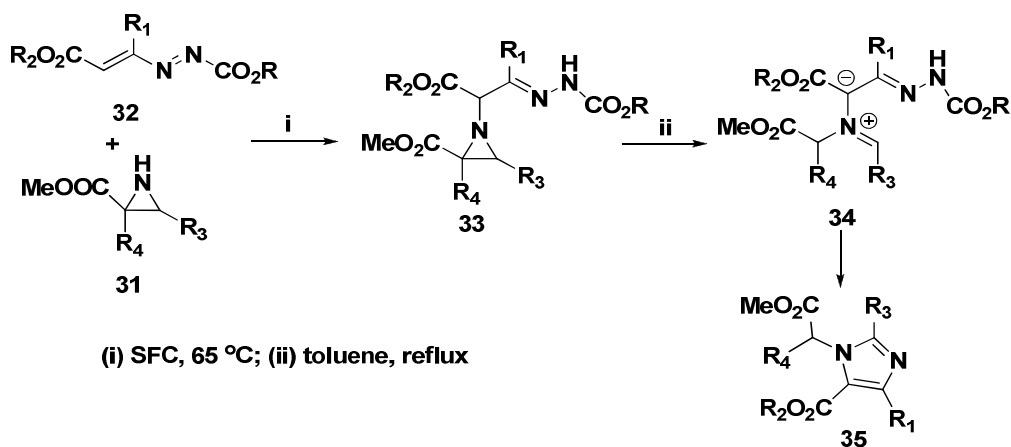
Basavaiah *et al.* reported the synthesis of variety of indolizine, benzofused indolizino, pyrrole[1,2-*a*]quinoline and pyrrole[1,2-*a*] isoquinoline derivative **30** from allyl bromide of MBH adduct **27** and pyridine derivative **28** via 1,5-electrocyclization (Scheme 5.6). Interestingly, the synthesized dihydroindolizine derivatives **29** underwent *in-situ* dehydrogenation provided indolizine framework **30** [Basavaiah, D. *et al.* 2009].



Scheme 5.6: Synthesis of indolizine derivatives via nucleophilic pyridine core activation.

5.2.7 Synthesis of imidazole derivative via 1,5-electrocyclization:

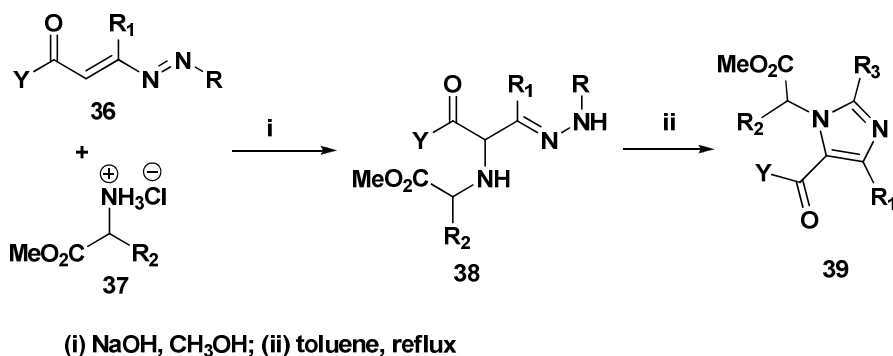
The imidazole derivative **35** has been synthesized from aziridinecarboxylates **31** with 1,2-diazo-1,3-butadiene **32** under solvent free condition (SFC) via 1,5-electrocyclization (Scheme 5.7). The compound **34** underwent 1,5-electrocyclization and aromatization by concomitant loss of carbamate residue by cleavage of *N-N* bond afforded imidazole derivative **35** by thermolytic cleavage of the aziridine [Attanasi, O. A. *et al.* 2007].



(i) SFC, 65 °C; (ii) toluene, reflux

Scheme 5.7: Synthesis of imidazole derivatives from aziridine via 1,5-electrocyclization.

This pioneer work has been extended to amino ester derivative **37** with 1,2-diazo-1,3-butadiene derivative **36** yielded imidazole derivative **39** via 1,5-electrocyclization (Scheme 5.8) [Attanasi, O. A. *et al.* 2009].



(i) NaOH, CH₃OH; (ii) toluene, reflux

Scheme 5.8: Synthesis of imidazole derivatives from amino acid via 1,5-electrocyclization.

With this background on electrocyclization concept, we can conclude that the combined utilization of 1,5-electrocyclization reaction of the pyridinium salt obtained from allyl bromide of MBH adduct of isatin and pyridine ring would be able to produce the stereo defined, pyridine core activated spirocyclic oxindoles.

5.3 Present work:

Nitrogen containing polyheterocycles have been found to be the basic skeleton in a numerous alkaloid natural products and bioactive compounds (Figure 5.3).

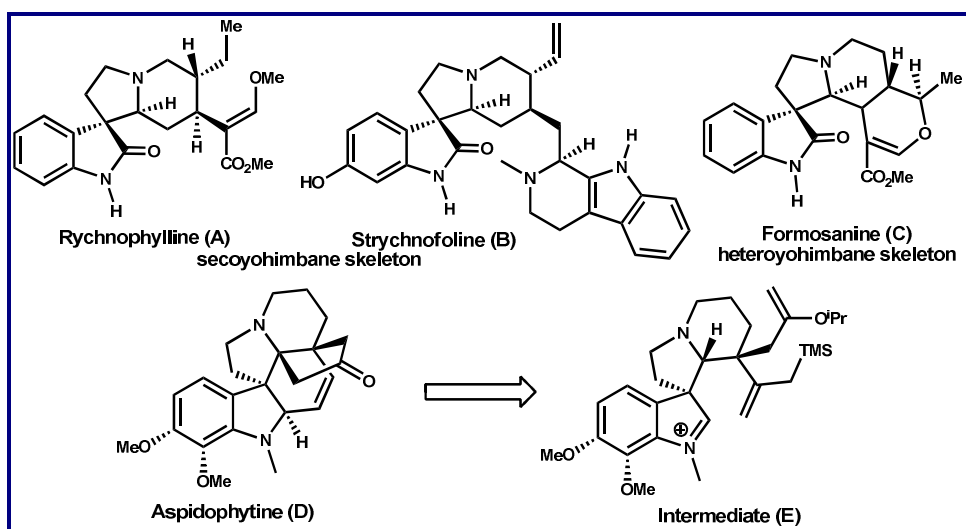


Figure 5.3: Natural products with 3-Spirooxindole core structure.

Especially, the spirocarbo- and heterocyclic derivatives at C3 position in oxindoles are elegant synthetic targets in organic synthesis due to their significant biological activities. The MBH adduct of isatin and their derivative has been paid less attention towards metal free pyridine core activation studies. Hence, in this chapter, we wish to synthesize 3-spiropyrazoline-2-oxindole derivatives by the combined utilization of the allyl bromide of oxindoles with pyridine nucleus and pyridine core activation as key step *via* 1, 5-electrocyclization process. The quarternization of pyridine nitrogen derived from allyl bromides of MBH adduct and pyridine readily undergoes intramolecular nucleophilic substitutions at C2 position to provide spirocyclic oxindole derivatives. The detail of the study on the 1,5-electrocyclization reaction of various

pyridine derivatives of allyl bromide MBH adduct of oxindoles is the subject matter of this Chapter.

5.4 Retrosynthetic analysis:

A retrosynthetic analysis for present study is outlined in Figure 5.4. The spirodihydroindolizine oxindole **A** can be derived from the pyridinium salt **B** with a base. The potential allyl bromide **C**, which could quarternize with pyridine to provide pyridinium salt **B**, could be synthesized from isatin derived MBH adduct **D** by isomerization with HBr. The MBH adduct could be formed from isatin **E** with methyl acrylate.

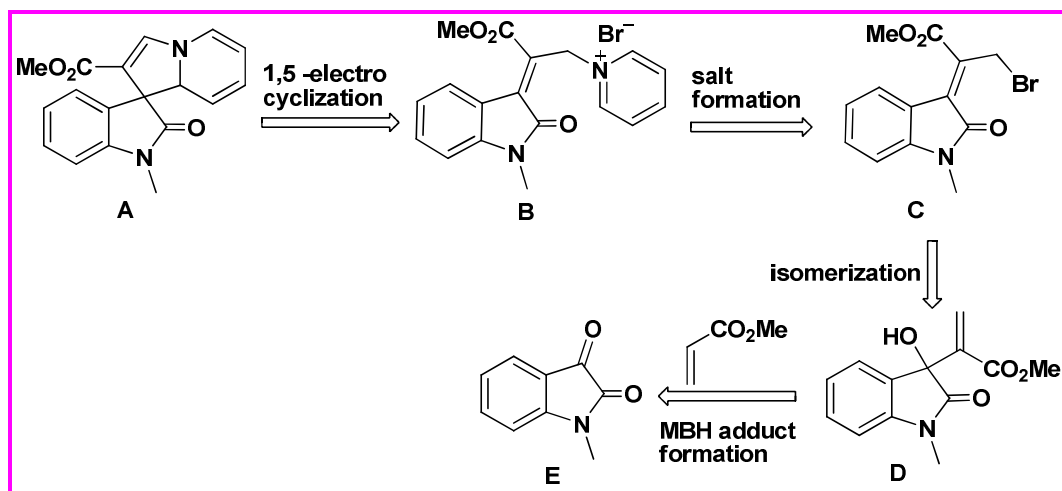


Figure 5.4: Retrosynthetic analysis of pyridine activation.

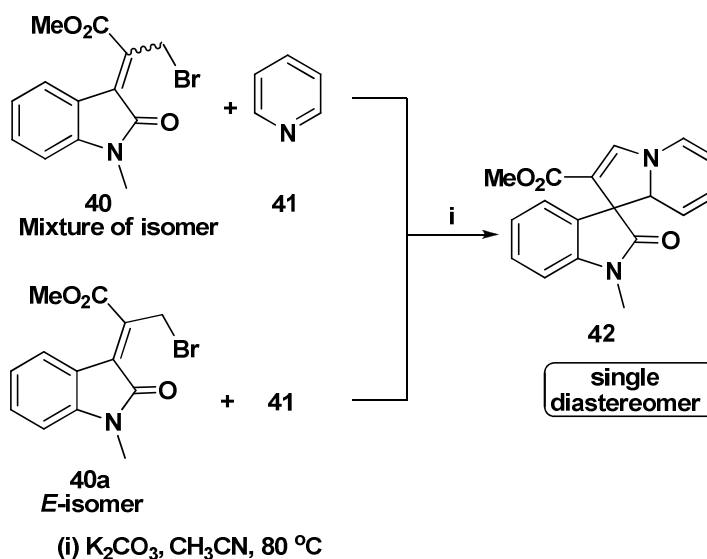
5.5 Results and Discussion:

5.5.1 Preparation of allyl bromide of oxindole from MBH adduct of isatin:

According to the retrosynthetic analysis, the starting precursor i.e. allyl bromide of oxindole was prepared under solvent free microwave irradiation from MBH adduct of isatin. The details of the synthesis of *E/Z*-isomers of **C** and characterization have already been discussed in Chapter IV (Figure 5.4).

5.5.2 Synthesis of 3-spirodihydroindolizine-2-oxindole derivative via 1,5 electrocyclization:

The preliminary study was initiated between the reactions of *E*-allyl bromide of oxindole **40a** with pyridine **41** in the presence of K_2CO_3 as base under reflux condition in acetonitrile. The reaction furnished poor yield (15%) of pyridine core activated spirocyclic product **42** via 1,5-electrocyclization reaction (Scheme 5.9). Interestingly, when the *E/Z*-isomeric mixture of allyl bromides of oxindole **40** and pyridine **41** have been subjected to 1,5-electrocyclization also furnished the single diastereomer of spirocyclic compound **42**.



Scheme 5.9: Synthesis of 3-spirodihydroindolizine-2-oxindole via 1,5-electrocyclization.

Before entering into the optimization, the structure of synthesized compound **42** has been characterized by spectroscopic analysis (FTIR, 1H , ^{13}C NMR and FAB-Mass).

The FTIR spectrum of the compound **42** showed the presence of amide and ester group absorptions at 1703 and 1721 cm^{-1} , respectively. In the 1H NMR spectrum, five protons of the dihydroindolizine six member ring appeared in the region between δ 4.68-6.46 ppm (Figure 5.5).

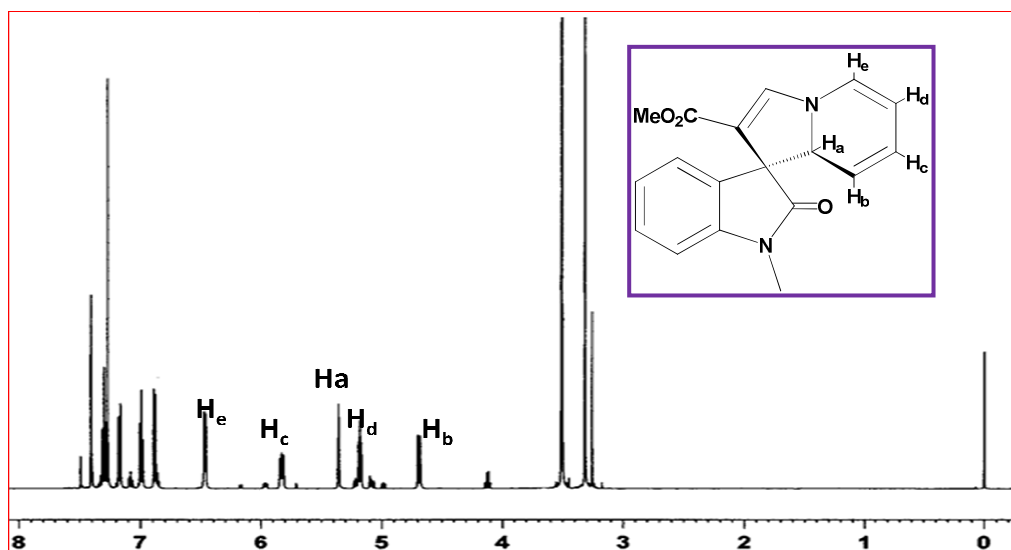


Figure 5.5: ^1H NMR Spectrum of compound **42**

The coupling nature of these protons in the ^1H - ^1H COSY spectrum further supported the assigned structure of compound **42** (Figure 5.6).

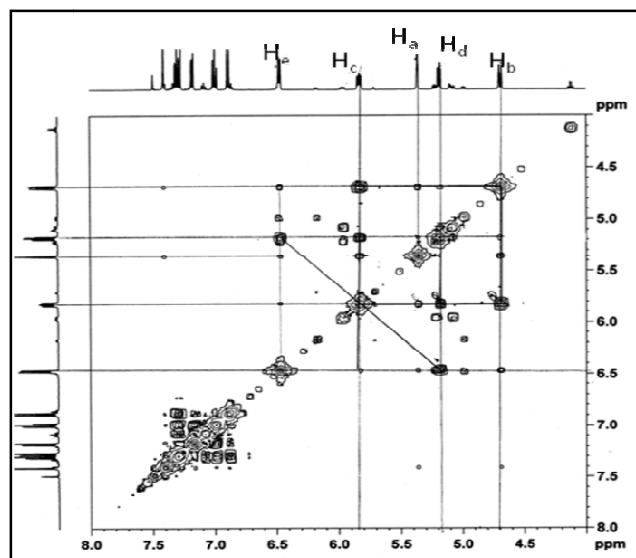


Figure 5.6: ^1H - ^1H -COSY Spectrum of compound **42** (Expanded region δ 4-8)

The dihydroindolizine ring sp^3 C-H proton marked as **H_a** appeared as a uncoupled singlet at δ 5.81 ppm. The **H_e** proton deshielded due to the nitrogen atom appeared at δ 6.46 ppm which showed the strong coupling with **H_d** proton visible at δ 5.35 ppm. The **H_c** proton appeared as a multiplet at δ 6.46 ppm and also coupled with **H_b** and **H_d**

protons. Interestingly, the **H_b** proton showed a strong coupling with **H_c** and not with **H_a** proton which may be in a perpendicular plane with indolizine ring protons. The alkene proton at the five member ring resonated at δ 7.40 ppm. The oxindole moiety aromatic protons were visible in the region of δ 6.88-7.29 ppm. The two singlets resonated at δ 3.31 and 3.50 ppm was assigned to *N*-methyl and ester methyl protons, respectively.

Analysis of the ^{13}C NMR spectrum of compound **42** showed signals at δ 26.92 and 51.16 ppm were assigned to *N*-methyl and ester methyl carbons, respectively (Figure 5.7). The sp^3 center carbon at the dihydroindolizine and spiro carbon were visible at δ 61.83 and 67.72 ppm, respectively. The presence of spiro carbon was confirmed from ^1H - ^{13}C correlation spectra by the absence of carbon hydrogen interaction and also from DEPT-135 signal disappeared at δ 67.72 ppm. The entire aromatic carbons were in good agreement with assigned structure and resonated between the region δ 108.19-144.88 ppm. The other carbonyl carbons such as amide and ester were appeared at δ 164.31 and 178.41 ppm, respectively.

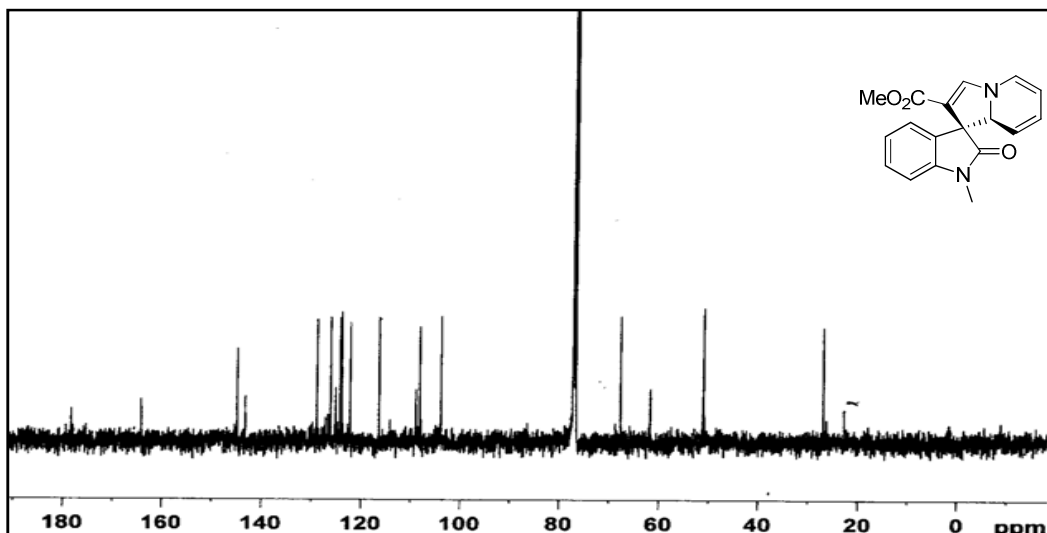


Figure 5.7: ^{13}C NMR Spectrum of compound **42**

Finally, the FAB-Mass showed a molecular ion peak [M^+] peak at $m/z = 308.31$ against the calculated value of $m/z = 308.12$ which supports the assigned structure and satisfactory elemental analysis (Figure 5.8).

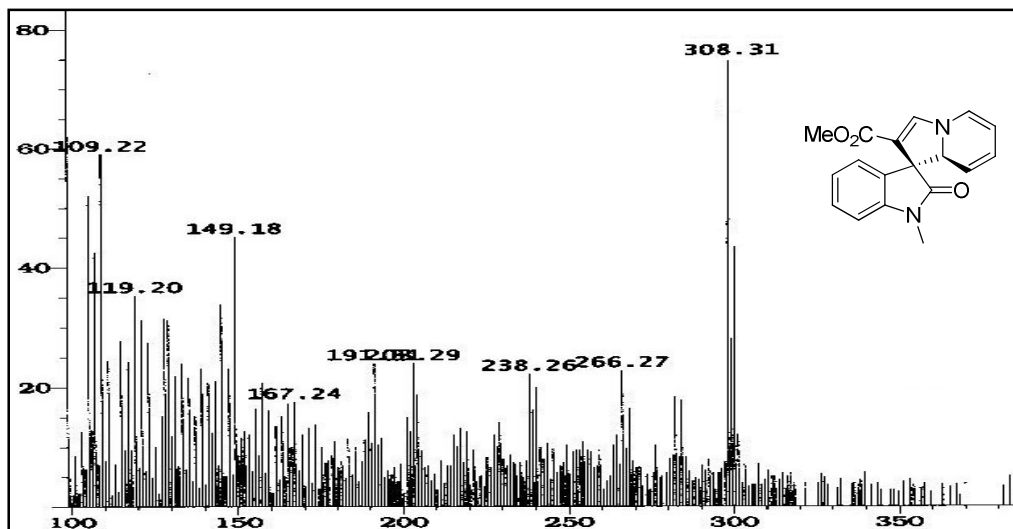


Figure 5.8: Mass spectrum of compound 42

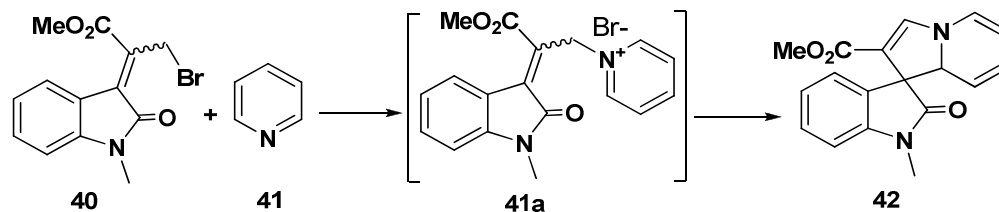
It is interesting to note that the synthesized compounds from both the isomers have had the similar core structure of the secoyohimbane type natural products (Figure 5.3).

5.5.3 Optimization study: Effect of solvent and catalyst load:

In order to improve the yield of the reaction, effect of variants such as solvent and catalyst requirement have been studied. For the optimization study, the *E/Z*- mixture of allyl bromide of oxindole **40** has been chosen as a model substrate. Experiments with various solvent systems such as acetonitrile, THF, acetone, DMF, etc and different bases were carried out and the results are given in the Table 5.2. After several test reactions, a combination of CH₃CN as a solvent with 2 h time delayed base addition (K₂CO₃) gave better yield (86%) and found to be an optimum condition (Table 5.2, entry 6). The time delayed addition of base to the reaction mixture gave better yield than immediate addition. The reason may be due to the immediate addition of base has led to decomposition of starting material before the formation of pyridinium salt **41a** under the reaction condition (Table 5.2, entries 1, 5). Interestingly, pyridine can also act as base, if the second equivalent of pyridine added to the reaction mixture and provided comparably better yield after 2 h (Table 5.2, entry 2). The other solvent systems and bases such as CH₃CN/Ag₂CO₃, acetone and DME/K₂CO₃ were found to be fruitless for this 1,5-electrocyclization with allyl bromide of oxindole (Table 5.2, entries 3, 7 and 9). All other

reaction conditions were afforded the expected products in moderate yield and the results are given in Table 5.2.

Table 5.2: Optimization of 1,5-electrocyclization reaction with allyl bromide of oxindole.



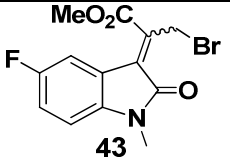
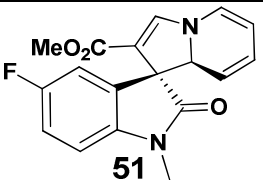
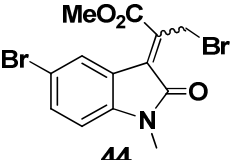
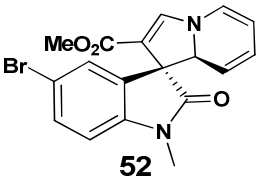
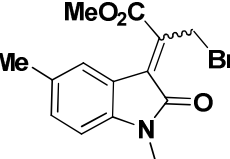
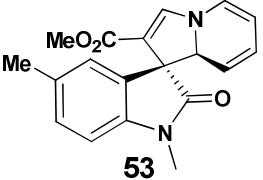
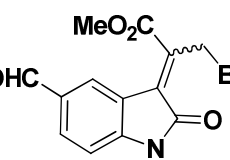
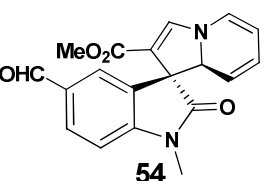
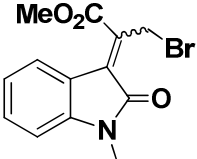
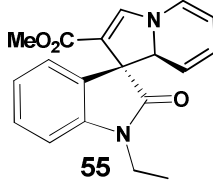
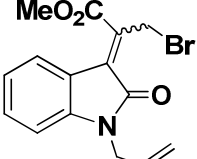
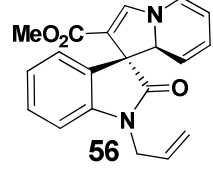
Entry	Solvent	Base	T °C	Time ^a	Yield (%)
1	CH ₃ CN	K ₂ CO ₃	80	0.5/3	15
2	CH ₃ CN	Pyridine	80	2/3	79
3	CH ₃ CN	Ag ₂ CO ₃	80	2/3	-
4	THF	K ₂ CO ₃	60	2/3	40
5	CH ₃ CN	K ₂ CO ₃	80	1/3	30
6	CH₃CN	K₂CO₃	80	2/3	86
7	Acetone	K ₂ CO ₃	56	2/3	-
8	DMF	K ₂ CO ₃	80	2/3	45
9	DME	K ₂ CO ₃	80	2/3	-

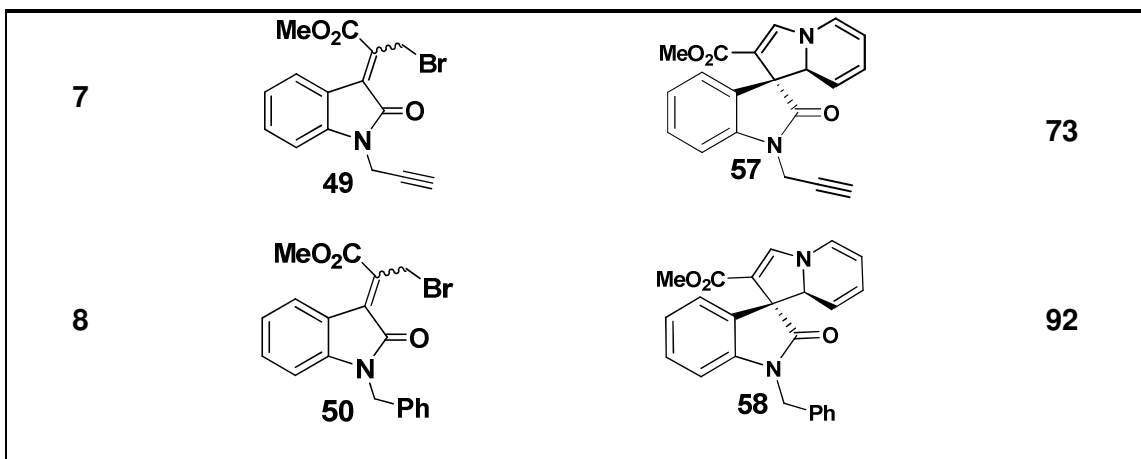
^a Base added after specified time / total reaction time.

5.5.4 Generality of pyridine core activation *via* 1,5-electrocyclization reaction:

In order to exemplify the 1, 5-electrocyclization reaction, with various allyl bromides of MBH adducts and pyridine, were carried out under optimized condition. All the reactions underwent the 1,5-electrocyclization smoothly and afforded the corresponding pyridine core activated spiroindolizine derivatives in excellent yield. The results are highlighted and given in Table 5.3.

Table 5.3: Generality of 1,5-electrocyclization with a various allyl bromide of oxindole derivatives.

Entry	Substrates (43-50)	Products (51-58)	Yield (%)
1	 <p>43</p>	 <p>51</p>	85
2	 <p>44</p>	 <p>52</p>	87
3	 <p>45</p>	 <p>53</p>	65
4	 <p>46</p>	 <p>54</p>	83
5	 <p>47</p>	 <p>55</p>	71
6	 <p>48</p>	 <p>56</p>	78



The presence of functional groups at aromatic and nitrogen position of oxindole core is an important factor to enhance the drugs essential properties such as solubility, promising cell permeability, hydrogen bond donor, acceptor property and inhibitory activity [Vintonyak, V. V. *et al.* 2010]. Hence, generality of this reaction was carried out with various allyl bromides of oxindole. This electrocyclization reaction was tolerable towards functional groups such as at *N*-position substituted by ethyl, benzyl, allyl and propargyl and also aromatic core of oxindole substituted by bromo, fluoro, methyl and formyl groups. Especially, the aromatic core of oxindole bearing electron withdrawing group showed to be better reactive substrate for the 1,5-electrocyclization reaction and also furnished spirocyclic product in good to excellent yield (Table 5.3, entries 1-4). The functional groups such as fluoro, bromo and formyl groups at aromatic core of oxindole are important constituent for further synthetic transformation. The 5-methyl allyl bromide of oxindole showed slow reactivity with low yield (Table 5.3, entry 5). Significantly, the *N*-benzyl derivatives gave best yield than the other substrates (Table 5.3, entry 8). Usually, the *N*-allyl and propargyl derivatives are playing vital role in stereochemistry of observed product in dipolar cycloaddition reaction [Pardasani, R. T. *et al.* 2003]. Hence, we were interested to check the reactivity of *N*-allyl **56** and *N*-propargyl **57** derivative of oxindole with 1,5-electrocyclization reaction and provided expected compound in good yield (Table 5.3, entries 6-7). It is interesting to mention that all the substituted isatin MBH derivatives furnished the expected spirocyclic compound as a diastereoselective product with trace of the other isomer.

For representative spectroscopic characterization of new compounds, *N*-propargyl derivative of spiroindolizine **57** was chosen for discussion. The FTIR spectrum showed the characteristic functional groups such as acetylene, amide and ester absorbance at 2250, 1701 and 1722 cm^{-1} , respectively.

The ^1H NMR spectrum of compound **57** showed the terminal acetylenic proton resonates at δ 2.26 ppm and the ester methyl proton appeared as a singlet at δ 3.48 ppm (Figure 5.9). The *N*-methylene proton resonated as a multiplet centered at 4.60 ppm. The five protons of dihydroindolizine ring appeared in the region at δ 4.70-6.46 ppm. Specifically, the dihydroindolizine C-H proton resonated as an uncoupled singlet at δ 5.36 ppm. The five member ring alkene proton from dihydroindolizine was visible at δ 7.31 ppm. All the aromatic protons of oxindole moiety were visible in the region at δ 7.03-7.31 ppm.

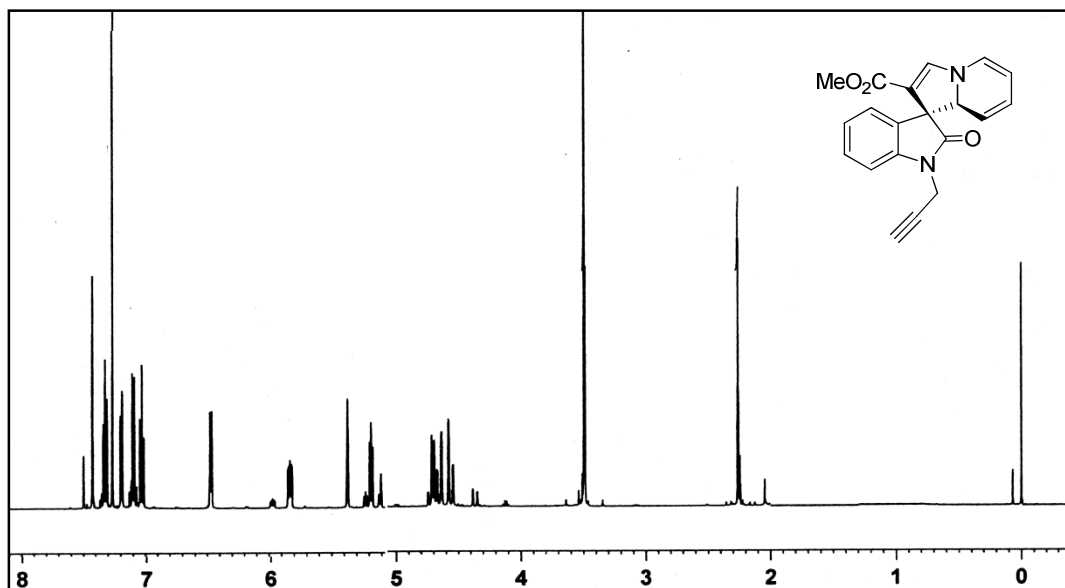


Figure 5.9: ^1H NMR Spectrum of compound **57**

The ^{13}C spectrum of compound **57** further supported the assigned structure and showed a signal at δ 51.07 ppm which corresponds to ester methyl carbon (Figure 5.10). The characteristic acetylene carbons of propargyl system were visible at 67.94 and 72.20 ppm, respectively.

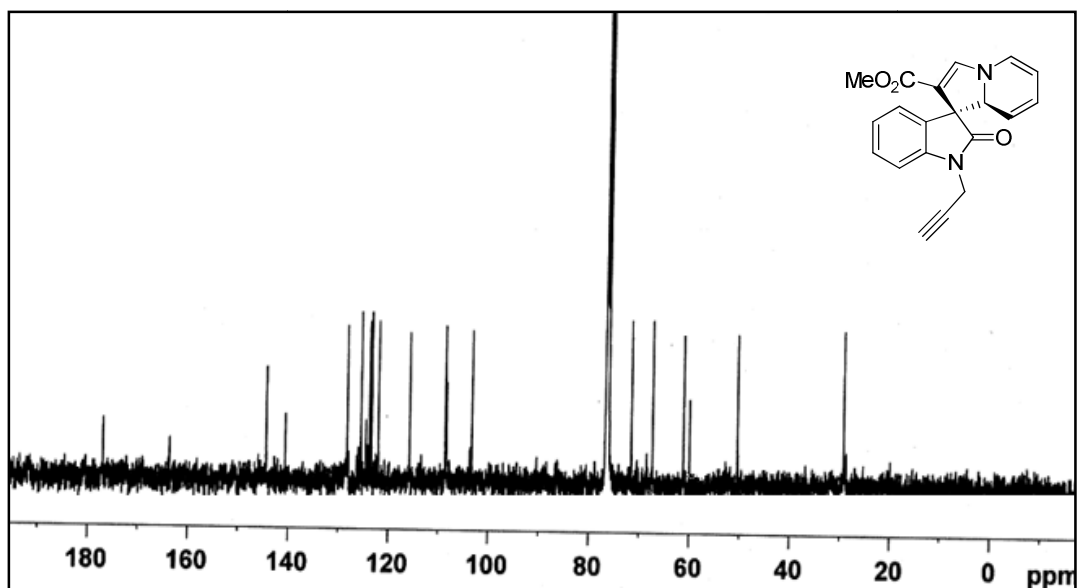


Figure 5.10: ^{13}C NMR spectrum of compound 57

The other aliphatic carbons such as *N*-methylene and spiro carbons resonated at 29.84 and 63.04 ppm, respectively. The sp^3 carbon from the dihydroindolizine was visible at δ 61.80 ppm. The remaining all aromatic carbon signals were accounted and appeared in the region at 103.92-145.04 ppm. The amide and ester carbonyl carbons appeared at 164.34 and 177.65 ppm, respectively.

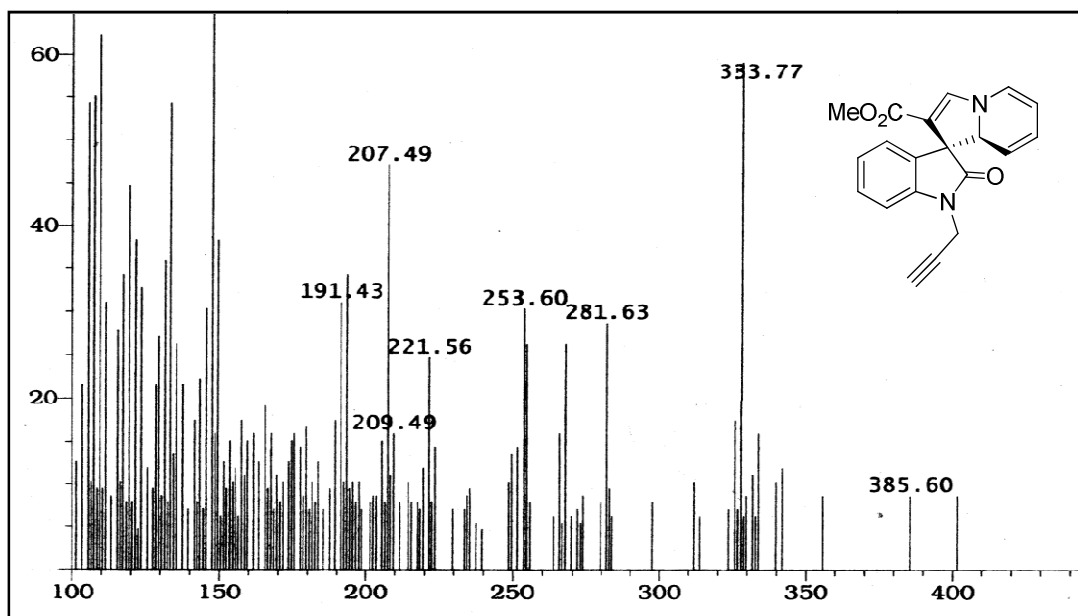


Figure 5.11: FAB mass spectrum of compound 57

Final proof of assigned structure of the compound **57** was supported by FAB mass spectrum as it showed a molecular ion peak [M+1] at $m/z = 333.77$ against the calculated value $m/z = 332.12$ (Figure 5.11). The spectroscopic data of all the new compounds are listed in the experimental section at the end of this chapter.

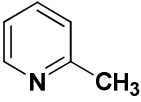
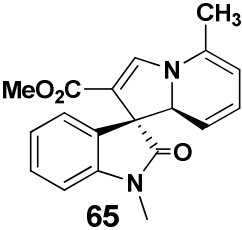
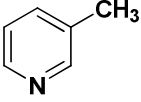
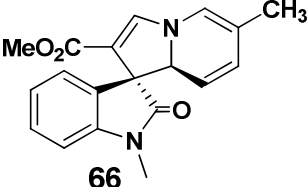
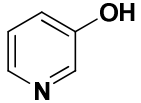
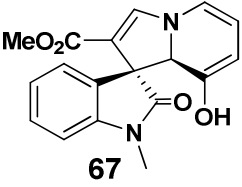
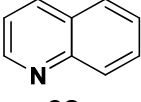
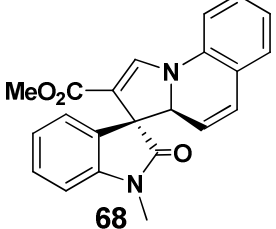
The spirocyclic compounds stored in CDCl_3 solvent at room temperature were found to be completely decomposed within 4 hour and were confirmed by *TLC* and ^1H NMR spectrum. Fatefully, we could not find any characteristic rearranged products from these decomposed spiroindolizine derivatives. In order to avoid the decomposition of product, we were taken the NMR spectrum of all the spirocyclic derivatives in CDCl_3 solvent after passing through capillary basic alumina column (Brockmann activity I, II). The reason may be traces of acidic impurity in CDCl_3 solvent which initiated the decomposition that has been removed in an alumina column.

5.5.5 Substituted pyridine and poly cyclic pyridine core involved 1,5-electrocyclization:

Encouraged by the preliminary results, we turned our attention to examine different substituted pyridines, and its polycyclic derivatives such as quinoline and isoquinoline for 1,5-electrocyclization reaction (Table 5.4). Hence, the *N*-methyl allyl bromide of oxindole **40** was chosen as model substrate and treated with various pyridine derivatives for 1,5-electrocyclization. During the substrate screening, only a few pyridine derivatives underwent smoothly the 1,5-electrocyclization reaction and provided the corresponding pyridine core activated spiroindolizine compounds in good yield. The results are given in Table 5.4. The 1,5-electrocyclization reaction of 2-picoline **59** provided the spirocyclic compound **65** in good yield without any compromise of selectivity (Table 5.4, entry 1). But in the case of 3-picoline **60**, an inseparable mixture of two regio-isomeric products **66** ratio 1:0.5 as estimated from ^1H NMR was obtained with combined yield of 71% (Table 5.4, entry 2). Among the hydroxyl group substituted pyridine derivatives, only the 3-hydroxyl pyridine **61** underwent 1,5-electrocyclization to produce inseparable two regio-isomeric products **67** (ratio 1:0.5) in combined good yield 66% (Table 5.4, entry 3). The screening of nitrogen found poly cyclic core with allyl

bromide of oxindole derivatives in pyridine core activation is synthetically important, which has led to the natural product core structure like secoyohimbane and heteroyohimbane (Figure 5.3). In order to make complex molecular framework of spirocyclic oxindoles, polycyclic pyridine derivatives such as quinoline **62** has been used. The reaction provided the benz-fused spiroindolizine compound **68** in good yield (Table 5.4, entry 4). Isoquinoline **63** was also used in 1,5-electrocyclization and provided a single regio-isomeric product **69** in good yield (Table 5.4, entry 5). The 4-bromoquinoline **64** furnished the expected spiro derivative **70** in good yield (Table 5.4, entry 6).

Table 5.4: Activation of pyridine derivatives core via 1,5-electrocyclization.

Entry	Substrate	Product	Yield (%)
1	 59	 65	78
2	 60	 66	71 ^a
3	 61	 67	66 ^{ab}
4	 62	 68	75



^a Mixture of regioisomer. ^b Reaction conducted in room temperature.

The structure of synthesized compound **70** was determined on the basis of detailed spectroscopic analysis. The FTIR spectrum showed absorptions at 1702 and 1719 cm^{-1} due to presence of functional groups such amide and ester, respectively.

In the ^1H NMR spectrum, two separate singlets at δ 3.44 and 3.54 ppm was assigned to *N*-methyl and ester methyl protons, respectively (Figure 5.12). The sp^3 C-H proton from dihydroindolizine appeared at δ 5.93 ppm as an uncoupled singlet. The alkene proton from the six membered indolizine ring resonated at δ 5.98 ppm. The remaining all aromatic protons were accounted and resonated in the region at 6.78-7.32 ppm.

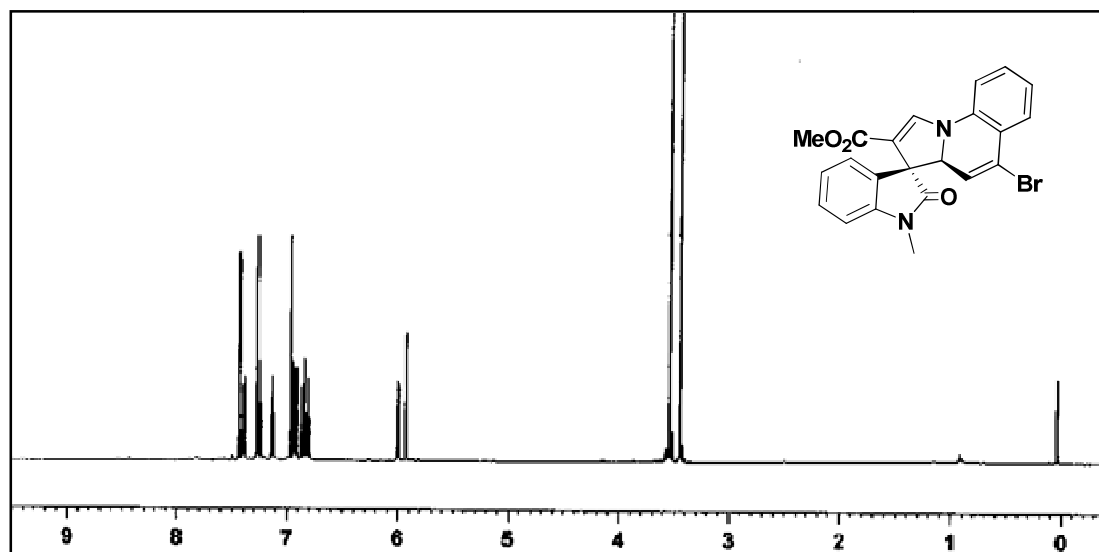


Figure 5.12: ^1H NMR spectrum of compound **70**

The ^{13}C NMR spectrum supported the structure of synthesized compound **70** and showed the signals at δ 27.17 and 51.18 ppm which were assigned to the *N*-methyl and methoxy carbon of the ester group (Figure 5.13). The characteristic sp^3 carbon from dihydroindolizine and spiro carbon were visible at δ 61.14 and 68.42 ppm, respectively. The remaining aromatic carbons were appeared in the chemical shift range between δ 101.14-143.09 ppm. The carbonyls carbon of amide and ester were detected at δ 163.80 and 177.81 ppm, respectively (Figure 5.13).

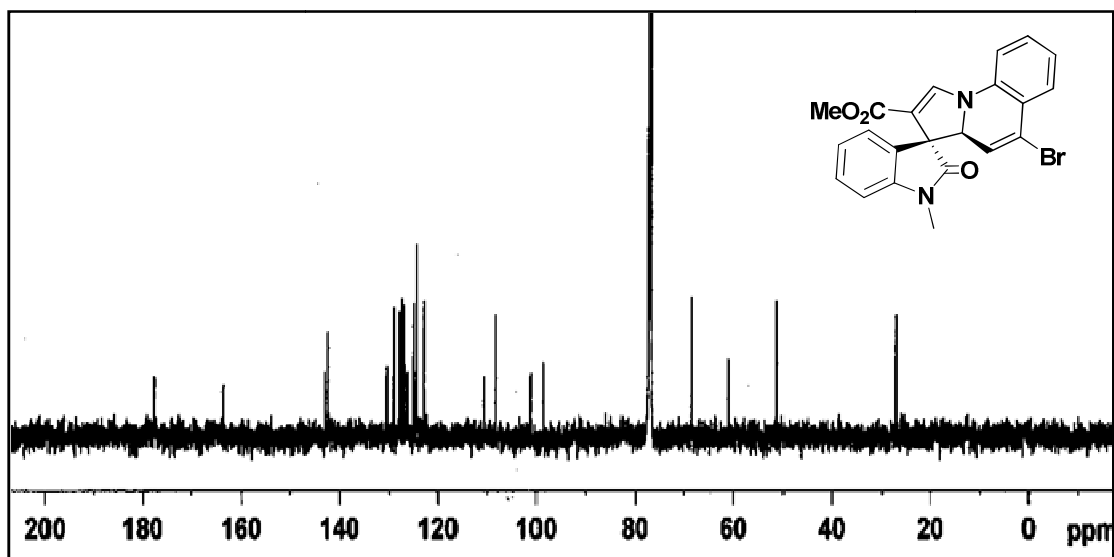


Figure 5.13: ^{13}C NMR spectrum of compound **70**

Finally, the assigned structure was supported by FAB mass spectrum as it showed a molecular ion peak $[\text{M}+2]$ at $m/z = 438.14$ against calculated value $m/z = 436.04$ and satisfactory elemental analysis. Unambiguous evidence for the structure of synthesized compound **70** and stereochemistry was obtained by single crystal X-ray analysis (Figure 5.14).

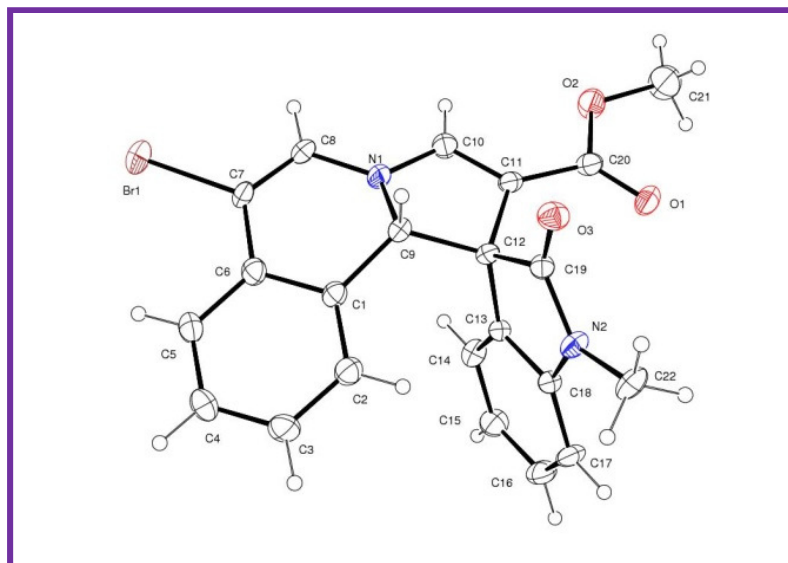
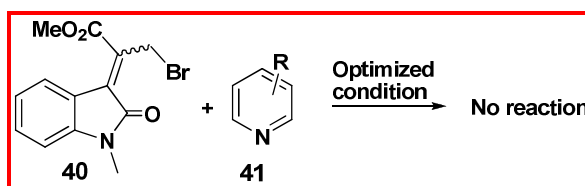


Figure 5.14: X-ray single crystal structure of the compound **70**

5.5.6 Limitations of 1, 5-electrocyclization reaction with pyridine derivative in allyl bromide of oxindole:

We found that a number of pyridine derivatives (Figure 5.15) along with allyl bromide of oxindole afforded decomposed products under the optimized reaction condition (Scheme 5.10).



Scheme 5.10: Screening of pyridine derivatives.

The decomposition of starting material might have happened due to inertness of the pyridine core on initial salt formation with allyl bromide of isatin under basic (presence of K_2CO_3) reaction condition. Due to the presence of electron withdrawing formyl groups at 2nd, 3rd and 4th position of the pyridine core of nitrogen atom got reduced and hence slow formation of the pyridinium salt resulted in the decomposition of starting materials in presence of K_2CO_3 (Figure 5.15, **71-73**). In the case of 2- and 4-amino pyridine derivatives, the substituted amine group act as strong nucleophile rather than pyridine nitrogen and resulted in the decomposition of starting materials (Figure 5.15, **74-75**). However, the 2- and 4-hydroxyl pyridine derivatives have also failed to

produce the spirocyclic product which may be due to the keto-enol tautomerism (Figure 5.15, **76-77**). The screening of various substituted pyridines for 1,5-electrocyclization inferred that 2-/3-picolines and 3-hydroxyl derivatives were suitable substrates along with allyl bromides of oxindoles leading to pyridine core activation.

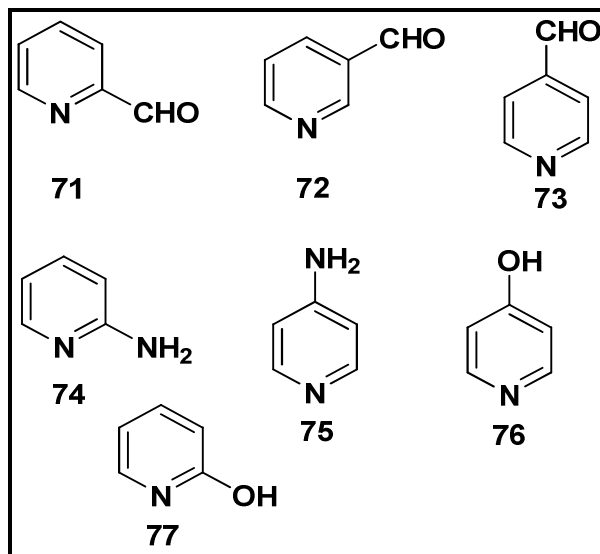
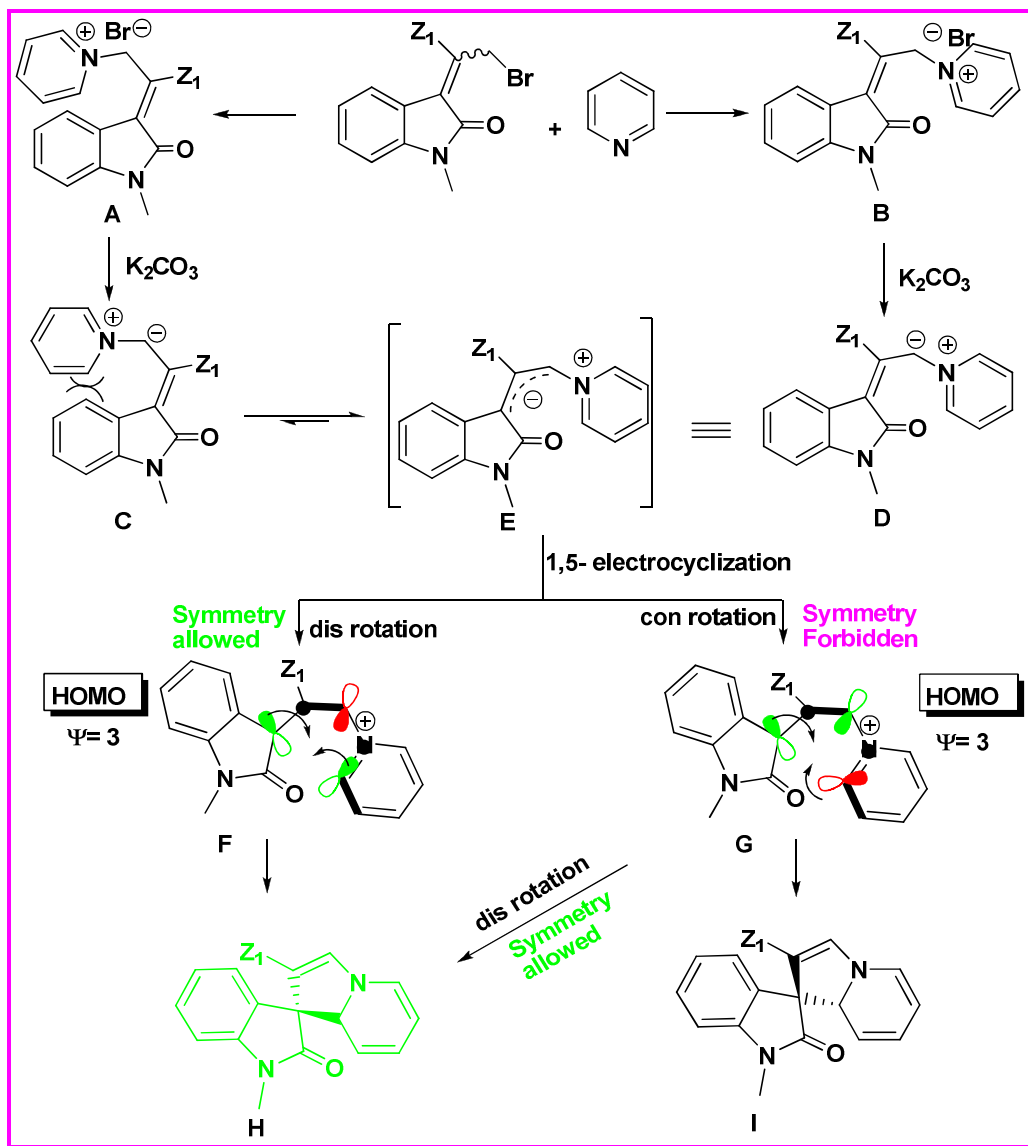


Figure 5.15: Failed substrate of substituted pyridine derivatives in 1,5-electrocyclization.

5.6 Reaction mechanism of pyridine core activation via 1,5-electrocyclization:

The reaction of pyridine core activation *via* 1,5-electrocyclization can be rationalized by invoking a mechanistic postulate (Scheme 5.11). In an initial event, mixture of pyridinium allylide **A** and **B** were formed from the *E/Z*-mixtures of allyl bromide of oxindole with pyridine. These pyridinium allylides upon deprotonated by K_2CO_3 and generated vinyl pyridinium ylide intermediates **C** and **D**. Due to the steric interaction between the pyridine core and the aryl part of oxindole, a resonance stabilized common intermediate **E** was formed. The formation of common intermediate **E** from a mixture of starting material was a key step which resulted in to the formation of single diastereomeric product **H**. According to the *Woodward-Hoffmann* rule, Ψ_3 is HOMO under thermal condition and the either mode of ring closing or ring opening reaction progressed *via* dis-rotation. The observed stereochemistry of all the synthesized compound stereocenter at C3 position to met the prediction of the *Woodward-Hoffmann*

rule of 1,5-electrocyclization which also an important factor for the natural product core structure synthesis such as secoyohimbane and heteroyohimbane (Scheme 5.11).



Scheme 5.11: Mechanistic postulates of pyridine core activation in allyl bromide of oxindole derivatives.

5.7 Conclusions:

- ❖ We have demonstrated an efficient synthesis of 3-spirodihydroindolizine-2-oxindoles and benz-fused 3-spirodihydroindolizine-2-oxindole derivatives from *E*- and *Z*-mixture of allyl bromide of oxindole by a metal free pyridine activation strategy.
- ❖ The scope and generality of 1,5-electrocyclization reaction with various MBH derivatives and pyridine derivatives were studied.
- ❖ The stereochemistry of the synthesized compound was assigned based on single crystal X-ray analysis and found to coincide with natural product analogues such as secoyohimbane and heteroyohimbane compounds.
- ❖ The mixture of *E*- and *Z*-allyl bromide of oxindole provided single diastereomer of spirodihydroindolizines and the observed diastereoselectivity was accounted by mechanistic postulates.
- ❖ All the new compounds were completely characterized by spectroscopic methods.

5.8 Experimental section:

5.8.1 General remarks:

All the reactions were carried out in oven-dried glassware. Progress of reactions was monitored by Thin Layer Chromatography (TLC) while purification of crude compounds was done by column chromatography using silica gel (100-200 mesh). Melting points were recorded on a Buchi melting point apparatus and are uncorrected. NMR spectra were recorded at 500 and 300 MHz (based on availability of instruments) 125 and 75 MHz (for ^{13}C) respectively on Bruker Avance DPX-500 MHz. and Bruker Avance DPX-300 MHz. Chemical shifts are reported in δ (ppm) relative to TMS (^1H) or CDCl_3 (^{13}C) as internal standards. Mass spectra were recorded using JEOL JMS 600H mass spectrometer. IR spectra were recorded on Bomem MB series FT-IR spectrometer, absorbencies are reported in cm^{-1} . Yields refer to quantities obtained after chromatography.

5.8.2 General experimental procedure for the preparation of Morita-Baylis-Hillman adducts of isatin:

The detailed experimental procedure for synthesis of MBH adduct of isatin was given in the experimental section of Chapter II at 2.9.2 and 2.9.3.

5.8.3 General experimental procedure for the preparation of bromo isomerized Morita-Baylis-Hillman adducts of isatin:

A mixture of MBH adduct of isatin derivatives (100 mg) was added with of 46% HBr (4 equiv.) and silica gel (200 mg) and made as slurry. The slurry was subjected to microwave irradiation (750 W) over a period of 5-15 min. The mixture was cooled to room temperature and then extracted with CH_2Cl_2 and the organic phase was washed with water. The organic layer was separated and dried over Na_2SO_4 and concentrated in *vacuo*. The crude mixture was purified by silica gel column chromatography using a gradient elution with hexane and EtOAc as eluent to afford pure isomerized bromo

derivatives 30-65% combined yield. The detailed spectral data are given in the experimental section of Chapter IV at 4.9.2.

5.8.4 General experimental procedure for 1, 5-electrocyclization:

To a refluxing solution of isomerized Morita-Baylis-Hillman derivatives (1 mmol) in acetonitrile (1 mL), was added pyridine (1 equiv.) derivative and kept stirring for 2 hours. After that, 1 equiv. of potassium carbonate was added and continued stirring. After completion of the reaction (monitored by TLC), the reaction mixture was subject to acid work-up and passed through a pad of celite and purified through column by neutral alumina column chromatography using EtOAc: Hexane (10: 90) as eluent to afford good to excellent yields (66-92 %).

5.8.5 Characterization of new compounds:

Yellow crystalline solid, mp: 118-120 °C;

R_f: 0.31 (15% EtOAc-Hexane);

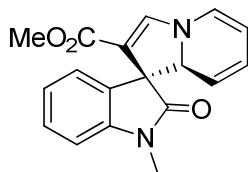
IR (KBr) ν_{\max} : 3025, 2921, 1721, 1703, 1623, 1536, 1306, 1216, 1115, 894, 792 cm^{-1} ;

¹H NMR(CDCl₃/TMS, 500.1 MHz): δ 3.31 (s, 3H), 3.50 (s, 3H), 4.68 (d, $J = 10.0$ Hz, 1 H), 5.17 (dd, $J = 6.0, 12.5$ Hz, 1H), 5.35 (t, $J = 2$ Hz, 1H), 5.81 (s, 1H), 6.46 (t, 7.0 Hz, 1H), 6.88 (d, $J = 7.8$ Hz, 1H), 6.98 (t, $J = 8.0$ Hz, 1H), 7.16 (d, $J = 7.5$ Hz, 1H), 7.29 (t, $J = 7.5$ Hz, 1H), 7.40 (s, 1H);

¹³C NMR (CDCl₃/TMS, 125.7 MHz): δ 26.92, 51.16, 61.83, 67.72, 108.19, 108.97, 116.47, 122.30, 124.01, 124.33, 125.28, 126.23, 126.77, 128.99, 143.29, 144.88, 164.31, 178.41;

FAB mass: Calcd. for C₁₈H₁₆N₂O₃ $m/z = 308.12$;
Found: 308.22 (M⁺);

Elemental Analysis: C₁₈H₁₆N₂O₃ Calcd. for C, 70.12%; H, 5.23%; N, 9.09 %; Found: C, 70.10; H,



Compound 42

5.21; N, 8.89.

Yellow crystalline solid, mp: 132-134 °C;

R_f: 0.29 (15% EtOAc-Hexane);

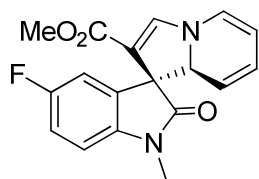
IR (KBr) ν_{\max} : 3104, 2851, 1718, 1701, 1621, 1519, 1321, 1245, 1210, 1121, 798 cm^{-1} ;

¹H NMR (CDCl₃/TMS, 500.1 MHz): δ 3.30 (s, 3H), 3.52 (s, 3H), 4.70 (d, $J = 10.0$ Hz, 1H), 5.18 (dd, $J = 6.5, 13.0$ Hz, 1H), 5.33 (s, 1H), 5.86 (m, 1H), 6.45 (d, $J = 7$ Hz, 1H), 6.77 (m, 1H), 6.90 (m, 1H), 6.95 (m, 1H), 7.37 (s, 1H);

¹³C NMR (CDCl₃/TMS, 125.7 MHz): δ 27.02, 51.0, 62.03, 67.55, 104.10, 108.47, 108.82, 112.40, 112.60, 115.16, 115.35, 116.07, 124.34, 126.19, 139.32, 144.75, 163.93, 177.89;

FAB mass: Calcd. for C₁₈H₁₅FN₂O₃ $m/z = 326.11$;
Found: 327.31 (M+1);

Elemental Analysis: C₁₈H₁₅FN₂O₃ Calcd. for : C, 66.25; H, 4.63; N, 8.58; Found: C, 66.20; H, 4.55; N, 8.42.



Compound 51

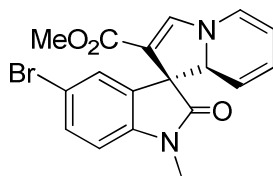
Yellow crystalline solid, mp: 138-140 °C;

R_f: 0.28 (15% EtOAc-Hexane);

IR (KBr) ν_{\max} : 3024, 2918, 2849, 1722, 1704, 1628, 1579, 1217, 1120, 1054, 882, 796 cm^{-1} ;

¹H NMR (CDCl₃/TMS, 500.1 MHz): δ 3.33 (s, 3H), 3.55 (s, 3H), 5.22 (dd, $J = 6.0, 7.0$ Hz, 1H), 5.36 (s, 1H), 5.89 (m, 1H), 6.48 (d, $J = 7.0$ Hz, 1H), 6.80 (m, 1H), 6.84 (m, 1H), 6.92 (d, $J = 2.5$ Hz, 1H), 6.96 (m, 1H), 7.57 (s, 1H);

¹³C NMR (CDCl₃/TMS, 125.7 MHz): δ 27.08, 51.06,



Compound 52

62.09, 67.61, 104.16, 108.54, 108.88, 112.47, 112.66, 115.23, 115.41, 116.14, 124.40, 126.25, 139.39, 144.82, 163.99, 177.95;

FAB mass: Calcd. for $C_{18}H_{15}BrN_2O_3$ $m/z = 386.03$;
Found: 388.78 (M+2);

Elemental Analysis: $C_{18}H_{15}BrN_2O_3$ Calcd. for: C, 55.83; H, 3.90; N, 7.23; Found: C, 55.31; H, 3.76; N, 6.96.

Yellow crystalline solid, mp: 120-122 °C;

R_f: 0.32 (15% EtOAc-Hexane);

IR (KBr) ν_{max} : 3014, 2981, 1726, 1702, 1624, 1222, 1128, 879, 792 cm^{-1} ;

¹H NMR ($CDCl_3/TMS$, 500.1 MHz): δ 2.28 (s, 3H), 3.28 (s, 3H), 3.51 (s, 3H), 4.69 (d, $J = 9.0$ Hz, 1H), 5.18 (dd, $J = 6.5, 12.5$ Hz, 1H), 5.33 (s, 1H), 5.81 (m, 1H), 6.46 (t, $J = 7.0$ Hz, 1H), 6.75 (d, $J = 8$ Hz, 1H), 6.96 (s, 1H), 7.07 (d, $J = 8$ Hz, 1H), 7.39 (s, 1H);

¹³C NMR ($CDCl_3/TMS$, 125.7 MHz): δ 21.11, 26.95, 51.01, 61.84, 67.70, 104.20, 107.85, 116.59, 123.96, 124.74, 125.24, 125.74, 126.22, 129.31, 131.72, 140.97, 142.77, 164.34, 178.33;

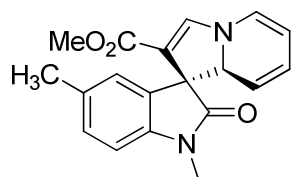
FAB mass: Calcd. for $C_{19}H_{18}N_2O_3$ $m/z = 322.13$;
Found: 323.64 (M+1);

Elemental Analysis: $C_{19}H_{18}N_2O_3$ Calcd. for C, 70.79%; H, 5.63%; N, 8.69%; Found: C, 70.75; H, 5.65; N, 8.65.

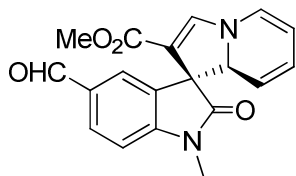
Yellow crystalline solid, mp: 126-128 °C;

R_f: 0.32 (15% EtOAc-Hexane);

IR (KBr) ν_{max} : 3046, 2953, 2850, 2750, 1718, 1701,



Compound 53



Compound 54

1642, 1475, 1375, 1243, 1142, 938, 786 cm^{-1} ;

$^1\text{H NMR}$ (CDCl_3/TMS , 500.1 MHz): δ 3.37 (s, 3H), 3.52 (s, 3H), 4.68 (d, $J = 9.5$ Hz, 1 H), 5.23 (dd, $J = 6.0, 13.0$ Hz, 1 H), 5.35 (s, 1 H), 5.86 (m, 1H), 6.49 (t, $J = 7.5$ Hz, 1H), 7.02 (d, $J = 8$ Hz, 1H), 7.43 (s, 1 H), 7.70 (s, 1H), 7.84 (d, $J = 8.0$ Hz, 1H), 7.87 (s, 1H);

$^{13}\text{C NMR}$ (CDCl_3/TMS , 125.7 MHz): δ 27.24, 51.13, 61.43, 67.60, 104.39, 108.23, 108.93, 113.66, 115.71, 124.43, 124.73, 126.30, 131.52, 133.96, 145.16, 148.89, 164.20, 178.88, 191.15;

FAB mass: Calcd. for $\text{C}_{19}\text{H}_{16}\text{N}_2\text{O}_4$ $m/z = 336.11$;
Found: 336.67 (M^+);

Elemental Analysis: $\text{C}_{19}\text{H}_{16}\text{N}_2\text{O}_4$ Calcd. for C, 67.85%; H, 4.79%; N, 8.33%. Found: C, 65.35; H, 3.76; N, 8.11.

Yellow crystalline solid, mp: 116-118 $^\circ\text{C}$;

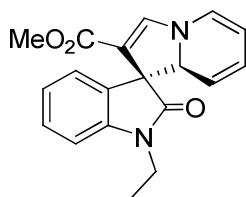
R_f : 0.32 (15% EtOAc-Hexane);

IR (KBr) ν_{max} : 3022, 2988, 1714, 1702, 1616, 1564, 1214, 1135, 879, 789 cm^{-1} ;

$^1\text{H NMR}$ (CDCl_3/TMS , 500.1 MHz): δ 1.45 (m, 3H), 3.98 (s, 3H), 4.35 (d, $J = 8.5$ Hz, 2H), 4.77 (m, 1H), 5.69 (m, 1H), 5.76 (m, 1H), 5.86 (m, 1H) 6.96 (m, 1H), 7.52 (d, $J = 7.5$ Hz, 1H), 7.56 (m, 1H), 7.69 (m, 1H), 7.81 (m, 1H), 7.92 (s, 1H);

$^{13}\text{C NMR}$ (CDCl_3/TMS , 125.7 MHz): δ 11.86, 29.96, 44.98, 51.14, 68.01, 103.98, 109.07, 109.31, 116.49, 122.77, 124.18, 124.55, 124.98, 125.26, 126.26, 129.04, 145.11, 164.41, 177.72;

FAB mass: Calcd. for $\text{C}_{19}\text{H}_{18}\text{N}_2\text{O}_3$ $m/z = 322.13$;
Found: 323.64 ($\text{M}+1$);



Compound 55

Elemental Analysis: Calcd. for C₁₉H₁₈N₂O₃: C, 70.79%; H, 5.63%; N, 8.69%; Found: C, 70.77; H, 5.65; N, 8.17.

Yellow crystalline solid, mp: 129-131 °C;

R_f: 0.29 (15% EtOAc-Hexane);

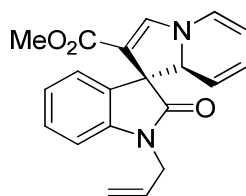
IR (KBr) ν_{\max} : 3268, 3017, 2924, 2136, 1723, 1703, 1677, 1612, 1467, 1108, 987, 751 cm⁻¹;

¹H NMR (CDCl₃/TMS, 500.1 MHz): δ 3.50 (s, 3H), 4.38 (m, 1H), 4.49 (m, 1H), 4.68 (d, *J* = 9.5 Hz, 1H), 5.18 (t, *J* = 7.0 Hz 1H), 5.28 (d, *J* = 10.5 Hz, 1H), 5.36 (s, 1H), 5.85 (m, 2H), 6.46 (d, *J* = 7.5 Hz, 1H), 6.85 (d, *J* = 8.0 Hz, 1H), 6.97 (t, *J* = 8.0 Hz, 1H), 7.17 (d, *J* = 8.0 Hz, 1H), 7.25 (m, 1H), 7.42 (s, 1H);

¹³C NMR (CDCl₃/TMS, 125.7 MHz): δ 42.91, 50.98, 61.85, 68.05, 103.83, 108.94, 109.18, 116.34, 117.46, 122.25, 124.08, 124.39, 125.27, 126.23, 128.84, 131.39, 142.35, 145.07, 164.31, 178.17;

FAB mass: Calcd. for C₂₀H₁₈N₂O₃: 334.13; Found: 335.78 (M+1);

Elemental Analysis: Calcd. for C₂₀H₁₈N₂O₃: C, 71.84; H, 5.43; N, 8.38; Found: C, 70.26; H, 5.45; N, 7.86.



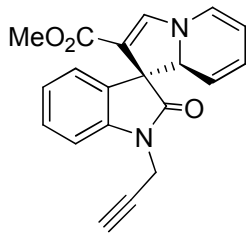
Compound 56

Yellow crystalline solid, mp: 135-137 °C;

R_f: 0.27 (15% EtOAc-Hexane);

IR (KBr) ν_{\max} : 3310, 2984, 2250, 1722, 1701, 1628, 1497, 1357, 1256, 1195, 1047, 915, 826, 787 cm⁻¹;

¹H NMR (CDCl₃/TMS, 500.1 MHz): δ 2.26 (s, 1H), 3.48 (s, 3H), 4.57 (d, *J* = 2.5 Hz, 1H), 4.63 (d, *J* = 2 Hz, 1H), 4.70 (d, *J* = 8.5 Hz, 1H), 5.17 (m, 1H), 5.36 (s, 1H), 5.82 (m, 1H), 6.46 (d, *J* = 7.5 Hz, 1H), 7.03 (t,



Compound 57

$J = 7.5$ Hz, 1H), 7.09 (d, $J = 8.0$ Hz, 1H) 7.19 (d, $J = 7.5$ Hz, 1H), 7.31(t, $J = 8.0$ Hz, 1H), 7.42 (s, 1H);

^{13}C NMR (CDCl₃/TMS, 125.7 MHz): δ 29.84, 51.07, 61.80, 63.04, 67.94, 72.20, 103.92, 109.0, 109.24, 116.43, 122.70, 124.11, 124.49, 125.19, 126.20, 128.97, 141.29, 145.04, 164.34, 177.65;

FAB mass: Calcd. for C₂₀H₁₆N₂O₃ $m/z = 332.12$;
Found: 333.77 (M+1);

Elemental Analysis: Calcd. for C₂₀H₁₆N₂O₃: C, 72.28;
H, 4.85; N, 8.43; Found: C, 71.66; H, 4.83; N, 7.86.

Yellow crystalline solid, mp: 135-137 °C;

R_f : 0.29 (10% EtOAc-Hexane);

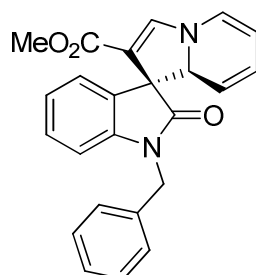
IR (KBr) ν_{max} : 3123, 2984, 1716, 1708, 1616, 1487, 1347, 1265, 1022, 915, 818, 794 cm⁻¹;

^1H NMR (CDCl₃/TMS, 500.1 MHz): δ 3.50 (s, 3H), 4.70 (d, $J = 10$ Hz, 1H), 4.94 (d, $J = 16.0$ Hz, 1H), 5.10 (d, $J = 15.5$ Hz, 1H), 5.18 (m, 1H), 5.44 (s, 1H), 5.85 (m, 1H), 6.49 (d, $J = 6.5$ Hz, 1H), 6.79 (d, $J = 7.5$ Hz, 1H), 6.95 (d, $J = 7.5$ Hz, 1H), 7.16 (m, 2H), 7.35 (m, 5H), 7.39 (s, 1H);

^{13}C NMR (CDCl₃/TMS, 125.7 MHz): δ 44.47, 50.99, 61.98, 68.40, 103.79, 109.12, 109.30, 116.40, 122.35, 124.15, 124.45, 125.31, 126.28, 127.34, 127.58 (2C), 128.79, 128.89 (2C), 135.91, 142.35, 145.09, 164.20, 178.45;

FAB mass: Calcd. for C₂₄H₂₀N₄O₃ $m/z = 384.15$;
Found: 385.23 (M+1);

Elemental Analysis: Calcd. for C₂₄H₂₀N₄O₃: C, 74.98%;
H, 5.24%; N, 7.29%; Found: C, 71.96; H,



Compound 58

5.22; N, 7.27.

Yellow crystalline solid, mp: 136-138 °C;

R_f : 0.29 (15% EtOAc-Hexane);

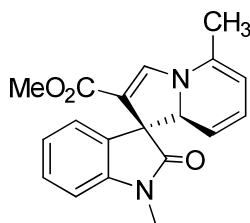
IR (KBr) ν_{\max} : 3112, 2976, 1723, 1706, 1621, 1467, 1343, 1243, 916, 816, 795 cm^{-1} ;

¹H NMR (CDCl_3/TMS , 500.1 MHz): δ 2.06 (s, 3H), 3.32 (s, 3H), 3.52 (s, 3H), 4.67 (d, $J = 9.5$ Hz, 1H), 5.03 (d, $J = 5.5$ Hz, 1H), 5.32 (s, 1H), 5.78 (m, 1H), 6.89 (d, $J = 7.5$ Hz, 1H), 6.95 (t, $J = 7.5$ Hz, 1H), 7.17 (t, $J = 7.5$ Hz, 1H), 7.29 (m, 1H), 7.60 (s, 1H);

¹³C NMR (CDCl_3/TMS , 125.7 MHz): δ 17.82, 26.92, 50.98, 61.58, 68.92, 103.00, 108.18, 108.72, 115.39, 122.26, 124.33, 124.48, 125.43, 128.90, 134.19, 142.59, 143.26, 166.19, 178.60;

FAB mass: Calcd. for $\text{C}_{19}\text{H}_{18}\text{N}_2\text{O}_3$ $m/z = 322.13$;
Found: 323.53 (M+1);

Elemental Analysis: Calcd. for $\text{C}_{19}\text{H}_{18}\text{N}_2\text{O}_3$: C, 70.79%; H, 5.63%; N, 8.69%; Found: C, 70.01; H, 5.23; N, 7.31.



Compound 65

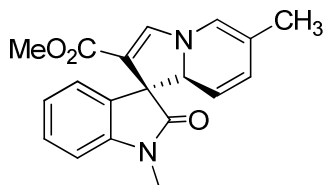
Yellow crystalline solid, mp: 138-140 °C;

R_f : 0.26 (15% EtOAc-Hexane);

IR (KBr) ν_{\max} : 3114, 2979, 1724, 1702, 1630, 1468, 1342, 1242, 914, 813, 791 cm^{-1} ;

¹H NMR (CDCl_3/TMS , 500.1 MHz): δ 0.90 (s, 3H), 3.25 (s, 3H), 3.43 (s, 3H), 5.03 (m, 1H), 5.36 (s, 1H), 5.47 (m, 1H), 6.29 (d, $J = 6.5$ Hz, 1H), 6.75 (m, 1H), 6.91 (m, 1H), 7.10 (m, 1H), 7.19 (m, 1H), 7.21 (s, 1H);

¹³C NMR (CDCl_3/TMS , 125.7 MHz): δ 17.57, 29.90, 50.96, 61.93, 71.35, 103.65, 108.16, 108.62, 120.66,



Compound 66

122.52, 123.37, 124.34, 126.74, 129.10, 133.97,
139.99, 144.49, 166.93, 177.02;

FAB mass: Calcd. for C₁₉H₁₈N₂O₃ m/z = 322.13;
Found: 323.19 (M+1);

Elemental Analysis: Calcd. for C₁₉H₁₈N₂O₃: C, 70.79;
H, 5.63; N, 8.69; Found: C, 69.21; H, 5.31; N, 8.41.

White crystalline solid, mp: 168-170 °C;

R_f : 0.24 (20% EtOAc-Hexane);

IR (KBr) ν_{\max} : 3467, 3123, 2985, 1716, 1704, 1616,
1485, 1346, 1263, 1021, 919, 811, 791 cm⁻¹;

¹H NMR (CDCl₃/TMS, 500.1 MHz): δ 3.75 (s, 3H),
3.93 (s, 3H), 5.51 (d, J = 6.0 Hz, 1H), 5.96 (s, 1H),
5.97 (d, J = 1 Hz, 1H), 6.79 (d, J = 7 Hz, 1H), 7.29
(m, 2H), 7.55 (m, 2H), 7.74 (s, 1H), 10.28 (b, 1H);

¹³C NMR (CDCl₃/TMS, 125.7 MHz): δ 27.14, 51.47,
62.09, 67.25, 104.16, 108.54, 108.88, 112.47, 112.66,
115.23, 115.41, 116.14, 124.25, 126.40, 139.39,
152.82, 164.99, 177.95;

FAB mass: Calcd. for C₁₈H₁₆N₂O₄ m/z = 324.11;

Found 325.16 (M+1);

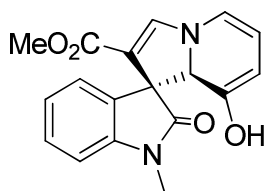
Elemental Analysis: Calcd. for C₁₈H₁₆N₂O₄: C, 66.66;
H, 4.97; N, 8.64; Found: C, 66.64; H, 4.95; N, 8.63.

Yellow crystalline solid, mp: 176-178 °C;

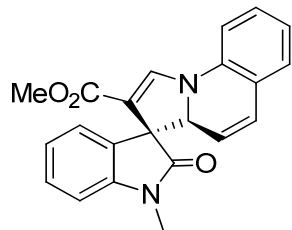
R_f : 0.24 (10% EtOAc-Hexane);

IR (KBr) ν_{\max} : 3269, 2923, 1722, 1712, 1676, 1612,
1467, 1102, 989, 751 cm⁻¹;

¹H NMR (CDCl₃/TMS, 500.1 MHz): δ 3.33 (s, 3H),
3.53 (s, 3H), 5.09 (d, J = 10 Hz, 1H), 5.50 (s, 1H), 6.30
(d, J = 10.0 Hz, 1H), 6.94 (m, 5H), 7.21 (m, 3H), 7.91



Compound 67



Compound 68

(s, 1H);

^{13}C NMR (CDCl_3/TMS , 125.7 MHz): δ 26.90, 50.96, 61.03, 68.08, 108.06, 109.39, 113.31, 119.15, 122.04, 122.22, 122.43, 123.06, 124.60, 126.43, 128.03, 129.03, 129.31, 135.99, 142.80, 143.29, 164.08, 177.90;

FAB mass: Calcd. for $\text{C}_{22}\text{H}_{18}\text{N}_2\text{O}_3$ m/z = 358.13; Found: 359.40 (M+1);

Elemental Analysis: Calcd. for $\text{C}_{22}\text{H}_{18}\text{N}_2\text{O}_3$: C, 73.73; H, 5.06; N, 7.82; Found: C, 72.13; H, 5.01; N, 6.94.

Yellow crystalline solid, mp: 178-180 °C;

R_f : 0.26 (10% EtOAc-Hexane);

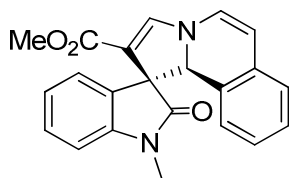
IR (KBr) ν_{max} : 3096, 3023, 2967, 1723, 1710, 1665, 1632, 1451, 1121, 991, 781 cm^{-1} ;

^1H NMR (CDCl_3/TMS , 500.1 MHz): δ 3.37 (s, 3H), 3.44 (s, 3H), 5.64 (d, J = 7.5 Hz, 1H), 5.81 (s, 1H), 5.93 (d, J = 7.5 Hz, 1.0 H), 6.52 (d, J = 7.5 Hz, 1.0 H), 6.66 (t, J = 7.2, Hz, 1 H), 6.77 (d, J = 7.8, Hz, 1 H), 6.91 (m, 3H), 7.15 (m, 3H);

^{13}C NMR (CDCl_3/TMS , 125.7 MHz): δ 27.13, 51.04, 61.11, 68.62, 106.88, 108.18, 109.59, 122.85, 124.42, 124.62, 125.14, 125.92, 126.36, 126.88, 127.06, 127.70, 128.98, 131.83, 143.06, 143.68, 164.30, 178.38;

FAB mass: Calcd. for $\text{C}_{22}\text{H}_{18}\text{N}_2\text{O}_3$ m/z = 358.13; Found: 359.56 (M+1);

Elemental Analysis: Calcd. for $\text{C}_{22}\text{H}_{18}\text{N}_2\text{O}_3$: C,



Compound 69

73.73%; H, 5.06%; N, 7.82%; Found: C, 73.71; H, 5.03; N, 7.81;

White crystalline solid, mp: 198-200 °C;

R_f: 0.27 (15% EtOAc-Hexane);

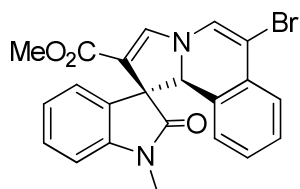
IR (KBr) ν_{\max} : 3098, 2936, 2841, 1719, 1702, 1632, 1056 cm^{-1} ;

¹H NMR (CDCl_3/TMS , 500.1 MHz): δ 3.44 (s, 3H), 3.54 (s, 3H), 5.93 (s, 1H), 5.98 (s, 1H), 6.78 (m, 6H); 7.13 (dd, $J = 8.0, 8.0$ Hz, 1 H), 7.18 (m, 1H), 7.32 (m, 1H);

¹³C NMR (CDCl_3/TMS , 125.7 MHz): δ 27.17, 51.18, 61.14, 68.42, 101.14, 102.94, 108.31, 110.73, 122.95, 124.46, 125.19, 126.35, 127.02, 127.13, 127.51, 128.07, 129.20, 130.59, 142.46, 143.09, 163.80, 177.81;

FAB mass: Calcd. for $\text{C}_{22}\text{H}_{17}\text{BrN}_2\text{O}_3$ $m/z = 436.04$; Found: 438.14 (M+2);

Elemental Analysis: Calcd. for $\text{C}_{22}\text{H}_{17}\text{BrN}_2\text{O}_3$: C, 60.43; H, 3.92; N, 6.41; Found: C, 60.41; H, 3.89; N, 6.24.



Compound 70

Bibliography and References:

- Aggarwal, V. K.; Fulford, S. Y.; Lloyd-Jones, G. C. "Reevaluation of the mechanism of the Baylis-Hillman reaction: Implications for asymmetric catalysis" *Angew. Chem., Int. Ed.* **2005**, *44*, 1706.
- Aizpurua, J. M.; Juaristi, M.; Lecea, B.; Palomo, C. "Reagents and synthetic methods-40. Halosilanes/chromium trioxide as efficient oxidizing reagents" *Tetrahedron.* **1985**, *41*, 2903.
- Appel, R.; Hartmann, N.; Mayr, H. "Scope and limitations of cyclopropanations with sulfur ylides" *J. Am. Chem. Soc.* **2010**, *132*, 17894.
- Ates, A.; Gautier, A.; Leroy, B.; Plancher, J. -M.; Quesnel, Y.; Marko', I. E. "Remarkably efficient deprotection of cyclic acetals and ketals" *Tetrahedron Lett.* **1999**, *40*, 1799.
- Attanasi, O. A.; Davoli, P.; Favi, G.; Filippone, P.; Forni, A.; Moscatelli, G.; Prati, F. "Azavinyl azomethine ylides from thermal ring opening of α -aziridinohydrazones: unprecedented 1,5-electrocyclization to imidazoles" *Org. Lett.* **2007**, *9*, 3461.
- Attanasi, O. A.; Caselli, E.; Davoli, P.; Favi, G.; Mantellini, F.; Ori, C.; Prati, F. " α -Aminoester-derived imidazoles by 1,5-electrocyclization of azavinyl azomethine ylides" *Org. Lett.* **2009**, *11*, 2840.
- Bacon, R. G. R.; Doggart, J. R. "Oxidation by persulphate. Part II. Oxidation effects with a methyl group and some substituted methyl groups on a benzene nucleus" *J. Chem. Soc.* **1960**, 1332.

- Barluenga, J.; Lonzi, G.; Riesgo, L.; Lo'pez, L. A.; Toma's, d. M. "Pyridine activation via copper(I)-catalyzed annulation toward indolizines" *J. Am. Chem. Soc.* **2010**, *132*, 13200.
- Barton, D. H. R.; Hui, R. A. H. F.; Lester, D. J.; Ley, S. V. "Preparation of aldehydes and ketones by oxidation of benzylic hydrocarbons with benzeneseleninic anhydride" *Tetrahedron Lett.* **1979**, *20*, 3331.
- Basavaiah, D.; Kumaragurubaran, N.; Sharada, D. S. "Baylis-Hillman chemistry: A novel synthesis of functionalized 1,4-pentadienes" *Tetrahedron Lett.* **2001**, *42*, 85.
- Basavaiah, D.; Sharada, D. S.; Kumaragurubaran, N.; Reddy, R. M. "The Baylis-Hillman reaction: One-pot facile synthesis of 2,4-functionalized 1,4-pentadienes" *J. Org. Chem.* **2002**, *67*, 7135.
- Basavaiah, D.; Rao, A. J.; Satyanarayana, T. "Recent advances in the Baylis-Hillman reaction and applications" *Chem. Rev.* **2003**, *103*, 811.
- Basavaiah, D.; Rao, K. V.; Reddy, R. J. "The Baylis-Hillman reaction: A novel source of attraction, opportunities, and challenges in synthetic chemistry" *Chem. Soc. Rev.* **2007**, *36*, 1581.
- Basavaiah, D.; Roy, S. "Dimethyl sulfide induced [3 + 2] annulation strategy: An efficient synthesis of functionalized dihydropyrazole derivatives using the Baylis-Hillman bromides" *Org. Lett.*, **2008**, *10*, 1819.
- Basavaiah, D.; Dandamudi, B. D.; Lenin, V. Satyanarayana, T. "The Baylis-Hillman bromides as versatile synthons: A facile one-pot synthesis of indolizine and benzofused indolizine frameworks" *Synlett.* **2009**, 411.

- Basavaiah, D.; Reddy, B. S.; Badsara, S. S. "Recent contributions from the Baylis-Hillman reaction to organic chemistry" *Chem. Rev.* **2010**, *110*, 5447.
- Basset, J-M.; Coperet, C.; Soulivong, D.; Taoufik, M.; Cazat, J. T. "Metathesis of alkanes and related reactions" *Acc. Chem. Res.*, **2010**, *43*, 323.
- Baylis, A. B.; Hillman, M. E. D. German Patent 2155113, *Chem. Abstr.* **1972**, *77*, 34174q.
- Bennasar, M.-L.; Zulaica, E.; Alonso, Y.; Bosch, J. "Nucleophilic addition to chiral pyridinium salts: Stereoselective synthesis of (-)-*N*_α-methylervitsine" *Tetrahedron: Asymmetry* **2003**, *14*, 469.
- Binder, J. T.; Kirsch, S. F. "Synthesis of highly substituted pyrroles *via* a multimetal-catalyzed rearrangement-condensation-cyclization domino approach" *Org. Lett.*, **2006**, *8*, 2151.
- Bonney, K. J.; Braddock, D. C.; White, A. J. P.; Yaqoob, M. "Intramolecular bromonium ion assisted epoxide ring-opening: Capture of the oxonium ion with an added external nucleophile" *Org. Chem.*, **2011**, *76*, 97.
- Bruhne, F.; Wright, E. Industrial organic chemicals: Starting materials and intermediates – an ullmann's encyclopedia, vol. 2, Wiley-VCH, Weinheim, **1999**, pp. 673–692.
- Byers, J. A.; Jamison, T. F. "On the synergism between H₂O and a tetrahydropyran template in the regioselective cyclization of an epoxy alcohol" *J. Am. Chem. Soc.* **2009**, *131*, 6383.
- Cao, H.; Vieira, T. O.; Alper, H. "Synthesis of unsaturated seven-membered ring lactams through palladium-catalyzed amination and intramolecular

- cyclocarbonylation reactions of amines and Baylis-Hillman acetates” *Org. Lett.*, **2011**, *13*, 11.
- ^aCarroll, M. F. “Addition of α , β -unsaturated alcohols to the active methylene group. Part I. The action of ethyl acetoacetate on linalool and geraniol” *J. Chem. Soc.* **1940**, 704.
- ^bCarroll, M. F. “Addition of β,γ -unsaturated alcohols to the active methylene group. Part II. The action of ethyl acetoacetate on cinnamyl alcohol and phenylvinylcarbinol” *J. Chem. Soc.* **1940**, 1266.
- Charette, A. B.; Grenon, M.; Lemire, A.; Pourashraf, M.; Martel, J. “Practical and highly regio- and stereoselective synthesis of 2-substituted dihydropyridines and piperidines: Application to the synthesis of (–)-Coniine” *J. Am. Chem. Soc.* **2001**, *123*, 11829.
- Charette, A. B.; Mathieu, S.; Martel, J. “Electrophilic activation of lactams with Tf₂O and pyridine: Expedient synthesis of (±)-Tetraonerine T4” *Org. Lett.* **2005**, *7*, 5401.
- Clayden, J.; Hamilton, S. D.; Mohammed, R. T. “Cyclization of lithiated pyridine and quinoline carboxamides: Synthesis of partially saturated pyrrolopyridines and spirocyclic β -lactams” *Org. Lett.* **2005**, *7*, 3673.
- Chen, Z.-H.; Zhang, Y.-Q.; Chen, Z.-M.; Tu, Y.-Q.; Zhang, F.-M. “Total synthesis of (–)-maistemone and (–)-Stemonamide” *Chem. Commun.*, **2011**, *47*, 1836.
- Chernyak, D.; Gadamsetty, S. B.; Gevorgyan, V. “Low temperature organocopper-mediated two-component cross coupling/cycloisomerization approach toward *N*-fused heterocycles” *Org. Lett.* **2008**, *10*, 2307.

- Choi, J.; Imai, E.; Mihara, M.; Oderaotoshi, Y.; Minakata, S.; Komatsu, M. “1,4-Silatropy of *S*-r-silylbenzyl thioesters: A convenient route to silyl enol and dienol ethers accompanied by C-C bond formation *via* thiocarbonyl ylides” *J. Org. Chem.* **2003**, *68*, 6164.
- Cho, C.-W.; Kong, J.-R.; Krische, M. J. “Phosphine-catalyzed regiospecific allylic amination and dynamic kinetic resolution of Morita-Baylis-Hillman acetates” *Org. Lett.*, **2004**, *6*, 1337.
- Chung, Y. M.; Im, Y.J.; Kim, J.N “Baylis-Hillman reaction of isatin derivatives: Isatins as a new entry for the Baylis-Hillman reaction” *Bull. Korean Chem. Soc.* **2002**, *23*, 1651.
- Chuprakov, S.; Malyshev, D.A.; Trofimov, A.; Gevorgyan, V. “Sila Morita-Baylis-Hillman reaction of cyclopropenes” *J. Am. Chem. Soc.* **2007**, *129*, 14868.
- Coldham, I.; Hufton, R.; “Intramolecular dipolar cycloaddition reactions of azomethine ylides” *Chem. Rev.* **2005**, *105*, 2765.
- Comins, D. L.; Zheng, X.; Goehring, R. R. “Total synthesis of the putative structure of the lupin alkaloid plumerinine” *Org. Lett.* **2002**, *4*, 1611.
- Cotelle, P.; Catteau, J.-P. “Selective synthesis of 2,5-dimethoxy-4-nitrobenzaldehyde” *Tetrahedron Lett.* **1992**, *33*, 3855.
- ^aCui, H.-L.; Peng, J.; Feng, X.; Du, W.; Jiang, K.; Chen, Y.-C. “Enantioselective allylic amination of Morita-Baylis-Hillman carbonates catalysed by modified cinchona alkaloids” *Chem.–Eur. J.*, **2009**, *15*, 1574.

- ^bCui, H.-L.; Feng, X.; Peng, J.; Lei, J.; Jiang, K.; Chen, Y.-C. "Chemoselective asymmetric *N*-allylic alkylation of indoles with Morita–Baylis–Hillman carbonates" *Angew. Chem. Int. Ed.* **2009**, *48*, 5737.
- da Silva J. F. M.; Garden, S. J.; Pinto, A.C. "The chemistry of isatins: A review from 1975 to 1999" *J. Braz. Chem. Soc.* **2001**, *12*, 273.
- Declerck, V.; Ribiere, P.; Nedellec, Y.; Allouchi, H.; Martinez, J.; Lamaty, F. "A microwave-assisted heck reaction in poly(ethylene glycol) for the synthesis of benzazepine" *Eur. J. Org. Chem.* **2007**, 201.
- Declerck, V.; Martinez, J.; Lamaty, F. "Aza-Baylis-Hillman reaction" *Chem. Rev.* **2009**, *109*, 1.
- del Villar, I. S.; Gradillas, A.; Domínguez, G.; Pe´rez-Castells, J. "Morita-Baylis-Hillman reaction of lactams and lactones with alkyl halides and epoxides catalyzed by hydroxysulfides" *Org. Lett.*, **2010**, *12*, 2418.
- Doering, W. v. E.; Roth, W. R. "The overlap of two allyl radicals or a four-centered transition state in the cope rearrangement" *Tetrahedron* **1962**, *18*, 67.
- Dong, D.-J.; Li, Y.; Wang J.-Q.; Tian, S.-K. "Tunable stereoselective alkene synthesis by treatment of activated imines with nonstabilized phosphonium ylides" *Chem. Commun.*, **2011**, *47*, 2158.
- Dounay, A. B.; Overman, L. E. "The asymmetric intramolecular heck reaction in natural product total synthesis" *Chem. Rev.*, **2003**, *103*, 2945.
- Drewes, S. E.; Roos, G. H. P. "Synthetic potential of the tertiary-amine-catalysed reaction of activated vinyl carbanions with aldehydes" *Tetrahedron*, **1988**, *44*, 4653.

- Drewes, E.; Njamela, O. L.; Emslie, N. D.; Ramesar, N.; Field, J. S. "Intramolecular Baylis-Hillman reaction: A pathway to substituted coumarins" *Synth. Commun.* **1993**, *23*, 2807.
- Du, Y.; Lu, X.; Zhang, C. "A catalytic carbon-phosphorus ylide reaction: Phosphane-catalyzed annulation of allylic compounds with electron-deficient alkenes" *Angew. Chem., Int. Ed.* **2003**, *42*, 1035.
- Du, Y.; Feng, J.; Lu, X. "A phosphine-catalyzed [3+6] annulation reaction of modified allylic compounds and tropone" *Org. Lett.* **2005**, *7*, 1987.
- Edwards, D. R.; Montoya-Peleaz, P.; Crudden, C. M. "Experimental investigation into the mechanism of the epoxidation of aldehydes with sulfur ylides" *Org. Lett.*, **2007**, *9*, 5481
- Fandrick, D. R.; Reeves, J. T.; Tan, Z.; Lee, H.; Song, J. J.; Yee, N. K.; Senanayake, C. H. "Regioselective allene synthesis and propargylations with propargyl diethanolamine boronates" *Org. Lett.*, **2009**, *11*, 5458.
- Firouzabadi, H.; Salehi, P.; Sardarian, A. R.; Seddighi, M. "Oxidation of benzylic hydrocarbons to carbonyl compounds by tetrapyridinesilver(II) peroxydisulfate $\text{Ag(Py)}_4\text{S}_2\text{O}_8$ under non-aqueous and aprotic condition" *Synth. Commun.* **1991**, *21*, 1121.
- Fitjer, L.; Klages, U.; Wehle, D.; Giersig, M.; Schormann, N.; Clegg, W.; Stephensen, D. S.; Binsch, G. "Sterically crowded cyclohexanes - 8. Synthesis, crystal structure, conformation and dynamics of pentaspiro[2.0.2.0.2.0.2.0.2.1]hexadecane, pentaspiro[3.0.2.0.3.0.2.0.3.1]-

- nonadecane and pentaspiro[3.0.3.0.3.0.3.0.3.1] heneicosane” *Tetrahedron.*, **1988**, *46*, 416.
- Fleming, I. “Frontier orbitals and organic chemical reactions”. John Wiley & Sons, Ltd. **1976**.
- Fletton, R. A.; Humber, D. C.; Roberts, S. M.; Wright, J. L. “Reaction of cerium(IV) ammonium nitrate with 3-methylce reaction of cerium(IV) ammonium nitrate with 3-methylcephalosporins: Synthesis of a 2-methoxy-3-methylcephalosporin phalosporins: Synthesis of a 2-methoxy-3-methylcephalosporin” *J. Chem. Soc., Perkin Trans.* **1985**, *1*, 1523.
- Fukuda, T.; Terauchi, T.; Goto, A.; Tsujii, Y.; Miyamoto, T. “Well-defined block copolymers comprising styrene acrylonitrile random copolymer sequences synthesized by “living” radical polymerization” *Macromolecules* **1996**, *29*, 3050.
- Galliford, C.V.; Scheidt, K. A. “Pyrrolidinyl-spirooxindole natural products as inspirations for the development of potential therapeutic agents” *Angew. Chem. Int. Ed.* **2007**, *46*, 8748.
- Garden, S. J.; Skakle, J. M. S. “Isatin derivatives are reactive electrophilic components for the Baylis–Hillman reaction” *Tetrahedron Lett.* **2002**, *43*, 1972.
- Gassman, P. C.; Hodgson, P. K. G.; Balchunis, R. J. “Base-promoted hydrolysis of amides at ambient temperatures” *J. Am. Chem. Soc.* **1976**, *98*, 1275.
- Gibson, V. C.; Redshaw, G. A.; Solan, G. A. “Bis(imino)pyridines: Surprisingly reactive ligands and a gateway to new families of catalysts” *Chem. Rev.* **2007**, *107*, 1745.

- Gilman, H.; Brannen, C. G.; Ingham, R. K. "Some tetraarylsilanes containing functional groups" *J. Am. Chem. Soc.* **1956**, *78*, 1689.
- Ghosh, S.; Dey, R.; Chattopadhyay, K.; C. Ranu B. C. "Water-promoted highly regio- and stereoselective synthesis of α -dehydro- β -amino esters and nitriles from Baylis–Hillman acetates" *Tetrahedron Lett.* **2009**, *50*, 4892.
- Groves, J. T.; Dias, R. M. "Rapid amide hydrolysis mediated by copper and zinc" *J. Am. Chem. Soc.* **1979**, *101*, 1033.
- Gupta, M.; Paul, S.; Gupta, R.; Loupy, A. "Microwave-induced selective synthesis of α -bromo and α,α -dibromoalkanones using dioxane–dibromide and silica gel under solvent-free conditions" *Tetrahedron Lett.* **2003**, *44*, 439.
- Halket, J. M.; Watkins, P. J.; Przyborowska, A.; Goodwin, B. L.; Clow, A.; Glover, V.; Sandler, M. "Isatin (indole-2,3-dione) in urine and tissues. Detection and determination by gas chromatography-mass spectrometry" *J. Chromatogr.* **1991**, *562*, 279.
- Harrison, T. J.; Kozak, J. A.; Corbella-Pane, M.; Dake, G. R. "Pyrrole synthesis catalyzed by AgOTf or cationic Au(I) complexes" *J. Org. Chem.* **2006**, *71*, 4525.
- Haque, A.-M. J.; Kim, K. "Aldehyde-functionalized benzenediazonium cation for multi probe immobilization on microelectrode array surfaces" *Langmuir*, **2011**, *27*, 882.
- Havrylyuk, D.; Mosula, L.; Zimenkovsky, B.; Vasylenko, O.; Gzella, A.; Lesyk, R. "Synthesis and anticancer activity evaluation of 4-thiozolidines containing benzothiazole moiety" *Eur. J. Med. Chem.* **2010**, *11*, 5012.
- Herndon, W. C. "Theory of cycloaddition reactions" *Chem. Rev.*, **1972**, *72*, 157.

- Heathcock, C. K.; Graham, S. L.; Pirrung Palvac, F.; White, C. T. “*Total synthesis of natural products*” Ed. ApSimon, J. Vol. 5, New York: John Wiley, **1983**; pp 264-314.
- Hill, J. S.; Isaacs, N. S. “Functionalization of the α - position of acrylate systems by the addition of carbonyl compounds: Highly pressure-dependent reactions” *Tetrahedron Lett.* **1986**, 27, 5007;
- Hill, J. S.; Isaacs, N. S. “Mechanism of α -substitution reactions of acrylic derivatives” *J. Phys. Org. Chem.* **1990**, 3, 285.
- Hoffmann, R.; Woodward, R. B. “The conservation of orbital symmetry”. *Acc. Chem. Res.*, **1968**, 1, 17.
- Hou, X. L.; Yang, Z.; Wong, H. N. C.; Gribble, G. W.; Gilchrist, T. L.; “*In progress in heterocyclic chemistry*” Eds.; Pergamon: Oxford, **2003**, 15, 167-205.
- Hosseinzadeh, R.; Tajbakhsh, M.; Vahedi, H. “Selective oxidation of methylarenes with pyridinium chlorochromate” *Synlett*, **2005**, 2769.
- Hua, D.; Ge, X.; Tang, J.; Zhu, X.; Bai, R. “Controlled free-radical polymerization of methyl acrylate in the presence of a cyclic trithiocarbonate under γ -ray irradiation at low temperature” *J. E. Polym.* **2007**, 43, 847.
- Hwu, J. R.; King, K. -Y. “Versatile reagent ceric ammonium nitrate in modern chemical synthesis” *Curr. Sci.* **2001**, 81, 1043.
- Imamoto, T.; Koide, Y.; Hiyama, S. “Cerium(IV) trifluoromethanesulfonate as a strong oxidizing agent” *Chem. Lett.* **1990**, 19, 1445.
- Ireland, R. E.; Mueller, R. H. “Claisen rearrangement of allyl esters” *J. Am. Chem. Soc.* **1972**, 94, 5897.

- Ireland, R. E.; Mueller, R. H.; Willard, A. K. "The ester enolate Claisen rearrangement. Stereochemical control through stereoselective enolate formation" *J. Am. Chem. Soc.* **1976**, *98*, 2868
- Ischia, M.; Palumbo, A.; Prota, G. "Adrenalin oxidation revisited. New products beyond the adrenochrome stage" *Tetrahedron* **1988**, *44*, 6441.
- Ito, H.; Taguchi, T. "Asymmetric Claisen rearrangement" *Chem. Soc. Rev.* **1999**, *28*, 43.
- Ji, S.; Wang, S. "Ultrasound-accelerated Michael addition of indole to α,β -unsaturated ketones catalyzed by ceric ammonium nitrate (CAN)" *Synlett* **2003**, 2074.
- Jiang, K.; Peng, J.; Cuia, H.-L.; Chen, Y.-C. "Organocatalytic asymmetric allylic alkylation of oxindoles with Morita–Baylis–Hillman carbonate" *Chem. Commun.*, **2009**, 3955.
- Johnson, W. S.; Werthemann, L.; Bartlett, W. R.; Brockson, T. J.; Li, T.; Faulkner, D. J.; Petersen, M. R. "Simple stereoselective version of the Claisen rearrangement leading to trans-trisubstituted olefinic bonds. Synthesis of squalene" *J. Am. Chem. Soc.* **1970**, *92*, 741.
- Johnson, M. M.; Naidoo, J. M.; Fernandes, M. A.; Mmutlane, E. M.; van Otterlo, W. A. L.; de Koning, C. B. "CAN-Mediated oxidations for the synthesis of xanthenes and related products" *J. Org. Chem.* **2010**, *75*, 8701.
- Joule, J. A.; Mills, K. "*Heterocyclic Chemistry*" 4th ed.; Blackwell: Oxford, U.K., **2000**.
- Joyasawal, S. S.; Lotesta, S. D.; Akhmedov, N. G.; Williams, L. J. "Spirodiepoxide strategy to the C ring of pectenotoxin 4: Synthesis of the C1-C19" *Org. Lett.*, **2010**, *12*, 988.

- Jurkauskas, V.; Buchwald, S. L. "Dynamic kinetic resolution *via* asymmetric conjugate reduction: Enantio and diastereoselective synthesis of 2,4-dialkyl cyclopentanones" *J. Am. Chem. Soc.* **2002**, *124*, 2892,
- Kappe, C. O. "A unified mechanistic view on the Morita-Baylis-Hillman reaction: Computational and experimental investigations" *J. Org. Chem.* **2010**, *75*, 8615.
- Kasprzyk-Hordern, B. "Pharmacologically active compounds in the environment and their chirality" *Chem. Soc. Rev.*, **2010**, *39*, 4466.
- Katritzky, A. R.; Rees, C. W. "*Comprehensive Heterocyclic Chemistry: The Structure, Reactions, Synthesis, and Uses of Heterocyclic Compounds*" Eds.; Pergamon Press: Oxford, U.K., **1984**; Vols. 1-8.
- Keay, B. A.; Dibble, P. W.; Katritzky, A. R.; Rees, C. W.; Scriven, E. F. V.; "In *Comprehensive Heterocyclic Chemistry II*" Eds.; Elsevier: Oxford, **1997**; Vol. 2, 395-436.
- Kelly, T. R.; Ohashi, N. "Synthesis of (\pm)-fredericamycin A" *J. Am. Chem. Soc.* **1986**, *108*, 7100;
- Kim, S. C.; Gowrisankar, S.; Kim, J. N. "Synthesis of 3-aryl-3-hydroxypyrrolidin-2-ones and 2-benzyl-9b-hydroxy-3,3a,5,9b-tetrahydro-2H-pyrrolo-3,4-c]quinoline-1,4-dione derivatives from the Baylis-Hillman adducts of isatins" *Tetrahedron Lett.* **2006**, *47*, 3463.
- Kim, J. M.; Kim, K. H.; Kim, T. H.; Kim, J. N. "The first successful intermolecular Heck reaction of Baylis-Hillman adducts: Synthesis of β -aryl substituted Baylis-Hillman adducts" *Tetrahedron Lett.* **2008**, *49*, 3248.

- Ko, S.; Lin, C.; Tu, Z.; Wang, Y. -F.; Wang, C.-C.; Yao, C.-F. "CAN and iodine-catalyzed reaction of indole or 1-methylindole with α,β -unsaturated ketone or aldehyde" *Tetrahedron Lett.* **2006**, *47*, 487.
- Kokotos, C. G.; Aggarwal, V. K. "Aminals as substrates for sulfur ylides: A synthesis of functionalized aziridines and *N*-heterocycles" *Org. Lett.*, **2007**, *9*, 2099.
- Knowles, R. R.; Carpenter, J.; Blakey, S. B.; Kayano, A.; Mangion, I. K.; Sinz, C. J. ; MacMillan, D. W. C. "Total synthesis of diazonamide" *Chem. Sci.*, **2011**, *2*, 308
- ^aKrafft, M. E.; Haxell, T. F. N. "Organomediated Morita-Baylis-Hillman cyclization reactions" *J. Am. Chem. Soc.* **2005**, *127*, 10168.
- ^bKrafft, M. E.; Seibert, K. A.; Haxell, T. F. N.; Hirosawa, C. "Unprecedented reactivity in the Morita-Baylis-Hillman reaction; intramolecular α -alkylation of enones using saturated alkyl halides" *Chem. Commun.* **2005**, 5772.
- ^aKrafft, M. E.; Haxell, T. F. N.; Seibert, K. A.; Abboud, K. A. "Mechanistic implications in the Morita-Baylis-Hillman alkylation: Isolation and characterization of an intermediate" *J. Am. Chem. Soc.* **2006**, *128*, 4174.
- ^bKrafft, M. E.; Wright, J. A. "New directions for the Morita-Baylis-Hillman reaction; homologous aldol adducts via epoxide opening" *Chem. Commun.*, **2006**, 2977
- Krafft, M. E. ; Campbell, M. J.; Kerrigan, S.; Cran, J. W. "Intermolecular Morita-Baylis-Hillman reactions using dicobalthexacarbonyl complexed acetylenic acetals" *Tetrahedron Lett.* **2011**, *52*, 1090.
- Krapcho, A. P. "Synthesis of carbocyclic spiro compounds **via** cycloaddition routes" *Synthesis* **1978**, 77.

- Lapierre, A. J. B. ; Geib, S. J.; Curran, D. P. “Low-temperature Heck reactions of axially chiral *O*-iodoacrylanilides occur with chirality transfer: Implications for catalytic asymmetric Heck reactions” *J. Am. Chem. Soc.* **2007**, *129*, 494.
- Laundon, B.; Morrison, G. A.; Brooks, J. S. “Naturally occurring compounds related to phenalenone. Part I. The synthesis of lachnanthocarpone” *J. Chem. Soc. C*, **1971**, 36.
- Lee, J. B.; Clarke, T. G. “Silver II complexes as oxidising agents” *Tetrahedron Lett.* **1967**, *8*, 415.
- Lee, J. G.; Ha, D. S. “Oxidation of olefins using chromic anhydride-chlorotrimethylsilane. A convenient synthesis of α -chloro ketones” *Tetrahedron Lett.* **1989**, *30*, 193.
- Li, W.-S.; Liu, L. K. A “Convenient oxidation of benzylic methyl, methylene, and methine groups with potassium permanganate/triethylamine reagent” *Synthesis* **1989**, 293.
- Lingam, K. A. P.; Shanmugam, P.; Selvakumar, K. “Stereoselective synthesis of geometrically strained, oxindole appended vinyl cyclopropanes and highly substituted cyclopentenes *via sulphur ylide* cyclopropanation and vinyl cyclopropane rearrangement” *Synlett.* **2012**, 278.
- Lingam, K. A. P.; Mandal, A. B.; Shanmugam P. “A novel MgI₂ mediated unusual dimerization–spirocyclopropanation of bromo isomerised Morita-Baylis-Hillman adduct of isatin: A facile synthesis of 3-spirocyclopropane-2-oxindole derivatives” *Tetrahedron Lett.* **2011**, *52*, 3610.

- Lipshutz, B. H. "Five-membered hetero-aromatic rings as intermediates in organic synthesis" *Chem. Rev.* **1986**, *86*, 795.
- Liu, Y.-L.; Wang, B.-L.; Cao, J.-J.; Chen, L.; Zhang, Y.-X.; Wang, C.; Zhou, J. "Organocatalytic asymmetric synthesis of substituted 3-hydroxy-2-oxindoles via Morita-Baylis-Hillman reaction" *J. Am. Chem. Soc.* **2010**, *132*, 15176.
- Liu, C.; Tan, B.-X.; Jin, J.-L.; Zhang, Y.-Y.; Dong, N. Li, X.; Cheng, J.-P. "Chiral bisquinoline alkaloid promoted asymmetric allylic alkylation of 3-substituted benzofuran-2(3h)-ones with Morita-Baylis-Hillman carbonates" *J. Org. Chem.* **2011**, *76*, 5838.
- Lutz, R. P. "Catalysis of the cope and Claisen rearrangements" *Chem. Rev.* **1984**, *84*, 205.
- Ma, G.-N.; Jiang, J.-J.; Shi, M.; Weib, Y. "Recent extensions of the Morita-Baylis-Hillman reaction" *Chem. Commun.*, **2009**, 5496.
- Madhavan, S.; Shanmugam, P. "Activated alkene dependent one-pot, three- component aza- Morita-Baylis-Hillman reaction of ferrocenealdehyde: Synthesis of highly functionalized diverse ferrocene derivatives" *Org. Lett.*, **2011**, *13*, 1590.
- Majumdar, K. C.; Chattopadhyay, B.; Samanta, S. "Synthesis of highly substituted dibenzoazocine derivatives by the aza-Claisen rearrangement and intramolecular Heck reaction via 8-exo-trig mode of cyclization" *Tetrahedron Lett.*, **2009**, *50*, 3178.
- Marko, I. E.; Ates, A.; Gautier, A.; Leroy, B.; Plancher, J.-M.; Quensel, Y.; Vanherck, J.-C. "Cerium(IV)-catalyzed deprotection of acetals and ketals under mildly basic conditions" *Angew. Chem., Int. Ed. Engl.* **1999**, *38*, 3207.

- Maryanoff, B. E.; Reitz, A. B.; Mutter, M. S.; Inners, R. R.; Almond, Jr. H. R., "Detailed rate studies on the Wittig reaction of non-stabilized phosphorus ylides via ^{31}P , ^1H , and ^{13}C NMR spectroscopy. Insight into kinetic vs. thermodynamic control of stereochemistry" *J. Am. Chem. Soc.*, **1985**, *107*, 1068.
- Masson, G.; Housseman, C.; Zhu, J. "The enantioselective Morita–Baylis–Hillman reaction and its aza counterpart" *Angew. Chem., Int. Ed.* **2007**, *46*, 4614.
- Mehta, G.; Srikrishna, A. "Synthesis of polyquinane natural products: An update" *Chem Rev.* **1997**, *97*, 671.
- Menz, H.; Kirsch, S. F. "Synthesis of stable 2h-pyran-5-carboxylates *via* a catalyzed propargyl-Claisen rearrangement/ oxa-6 δ electrocyclization strategy" *Org. Lett.* **2006**, *8*, 4795.
- Merlin, P.; Braekman, J. C.; Daloz, D.; Pasteels, J. M. "Tetraponerines, toxic alkaloids in the venom of the Neo-Guinean pseudomyrmecine ant *Tetraponera* sp." *J. Chem. Ecol.* **1988**, *14*, 517.
- Michael, J. P.; "Simple indolizidine and quinolizidine alkaloids" San Diego: Academic Press; *The Alkaloids*. **2001**, *55*, 91.
- Micheal, J. P. "Quinoline, quinoxaline and acridone alkaloids" *Nat. Prod. Rep.* **2002**, *19*, 742.
- Miyamoto, H.; Okawa, Y.; Nakazaki, A.; Kobayashi, S. "Highly diastereoselective one-pot synthesis of spirocyclic oxindoles through intramolecular Ullmann coupling and Claisen rearrangement" *Angew. Chem., Int. Ed.* **2006**, *45*, 2274.

- Miyamoto, H.; Okawa, Y.; Nakazaki, A.; Kobayashi, S. "Total synthesis of (\pm)-debromoflustramine B and E and (\pm)-debromoflustramide B based on one-pot intramolecular Ullmann coupling and Claisen rearrangement" *Tetrahedron Lett.*, **2007**, *48* 1805.
- Moghaddam, F. M.; Ghaffarzadeh, M. "Microwave-assisted rapid hydrolysis and preparation of thioamides by Willgerodt-Kindler reaction" *Synth. Commun.* **2001**, *31*, 317.
- Morrison, R. T.; Boyd, R. N. "Organic chemistry" 6th Ed.; Prentice-Hall, Inc. **1992**. 1005-1013.
- Morten, C. J.; Jamison, T. F. "Water overcomes methyl group directing effects in epoxide-opening cascades" *J. Am. Chem. Soc.* **2009**, *131*, 6678.
- Mortia, K., Suzuki, Z., Hirose, H. "A tertiary phosphine-catalyzed reaction of acrylic compounds with aldehydes" *Bull. Chem. Soc. Jap.* **1968**, *41*, 2815.
- Marx, J. N.; Bih, Q. -R. "Spirocyclic sesquiterpene synthesis *via* quinone methide coupling reactions. Anhydro- β -rotunol" *J. Org. Chem.* **1987**, *52*, 336.
- Myers, E. L.; de Vries, J. G.; Aggarwal, V. K. "Reactions of iminium ions with Michael acceptors through a Morita-Baylis-Hillman-type reaction: Enantiocontrol and applications in synthesis" *Angew. Chem. Int. Ed.* **2007**, *46*, 1893.
- Naidu, M. V.; Krishna Rao, G. S.; "Synthetic studies in aromatic hemiterpenes of natural origin, Part 5: Synthesis of 6-acetyl-2,2-dimethyl-8-methoxychromene *via* benzylic oxidation route" *Synthesis*, **1979**, 144.
- Nair, V.; Mathew, J.; Prabhakaram, J. "Carbon-carbon bond forming reactions mediated by Cerium(IV) reagents" *Chem. Soc. Rev.* **1997**, 127.

- Nair, V.; Jayan C. N.; Ros, S. "Novel reactions of reagent of indium reagent with 1,2-diketone; A facile synthesis of α -hydroxy ketone" *Tetrahedron*. **2001**, *57*, 9453.
- Nair, V.; Rajan, R.; Rath, N. P. "A CAN-induced cyclodimerization-Ritter trapping strategy for the one-pot synthesis of 1-amino-4-aryltetralins from styrenes" *Org. Lett.* **2002**, *4*, 1575.
- Nair, V.; Panicker, S. B.; Nair, L. G.; George, T. G.; Augustine, A. "Carbon-heteroatom bond-forming reactions mediated by Cerium(IV) ammonium nitrate: An overview" *Synlett* **2003**, 156.
- Nair, V.; Balagopal, L.; Rajan, R.; Mathew, J. "Recent advances in synthetic transformations mediated by cerium(IV) ammonium nitrate" *Acc. Chem. Res.* **2004**, *37*, 21.
- Nair, V.; Sreekumar, V.; Poonoth, M.; Mohan, R.; Suresh, E. "N-Heterocyclic carbene catalyzed reaction of enals and 1,2-dicarbonyl compounds: Stereoselective synthesis of spiro γ -butyrolactones" *Org. Lett.* **2005**, *7*, 2297.
- ^aNair, V.; Deepthi A. "Cerium (IV) ammonium nitrates a versatile single-electron oxidant" *Chem. Rev.* **2007**, *107*, 1862.
- ^bNair, V.; Mathew, S. C.; Biju, A.T.; Suresh, E. "A novel reaction of the "Huisgen zwitterion" with chalcones and dienones: An efficient strategy for the synthesis of pyrazoline and pyrazolopyridazine derivatives" *Angew. Chem.*, **2007**, *46*, 2070.
- Nair, V.; Deepthi, A. "Recent advances in CAN mediated reactions in organic synthesis" *Tetrahedron* **2009**, *65*, 10745.

- Nicolaou, K. C.; Montagnon, T.; Baran, P. S.; Zhong, Y. -L. "Iodine(V) reagents in organic synthesis. Part 4. O-Iodoxybenzoic acid as a chemospecific tool for single electron transfer-based oxidation processes" *J. Am. Chem. Soc.* **2002**, *124*, 2245.
- Negishi, E.; Cope'ret, C.; Ma, S.; Lou, S.-Y.; Liu, F. "Cyclic carbopalladation. A versatile synthetic methodology for the construction of cyclic organic compounds" *Chem. Rev.* **1996**, *96*, 365;
- Nishiguchi, I.; Hirashima, T. "Electroorganic synthesis. 4. Facile synthesis of aromatic aldehydes by direct anodic oxidation of para-substituted toluenes" *J. Org. Chem.* **1985**, *50*, 539.
- Nishinaga, A.; Itahara, T.; Matsuura, T. "Selective oxidation of the methyl group of *p*-cresols by base-catalyzed oxygenation" *Angew. Int. Ed.* **1975**, *14*, 356.
- Palumbo, A.; Ischia, M.; Misuraca, G.; Prota, G. "A new look at the rearrangement of adrenochrome under biomimetic conditions" *Biochim. Biophys. Acta.* **1989**, *990*, 297.
- Pandey, G.; Banerjee, P.; Gadre, S. R. "Construction of enantiopure pyrrolidine ring system *via* asymmetric [3+2]-cycloaddition of azomethine ylides" *Chem. Rev.* **2006**, *106*, 4484.
- Pardasani, R. T.; Pardasani, P.; Chaturvedi, V.; Yadav, S. K.; Saxena, A.; Sharma, I. "Theoretical and synthetic approach to novel spiroheterocycles derived from isatin derivatives and *L*-proline *via* 1,3-dipolar cycloaddition" *Heteroatom Chem.* **2003**, *14*, 361.

- Peddibhotla, S. "3-substituted-3-hydroxy-2-oxindole, an emerging new scaffold for drug discovery with potential anti-cancer and other biological activities" *Curr. Bioact. Compd.* **2009**, *5*, 20.
- Peng, J.; Huang, X.; Cui, H-L.; Chen, Y-C. "Organocatalytic and electrophilic approach to oxindoles with C3-quaternary stereocenters" *Org. Lett.*, **2010**, *12*, 4260.
- Perez, R.; Veronese, D.; Coelhob, F.; Antunes, O. A. C. "Palladium catalyzed Heck reaction of arenediazonium tetrafluoroborate salts with Baylis–Hillman adducts: production of α -benzyl- β -keto esters" *Tetrahedron Lett.* **2006**, *47*, 1325.
- Pohjala, E. "A facile synthesis of stable dihydroindolizines *via* intramolecular 1,5-cyclization of ylides" *Tetrahedron Lett.* **1972**, *13*, 2585.
- Popp, F. D. "Potential anticonvulsants. V. The condensation of isatins with C-acetyl heterocyclic compounds" *J. Heterocycl. Chem.* **1982**, *19*, 589.
- Pothast, A.; Rosenau, T.; Chen, C. -L.; Gratzl, J. S. "Selective enzymatic oxidation of aromatic methyl groups to aldehydes" *J. Org. Chem.* **1995**, *60*, 4320.
- ^aPrice, K. E.; Broadwater, S. J.; Jung, H. M.; McQuade, D. T. "Baylis-Hillman mechanism: A new interpretation in aprotic solvents" *Org. Lett.* **2005**, *7*, 147.
- ^bPrice, K. E.; Broadwater, S. J.; Walker, B. J.; McQuade, D. T. "A new interpretation of the Baylis-Hillman mechanism" *J. Org. Chem.* **2005**, *70*, 3980.
- Pryde, D. C.; Dalvie, D.; Hu, Q.; Jones, P.; Obach, R. S.; Tran T.-D. "aldehyde oxidase: An enzyme of emerging importance in drug discovery" *J. Med. Chem.*, **2010**, *53*, 8441.

- Qiao, Z.; Shafiq, Z.; Liu, L.; Yu, Z.-B.; Zheng, Q.-Y.; Wang, D.; Chen, Y.-J. "An organocatalytic, δ -regioselective, and highly enantioselective nucleophilic substitution of cyclic Morita–Baylis–Hillman alcohols with indoles" *Angew. Chem. Int. Ed.* **2010**, *49*, 7294.
- Qu, H.; Gu, X.; Min, B. J.; Liu, Z.; Hruby, V. J. "Synthesis of anti- β -substituted γ,δ -unsaturated amino acids via Eschenmoser-Claisen rearrangement" *Org. Lett.*, **2006**, *8*, 4215.
- Rama Rao, A. V.; Singh, A. K.; Venkateswara Rao, B.; Reddy, M. "Synthesis of (\pm) Fredericamycin A" *Tetrahedron Lett.* **1993**, *34*, 2665.
- Rassadin, V. A.; Tomashevskiy, A. A.; Sokolov, V. V.; Ringe, A.; Magull, J.; de Meijere, A. "Facile access to bicyclic sultams with methyl 1-sulfonylcyclopropane-1-carboxylate moieties" *Eur. J. Org. Chem.* **2009**, 2635.
- Redondo, M. C.; Ribagorda, M.; Carren˜o, M. C. "Exploring Morita-Baylis-Hillman reactions of *p*-quinols" *Org. Lett.*, **2010**, *12*, 568.
- Rhoads, S. J.; Cockroft, R. D. "Valence tautomerism in cis-2-vinylcyclopropane-carboxaldehyde. 2,5-dihydrooxepin" *J. Am. Chem. Soc.* **1969**, *91*, 2815.
- Ribiere, P.; Declerck, V.; Nedellec, Y.; Yadav-Bhatnagar, N.; Martinez, J.; Lamaty, F. "Synthesis of novel poly(ethylene glycol) supported benzazepines: The crucial role of PEG on the selectivity of an intramolecular Heck reaction" *Tetrahedron* **2006**, *62*, 10456.
- Ryu, I.; Sonoda, N.; Curran, D. P. "Tandem radical reactions of carbon monoxide, isonitriles, and other reagent equivalents of the geminal radical acceptor/radical precursor synthons" *Chem. Rev.*, **1996**, *96*, 177.

- Sadana A. K.; Mirza, Y.; Aneja, K. R.; Prakash, O. "Hypervalent iodine mediated synthesis of 1-aryl/hetryl-1,2,4-triazolo[4,3-*a*] pyridines and 1-aryl/hetryl 5-methyl-1,2,4-triazolo[4,3-*a*]quinolines as antibacterial agents" *Eur. J. Med. Chem.* **2003**, *38*, 533.
- Sadeka, K. U.; Al-Qalaf, F.; Mekheimer, R. A.; Elnagdi, M. H. "Cerium (IV) ammonium nitrate-mediated reactions: Simple route to benzimidazole derivatives" doi:10.1016/j.arabjc.2010.07.024.
- Sannigrahi, M. "Stereocontrolled synthesis of spirocyclics" *Tetrahedron* **1999**, *55*, 9007.
- Santamaria, J.; Jroundi, R. "Electron transfer activation - A selective photooxidation method for the preparation of aromatic aldehydes and ketones" *Tetrahedron Lett.* **1991**, *32*, 4291.
- Santos, L. S.; Pavam, C. H.; Almeida, W. P.; Coelho, F.; Eberlin, M. N. "Probing the mechanism of the Baylis–Hillman reaction by electrospray ionization mass and tandem mass spectrometry" *Angew. Chem. Int. Ed.* **2004**, *43*, 4330.
- Schwier, T.; Sromek, A. W.; Yap, D. M. L.; Chernyak, D.; Gevorgyan, V. "Mechanistically diverse copper-, silver-, and gold-catalyzed acyloxy and phosphatyloxy migrations: Efficient synthesis of heterocycles via cascade migration/cycloisomerization approach" *J. Am. Chem. Soc.* **2007**, *129*, 9868.
- Seregin, I. V.; Gevorgyan, V. "Gold-catalyzed 1,2-migration of silicon, tin, and germanium en route to C-2 substituted fused pyrrole-containing heterocycles" *J. Am. Chem. Soc.* **2006**, *128*, 12050.

- Seregin, I. V.; Schammel, A. W.; Gevorgyan, V. "Multisubstituted *N*-fused heterocycles via transition metal-catalyzed cycloisomerization protocols" *Tetrahedron* **2008**, *64*, 6876.
- Senapati, B. K.; Hwang, G-S.; Lee, S.; Ryu, D. H. "Enantioselective synthesis of β -iodo Morita–Baylis–Hillman esters by a catalytic asymmetric three-component coupling reaction" *Angew. Chem. Int. Ed.* **2009**, *48*, 4398.
- Shanmugam, P.; Rajasingh, P. "Studies on montmorillonite K10-microwave assisted isomerisation of Baylis–Hillman adduct: Synthesis of *E*-trisubstituted alkenes and synthetic application to lignan core structures by vinyl radical cyclization" *Tetrahedron* **2004**, *60*, 9283.
- ^aShanmugam, P.; Vaithyanathan, V.; Viswambharan, B. "Activation of the *N*-C–H bond of Baylis–Hillman adducts of *N*-methylisatin with CAN/ROH" *Tetrahedron Lett.* **2006**, *47*, 6851.
- ^bShanmugam, P.; Vaithyanathan, V.; Viswambharan, B. "Synthesis of functionalized 3-spirocyclopropane-2-indolones from isomerised Baylis-Hillman adducts of isatin" *Tetrahedron* **2006**, *62*, 4342.
- ^aShanmugam, P.; Vaithyanathan, V.; Viswambharan, B.; Madhavan, S. "A facile and efficient stereoselective synthesis of highly functionalised trisubstituted alkene derivatives of ferrocenealdehyde" *Tetrahedron Lett.* **2007**, *48*, 9190.
- ^bShanmugam, P.; Vaithyanathan, V.; Viswambharan, B. "A facile and efficient synthesis of functionalized γ -butyrolactones from Baylis-Hillman Adducts of isatin" *Aust. J. Chem.* **2007**, *60*, 296.

^cShanmugam, P.; Viswambharan, B.; Madhavan, S. “Synthesis of novel functionalized 3-spiropyrrrolizidine and 3-spiropyrrrolidine oxindoles from Baylis-Hillman adducts of isatin and heteroaldehydes with azomethine ylides *via* [3+2]-cycloaddition” *Org. Lett.* **2007**, *9*, 4095.

^aShanmugam, P.; Vaithyanathan, V. “Stereoselective synthesis of 3-spiro- α -methylene- δ -butyrolactoneoxindoles from Morita-Baylis-Hillman adducts of isatin” *Tetrahedron* **2008**, *64*, 3322.

^bShanmugam, P.; Viswambharan, B. “Short and efficient synthesis of 3-spiro- α -methylene- γ -butyrolactone oxindolone from isomerized bromoderivatives of Morita-Baylis-Hillman adduct” *Synlett.* **2008**, 2763.

^cShanmugam, P.; Viswambharan, B.; Selvakumar, K.; Madhavan, S. “A facile and efficient synthesis of highly functionalised 3,30-dispiropyrrrolidine- and 3,30-dispiropyrrrolizidine bisoxindoles *via* [3+2] cycloaddition” *Tetrahedron Lett.* **2008**, *47*, 2611.

Shanmugam, P.; Madhavan, S.; Selvakumar, K.; Vaithyanathan, V.; Viswambharan, B. “A first one-pot synthesis, isomerization and synthetic utility of mono- and bis Morita-Baylis-Hillman adducts of 1, 10-ferrocenedialdehyde” *Tetrahedron Lett.* **2009**, *50*, 2213.

Sharma, V.; McLaughlin, M. L “Efficient Assembly of 2,5,6-Substituted Pyrimidines *via* MgI₂-Mediated Morita-Baylis-Hillman Reaction” *J. Comb. Chem.* **2010**, *12*, 327.

- Shawali, A. S.; Gomha, S. M. "Regioselectivity in 1,5-electrocyclization of *N*-[*as*-triazin-3-yl]nitrilimines. Synthesis of *s*-triazolo[4,3-*b*]-*as*-triazin-7(8*H*)-ones" *Tetrahedron*, **2002**, 58, 8559.
- Sherry, B. D.; Toste, F. D. "Gold(I)-catalyzed propargyl Claisen rearrangement" *J. Am. Chem. Soc.* **2004**, 126, 15978.
- Sherry, B. D.; Maus, L.; Laforteza, B. N.; Toste, F. D. "Gold(I)-catalyzed synthesis of dihydropyrans" *J. Am. Chem. Soc.* **2006**, 128, 8132.
- Shibata, T.; Kadowaki, S.; Takagi, K. "Chemo- and regioselective intramolecular hydrosilylative carbocyclization of allenynes" *Organometallics* **2004**, 23, 4116.
- Shipman, M. "Indolizines" *Sci. Synth.* **2001**, 10, 745.
- Shvekhgeimer, M. G. A. "Synthesis of heterocyclic compounds by the cyclization of isatin and its derivatives" *Chem. Heterocycl. Compd. (Engl. Transl.)*. **1996**, 32, 249.
- Singh, J.; Sharma, M.; Kad, G. L.; Chhabra, B. R. "Selective oxidation of allylic methyl groups over a solid support under microwave irradiation" *J. Chem. Res. (S)*, **1997**, 264.
- Singh, V.; Batra, S. "Advances in the Baylis–Hillman reaction-assisted synthesis of cyclic frameworks" *Tetrahedron* **2008**, 64, 4511.
- Singh, V.; Hutait, S.; Batra, S. "Advancing the Morita–Baylis–Hillman chemistry of 1-formyl- β -carbolines for the synthesis of indolizino-indole derivatives" *Eur. J. Org. Chem.* **2010**, 3684

- Smith, C. D.; Zilfou, J. T.; Stratmann, K.; Patterson, G. M.; Moore, R. E. “Welwitindolinone analogues that reverse P-glycoprotein-mediated multiple drug resistance” *Mol. Pharmacol.* **1995**, *47*, 241.
- Smith, N. D.; Mancuso, J.; Lautens, M. “Metal-catalyzed hydrostannations” *Chem. Rev.* **2000**, *100*, 3257.
- Sonnenschein, H.; Hennrich, G.; Resch-Genger, U.; Schulz, B. “Fluorescence and UV/Vis spectroscopic behaviour of novel biindolizines” *Dyes Pigm.* **2000**, *46*, 23.
- Sridharan, V.; Mene´ndez, J. C. “Cerium(IV) ammonium nitrate as a catalyst in organic synthesis” *Chem. Rev.* **2010**, *110*, 3805.
- Stylianakis, I.; Kolocouris, A.; Kolocouris, N.; Fytas, G.; Foscolos, G. B.; Padalko, E.; Neyts, J.; De Clercq, E. “Spiro[pyrrolidine-2,20-adamantanes]: Synthesis, anti-Influenza virus activity and conformational properties” *Bioorg. Med. Chem. Lett.* **1999**, *9*, 3465.
- Suhre, M. H.; Reif, M.; Kirsch, S. F. “Gold(I)-catalyzed synthesis of highly substituted furans” *Org. Lett.* **2005**, *7*, 3925.
- Sumpter, W. C. “The chemistry of oxindole” *Chem. Rev.* **1945**, *34*, 407.
- Syper, L. “Partial oxidation of aliphatic side chains with cerium (IV)” *Tetrahedron Lett.* **1966**, *37*, 4493.
- Tamura, Y.; Tsujimoto, N.; Sumida, Y.; Ikeda, M. “Intramolecular 1,5-cyclization of ylides : Synthesis of pyrazolo-[1,5-a]pyridines and indolizines” *Tetrahedron* **1972**, *28*, 21.

- Thommen, M.; Keese, R. "Fenestranes in recent synthetic developments" *Synlett*, **1997**, 231.
- Thyrann, T.; Lightner, D. A. "Oxidation of pyrrole α -methyl to formyl with Ceric ammonium nitrate" *Tetrahedron Lett.* **1995**, *36*, 4345.
- Tian, X.; Hutters, A. D.; Douglas, C. J. ; Garg, N. K. "Concise synthesis of the bicyclic scaffold of *N*-methylwelwitindolinone C isothiocyanate *via* an indolyne cyclization" *Org. Lett.* **2009**, *11*, 2349.
- Tian, J.; Zhou, R.; Sun, H.; Song, H.; He, Z. "Phosphine-catalyzed [4 + 1] annulation between α,β -unsaturated imines and allylic carbonates: Synthesis of 2-Pyrrolines" *J. Org. Chem.* **2011**, *76*, 2374.
- Togni, A.; Venanzi, L. M. "Nitrogen donors in organometallic chemistry and homogeneous catalysis" *Angew. Chem. Int. Ed. Engl.* **1994**, *33*, 497.
- Trahanovsky, W. S.; Young, L. B. "Controlled oxidation of organic compounds with cerium(IV): The oxidation of toluenes" *J. Org. Chem.* **1966**, *31*, 2033.
- Unthank, M. G.; Tavassoli, B.; Aggarwal, V. K. "Epoxy-annulations by reactions of *R*-amido ketones with vinyl sulfonium salts. Reagent versus substrate control and kinetic resolution" *Org. Lett.* **2008**, *10*, 1501.
- Vasudevan, A.; Tseng, P.-S.; Djuric, S. W. "A post aza Baylis-Hillman/Heck coupling approach towards the synthesis of constrained scaffolds" *Tetrahedron Lett.* **2006**, *47*, 8591.
- Vetelino, M. G.; Coe, J. W.; "A mild method for the conversion of activated aryl methyl groups to carboxaldehydes *via* the uncatalyzed periodate cleavage of enamines" *Tetrahedron Lett.* **1994**, *35*, 219.

- Vintonyak, V. V.; Warburg, K.; Kruse, H.; Grimme, S.; Bel, K. H.; Rauh, D.; Waldmann, H. "Identification of thiazolidinones spiro-fused to indolin-2-ones as potent and selective inhibitors of the mycobacterium tuberculosis protein tyrosine phosphatase B" *Angew. Chem. Int. Ed.* **2010**, *49*, 5902.
- Vlahovici, A.; Druta, I.; Andrei, M.; Cotlet, M.; Dinica, R. "Photophysics of some indolizines, derivatives from bipyridyl, in various media" *J. Lumin.* **1999**, *82*, 155.
- Vlahovici, A.; Andrei, M.; Druta, I. "A study of the dimethyl 3-benzoyl-5(2'-pyridyl)-indolisine-1,2-dicarboxylate exciplexes with alcohols" *J. Lumin.* **2002**, *96*, 279.
- Wan, Y.; Barnhurst, L. A.; Kutateladze, A. G. "Photooxidation of methylthiopyrins into thiopyrin carboxaldehydes in carbon tetrachloride" *Org. Lett.* **1999**, *1*, 937.
- Wang, S. -Y.; Ji, S. -J. "Facile synthesis of 3,3-di(heteroaryl)indolin-2-one derivatives catalyzed by ceric ammonium nitrate (CAN) under ultrasound irradiation" *Tetrahedron* **2006**, *62*, 1527.
- Wille, G.; Steglich, W. "A short synthesis of the bacterial pigments violacein and deoxyviolacein" *Synthesis*, **2001**, 759.
- Wilson, J. E.; Fu, G. C. "Synthesis of functionalized cyclopentenes through catalytic asymmetric [3+2] cycloadditions of allenes with enones" *Angew. Chem. Int. Ed.* **2006**, *45*, 1426.
- Woodward, R. B.; Hoffmann, R. "The conservation of orbital symmetry" *Angew. Chem. Int. Ed. Engl.* **1969**, *8*, 781.

- Wurz, R. P.; Fu, G. C. "Catalytic asymmetric synthesis of piperidine derivatives through the [4 + 2] annulation of imines with allenes" *J. Am. Chem. Soc.* **2005**, *127*, 12234.
- Xie, P.; Huang, Y.; Chen, R. "Phosphine-catalyzed domino reaction: Highly stereoselective synthesis of *trans*-2,3-dihydrobenzofurans from salicyl *n*-thiophosphinyl imines and allylic carbonates" *Org. Lett.* **2010**, *12*, 3768.
- Ye, L.-W.; Sun, X.-L.; Wang, Q.-G.; Tang, Y. "Phosphine-catalyzed intramolecular formal [3+2] cycloaddition for highly diastereoselective synthesis of bicyclo[n.3.0] Compounds" *Angew. Chem. Int. Ed.* **2007**, *46*, 5951.
- Ye, L.-W.; Han, X.; Sun, X.-L.; Tang, Y. "PPh₃-catalyzed ylide cyclization for the controllable synthesis of benzobicyclo[4.3.0] compounds: base effects and scope" *Tetrahedron* **2008**, *64*, 1487.
- Yoshikawa, M.; Murakami, T.; Kishi, A.; Sakurama, T.; Matsuda, H.; Nomura, M.; Matsuda, H.; Kubo, M. "Novel indole S, O-bisdesmoside, calanthoside, the precursor glycoside of tryptanthrin, indirubin, and isatin, with increasing skin blood flow promoting effects, from two *Calanthe* species (Orchidaceae)" *Chem. Pharm. Bull.* **1998**, *46*, 886.
- Zhang, X.; Smith, C. D. "Microtubule effects of Welwistatin, a cyanobacterial indolinone that circumvents multiple drug resistance" *Mol. Pharmacol.* **1996**, *49*, 288.
- Zhang, R.; Mamai, A.; Madalengoitia, J. S. "Cyclopropanation reactions of pyroglutamic acid-derived synthons with akylidene transfer reagents" *J. Org. Chem.* **1999**, *64*, 547.

- Zhang, Y.; Panek, J. S. "Stereocontrolled synthesis of spirooxindoles through Lewis acid-promoted [5 + 2]-annulation of chiral silyl alcohols" *Org. Lett.* **2009**, *11*, 3366.
- Zhang, X.; Rao, W.; Sally.; Chan, P. W.H. "Iron(III) chloride-catalysed direct nucleophilic *a*-substitution of Morita-Baylis-Hillman alcohols with alcohols, arenes, 1,3-dicarbonyl compounds, and thiols" *Org. Biomol. Chem.* **2009**, *7*, 4186.
- Zhao, D.; Lee, D. G. "Heterogeneous permanganate oxidations; part 6: Selective oxidation of arenes" *Synthesis* **1994**, 915.
- Zheng, J.-C.; Zhu, C.-Y.; Sun, X.-L.; Tang, Y.; Dai, L.-X. "Highly diastereoselective and enantioselective formal [4 + 1] ylide annulation for the synthesis of optically active dihydrofurans" *J. Org. Chem.* **2008**, *73*, 6909.
- Zheng, S.; Lu, X. "Phosphine-catalyzed [3 + 2] annulation reaction of modified allylic compounds and *n*-tosylimines" *Org. Lett.* **2008**, *10*, 4481.
- Zheng, S.; Lu, X. "Phosphine-catalyzed [3+3] annulation reaction of modified tert-butyl allylic carbonates and substituted alkylidenemalononitriles" *Tetrahedron Lett.* **2009**, *50*, 4532.
- Zheng, S.; Lu, X. "Phosphine-catalyzed [4 + 3] annulation for the synthesis of highly functionalized bicyclo[3.2.2] nonadienes" *Org. Lett.* **2009**, *11*, 3978.
- Zhong, F.; Han, X.; Wang, Y.; Lu, Y. "Highly enantioselective [3+2] annulation of Morita-Baylis-Hillman adducts mediated by l-threonine-derived phosphines: Synthesis of 3-spirocyclopentene-2-oxindoles having two contiguous quaternary centers" *Angew. Chem. Int. Ed.* **2011**, *50*, 7839.

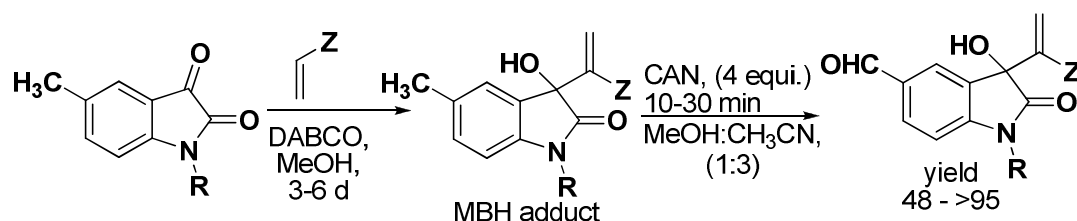
- Zhou, H. Xing, A.; Yao, J.; Lu, Y. J. "Heteroatom as a promotor: Synthesis of polyfunctionalized benzenes and naphthalenes" *J. Org. Chem.* **2011**, *76*, 4582.
- Zhou, R.; Wang, J.; Song, H.; He, Z. "Phosphine-catalyzed cascade [3 + 2] cyclization-allylic alkylation, [2 + 2 + 1] annulation, and [3 + 2] cyclization reactions between allylic carbonates and enones" *Org. Lett.* **2011**, *13*, 580.
- Zimmer, R.; Dinesh, C. U.; Nandan, E.; Khan, F. A. "Palladium-catalyzed reactions of allenes" *Chem. Rev.* **2000**, *100*, 3067.
- Ziegler, F. E. "Stereo- and regiochemistry of the Claisen rearrangement: Applications to natural products synthesis" *Acc. Chem. Res.* **1977**, *10*, 227.
- Ziegler, F. E. "The thermal, aliphatic Claisen rearrangement" *Chem. Rev.* **1988**, *88*, 1423.

SUMMARY

The thesis entitled “**Synthesis of Functionalized 2-Oxindoles and 3-Spirocyclic-2-Oxindoles from Morita-Baylis-Hillman Adduct of Isatin**” presents the results of our investigation on novel synthetic transformations of Morita-Baylis-Hillman (MBH) adduct and its derivatives of isatin towards synthesis of spirocyclic oxindole derivatives. The thesis is divided in to five chapters which deals with detailed discussion on synthetic transformation of isatin MBH adduct.

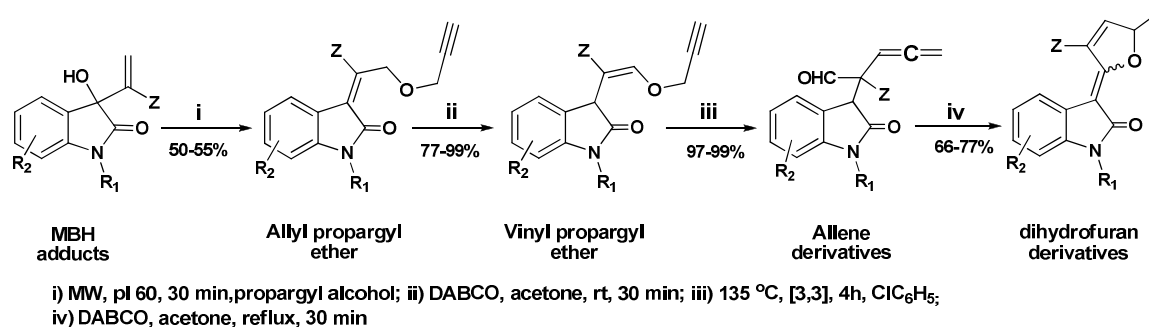
The thesis **Chapter I** embody a brief general introductory discussion on the genesis, recent kinetic studies and development of mechanistic details of MBH adduct formation, new catalytic systems used and substrates scope in MBH chemistry. In continuation with this discussion, example of isatin core involved natural, bioactive molecule synthesis and isatin MBH adducts involved synthetic transformations were briefly explored.

In **Chapter II**, synthesis of 5-formyl MBH adduct derivatives by controlled oxidation from 5- methyl MBH adducts of isatin using CAN as a mild oxidant in acid free reaction condition is described (Scheme-1). Due to the various oxidation states of other metal salts in strong acidic media at elevated temperatures, controlled oxidation for the synthesis of aromatic aldehyde remains a challenging task for organic chemists. This chapter encompasses detailed studies on MBH adduct aromatic side chain oxidation including the substrate scope and limitation, spectroscopic characterization of the newly synthesized products and plausible reaction mechanism. (Shanmugam, P. Vaithyanathan, V. and Selvakumar, K. *Tetrahedron Lett.* **2008**, 49, 2119.)



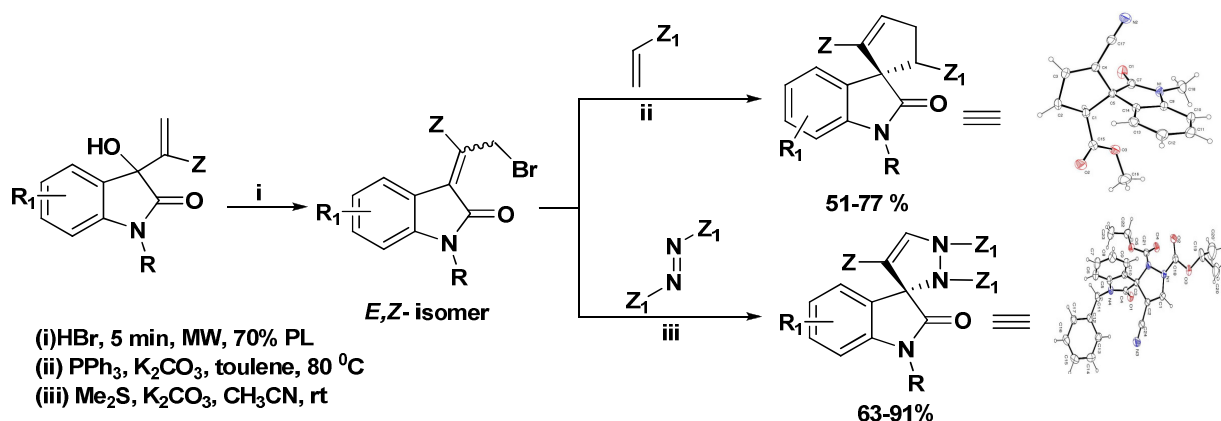
Scheme 1. CAN mediated side chain oxidation of 5-Methyl MBH adduct of isatin

Chapter III describes the synthesis of highly functionalized allene incorporated oxindole derivatives from propargyl isomerized MBH adducts of isatin *via* [3,3]-sigmatropic Claisen rearrangement reaction as the key step. The synthetic utility of allene derivatives have been demonstrated by the synthesis of dihydrofuran appended oxindole derivative *via* base mediated intramolecular cyclization. In addition, the formation of dihydrofuran derivatives has been rationalized *via* a mechanistic proposal (Scheme 2). (Shanmugam, P. Vaithianathan, V. and Selvakumar, K. *Synlett.* **2009**, 1591.)



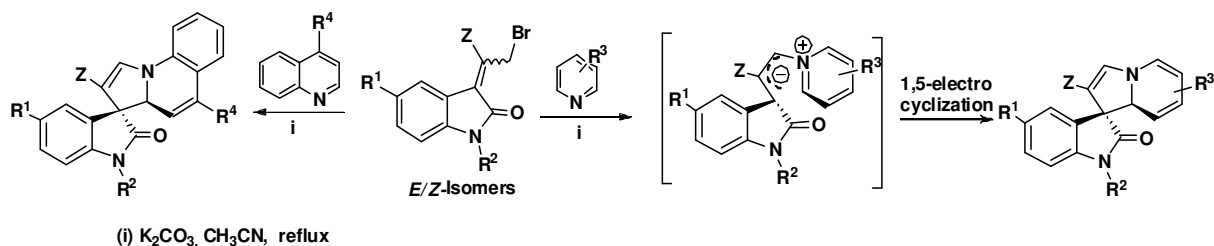
Scheme 3: Claisen rearrangement reaction of MBH adduct of isatin

Spirooxindoles are commonly occurring heterocyclic ring systems which found in many natural products and pharmaceuticals units. Hence we embarked upon the synthesis of various spiro carbo- and heterocyclic frame works from the allyl bromide of oxindoles *via* [3+2] annulation strategy (Scheme-3) and is the central theme of **Chapter IV**. Utilizing the recently well explored sulphur and phosphorous ylide chemistry, we have synthesized spirocyclopentene and spiropyrazole derivatives diastereoselectively from a mixture of *E*- and *Z*- isomerised allyl bromide of oxindole *via* [3+2] dipolar strategy. The stereochemistry of the product was assigned based on the single crystal X-ray analysis. (Selvakumar, K, Vaithianathan, V and Shanmugam, P. *Chem. Commun.*, **2010**, 46, 2826.)



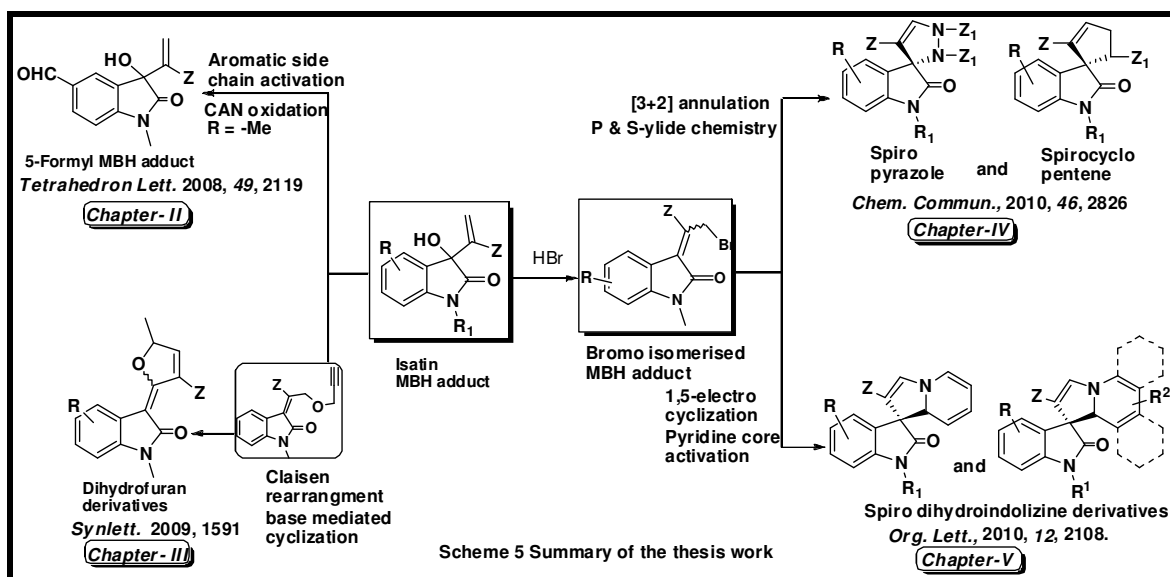
Scheme 3. Synthesis of spiro carbo- and heterocycles from MBH adducts of isatin

In **Chapter V**, diastereoselective synthesis of spirodihydroindolizine compound from bromo isomerized MBH adduct of isatin *via* pyridine core activation as the key step is described. Pyridine core activation is an important synthetic transformation and functionalization of pyridine in metal free condition remains an important and challenging issue in synthetic organic chemistry. The details of the study on the 1,5-electrocyclization reaction of various pyridine derivatives of allyl bromide MBH adduct of oxindoles is described in this chapter (Scheme 4). The method has been successfully applied for an efficient synthesis of a number of 3-spirodihydroindolizine-2-oxindoles, which have been found as core structure of secoyohimbane and heteroyohimbane alkaloid natural products. (Viswambharan, B. **Selvakumar**, K. Madhavan, S and Shanmugam, P. *Org. Lett.*, **2010**, *12*, 2108.)



Scheme 4. Synthesis of spiro heterocycles via pyridine core activation

The overall work carried out for this thesis is shown in the Scheme 5.



PUBLICATIONS

1. An efficient stereoselective synthesis of 3-spirocyclopentene- and 3-spiro pyrazole-2-oxindoles *via* 1,3-dipolar cycloaddition reaction. **Selvakumar, K.** Vaithyanathan, V. and Shanmugam, P. *Chem. Commun.*, **2010**, *46*, 2826–2828.
2. Synthesis of 3-spirodihydroindolizine oxindoles by 1,5-electrocyclization: Pyridine core activation *via* quaternization with bromo isomerised Morita-Baylis-Hillman adducts of isatin. Viswambharan. B, **Selvakumar, K.** Madhavan. S and Shanmugam, P. *Org. Lett.*, **2010**, *12*, 2108-2111.
3. A mild and efficient CAN mediated oxidation of Morita-Baylis-Hillman adducts of 5-methyl-N-alkyl isatin to 5-formyl-N-alkyl isatin. Shanmugam, P. Vaithyanathan, V. and **Selvakumar, K.** *Tetrahedron Lett.* **2008**, *49*, 2119-2123.
4. Synthesis of highly functionalized Allene- appended oxindole and 2-Oxo-1,2 dihydroindole- 3-ylidene-2,5 dihydrofuran *via* Claisen rearrangement and cyclization. Shanmugam, P. Vaithyanathan V. and **Selvakumar, K.** *Synlett.* **2009**, *10*, 1591-1596.
5. Synthesis of multifunctional 3, 3'-dispiro pyrrolidine- and 3, 3'-dispiro pyrrolizidine bisoxindoles from isomerised Morita-Baylis-Hillman adducts of isatin with azomethine ylides *via* [3+2]-Cycloaddition. Shanmugam, P. Viswambharan, B. **Selvakumar, K.** and Madhavan. S. *Tetrahedron Lett.* **2008**, *49*, 2611-2616.
6. A first one-pot synthesis, isomerization and synthetic utility of mono and bis Morita-Baylis-Hillman adducts of 1, 1'-ferrocenedialdehyde. Shanmugam, P. Madhavan. S **Selvakumar, K.** Vaithyanathan, V. and Viswambharan, B. *Tetrahedron Lett.* **2009**, *50*, 2213-2493.
7. Synthesis of functionalized 1, 2, 3-triazole derivatives of 2-indolones from Morita-Baylis-Hillman adducts of isatin *via* "click chemistry" Shanmugam, P. Damodiran, M. **Selvakumar, K.** and Perumal. P.T.; *J. Heterocyclic Chem.* **2009**, *46*, 919.

8. Stereoselective synthesis of geometrically strained, oxindole appended vinyl cyclopropanes and highly substituted cyclopentenes *via sulphur ylide* cyclopropanation and vinyl cyclopropane rearrangement . Arun Prasath Lingam, K. Shanmugam, P. and **Selvakumar, K.** *Synlett*, **2012**, 278.

MANUSCRIPTS UNDER PREPARATION:

1. Synthesis of Highly Functionalized Oxindole Derivatives *via* Isomerization of Bis Morita-Baylis-Hillman Adduct of Isatin: Unforeseen Rate Acceleration of Second Morita-Baylis-Hillman Reaction due to Hydrogen Bonding. Shanmugam, P. **Selvakumar, K.** and Vaithiyanathan, V. (Communicated to *JOC*)
2. Development of Green Protocol for One-Pot Protection/ Isomerization and *O*-Alkylation of Tertiary Allyl Alcohols with Potassium Carbonate as Base under Microwave Irradiation. **Selvakumar, K.** Solaiselvi, R. Luxmi Varma, Shanmugam, P. (To be communicated)
3. Direct Synthesis of Quinoline Derivatives *via* Palladium Catalyzed Tandem Heck Reaction–Condensation Cyclization from Morita-Baylis-Hillman Adducts. **Selvakumar, K.**, R. Luxmi Varma, Shanmugam, P. (To be communicated)

PAPERS PRESENTED AT CONFERENCES:

1. Participated and Presented Poster at the *10th CRSI symposium*, held on Feb11-13, 2008 at IISc Bangalore.
2. Participated and Presented Poster at the *12th CRSI symposium*, held on Feb 06-10, 2010 at ICT, Hyderabad.
3. Participated and Presented Poster at *the 5th Midyear CRSI symposium*, held on July 23-24, 2009 at NIIST, Trivandrum.
4. Participated at the *14th CRSI symposium*, held on Feb 03-5, 2012 at NIIST, Trivandrum.